

AN OPTIMAL DESIGN METHODOLOGY FOR A
CLASS OF AIR-BREATHING LAUNCH VEHICLES

by

Philip David Hattis

Submitted to the Department of
Aeronautics and Astronautics on June, 1980,
in partial fulfillment of the requirements for
the degree of Doctor of Philosophy

ABSTRACT

A generalized two-point boundary value problem methodology applicable to the design of flight vehicles is developed and subsequently applied to a two-staged air-breathing launch vehicle. Methods are developed to simultaneously consider configuration and trajectory by treating geometry, dynamic discontinuities, and time-dependent flight variables all as controls to be optimized with respect to a single mathematical performance measure. In the air-breathing launch vehicle application, inequality constraint bounds are applied to dynamic pressure and specific force, and the effect of their variation is evaluated and discussed.

Thesis Supervisor: Wallace E. Vander Velde
Title: Professor of Aeronautics and
Astronautics

Thesis Supervisor: Steven R. Croopnick
Title: Staff, Flight Control and Dynamics
Group, C.S. Draper Laboratory

Thesis Supervisor: Donald C. Fraser
Title: Lecturer, Aeronautics and
Astronautics

Thesis Supervisor: Manuel Martinez-Sanchez
Title: Associate Professor of Aeronautics
and Astronautics

Thesis Supervisor: Rudrapatna Ramnath
Title: Lecturer, Aeronautics and
Astronautics and Mechanical
Engineering

ACKNOWLEDGMENT

I wish to express my sincere gratitude to my thesis committee. This includes Professor Wallace E. Vander Velde who served both as chairman and frequent technical consultant, Dr. Steven R. Croopnick who helped originate the topic and consistently provided technical support and advice, Dr. Donald C. Fraser whose frequent advice assured practical application and direction for the thesis, Professor Manuel Martinez-Sanchez who provided much useful advice and many ideas on modelling and interpreting the behavior of air-breathing vehicles, and Dr. Rudrapatna Ramnath whose mathematical expertise was invaluable.

I also wish to express my deep appreciation to Robert A. Jones, William J. Small, and F. Steven Kirkham of the NASA Langley Research Center who provided much useful technical data and advice.

I would like to thank all the members of The Charles Stark Draper Laboratory Control and Flight Dynamics Division for their comments and suggestions during my doctoral program, especially for the moral support provided by Christopher B. Kirchwey, Harvey L. Malchow, Alexander Penchuk, Edward V. Bergmann, and fellow students Steven D. Ginter and Sean K. Collins.

This thesis was prepared at The Charles Stark Draper Laboratory, Inc., under Contract NAS9-13809 with the Johnson Space Center of the National Aeronautics and Space Administration. Publication of this thesis does not constitute approval by NASA or The Charles Stark Draper Laboratory, Inc., of the findings or conclusions contained herein.

TABLE OF CONTENTS

<u>Section</u>		<u>Page</u>
I	INTRODUCTION.....	18
II	THE VEHICLE AND ENVIRONMENT MODEL.....	22
	2.1 An Overview.....	22
	2.2 The First-Stage Model.....	23
	2.3 The Second-Stage Model.....	36
III	SYSTEM DYNAMICS.....	42
IV	A SUITABLE OPTIMIZATION ALGORITHM.....	46
V	SPECIFIC FUNCTIONAL, DERIVATIVE, AND BOUNDARY CONDITION RELATIONS.....	65
	5.1 The Cost Function.....	65
	5.2 The Initial State Boundary Condition.....	67
	5.3 The Equality Constraints and the State Integration Cutoff Condition.....	68
	5.4 The Derivative Terms.....	70
	5.5 The Boundary Conditions of the Adjoined Functions.....	75
VI	NUMERICAL DIFFICULTIES AND THEIR RESOLUTION.....	77
	6.1 An Overview.....	77
	6.2 Loss of Significant Information.....	77
	6.3 Equality Constraint Effect on Stability of Convergence.....	77
	6.4 Choosing Metrics.....	80
	6.5 Choosing a Penalty Function Weighting Factor.....	82
	6.6 Choosing a Specified Cost Improvement.....	82
VII	COMPUTER RESULTS.....	84
	7.1 An Overview.....	84
	7.2 Details of Computer Cases.....	84
	7.3 Optimization Data.....	85
	7.4 Physical Effects in Optimal Results.....	88
	7.5 Some Comments About the Scramjet.....	104
	7.6 Summary.....	105

TABLE OF CONTENTS (Cont.)

<u>Section</u>	<u>Page</u>
VIII	CONCLUSIONS AND SUGGESTIONS FOR FUTURE RESEARCH.....107
8.1	An Overview.....107
8.2	Conclusions.....107
8.3	Suggested Future Research.....109
<u>Appendix</u>	
	OPTIMIZATION SOFTWARE PROGRAM.....112
	LIST OF REFERENCES.....282
	BIOGRAPHY.....285

LIST OF ILLUSTRATIONS

<u>Figure</u>	<u>Page</u>
II-1	28
III-1.....	43
IV-1.....	48
IV-2.....	53
VI-1.....	78
VII-1	89
Angle of attack α vs. t. First 240 seconds. Specific force bound = 3 g's. Dynamic pressure bound varied.....	
VII-2	89
Angle of attack α vs. t. Full flight time. Specific force bound = 3 g's. Dynamic pressure bound varied.....	
VII-3	89
Throttle setting ϕ vs. t. First 240 seconds. Specific force bound = 3 g's. Dynamic pressure bound varied.....	
VII-4	90
Throttle setting ϕ vs. t. Full flight time. Specific force bound = 3 g's. Dynamic pressure bound varied.....	
VII-5	90
Dynamic pressure q vs. t. Through dense atmos- phere. Specific force bound = 3 g's. Dynamic pressure bound varied.....	
VII-6	90
Specific force F_{sp} vs. t. First 240 seconds. Specific force bound = 3 g's. Dynamic pressure bound varied.....	
VII-7	91
Specific force F_{sp} vs. t. Full flight time. Specific force bound = 3 g's. Dynamic pressure bound varied.....	
VII-8	91
Radial velocity \dot{r} vs. t. Through first stage flight. Specific force bound = 3 g's. Dynamic pressure bound varied.....	
VII-9	91
Tangential air speed $r(\dot{\theta} - \omega_e)$ vs. t. Through first stage flight. Specific force bound = 3 g's. Dynamic pressure bound varied.....	
VII-10	92
Mach number M vs. t. Through first stage flight. Specific force bound = 3 g's. Dynamic pressure bound varied.....	
VII-11	92
Angle of attack α vs. t. First 240 seconds. Dynamic pressure bound = 800 psf. Specific force bound varied.....	
VII-12	92
Angle of attack α vs. t. Full flight time. Dynamic pressure bound = 800 psf. Specific force bound varied.....	

LIST OF ILLUSTRATIONS (Cont.)

<u>Figure</u>	<u>Page</u>
VII-13	Throttle setting ϕ vs. t. First 240 seconds. Dynamic pressure bound = 800 psf. Specific force bound varied.....93
VII-14	Throttle setting ϕ vs. t. Full flight time. Dynamic pressure bound = 800 psf. Specific force bound varied.....93
VII-15	Dynamic pressure q vs. t. Through dense atmosphere. Dynamic pressure bound = 800 psf. Specific force bound varied.....93
VII-16	Specific force F_{sp} vs. t. First 240 seconds. Dynamic pressure bound = 800 psf. Specific force bound varied.....94
VII-17	Specific force F_{sp} vs. t. Full flight time. Dynamic pressure bound = 800 psf. Specific force bound varied.....94
VII-18	Radial velocity \dot{r} vs. t. Through first stage flight. Dynamic pressure bound = 800 psf. Specific force bound varied.....94
VII-19	Tangential air speed. $r(\dot{\theta} - \omega_e)$ vs. t. Through first stage flight. Dynamic pressure bound = 800 psf. Specific force varied.....95
VII-20	Mach number M vs. t. Through first stage flight. Dynamic pressure bound = 800 psf. Specific force bound varied.....95
VII-21	Dynamic pressure q vs. t. Bound violation region. Specific force bound = 2 g's. Dynamic pressure bound = 800 psf.....103
VII-22	Specific force F_{sp} vs. t. Early flight. Specific force bound = 2 g's. Dynamic pressure bound = 800 psf.....103
VII-23	Specific force F_{sp} vs. t. Full flight time. Specific force bound = 2 g's. Dynamic pressure bound = 800 psf.....103

LIST OF TABLES

<u>Table</u>	<u>Page</u>
II-1	Delta wing lift and drag coefficients.....25
II-2	First stage parasitic drag coefficients. (Based on scaled shuttle data—scale factor = 1/3).....26
II-3	Scramjet mass capture ratio.....36
II-4	Space shuttle physical properties.....37
II-5	Space shuttle aerodynamic data.....39
II-6	Atmospheric properties.....41
VII-1	Inequality constraints on computer runs.....85
VII-2	Parameter values.....86
VII-3	Transition and flight times.....86
VII-4	Transition point state functions.....87
VII-5	Ground value of propellant masses.....87
VII-6	Data from 2.0 g's, 800 psf bound case. (Not a fully converged solution.).....102

LIST OF SYMBOLS

a	the dimension of the state vector (x)
a_d	the bound on the desired acceleration excluding gravity (the specific force bound)
A	(1) aspect ratio (2) a matrix term in the differential equation for Λ defined in Eq. (4-45)
A_{f_s}	fuselage surface area
A_S	scramjet inlet area
A_T	turbojet inlet area
A_P	second stage planform area
A_{P_0}	space shuttle planform area (a reference value)
A_{w_p}	area of first stage wing planform
b	the dimension of the control vector (u)
B	a matrix term in the variation equations defined in Eq. (4-70a)
c	the dimension of the parameter vector (p)
C	a vector used in the variation equations defined in Eq. (4-70b)
C_A	a constant to establish the desired weight given to specific force bound violation penalties
C_D	aerodynamic drag coefficient
C_{D_0}	aerodynamic parasitic drag coefficient

LIST OF SYMBOLS (CONT.)

C_J	a coefficient to establish the desired weight given to cost improvement contributions to variation terms
C_L	aerodynamic lift coefficient
C_Ψ	a coefficient to establish the desired weight given to equality constraint violation improvements in variation terms
d	(1) a mathematical symbol for a total derivative (2) the dimension of the switch time vector (t_s)
D	total vehicle drag
D_1	vehicle first stage drag
D_2	vehicle second stage drag
D_w	drag due to first stage wing
f	derivative of state vector with respect to time
f_s	the derivative of the state vector with respect to time evaluated at the switch points (a vector)
f_{s_i}	the derivative of the state vector with respect to time evaluated at the i^{th} switch point
f_p	the partial derivative of the vector f with respect to the vector p (a matrix)
f_x	the partial derivative of the vector f with respect to the vector x (a matrix)
F	a symbol for the matrix f_x
F_g	the gravitational force component
F_r	the radial force component
F_{sp}	the specific force
F_θ	the tangential force component
g	(1) the gravitational acceleration (2) a vector used in the variation equations defined in Eq. (4-56a)

LIST OF SYMBOLS (CONT.)

g_0	the gravitational acceleration at the earth's surface
G	(1) the universal gravitation constant (2) the partial derivatives of the vector f with respect to the vector u (a matrix)
h_S	the scramjet inlet height
h_T	the turbojet inlet height
h_0	the desired orbital altitude
H	the Hamiltonian defined in Eq. (4-3)
H_p	the partial derivatives of H with respect to the vector p (a vector)
H_u	the partial derivatives of H with respect to the vector u (a vector)
i	a subscript denoting the element of a vector
I_{JJ}	an influence function of cost (a scalar)
I_{spR}	rocket specific impulse
I_{spS}	scramjet specific impulse
I_{spT}	turbojet specific impulse
$I_{\psi J}$	an influence function of constraint and cost (a vector)
$I_{\psi\psi}$	an influence function of constraints (a matrix)
J	the mathematical cost imposed on the system
\bar{J}	a mathematical cost of J plus adjoined terms
J_S	a specified cost
k	the dimension of the vector ψ
K	a symbol for the matrix f_p
l	fuselage length

LIST OF SYMBOLS (CONT.)

L	(1) the total vehicle lift (2) the distributed mathematical cost term
L_p	the partial derivatives of the distributed cost with respect to the vector p (a vector)
L_u	the partial derivatives of the distributed cost with respect to the vector u (a vector)
L_w	the lift due to the first stage wing
L_x	the partial derivatives of the distributed cost with respect to the vector x (a vector)
L_1	(1) net first stage lift (2) penalty term on dynamic pressure
L_2	(1) net second stage lift (2) penalty term on specific force
m	the net vehicle mass
m_{d_s}	the second stage dry mass
m_{d_0}	the nominal shuttle dry mass
m_{f_a}	the first stage fuselage mass due to surface area
m_{f_s}	the second stage propellant tank fuel mass capacity
m_{f_t}	the first stage dry mass contribution of the fuel tanks
m_i	the i^{th} component of the three propellant mass states
m_S	the dry mass of the scramjet
m_T	the dry mass of the turbojet
m_w	the dry mass of the first stage wing
m_1	the turbojet fuel mass
m_2	the scramjet fuel mass
m_3	the rocket propellant mass

LIST OF SYMBOLS (CONT.)

M	a matrix term used in the variation equations defined in Eq. (4-56c)
M_e	the earth's mass
M_0	the free stream Mach number
M_1	the Mach number immediately following the nose shock (and also at the air-breathing engine inlets)
N	the aerodynamic force normal to the vehicle body x-axis
p	the parameter vector
\dot{p}_p	the partial derivatives of the parameter vector time derivatives with respect to the parameter vector (a matrix)
\dot{p}_x	the partial derivatives of the parameter vector time derivatives with respect to the state vector (a matrix)
p_1	the first stage nose angle
p_2	the first stage fuselage width
p_3	the scramjet inlet height
p_4	the turbojet inlet height
p_5	the first stage wing span
p_6	the first stage wing delta angle
p_7	the ratio of the turbojet tank volume to total first stage tank volume
p_8	the first stage fuselage length
p_9	the second stage maximum propellant tank mass capacity
p_{10}	the maximum rocket thrust
p	the aerodynamic force parallel to the body x-axis
p_1	the pressure after the first-stage nose shock (and at the air-breathing engine inlets)
q	dynamic pressure
q_d	the bound on the desired dynamic pressure range

LIST OF SYMBOLS (CONT.)

q_0	the free stream dynamic pressure
Q	a constant to establish the desired weight given to dynamic pressure bound violation penalties
r	the distance from the earth's center
r_{fS}	the stoichiometric scramjet fuel/air mass ratio
r_{fT}	the stoichiometric turbojet fuel/air mass ratio
r_S	the scramjet fuel tank mass/volume ratio
r_T	the turbojet fuel tank mass/volume ratio
R	the universal gas constant
R_e	the earth's radius
R_f	the turbojet fuel tank volume/total first stage fuel tank volume ratio
S	step size
S_T	advanced turbojet mass scaling factor
t_s	the vector of switch times
t_{s_i}	the i^{th} component of t_s
T	(1) the matrix transpose sign when used as a superscript (2) the total vehicle thrust
T_{\max_s}	the second-stage maximum thrust
T_R	the rocket thrust
T_S	the scramjet thrust
T_T	the turbojet thrust
T_0	the free stream temperature
T_1	the post first-stage nose shock temperature (also the temperature at the air-breathing engine inlets)

LIST OF SYMBOLS (CONT.)

u	the control vector
u_f	an unbounded fuel flow function
u_0	a unit step function
u_1	air velocity after first-stage nose shock compression (also the velocity at the air-breathing engine inlets)
U	a matrix to weight different elements of the control variation vector
V	a matrix to weight different elements of the parameter variation vector
V_f	the first stage fuselage volume
V_T	the second stage propellant tank volume
V_0	the shuttle nominal volume (a reference value)
w_f	the first stage fuselage width
w_s	the first stage wing span
x	the state vector
x_1	the distance from earth's center
x_2	the radial velocity
x_3	the orbital angle (in polar coordinates—two dimensional)
x_4	the angular velocity
x_5	the turbojet fuel mass
x_6	the scramjet fuel mass
x_7	the rocket fuel mass
z	an intermediate vector in the derivation of the variation equations
α	the angle of attack
α_n	the first-stage nose angle

LIST OF SYMBOLS (CONT.)

α_t	the first-stage tail angle
β_s	the first-stage nose shock angle
γ_0	the free stream specific heat ratio
δ	(1) a mathematical symbol for a variation (2) the vehicle body x-axis angle relative to the local horizontal
δ_a	the first stage wing delta angle
η	a Lagrange multiplier scalar
θ	the orbital angle (in polar coordinates—two dimensional)
θ_f	the first stage nose flow deflection angle
λ	the costate vector
Λ	a matrix influence function of the equality constraints
Λ_0	a coefficient of some terms in the Λ_1 boundary condition
Λ_1	a state equality constraint matrix influence function
Λ_2	a parameter equality constraint matrix influence function
ν	a Lagrange multiplier vector
ρ	air density
ρ_0	free stream air density
ρ_1	air density after the first-stage nose shock compression (also the density at the air-breathing engine inlets)
τ	the terminal time of the trajectory
ϕ	the terminal cost terms
ϕ_x	the partial derivatives of the terminal cost terms with respect to the states (a vector)
ϕ	proportion of stoichiometric fuel mixture used (where $\phi=1$ is assumed as an upper limit)

LIST OF SYMBOLS (CONT.)

Ψ	the equality constraint vector
Ψ_p	the partial derivatives of the Ψ vector with respect to parameters (a matrix)
Ψ_x	the partial derivatives of the Ψ vector with respect to states (a matrix)
ω_e	the earth's angular velocity in an inertial frame
ω_0	the desired orbital angular velocity
Ω	the state integration cutoff function
Ω_x	the derivative of Ω with respect to states (a vector)
∂	the partial derivative sign
\cdot	when over a symbol, a derivative with respect to time
$+$	as a superscript, indicates a small positive time displacement
$-$	as a superscript, indicates a small negative time displacement

CHAPTER I

INTRODUCTION

At a time when the first reusable space transportation system is in the final developmental stages, considerable attention is being given to new space applications. Investigations of required flight frequencies, orbital payload masses, and associated transportation costs have been performed^[1] with the presumption that any one of several proposed new uses of the space environment will occur, resulting in vastly expanded space operations.

With the probability that the next quarter century will lead to many imaginative and unanticipated uses of space, it seems likely that improvements in performance over what can be achieved with the space shuttle will be desirable, and probably necessary. Given the uncertainty of the economic evaluation methods (i.e., trying to establish dollar figures for development and flight costs years before actual flight), it seems reasonable to judge the design requirements of advanced space transportation concepts, where approval is still years in the future, on strict engineering performance requirements. In particular, the propellant mass consumption requirement for a variety of propulsion methods, along with the sensitivity of this quantity to the application of constraints on specific force and dynamic pressure, seems an unambiguous performance measure which will permit a lucid comparison of alternate space transportation concepts.

One class of launch vehicle that promises considerable improvement in the propellant mass performance measure when compared to space shuttle technology is the air-breathing launch system.

Since the end of World War II, much attention has been given to high performance air-breathing engines for both aircraft and launch vehicle propulsion. Most interest has been in the area of ramjet propulsion, due to its simplicity and high performance to beyond Mach 4.^[2] In the early 1960's interest developed in the possibility of ramjet designs using supersonic combustion (scramjets) due to the decreased

inlet losses expected, and improved specific impulse at high Mach number. The potential of operating to beyond Mach 10 was recognized.^[3]

As spaceflight became routine in the mid 1960's, and the potential for vastly increased flight activity was foreseen, consideration was given to the possible economic benefit of space operations similar to the routine commercial aircraft operations.^[4] The potential of an orbital craft that used an aircraft type launching platform was recognized.

At about the same time NASA was investigating design concepts for the space shuttle. To support the investigation, work was done at NASA's Langley Research Center on design concepts for a two stage vehicle with an air-breathing first stage, and a rocket-powered second stage that would achieve orbit. Two papers were submitted to the AIAA Advanced Space Transportation meeting in 1970 that gave considerable thought to the necessary technology, the general geometry, the development requirements, the operational considerations, and the expected performance of the air-breathing system as compared to more conventional launch concepts.^[5,6]

Due to concern about the technology development time, along with a general conservatism about proven vs. new systems, the air-breathing system was dropped as a contender for the space shuttle design. However, technology development has continued on a low key in the context of hypersonic transport research. The technology and potential for hypersonic transports were assessed at Lockheed in a 1970 report,^[7] and at NASA's Langley Research Center propulsion/airframe integration concepts have been assessed along with thermal and structural problems,^[8-11] and supersonic hydrogen fuel mixing and combustion.^[12]

Recently, the case has been argued for the development of a flight-test platform for experimental hypersonic propulsion, structural, and fuel systems.^[13] It seems likely that the technology base for construction of reusable air-breathing launch vehicles will soon exist.

As generally proposed, the air-breathing launch vehicle consists of a two-staged horizontal takeoff configuration with air-breathing capability on the first stage and with the second stage operating as a conventional rocket. The first stage would have turbojet engines for flight to about Mach 3. At some point above Mach 1, dual mode ramjet engines, with both subsonic and supersonic combustion capability are phased into use. At some point between Mach 4 and Mach 12, separation of the stages occurs, and the first stage returns in an aircraft type

operation, while the second stage attains orbital velocity on rocket power.

Almost without exception, the first stage is presumed to use liquid hydrogen fuel at the higher Mach numbers because of the capacity of the fuel as a heat sink in active structural cooling, along with its high energy/mass density. At low Mach numbers, however, consideration has been given to the alternative fuels due to the low volumetric energy capacity of hydrogen.

Given the potential of full system reusability, more routine aircraft type operation, safer abort capability, and improved performance values, it seems appropriate at this time to develop a design methodology for the optimization of two-staged air-breathing launch vehicles based on propellant mass performance criteria. (A two-staged concept is considered to prevent the fuel penalty of transporting the dry weight of heavy air-breathing propulsion systems to orbit, since they have little utility in flight near orbit.) Consideration will be given to trajectory shape, aerodynamic design, propulsion system performance, and propulsion system changeover points. Since the overall problem consists of a complicated nonlinear two point boundary value problem, it is essential that efficient methods be devised to find the optimal solutions, to help keep the cost of computation down. It is believed that any efficient solution techniques derived for this problem will represent a contribution to the solution of many similar problems.

Many aspects of flight vehicle optimization have been addressed in the last twenty-five years, though generally individually. The aerospace Research Laboratory supported the development of an optimization technique to evaluate the configuration of a two-dimensional hypersonic cruise vehicle, with the cruise condition specified, using the lift-to-drag ratio as the primary cost consideration.^[14] Optimal rocket trajectories, with aerodynamic effects included, have been evaluated for fixed rocket configurations.^[15] Minimum time to climb and maximum altitude paths have been evaluated for air-breathing crafts (fighters) with specified geometry and performance models.^[16] Recently, attempts have been made to treat trajectory and configuration simultaneously for a single stage to orbit launch vehicle^[17] although in this case the method involved iterative optimization of each part separately with intermediate efforts to match the results of the different computations. When the aggregate objectives of these studies are considered, the need for a unified mathematical treatment to simultaneously optimize flight vehicle configuration and trajectory is clear.

A solid data base exists for the general performance characteristics of hypersonic lifting vehicles and propulsion systems. General conceptualization studies have been done for the design of air-breathing launch vehicles. Also, operational requirements of reusable space transportation systems have been established. The need for post-shuttle launch vehicles with improved performance seems likely to develop. Therefore, it appears to be timely to develop an optimal design methodology for a reusable air-breathing launch platform.

In the following material a methodology to establish an optimal configuration and flight path of sophisticated systems with complicated dynamics is developed and subsequently applied to a class of air-breathing launch vehicles. Chapter II specifies a parametric vehicle model, suitable for the optimization methodology, used for demonstration of the technique. Chapter III defines the system dynamics model used. Chapter IV outlines the mathematical development of the optimization algorithm, while Chapter V relates the material in Chapters II and III to the equations in Chapter IV. Chapters VI and VII discuss and interpret the results, and note numerical difficulties to be avoided when implementing the methodology. Conclusions are drawn, future research extensions are suggested and a listing of a computer algorithm is given in Chapter VIII and the Appendix.

CHAPTER II

THE VEHICLE AND ENVIRONMENT MODEL

In the following material, a parametric model of the two-staged air-breathing launch vehicle is developed, and the vehicle thrust and aerodynamic properties are defined, in a form suitable for computer algorithm application.

2.1 An Overview

The class of vehicle to be considered is a two-staged configuration, the second of which is a conventional rocket propelled orbiter with reentry glider configuration resembling the space shuttle. The first stage is propelled by air-breathing propulsion systems. Turbojets operate at low Mach numbers. Convertible subsonic/supersonic combustion ramjets (scramjets) are available to operate at high Mach number. Overlapping operation of the two air-breathing propulsion systems is possible at intermediate Mach numbers. The vehicle is configured for horizontal takeoff. The payload to be delivered to low earth orbit is assumed comparable to the space shuttle.

The vehicle parametric model is a function of aerodynamic geometry, propulsion geometry, fuel capacity, and propellant properties.

A shuttle-derived liquid hydrogen/liquid oxygen system is assumed for the second stage. Due to the heat sink capacity of liquid hydrogen upon conversion to combustible fuel, and the anticipated high heat loading on hypersonic air frames and propulsion systems, liquid hydrogen is assumed as the propellant in the scramjet propulsion mode. For low Mach number, in the turbojet mode, a hydrocarbon fuel is assumed due to its high volumetric energy capacity, its simpler handling and storage requirements, and its ready use by existing and extrapolated turbojet technology.

The propulsion dynamics are modeled to allow for the three thrust magnitude discontinuities which are associated with changes in propulsive mode. The first discontinuity following takeoff represents transition from the turbojet-only mode to mixed turbojet/scramjet operation. The second discontinuity represents transition to the scramjet-only mode. The third discontinuity represents simultaneous staging and initiation of the second-stage rocket thrust.

The atmosphere is modeled as variable with altitude only, and is assumed to rotate with the earth's surface.

Gravity is assumed to depend on altitude only, with variations modeled on a homogeneous sphere representation of the earth.

2.2 The First-Stage Model

A principal objective in the development of a parametric model of the physical characteristics of the air-breathing stage has been to obtain a reasonable representation of vehicle performance while requiring a minimum quantity of independent parameters. The desire to hold down the number of parameters is associated with the strong influence of the dimension of the parameter vector on computation time.

The basic dynamic behavior of the vehicle can be determined by giving consideration to wing, fuselage, and propulsion system dimension, along with component mass models, propulsion system performance data, and aerodynamic characteristics as a function of exterior geometry. If component geometry and aerodynamic models are limited to two dimensions, a further savings in parameter vector dimension is possible with little loss in solution accuracy, since very little cross coupling between down track and cross track motion would normally be expected.

2.2.1 The Wing

A simple body-integrated delta wing is considered, and the resulting configuration is treated as the sole source of aerodynamic lift and drag. The data on the propulsion system, given later, specifies installed performance. Consequently, most of the expected drag not attributable to the wing is incorporated into the propulsion model. Data on body-integrated delta wing lift and drag coefficients is available as a function of Mach number, aspect ratio, and angle of attack, as long as the angle of attack does not stray too far from zero.

The interpolation variables are A, and M_0 , where

A = aspect ratio

M_0 = free stream Mach number

One has

$$A = \frac{w_s^2}{A_{wp}} \quad (2-1a)$$

$$C_L = \frac{L_w}{q_0 A_{wp}} \quad (2-1b)$$

$$C_D = \frac{D_w}{q_0 A_{wp}} \quad (2-1c)$$

where

w_s = wing span

A_{wp} = area of wing planform

q_0 = free stream dynamic pressure

L_w = lift due to wing

D_w = nonparasitic drag due to wing

The resultant lift and drag equations are

$$L_1 = \left[\left(\frac{dC_L}{d\alpha} \right) \alpha \right] q_0 A_{wp} \quad (2-2a)$$

$$D_1 = \left[\left(\frac{dC_D}{dC_L^2} \right) C_L^2 + C_{D0} \right] q_0 A_{wp} \quad (2-2b)$$

where

L_1 = net lift on first stage

D_1 = net drag on first stage

C_{D0} = parasitic drag term

The data in Table II-1^[18] is the basis of an aerodynamic data linear interpolation scheme used to calculate lift and drag coefficients.

The interpolation results are the quantities $dC_L/d\alpha$, and dC_D/dC_L^2 , where

C_L = lift coefficient

C_D = drag coefficient

α = angle of attack

Table II-1. Delta wing lift and drag coefficients.

$$\frac{dC_L}{d\alpha} \text{ data}$$

Aspect Ratio	Mach Number									
	0.25	0.6	0.7	0.9	1.1	1.2	1.5	2.0	4.0	8.0
0.5	0.0120	0.0130	0.0140	0.0145	0.0155	0.0150	0.0145	0.0140	0.0120	0.0075
1.0	0.0200	0.0230	0.0250	0.0280	0.0320	0.0300	0.0280	0.0240	0.0150	0.0075
2.0	0.0400	0.0440	0.0480	0.0530	0.0680	0.0620	0.0530	0.0380	0.0175	0.0075
3.0	0.0530	0.0590	0.0630	0.0720	0.0870	0.0740	0.0620	0.0420	0.0180	0.0075
4.0	0.0650	0.0700	0.0730	0.0810	0.0980	0.0800	0.0700	0.0440	0.0190	0.0075

$$\frac{dC_D}{dC_L^2} \text{ data}$$

Aspect Ratio	Mach Number									
	0.25	0.6	0.7	0.9	1.1	1.2	1.5	2.0	4.0	8.0
0.5	0.77	0.79	0.80	0.86	0.89	0.92	1.00	1.10	1.45	2.00
1.0	0.47	0.48	0.42	0.39	0.41	0.43	0.58	0.69	1.10	1.99
2.0	0.30	0.30	0.27	0.24	0.26	0.27	0.34	0.48	1.00	1.99
3.0	0.25	0.25	0.23	0.21	0.22	0.24	0.31	0.46	1.00	1.99
4.0	0.22	0.22	0.21	0.195	0.21	0.22	0.28	0.45	1.00	1.99

Data for evaluation of C_{D_0} are given in Table II-2^[19], and are based on shuttle zero angle of attack drag properties with a scaling factor used to approximate the effect of assumed improved aerodynamic properties of the air-breathing stage. (The shuttle parasitic drag is very high because of the silica thermal protection tile surface properties).

Table II-2. First stage parasitic drag coefficients. (Based on scaled shuttle data—scale factor = 1/3).

Mach Number	C_{D_0}	Mach Number	C_{D_0}
0.25	0.0203	1.30	0.0521
0.60	0.0208	1.50	0.0516
0.80	0.0228	2.00	0.0470
0.90	0.0268	3.00	0.0378
0.95	0.0351	4.00	0.0327
1.05	0.0492	5.00	0.0295
1.10	0.0507	8.00	0.0263
1.20	0.0518	10.00	0.0260

Similar to the parasitic drag scaling factor, a scaling factor is allowed for the net lift and drag computations to approximate aerodynamic refinement of wing design or more complex wing geometries (~0.7 for drag; ~1.7 for lift).

The result of the data format is a requirement for two wing-associated independent parameters, wing span and wing area. However, for a simple delta wing one has

$$A_{w_p} = \frac{w_s^2}{(4 \tan \delta_a)} \quad (2-3)$$

where

δ_a = delta wing angle, the forward wing edge angle with the fuselage

The quantity δ_a is used in place of the wing planform area as one of the two wing-associated parameters.

Without going into detailed analysis of thermal protection requirements, one can roughly judge wing mass from wing planform area. A useful approximation in terms of slugs mass vs. square feet of wing area is^[20]

$$m_w = 0.25 A_{wp} \quad (2-4)$$

where

$$m_w = \text{mass of wing}$$

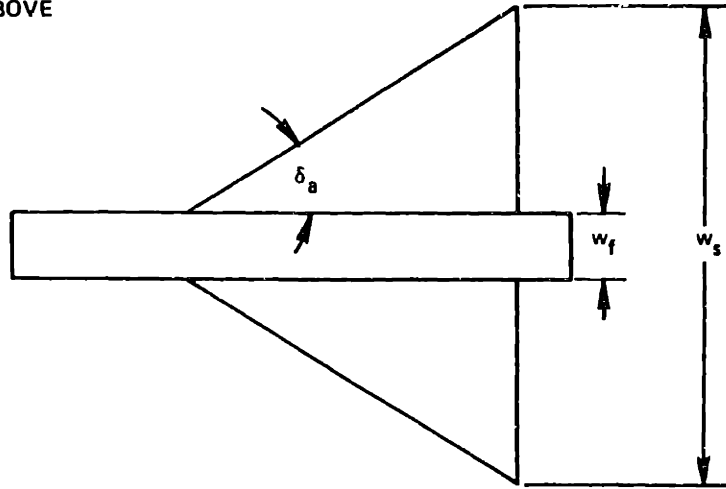
2.2.2 The Fuselage

For numerical simplicity it is desirable to keep the vehicle aerodynamics model two dimensional. This consideration mandates a fuselage design with constant geometry in a x-z body axis plane cross section as shown in the side view of Figure II-1. Therefore, a representation of the fuselage geometry simply requires a shape for the upper and lower surfaces. The complete characterization of the fuselage physical properties also requires internal propellant tank capacity, and dry mass properties.

For vehicles expected to use air-breathing propulsion at high Mach numbers, the body geometry must incorporate features beneficial to propulsion system performance. The forward surface should provide some compression prior to the propulsion system ingestion of air. The aft surface should serve as an expansion region extending beyond the propulsion system internal expansion nozzle. Good propulsion system behavior requires much attention to the geometry of the aft expansion surface to avoid undesirable effects such as separation. Consequently, to retain simplicity in the parametric model, the aft surface angle is assumed to be fixed, and is incorporated into the installed propulsion system performance data. The vehicle nose angle and the overall fuselage length are left as parameters to be evaluated. The general vehicle geometric configuration is shown in Figure II-1. Note that the propulsion system is assumed to be under the fuselage, permitting a flat upper surface.

The propellant tank capacity is constrained to match the propellant requirements. To allow the volume to meet the constraint, fuselage width is made a parameter.

FROM ABOVE



FROM SIDE

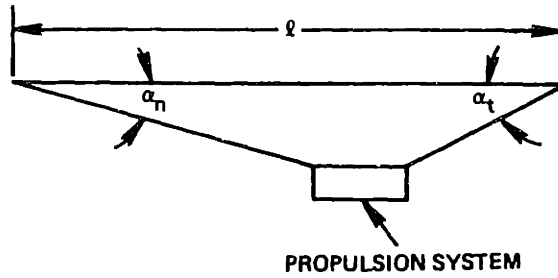


Figure II-1. First stage cross-section.

One has

$$V_f = \frac{w_f l^2 \sin(\alpha_n) \sin(\alpha_t)}{2 \sin(\alpha_n + \alpha_t)} \quad (2-5a)$$

$$A_{f_s} = w_f l \left(1 + \frac{\sin(\alpha_n) + \sin(\alpha_t)}{\sin(\alpha_n + \alpha_t)} \right) + \frac{2V_f}{w_f} \quad (2-5b)$$

where

V_f = fuselage volume

A_{f_s} = fuselage surface area

w_f = fuselage width
 l = fuselage length
 α_n = nose angle
 α_t = tail angle

The most important aerodynamic property of the fuselage not incorporated into propulsion performance models is the free stream compression by the vehicle nose. On the basis of the already assumed simple vehicle geometry, one can use oblique shock/normal shock/Prandtl-Meyer expansion fan theory for the supersonic compression calculations prior to the propulsion system ingestion of the flow. (Perfect gas behavior assumption is implied). Since the nose angle solution value is likely to be small, and since vehicle rotational dynamics will not be considered, eliminating the need for body pressure distributions, subsonic compression effects are neglected. Thus, one need only consider the nose effect when the free stream Mach number exceeds one. If the nose angle plus the angle of attack exceeds zero, a shock will result, otherwise an expansion will result. The shock can be oblique or normal depending on the turning angle of the free stream, and the Mach number. The following equations apply to normal shocks^[21]

$$M_1 = \left(\frac{1 + \frac{\gamma_0 - 1}{2} M_0^2}{\gamma_0 M_0^2 - \frac{\gamma_0 - 1}{2}} \right)^{1/2} \quad (2-6a)$$

$$T_1 = \left(1 + \frac{2(\gamma_0 - 1)}{(\gamma_0 + 1)^2} \frac{(\gamma_0 M_0^2 + 1)}{M_0^2} (M_0^2 - 1) \right) T_0 \quad (2-6b)$$

$$\rho_1 = \left(\frac{(\gamma_0 + 1) M_0^2}{(\gamma_0 - 1) M_0^2 + 2} \right) \rho_0 \quad (2-6c)$$

$$P_1 = \rho_1 R T_1 \quad (2-6d)$$

ere

- M_0 = free stream Mach number
 M_1 = post nose compression Mach number
 T_0 = free stream temperature
 T_1 = post nose compression temperature
 ρ_1 = post nose compression density
 P_1 = post nose compression pressure
 R = universal gas constant
 γ_0 = free stream specific heat ratio

The following equations apply to oblique shocks^[22]

$$M_1 = \left(\frac{1}{\sin^2 (\beta_s - \theta_f)} \frac{1 + \frac{\gamma_0 - 1}{2} M_0^2 \sin^2 \beta_s}{\gamma_0 M_0^2 \sin^2 \beta_s - \frac{\gamma_0 - 1}{2}} \right)^{1/2} \quad (2-7a)$$

$$T_1 = \left(1 + \frac{2(\gamma_0 - 1)}{(\gamma_0 + 1)^2} \frac{(\gamma_0 M_0^2 \sin^2 \beta_s + 1)}{M_0^2 \sin^2 \beta_s} (M_0^2 \sin^2 \beta_s - 1) \right) T_0 \quad (2-7b)$$

$$\rho_1 = \left(\frac{(\gamma_0 + 1) M_0^2 \sin^2 \beta_s}{(\gamma_0 - 1) M_0^2 \sin^2 \beta_s + 2} \right) \rho_0 \quad (2-7c)$$

$$P_1 = \rho_1 R T_1 \quad (2-7d)$$

$$\tan \theta_f = 2 \cot \beta_s \frac{M_0^2 \sin^2 \beta_s - 1}{M_0^2 (\gamma_0 + \cos 2\beta_s) + 2} \quad (2-7e)$$

ere

- θ_f = flow deflection angle
 β_s = shock angle

The following equations apply for expansion [23]

$$\theta_f = \sqrt{\frac{\gamma_0 + 1}{\gamma_0 - 1}} \left(\tan^{-1} \left(\frac{\gamma_0 - 1}{\gamma_0 + 1} (M_0^2 - 1) \right)^{1/2} - \tan^{-1} \left(\frac{\gamma_0 - 1}{\gamma_0 + 1} (M_1^2 - 1) \right)^{1/2} \right) - \left(\tan^{-1} (M_0^2 - 1)^{1/2} - \tan^{-1} (M_1^2 - 1)^{1/2} \right) \quad (2-8a)$$

$$T_1 = \left(\frac{1 + \frac{\gamma_0 - 1}{2} M_0^2}{1 + \frac{\gamma_0 - 1}{2} M_1^2} \right) T_0 \quad (2-8b)$$

$$\rho_1 = \rho_0 \left(\frac{T_1}{T_0} \right)^{\frac{1}{\gamma_0 - 1}} \quad (2-8c)$$

$$P_1 = \rho_1 R T_1 \quad (2-8d)$$

Also one needs a relation for the flow turning angle

$$\theta_f = \alpha_n + \alpha \quad (2-9)$$

If θ_f is negative one should use Eq. (2-8) with an iterative solution of Eq. (2-8a) required. If θ_f is not negative, either Eq. (2-7) or (2-6) should be used.

The distinction between use of Eq. (2-7) and (2-6) is dependent on whether a solution to Eq. (2-7) exists. If there is a solution then Eq. (2-7) is used. Otherwise Eq. (2-6) is used. (The principle that the weak shock solution applies when possible is used). To determine if a solution to Eq. (2-7) exists, it is necessary to investigate Eq. (2-7e) in detail. Differentiation, and evaluation where the derivative $d\theta_f/d\beta_s$ vanishes yields a value of β_s for the maximum θ_f that permits a real solution

$$\sin(\beta_{s_{\max}}) = \left[\left(\{(\gamma_0 + 1)M_0^2\} - 4 + \left((\gamma_0 + 1) \{(\gamma_0 + 1)M_0^4\} + \{8(\gamma_0 - 1)M_0^2\} + 16 \right)^{1/2} \right) / (4\gamma_0 M_0^2) \right]^{1/2} \quad (2-10)$$

Substitution of Eq. (2-10) into Eq. (2-7e) yields a maximum value for θ_f for which Eq. (2-7) can be applied.

The fuselage mass can be modeled to be a function of surface area, propellant tank volume, and fuel type within a given tank.

Using the same approximation as is used in Eq. (2-4) one gets

$$m_{f_a} = 0.25 A_{f_s} \quad (2-11)$$

where

m_{f_a} = mass of the fuselage due to area

The mass contribution of the propellant tanks must be based on the volume available to each tank. Something less than the entire fuselage volume is available for fuel storage due to the space requirement of various nonpropellant systems. A simple approximation is to presume that 80% of the total fuselage volume is available for fluid storage. Of the volume available, allocation of space must be made for both the turbojet and scramjet fuels, each having tanks with different mass properties due to the different fuel handling requirements. A parameter is created to specify the relative space allocation.

One gets

$$m_{f_t} = 0.8(r_T R_f + r_S(1 - R_f))V_f \quad (2-12)$$

where

m_{f_t} = mass of fuselage due to propellant tanks

R_f = turbojet fuel tank volume/total fuel volume ratio

r_T = turbojet tank mass/volume ratio

r_S = scramjet tank mass/volume ratio

r_T and r_S are constants requiring specification. Since the scramjet fuel is cryogenic, with the associated added storage burdens (e.g., insulation), one expects r_S to be larger than r_T . Analysis of material and storage requirements suggest

$$0.01 < r_T < 0.02 \quad \text{in slugs/ft}^3 \quad (2-13a)$$

$$0.03 < r_S < 0.04 \quad (2-13b)$$

2.2.3 The Propulsion Systems

The information necessary to characterize the propulsion system includes the external geometry, the mass, and the operational performance.

The geometry information can be limited to inlet area in the simplest case. On the basis of the two-dimensional aerodynamic approximations already made, the required information can be stated by providing inlet width and height for each propulsion system. Since the entire fuselage width is expected to provide precompression of the free stream, a further simplification is to assume the propulsion system width is equal to that of the fuselage, and all the compressed flow enters the system. One therefore requires two geometric parameters to define the air breathing propulsion system: the turbojet inlet height, and the scramjet inlet height. One gets

$$A_T = h_T w_f \quad (2-14a)$$

$$A_S = h_S w_f \quad (2-14b)$$

where

A_T = turbojet inlet area

A_S = scramjet inlet area

h_T = turbojet inlet height

h_S = scramjet inlet height

Models of propulsion system mass are somewhat speculative due to the experimental nature of scramjets and advanced lightweight turbojets. However, some data has been generated, and can be suitably simplified for use in the present problem.

In the case of the turbojet, one can extrapolate advanced lightweight designs from tabulated data of existing turbojet designs and historical weight reduction trends, [24] to derive an approximate system mass per unit of inlet area. The result yields

$$m_T = (7.5)S_T A_T \quad \text{with: } m_T \text{ in slugs} \quad (2-15)$$

$$A_T \text{ in ft}^2$$

where

m_T = mass of turbojet in slugs

S_T = advanced turbojet scale factor $\approx 2/3$

The scramjet mass model must be extrapolated from data on experimental configurations. Information on modularized designs has been produced^[25] and can be converted into a function of inlet area. The models lead to rather heavy systems designed to tolerate heat flux loads expected until well above Mach 6. The result is

$$m_S = ((15.2 h_S) - (4.6/h_S))w_f \quad (2-16)$$

where

m_S = scramjet mass in slugs if h_S , w_f are in feet

As h_S drops below about 1.25 ft, then the accuracy of Eq. (2-16) is rapidly reduced due to the growing relative contribution of propulsion system support equipment. A lower bound on mass per width can be used to resolve the problem. Analysis of the support system mass requirements suggests the bound^[26]

$$m_S \geq (15.0)w_f \quad (m_S \text{ in slugs}) \quad (2-17)$$

The performance data for propulsion systems intended for a body-integrated design application is usually presented in the form of installed specific impulse^[27] with the implicit assumption of nearly stoichiometric fuel/air mixture ratios. The data includes losses due to engine cowl effects and nozzle expansion. The data can be made to be a function of the aft fuselage angle, but a desirable angle is usually given as

$$\alpha_t = 12^\circ \quad (2-18)$$

On the basis of approximate curve fits for the Mach number dependence of the specific impulse data one gets

$$I_{SP_T} = 3800 - (300 M_1) - (100 M_1^2) \quad (2-19a)$$

$$I_{SP_S} = 15000 (M_1^{1.6}) e^{-1.73 (M_1^{0.52})} \quad (2-19b)$$

where

I_{SP_T} = turbojet installed specific impulse

I_{SP_S} = scramjet installed specific impulse

Accurate computation of system thrust generally requires knowledge of the variation of specific impulse with fuel/air mix. In most cases, however, the specific impulse has little change near the stoichiometric mixture ratio. As an approximation, the impulse is not made a function of the fuel/air mix. This gives

$$T_T = \rho_1 u_1 A_T I_{SP_T} g_0 r_{f_T} \phi \quad (2-20a)$$

$$T_S = \rho_1 u_1 A_S I_{SP_S} g_0 r_{f_S} \phi m_{CR} \quad (2-20b)$$

where

T_T = turbojet thrust

T_S = scramjet thrust

ρ_1 = air density after nose compression

u_1 = air velocity after nose compression

g_0 = gravity at earth's surface

r_{f_T} = stoichiometric turbojet fuel/air mass ratio
(≈ 0.0633 for octane)

r_{f_S} = stoichiometric scramjet fuel/air mass ratio
(≈ 0.027778)

ϕ = proportion of stoichiometric fuel mixture used
(where $\phi = 1$ is assumed as an upper limit)

m_{CR} = scramjet mass capture ratio
(proportion of inlet flow used in engine)

The quantity ϕ is used in both parts of Eq. (2-20) since it is assumed that if the scramjet and turbojet operate together, then they are equally throttled. The mass capture ratio for the scramjet is required to model the spillage effects at low supersonic Mach numbers typical of these engines. (Data is available on the Langley three dimensional propulsion system design and is given in Table II-3). [28]

2.2.4 A Summary of First Stage Parameters

If the independent geometric parameters are assumed to be elements of a vector p , one can define the following:

Table II-3. Scramjet mass capture ratio.

Mach Number	Mass Capture Ratio
2.5	0.35
3.5	0.60
5.0	0.80
5.5	0.85
8.0	0.95

p_1 = nose angle (α_n)

p_5 = wing span (w_s)

p_2 = fuselage width (w_f)

p_6 = delta wing angle (δ_a)

p_3 = scramjet height (h_s)

p_7 = turbojet tank volume/first-stage tank volume ratio (R_f)

p_4 = turbojet height (h_T)

p_8 = fuselage length (l)

2.3 The Second-Stage Model

The assumption is made that the second stage is a scaled version of the space shuttle, somewhat refined to improve aerodynamics. The thrust is assumed to be selectable. The fuel is assumed to be internally carried. Nominal space shuttle physical properties are given in Table II-4.

Table II-4. Space shuttle physical properties.

Mass (with 65,000 lbm payload)	=	7,000 slugs
Planform area	=	4,000 ft ²
Thrust (in vacuum)	=	1,500,000 lbf
Engine mass	=	600 slugs
Vehicle volume	=	59,000 ft ³

2.3.1 The Physical Characteristics

To compute the planform area of the second stage one uses elementary scaling theory. Since area is a function of linear dimension squared, and the volume is a function of linear dimension cubed one expects a 2/3 power growth factor of planform area vs. volume. One gets

$$A_p = A_{p_0} \left(1 + \left(\frac{V_T}{V_0} \right) \right)^{2/3} \quad (2-21)$$

where

A_p = second stage planform area

A_{p_0} = shuttle planform area

V_T = volume required for propellant tank

V_0 = shuttle nominal volume

The space shuttle uses an H₂/O₂ fuel flow ratio 1.6 times stoichiometric. This is because the increase in hydrogen flow beyond a stoichiometric ratio can reduce the average molecular weight of exhaust products more rapidly than the preexpansion temperature. The result is a higher exhaust velocity and thus a higher specific impulse. It seems appropriate to assume the same fuel mixture for the second stage being considered. Also, an 80% use of available volume for propellant storage seems likely after structure and insulation have been accommodated. One gets

$$A_p = A_{p_0} \left(1 + \left(0.0000334 m_{fs} \right) \right)^{2/3} \text{ in ft}^2$$

where

m_{fs} = mass capacity in slugs of fuel tanks for the second stage

Mass property calculations require fuel tank mass contributions and rocket propulsion system mass contributions. On the basis of modest improvements in space shuttle external tank and main engine construction technologies one gets^[29]

$$m_{d_s} = m_{d_0} + (0.04 m_{f_s}) + T_{\max_s} / 3220. \quad (2-22)$$

where

m_{d_s} = second-stage dry mass

m_{d_0} = nominal shuttle dry mass

T_{\max_s} = second-stage maximum thrust

(Equation (2-22) is derived from scaling shuttle data with a 15% mass reduction assumed possible compared to shuttle orbiter vehicle 102.

The aerodynamic properties of the second stage are assumed to have characteristics identical to the shuttle, though scaled to a degree assumed possible by significant utilization of new aerodynamic technology (~0.7 for drag; ~1.7 for lift.) The baseline shuttle data is in Table II-5.^[30]

Using the data in Table II-5 one has

$$L_2 = C_L A_P q_0 \quad (2-23a)$$

$$D_2 = C_D A_P q_0 \quad (2-23b)$$

where

L_2 = lift due to second stage

D_2 = drag due to second stage

The thrust level of the rocket propulsion has a maximum value, but may be varied to any nonnegative value less than the maximum. The equation is

$$T_R = T_{\max_s} \phi \quad (2-24)$$

Table II-5. Space shuttle aerodynamic data.

Angle of Attack †	C_L															
	Mach Number															
	0.25	0.60	0.80	0.90	0.95	1.05	1.1	1.2	1.3	1.5	2.0	3.0	4.0	5.0	8.0	10.0
-10°	-0.4974	-0.5239	-0.5734	-0.6084	-0.6373	-0.6388	-0.6283	-0.6034	-0.5590	-0.4784	-0.3735	-0.3011	-0.2390	-0.2073	-0.1860	-0.1800
0	-0.0393	-0.0469	-0.0501	-0.0500	-0.0501	-0.0298	-0.0257	-0.0197	-0.0118	-0.0168	-0.0348	-0.0402	-0.0595	-0.0578	-0.0529	-0.0520
10°	0.4281	0.4383	0.4419	0.4521	0.5123	0.5458	0.5417	0.5236	0.4993	0.4336	0.3281	0.2114	0.1674	0.1399	0.1069	0.1010
20°	1.0001	0.9432	0.8966	0.8770	0.9360	1.0163	0.9958	0.9585	0.9269	0.8433	0.6792	0.5118	0.4505	0.4180	0.3733	0.3621
25°	1.1420	1.0618	0.9138	0.9109	0.9560	1.1198	1.1137	1.0934	1.0748	0.9967	0.8401	0.6580	0.6007	0.5621	0.5174	0.5093

Angle of Attack †	C_D															
	Mach Number															
	0.25	0.60	0.80	0.90	0.95	1.05	1.1	1.2	1.3	1.5	2.0	3.0	4.0	5.0	8.0	10.0
-10°	0.1047	0.1194	0.1533	0.1877	0.2220	0.2674	0.2703	0.2683	0.2621	0.2477	0.2177	0.1839	0.1628	0.1519	0.1414	0.1400
0	0.0610	0.0625	0.0683	0.0805	0.1052	0.1477	0.1522	0.1557	0.1563	0.1547	0.1410	0.1135	0.0982	0.0884	0.0788	0.0784
10°	0.0891	0.0969	0.1271	0.1538	0.1884	0.2421	0.2448	0.2426	0.2364	0.2149	0.1817	0.1347	0.1125	0.0990	0.0849	0.0827
20°	0.2823	0.3578	0.3870	0.4093	0.4518	0.5227	0.5200	0.5051	0.4867	0.4381	0.3576	0.2751	0.2423	0.2259	0.2023	0.1981
25°	0.4753	0.5074	0.4965	0.5274	0.5706	0.6812	0.6630	0.6673	0.6501	0.5928	0.4976	0.3917	0.3587	0.3373	0.3102	0.3063

where

T_R rocket thrust

It is assumed that rocket specific impulse is constant at 450 seconds for mass flow calculations.

2.3.2 A Summary of Second Stage Parameters

Using the notation adopted for the first-stage independent geometric parameters, one gets the following for the second stage

P_9 = maximum fuel capacity (m_{f_s})

P_{10} = maximum rocket thrust (T_{max_s})

2.3.3 The Environment Model

The physical properties influencing vehicle behavior, but independent of vehicle design constitute the environment. In the problem under consideration, the atmosphere and gravity fit this category. Both are assumed functions only of radial distance from the earth's surface.

Table II-6 lists the data modeling the atmosphere, and used as the basis for computing free stream properties.^[31] For Mach number and dynamic pressure calculations, the assumption is made that the air mass rotates with the earth's surface uniformly. Between data points, the density is assumed to exponentially decrease with altitude increase as the basis of interpolation. Temperature is linearly interpolated.

Gravitation is modeled as though the earth were a perfect, homogeneous sphere. That is

$$g = \frac{GM_e}{r^2} \quad (2-25)$$

where

G = universal gravitation constant

M_e = mass of the earth

r = distance from earth center

g = gravitation acceleration

Table II-6. Atmospheric properties.

Altitude (km)	$\frac{\rho}{\rho_0}$	Temp (°C)	Altitude (km)	$\frac{\rho}{\rho_0}$	Temp (°C)	Altitude (km)	$\frac{\rho}{\rho_0}$	Temp (°C)
0	1.00000	288.150	68	9.3051×10^{-5}	227.529	136	3.714×10^{-9}	642.32
4	0.66885	262.166	72	5.4361×10^{-5}	211.876	140	2.770×10^{-9}	714.22
8	0.42921	236.215	76	3.050×10^{-5}	196.24	144	2.129×10^{-9}	785.87
12	0.25464	216.650	80	1.632×10^{-5}	180.65	148	1.676×10^{-9}	857.24
16	0.13589	216.650	84	7.807×10^{-6}	180.65	152	1.359×10^{-9}	918.94
20	0.072579	216.650	88	3.738×10^{-6}	180.65	156	1.128×10^{-9}	970.88
24	0.038317	220.560	92	1.584×10^{-6}	182.62	160	9.459×10^{-10}	1022.23
28	0.020470	224.527	96	8.229×10^{-7}	198.45	164	8.139×10^{-10}	1054.67
32	0.011065	228.490	100	4.060×10^{-7}	210.02	168	7.040×10^{-10}	1087.01
36	0.0059248	239.282	104	2.034×10^{-7}	229.18	172	6.149×10^{-10}	1115.73
40	0.0032618	250.350	108	1.080×10^{-7}	247.85	176	5.415×10^{-10}	1136.02
44	0.0018440	261.403	112	5.839×10^{-8}	275.85	180	4.782×10^{-10}	1156.12
48	0.0010749	270.650	116	3.294×10^{-8}	313.01	184	4.236×10^{-10}	1176.03
52	6.5389×10^{-4}	270.650	120	1.988×10^{-8}	349.49	188	3.762×10^{-10}	1195.73
56	4.0622×10^{-4}	263.628	124	1.171×10^{-8}	423.90	192	3.359×10^{-10}	1211.66
60	2.4973×10^{-4}	255.772	128	7.533×10^{-9}	497.36	196	3.014×10^{-10}	1223.88
64	1.5377×10^{-4}	243.202	132	5.165×10^{-9}	570.09	200	2.708×10^{-10}	1235.95

CHAPTER III

SYSTEM DYNAMICS

To complete the dynamics model needed for computer analysis of the air-breathing vehicle, the orbital mechanics model is needed.

The time dependent behavior of the air-breathing launch vehicle can be represented by a set of differential equations. The equations provide the necessary information to evaluate system position, velocity, and mass state provided an appropriate reference frame and a set of initial conditions are defined.

The real problem of the general launch vehicle trajectory analysis requires three components each of position, velocity, and force. However, for the sake of keeping computation requirements to a minimum (due to the strong association of computation time and component dimension), a two dimensional orbital dynamics model is used. Specifically, only an equatorial launch to achieve an equatorial orbit is considered.

If an earth-centered set of polar coordinates is used, Newton's laws of motion yield

$$F_r = m \left(\frac{d^2 r}{dt^2} - r \left(\frac{d\theta}{dt} \right)^2 \right) \quad (3-1a)$$

$$F_\theta = m \left(r \frac{d^2 \theta}{dt^2} + 2 \frac{dr}{dt} \frac{d\theta}{dt} \right) \quad (3-1b)$$

where

m = vehicle mass

F_r = force in radial direction

F_θ = force in tangential direction

Also, r and θ are polar coordinates whose sign convention is shown in Figure 3-1.

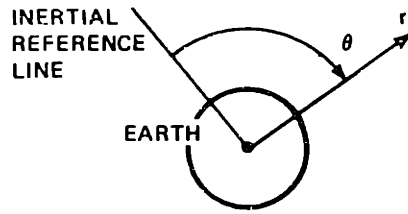


Figure III-1.

Equation (3-1), along with mass flow relations, can be resolved into a set of first-order differential equations in time, constituting a state space representation of the system convenient for future use.

Solving Eq. (3-1) for the second derivatives of r , θ one gets

$$\frac{d^2 r}{dt^2} = \frac{F_r}{m} + r \left(\frac{d\theta}{dt} \right)^2 \quad (3-2a)$$

$$\frac{d^2 \theta}{dt^2} = \frac{F_\theta}{mr} - \frac{2}{r} \frac{dr}{dt} \frac{d\theta}{dt} \quad (3-2b)$$

The system mass flow can be separated into three components, one for each propulsive mode. That gives

$$\dot{m} = \sum_i \dot{m}_i \quad (3-3)$$

where

\dot{m}_i = mass flow of i^{th} propulsive mode

$i = 1$ implies the turbojet

$i = 2$ implies the scramjet

$i = 3$ implies the rocket

One also has

$$\frac{d\left(\frac{dr}{dt}\right)}{dt} = \frac{d^2 r}{dt^2} \quad (3-4a)$$

$$\frac{d\left(\frac{d\theta}{dt}\right)}{dt} = \frac{d^2\theta}{dt^2} \quad (3-4b)$$

Suppose a vector x is defined as the state where

$$x = \begin{pmatrix} r \\ \dot{r} \\ \theta \\ \dot{\theta} \\ m_1 \\ m_2 \\ m_3 \end{pmatrix} \quad (3-5)$$

Where the dot indicates differentiation with respect to time.

One has

$$\dot{x} = \begin{pmatrix} \dot{r} \\ \ddot{r} \\ \dot{\theta} \\ \ddot{\theta} \\ \dot{m}_1 \\ \dot{m}_2 \\ \dot{m}_3 \end{pmatrix} \quad (3-6)$$

Substitution of Eq. (3-2) into Eq. (3-6) yields

$$\dot{x} = \begin{pmatrix} \dot{r} \\ r\dot{\theta}^2 + \frac{F_r}{m} \\ \dot{\theta} \\ -\frac{2r\dot{\theta}}{r} + \frac{F_\theta}{mr} \\ \dot{m}_1 \\ \dot{m}_2 \\ \dot{m}_3 \end{pmatrix} \quad (3-7)$$

Equation (3-7) is the state space dynamics equation sought. The models given in Chapter II must be used to solve for F_r , F_θ , and \dot{m}_i as a function of states, parameters, and controls.

CHAPTER 4

A SUITABLE OPTIMIZATION ALGORITHM

Suppose one has a set of m ordinary differential equations, each of order n , defining the dynamic state of a physical system as a function of time. The equations can be reduced to a system of $m \times n$ first-order differential equations. Such a mathematical system can be put in state space notation by solving each resultant equation algebraically for the first derivative it contains.

Suppose the mathematical representation just described already exists, with the vector x representing the physical system states.

Define

$$\dot{x} = \frac{dx}{dt} = f(x, u, p, t_s) \quad (4-1)$$

where

- x = a state vector of dimension a
- u = a control vector of dimension b
- p = a parameter vector of dimension c
- t_s = a switch time vector of dimension d
(points of discontinuities in some component of the forces contained in the dynamics)

The function f therefore represents the system dynamical behavior in a form suitable for further manipulation.

In any problem where the objective is to find an extremal value of a performance measure, it is possible to define the performance measure in terms of a function that places a mathematical cost on the system behavior. When the extremal value of the mathematical cost function is found, the extremal performance is achieved. The mathematical function can, in one form, be represented by two terms. One is a terminal time cost term, the other is a distributed cost term.

Define

$$J(\tau) = \phi(x(\tau)) + \int_{\tau}^0 L(x(t), u(t), p'(t)) dt \quad (4-2)$$

where

$J(\tau)$ = the mathematical cost imposed on the system at time τ

$\phi(x(\tau))$ = a terminal cost term evaluated at τ , dependent only on state

$L(x(t), u(t), p(t))$ = the distribution function for the distributed cost term, dependent on the states, controls, and parameters

τ = the terminal time. Since τ will have a negative value later, it is given as the integral lower bound.

By the above formulation, ϕ and L have no explicit time dependence.

From the present formulation, one can create a Hamiltonian function appropriate to finding an extremal, of the the cost.

Define

$$H = L + \lambda^T f \quad (4-3)$$

where

H = a Hamiltonian function based on the cost

λ = a vector known as the costate variable whose differential equation will be defined later.

The intent is to find a minimum value of J . It seems likely that J will be a smooth function of the control variables and design parameters, justifying a search for optimal solutions at stationery points only. Thus, a desired set of states, controls, parameters, and switch times are found when $dJ = 0$.

To start, differentiate Eq. (4-2). One gets

$$dJ = \phi_x dx(\tau + d\tau) + \int_{\tau}^0 (L_x \delta x + L_u \delta u + L_p \delta p) dt - L \Big|_{\tau} d\tau \quad (4-4)$$

where

$$\phi_x = \frac{\partial \phi}{\partial x}, \text{ a row vector of dimension } a$$

$$L_x = \frac{\partial L}{\partial x}, \text{ a row vector of dimension } a$$

$$L_u = \frac{\partial L}{\partial u}, \text{ a row vector of dimension } b$$

$$L_p = \frac{\partial L}{\partial p}, \text{ a row vector of dimension } c$$

δx = a variation of x , a vector of dimension a

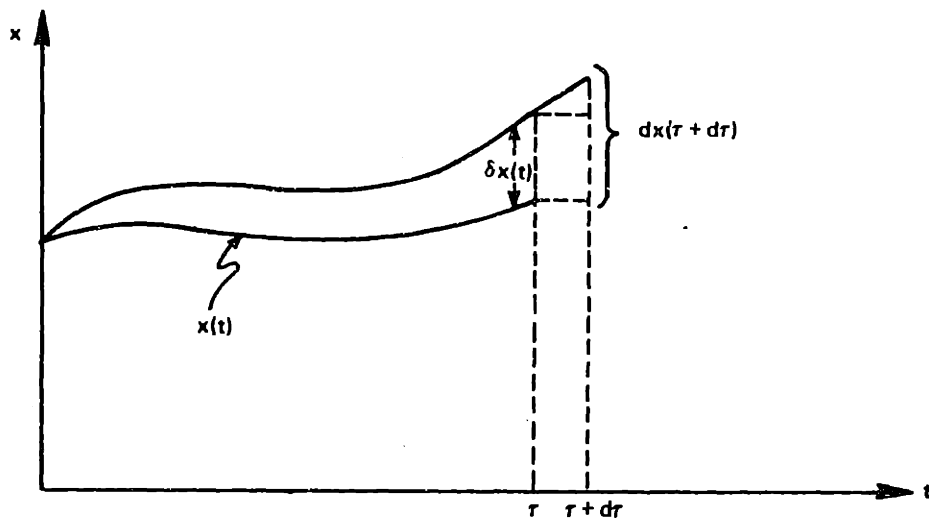
δu = a variation of u , a vector of dimension b

δp = a variation of p , a vector of dimension c

One can geometrically demonstrate that to first order

$$dx(\tau + d\tau) = \delta x(\tau) + f(\tau)d\tau \quad (4-5)$$

(See Figure IV-1 for a scalar function representation.)



$$dx(\tau + d\tau) = \delta x(\tau) + \frac{dx}{dt}(\tau) d\tau + \text{TERMS HIGHER THAN FIRST ORDER}$$

$$dx(\tau + d\tau) = \delta x(\tau) + f(\tau) d\tau \text{ TO FIRST ORDER}$$

Figure IV-1.

The first order approximation for dx is used since the algorithm to be developed will itself be first order. Specifically, gradient information will be used. If all information used is valid to first order then no information necessary to the algorithm is lost.

Equations (4-4) and (4-5) are combined to yield

$$dJ = \phi_x \delta x + (\phi_x f - L) \Big|_{\tau} d\tau + \int_{\tau}^0 (L_x \delta x + L_u \delta u + L_p \delta p) dt \quad (4-6)$$

It is necessary to find a relation between δx and $d\tau$ to eliminate the $d\tau$ term in Eq. (4-6).

The solution of the optimization problem requires integration of the states x starting at time = 0 until time = τ . The termination of the state integration will have to be determined by some cutoff function at $t = \tau$ since τ is a free quantity not known a priori. Suppose $\Omega(x(\tau))$ is such a cutoff condition.

Let

$$\Omega(x(\tau)) = 0 \quad (4-7)$$

One gets

$$\Omega(x(\tau) + dx(\tau + d\tau)) = 0 \quad (4-8)$$

Using an expansion series one gets

$$\Omega(x(\tau) + dx(\tau + d\tau)) = \Omega(x(\tau)) + \Omega_x dx(\tau + d\tau) \quad (4-9)$$

to first order

Use of Eqs. (4-7) and (4-8) in Eq. (4-9) yields

$$\Omega_x dx(\tau + d\tau) = 0 \quad (4-10)$$

Use of Eq. (4-5) in Eq. (4-10) yields

$$\Omega_x (\delta x(\tau) + f(\tau)d\tau) = 0 \quad (4-11)$$

Equation (4-11) can be algebraically solved for $d\tau$ to get

$$d\tau = - \frac{\Omega_x \delta x(\tau)}{\Omega_x^f} \quad (4-12)$$

Substitution of Eq. (4-12) into Eq. (4-6) yields

$$dJ = \left(\phi_x - \frac{(\phi_x^f - L)}{\Omega_x^f} \Omega_x \right) \Big|_{\tau} \delta x(\tau) + \int_{\tau}^0 (L_x \delta x + L_u \delta u + L_p \delta p) dt \quad (4-13)$$

Two point boundary value problems are usually formulated by defining an adjoint function or sensitivity function which obeys a differential equation of adjoint form. Applying this approach in this case, one defines

$$\dot{\lambda} = \frac{d\lambda}{dt} = -F^T \lambda - L_x^T \quad (4-14)$$

where

$$F = \frac{\partial f}{\partial x} \text{ a matrix of dimension } a \times a \quad (4-15)$$

One has

$$\frac{d}{dt} (\lambda^T \delta x) = \dot{\lambda}^T \delta x + \lambda^T \delta \dot{x} \quad (4-16)$$

Use of Eq. (4-16) requires that a representation of $\delta \dot{x}$ be developed, but \dot{x} can change discontinuously due to the switch points at t_s . This can be treated by considering the influence on \dot{x} of each of the switch points separately.

Define

$$\delta x = \delta x_0 + \sum_i \delta x_i$$

yielding

$$\delta \dot{x} = \delta \dot{x}_0 + \sum_i \delta \dot{x}_i \quad (4-17)$$

where

x_0 = state value without switch point contributions

x_i = state contribution due to switch point i

One has

$$\delta \dot{x}_0 = \frac{\partial \dot{x}_0}{\partial x} \delta x_0 + \frac{\partial \dot{x}_0}{\partial u} \delta u + \frac{\partial \dot{x}_0}{\partial p} \delta p \quad (4-18a)$$

$$\delta \dot{x}_i = \frac{\partial \dot{x}_i}{\partial x} \delta x_i + \frac{\partial \dot{x}_i}{\partial u} \delta u + \frac{\partial \dot{x}_i}{\partial p} \delta p \quad (4-18b)$$

One notices, however, that x_i was chosen to represent the effect on x of the switch point i . The switch point does not influence the behavior of x in response to u or p . One, therefore, has in Eq. (4-18b)

$$\delta u = \delta p = 0 \quad (4-19)$$

It is convenient to define two new variables

$$G = \frac{\partial \dot{x}}{\partial u} \quad (4-20a)$$

$$K = \frac{\partial \dot{x}}{\partial p} \quad (4-20b)$$

Substitution of Eqs. (4-20), (4-19), and (4-15) into Eq. (4-18) yields

$$\delta \dot{x}_0 = F \delta x_0 + G \delta u + K \delta p \quad (4-21a)$$

$$\delta \dot{x}_i = F \delta x_i \quad (4-21b)$$

Substitution of Eqs. (4-21) and (4-14) into Eq. (4-16) yields

$$\frac{d}{dt} (\lambda^T \delta x) = (-\lambda^T F - L_x) \delta x + \lambda^T \left(F \delta x_0 + \sum_i F \delta x_i + G \delta u + K \delta p \right) \quad (4-22)$$

Simplification of Eq. (4-22) and use of Eq. (4-17) gives

$$\frac{d}{dt}(\lambda^T \delta x) = -L_x \delta x + \lambda^T (G \delta u + K \delta p) \quad (4-23)$$

One has

$$\delta x(0) = 0 \quad (4-24)$$

since the desired state at $t = 0$ is specified explicitly.

Combination of Eqs. (4-24) and (4-17) yields

$$\delta x_0(0) = \delta x_i(0) = 0 \quad (4-25)$$

Integration of Eq. (4-23) from $t = \tau$ to $t = 0$ can now be done, using Eq. (4-25) and the fact that $\delta x_i = 0$ for $\tau \leq t < t_{s_i}$, or in other words the switch points contribute nothing until they occur, permitting integration of their contribution from the times of the switch points to the end only. (Note: the inequality is based on $\tau < 0$.)

One gets

$$-\lambda^T(\tau) \delta x_0(\tau) - \sum_i \lambda^T(t_{s_i}) \delta x_i(t_{s_i}) = \int_{\tau}^0 (-L_x \delta x + \lambda^T (G \delta u + K \delta p)) dt \quad (4-26)$$

By geometric arguments one can show

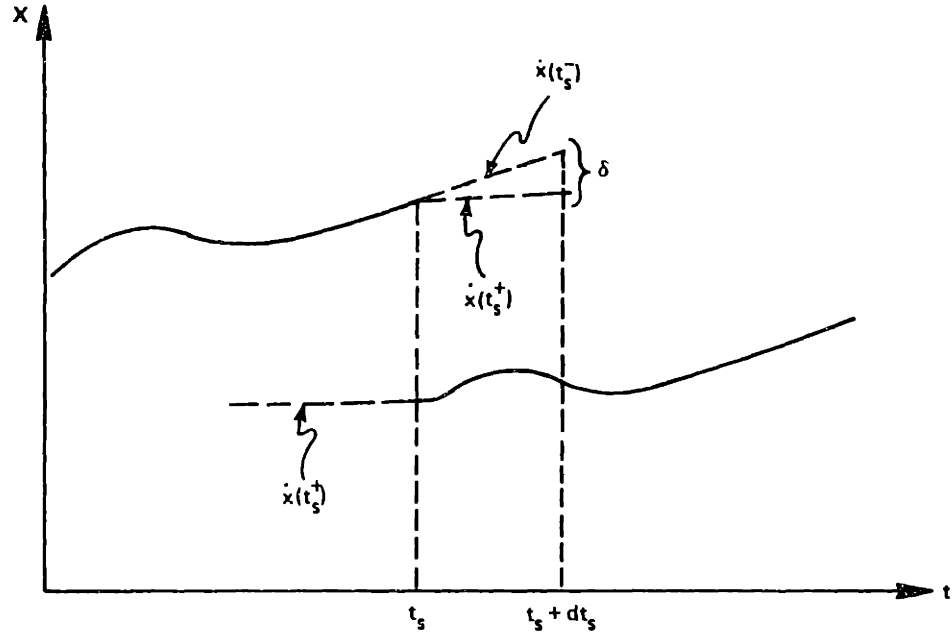
$$\delta x_i(t_{s_i}) = -\left(f_{s_i}^+ - f_{s_i}^-\right) dt_{s_i} \quad (4-27)$$

where

$$f_s^+ = \dot{x}(t_s^+) \quad (4-28a)$$

$$f_s^- = \dot{x}(t_s^-) \quad (4-28b)$$

(See Figure IV-2 for a scalar function representation.)



$$\begin{aligned}
 \delta &= (\dot{x}(t_s^-) - \dot{x}(t_s^+))dt_s \\
 &= (f_s^- - f_s^+)dt_s \\
 \therefore \delta x_i &= -(f_{s_i}^+ - f_{s_i}^-)dt_{s_i}
 \end{aligned}$$

Figure IV-2.

Use of Eq. (4-28) in Eq. (4-26) yields

$$\begin{aligned}
 -\lambda^T(\tau)\delta x_0(\tau) &= \int_{\tau}^0 (-L_x \delta x + \lambda^T G \delta u + \lambda^T K \delta p) dt \\
 &\quad - \sum_i \lambda^T(t_{s_i}) (f_{s_i}^+ - f_{s_i}^-) dt_{s_i}
 \end{aligned} \tag{4-29}$$

However, since the transition points have no effect at $t = \tau$, one has

$$\delta x_0(\tau) = \delta x(\tau) \tag{4-30}$$

Substitution of Eq. (4-30) into Eq. (4-29) yields

$$\begin{aligned}
 -\lambda^T(\tau) \delta \mathbf{x}(\tau) &= \int_{\tau}^0 (-L_x \delta \mathbf{x} + \lambda^T G \delta u + \lambda^T K \delta p) dt \\
 &\quad - \sum_i \lambda^T(t_{s_i}) (f_{s_i}^+ - f_{s_i}^-) dt_{s_i} \quad (4-31)
 \end{aligned}$$

Comparison of Eq. (4-31) and Eq. (4-13) implies an appropriate definition of $\lambda(\tau)$.

Define

$$\lambda^T(\tau) = - \left(\phi_x - \frac{\phi_x f - L}{\Omega_x f} \Omega_x \right) \Big|_{\tau} \quad (4-32)$$

Equation (4-32) is substituted into Eq. (4-31) and the result is substituted into Eq. (4-13) to obtain

$$dJ = \int_{\tau}^0 (L_u \delta u + L_p \delta p + \lambda^T G \delta u + \lambda^T K \delta p) dt - \sum_i \lambda^T(t_{s_i}) (f_{s_i}^+ - f_{s_i}^-) dt_{s_i} \quad (4-33)$$

One has

$$H_u = L_u + \lambda^T G \quad (4-34a)$$

$$H_p = L_p + \lambda^T K \quad (4-34b)$$

Substitution of Eq. (4-34) into Eq. (4-33) yields

$$dJ = \int_{\tau}^0 H_u \delta u dt + \int_{\tau}^0 H_p \delta p dt - \sum_i \lambda^T(t_{s_i}) (f_{s_i}^+ - f_{s_i}^-) dt_{s_i} \quad (4-35)$$

Note that p defines geometric parameters, so it must be time invariant. One has

$$\frac{dp}{dt} = 0 \quad (4-36)$$

Use of Eq. (4-36) in Eq. (4-35) yields

$$dJ = \int_{\tau}^0 H_u \delta u dt + \left(\int_{\tau}^0 H_p dt \right) \delta p - \sum_i \lambda^T(t_{s_i}) (f_{s_i}^+ - f_{s_i}^-) dt_{s_i} \quad (4-37)$$

Up to this point, the problem has assumed a specified state at $t = 0$, and a free state at terminal time. Typically, however, the terminal time state is constrained in some manner that may include a dependence on the parameters p . This is treated by creating a set of terminal state constraint functions, and a set of constraint influence functions, that establish a gradient contribution in the desired control parameter, and transition time variations as a function of the violations of the constraints.

Suppose one has several relations defining some equality constraints on state and parameters at terminal time in addition to Ω in Eq. (4-7). Call the constraint vector Ψ .

One has

$$\Psi = \Psi(x(\tau), p(\tau)) = \Psi(x(\tau), p) = 0 \quad (4-38)$$

where

$\Psi =$ a vector of dimension k

Differentiation of Eq. (4-38) yields

$$d\Psi = \Psi_x dx(\tau + d\tau) + \Psi_p dp(\tau + d\tau) \quad (4-39)$$

In analogy to Eq. (4-5) one gets

$$dp(\tau + d\tau) = \delta p(\tau) + \frac{dp}{dt}(\tau) d\tau \quad (4-40)$$

Substitution of Eq. (4-36) into Eq. (4-40) and subsequent use of the result and Eq. (4-5) in Eq. (4-39) yields

$$d\Psi = \Psi_x(\delta x(\tau) + f(\tau)d\tau) + \Psi_p \delta p \quad (4-41)$$

It is necessary to create a set of differential equations that will incorporate the results of Eq. (4-41), and will propagate the influence of the equality constraints through the vehicle trajectory and geometry. To achieve this, one must define a matrix function Λ of dimension $(a + c) \times k$.

One has

$$\frac{d}{dt} \left(\Lambda^T \begin{pmatrix} \delta x \\ \delta p \end{pmatrix} \right) = \dot{\Lambda}^T \begin{pmatrix} \delta x \\ \delta p \end{pmatrix} + \Lambda^T \begin{pmatrix} \delta \dot{x} \\ \delta \dot{p} \end{pmatrix} \quad (4-42)$$

Use of Eq. (4-36) in Eq. (4-42) yields

$$\frac{d}{dt} \left(\Lambda^T \begin{pmatrix} \delta x \\ \delta p \end{pmatrix} \right) = \dot{\Lambda}^T \begin{pmatrix} \delta x \\ \delta p \end{pmatrix} + \Lambda^T \begin{pmatrix} \delta \dot{x} \\ 0 \end{pmatrix} \quad (4-43)$$

As with the influence function for the cost variation, an influence function satisfying the adjoint differential equation can be used to express the effect of control variations on the constraint functions.

$$\dot{\Lambda} = -A^T \Lambda \quad (4-44)$$

where

$$A = \begin{pmatrix} f_x & f_p \\ \dot{p}_x & \dot{p}_p \end{pmatrix} \quad (4-45)$$

The matrix A definition is selected to separate state and parameter equality constraint sensitivity effects.

$$A = \begin{pmatrix} f_x & f_p \\ 0 & 0 \end{pmatrix} \quad (4-46)$$

Substitution of Eqs. (4-44) and (4-21) into Eq. (4-43) yields

$$\frac{d}{dt} \left(\Lambda^T \begin{pmatrix} \delta x \\ \delta p \end{pmatrix} \right) = -\Lambda^T A \begin{pmatrix} \delta x \\ \delta p \end{pmatrix} + \Lambda^T \begin{pmatrix} F\delta x + G\delta u + K\delta p \\ 0 \end{pmatrix} \quad (4-47)$$

Substitution of Eq. (4-46) into Eq. (4-47) and simplification yields

$$\frac{d}{dt} \left(\Lambda^T \begin{pmatrix} \delta x \\ \delta p \end{pmatrix} \right) = \Lambda^T \begin{pmatrix} G\delta u \\ 0 \end{pmatrix} \quad (4-48)$$

Integration of Eq. (4-48), use of Eq. (4-25) and the fact that the influence of the switch at t_{s_i} is zero for $(\tau \leq t < t_{s_i})$ if $\tau < 0$ and the integration is from $t = \tau$ to $t = 0$ yields

$$\Lambda^T(0) \begin{pmatrix} 0 \\ \delta p \end{pmatrix} - \Lambda^T(\tau) \begin{pmatrix} \delta x(\tau) \\ \delta p \end{pmatrix} - \sum_i \Lambda^T(t_{s_i}) \begin{pmatrix} \delta x_i(t_{s_i}) \\ 0 \end{pmatrix} = \int_{\tau}^0 \Lambda^T \begin{pmatrix} G\delta u \\ 0 \end{pmatrix} dt \quad (4-49)$$

where the t_{s_i} terms are derived in a manner similar to Eq. (4-26).

Substitution of Eq. (4-27) into Eq. (4-49) yields

$$\Lambda^T(0) \begin{pmatrix} 0 \\ \delta p \end{pmatrix} - \Lambda^T(\tau) \begin{pmatrix} \delta x(\tau) \\ \delta p \end{pmatrix} = \int_{\tau}^0 \Lambda^T \begin{pmatrix} G\delta u \\ 0 \end{pmatrix} dt - \sum_i \Lambda^T(t_{s_i}) \left(\begin{pmatrix} f_{s_i}^+ & -f_{s_i}^- \\ 0 \end{pmatrix} dt_{s_i} \right) \quad (4-50)$$

Suppose, for convenience, Λ is partitioned into two separate matrices.

Define

$$\Lambda = \begin{pmatrix} \Lambda_1 \\ \Lambda_2 \end{pmatrix} \quad (4-51)$$

where

Λ_1 = a matrix of dimension $a \times k$

Λ_2 = a matrix of dimension $c \times k$

Substitution of Eq. (4-51) into Eq. (4-50) yields

$$-\Lambda_1^T(\tau) \delta x(\tau) + (\Lambda_2^T(0) - \Lambda_2^T(\tau)) \delta p = \int_{\tau}^0 \Lambda_1^T G \delta u dt - \sum_i \Lambda_1^T(t_{s_i}) \left(f_{s_i}^+ - f_{s_i}^- \right) dt_{s_i} \quad (4-52)$$

Substitution of Eq. (4-12) into Eq. (4-41) yields

$$d\Psi = \left(\Psi_{\mathbf{x}} - \frac{\Psi_{\mathbf{x}} f_{\Omega} \mathbf{x}}{\Omega_{\mathbf{x}} f} \right) \delta \mathbf{x} + \Psi_{\mathbf{p}} \delta \mathbf{p} \quad (4-53)$$

Comparing the forms of Eq. (4-52) with (4-53), it is clear that useful definitions of the boundary conditions are

$$\Lambda_1^T(\tau) = - \left(\Psi_{\mathbf{x}} - \frac{\Psi_{\mathbf{x}} f_{\Omega} \mathbf{x}}{\Omega_{\mathbf{x}} f} \right) \quad (4-54a)$$

$$\Lambda_2^T(\tau) = -\Psi_{\mathbf{p}} \quad (4-54b)$$

Substitution of Eq. (4-54) into Eq. (4-52) and subsequently the result into Eq. (4-53) yields

$$d\Psi = \int_{\tau}^0 \Lambda_1^T G \delta u dt - \Lambda_2^T(0) \delta \mathbf{p} - \sum_i \Lambda_1^T(t_{s_i}) (f_{s_i}^+ - f_{s_i}^-) dt_{s_i} \quad (4-55)$$

A certain amount of notational simplicity is useful for future manipulation. The following definitions are therefore useful.

Define

$$\mathbf{g} = \begin{pmatrix} \int_{\tau}^0 H_{\mathbf{p}}^T dt \\ -\lambda^T(t_{s_1}) (f_{s_1}^+ - f_{s_1}^-) \\ -\lambda^T(t_{s_2}) (f_{s_2}^+ - f_{s_2}^-) \\ \vdots \end{pmatrix} \quad (4-56a)$$

$$\delta \mathbf{v} = \begin{pmatrix} \delta \mathbf{p} \\ dt_{s_1} \\ dt_{s_2} \\ \vdots \end{pmatrix} \quad (4-56b)$$

$$M = \left[-\Lambda_2^T(0) \mid -\Lambda_1^T(t_{s_1}) \left(f_{s_1}^+ - f_{s_1}^- \right) \mid -\Lambda_1^T(t_{s_2}) \left(f_{s_2}^+ - f_{s_2}^- \right) \mid - \dots \right] \quad (4-56c)$$

Substitution of Eq. (4-56) into Eq. (4-55) and (4-37) yields

$$dJ = \int_{\tau}^0 H_u \delta u dt + g^T \delta v \quad (4-57a)$$

$$d\Psi = \int_{\tau}^0 \Lambda_1^T G \delta u dt + M \delta v \quad (4-57b)$$

Inspection of Eq. (4-57) reveals that simplification of the desired decreases in J and $|\Psi|$ functionally imply desired variations in δu and δv . It is necessary to control the size of the steps taken by u and v , however, to assure that the first order approximations made thus far do not prevent convergence to the extremal solution one seeks.

An appropriate way to define step size is to create a quantity which is quadratic in δu and δv to assure a step whose measure is positive.

Define

S = step size

$$S^2 = \frac{1}{2} \int_{\tau}^0 \delta u^T U^{-1} \delta u dt + \frac{1}{2} \delta v^T V^{-1} \delta v \quad (4-58)$$

where

- V = a symmetric positive definite matrix to weight relative δv variations per iteration (dimension $[c+d] \times [c+d]$)
- $U(t)$ = a symmetric time function matrix, positive definite at all times, to weight δu variations per iteration (dimension $b \times b$)

It is appropriate to seek improvement in the equality constraint violations in direct proportion to the violations.

Define

$$d\psi = -C_\psi \psi \quad (4-59)$$

where

C_ψ is a constant to be specified

The step size control, the constraint violation improvement, and the cost improvement relations must be unified into a single set of relations. This is accomplished by adjoining a combination of Eqs. (4-59), (4-58), and (4-57) with Lagrange multipliers.

One defines η , ν as Lagrange multipliers. Substitution of Eq. (4-59) into Eq. (4-57b), and combining the result with Eqs. (4-57a) and (4-58) yields

$$\begin{aligned} d\bar{J} = & \int_{\tau}^0 H_u \delta u dt + g^T \delta v + \eta \left(\frac{1}{2} \int_{\tau}^0 \delta u^T U^{-1} \delta u dt + \frac{1}{2} \delta v^T V^{-1} \delta v - s^2 \right) \\ & + \nu^T \int_{\tau}^0 \left(\Lambda_1^T G \delta u dt + M \delta v + C_\psi \psi \right) \end{aligned} \quad (4-60)$$

At the extremal, the variation of $d\bar{J}$ with respect to δu and δv will vanish.

One gets

$$\begin{aligned} \delta d\bar{J} = 0 = & \int_{\tau}^0 \left(H_u + \eta \delta u^T U^{-1} + \nu^T \Lambda_1^T G \right) \delta \delta u dt \\ & + \left(g^T + \eta \delta v^T V^{-1} + \nu^T M \right) \delta \delta v \end{aligned} \quad (4-61)$$

Since the variations $\delta \delta u$ and $\delta \delta v$ are independent, the $\delta \delta u$ term and the $\delta \delta v$ term must separately vanish.

One gets

$$H_u + \eta \delta u^T U^{-1} + \nu^T \Lambda_1^T G = 0 \quad (4-62a)$$

$$g^T + \eta \delta v^T V^{-1} + v^T M = 0 \quad (4-62b)$$

One can solve Eq. (4-62) for δu , δv explicitly, yielding

$$\delta u = -\frac{1}{\eta} U(H_u^T + G^T \Lambda_1 v) \quad (4-63a)$$

$$\delta v = -\frac{1}{\eta} V(g + M^T v) \quad (4-63b)$$

Future notational simplicity suggests the following definitions

$$C_J = \frac{1}{\eta} \quad (4-64a)$$

$$z = -\frac{1}{\eta} v \quad (4-64b)$$

The following results are obtained upon substitution of Eq. (4-64) into Eq. (4-63)

$$\delta u = U(-C_J H_u^T + G^T \Lambda_1 z) \quad (4-65a)$$

$$\delta v = -C_J Vg + VM^T z \quad (4-65b)$$

Substitution of Eq. (4-65) into Eq. (4-57b), and use of Eq. (4-59) yields

$$-C_\psi \Psi = \int_{\tau}^0 \Lambda_1^T G U (-C_J H_u^T + G^T \Lambda_1 z) dt + M(-C_J Vg + VM^T z) \quad (4-66)$$

Some algebraic manipulation of Eq. (4-66) yields

$$\int_{\tau}^0 \Lambda_1^T G U G^T \Lambda_1 dt z + MVM^T z = -C_\psi \Psi + C_J \int_{\tau}^0 \Lambda_1^T G U H_u^T dt + C_J M V g \quad (4-67)$$

Further notational simplification suggests the definitions

$$I_{\psi\psi} = \int_{\tau}^0 \Lambda_1^T G U G^T \Lambda_1 dt \quad (4-68a)$$

$$I_{\Psi J} = \int_{\tau}^0 \Lambda_1^T G U H_u^T dt \quad (4-68b)$$

Substitution of Eq. (4-68) into Eq. (4-67) yields

$$(I_{\Psi\Psi} + MVM^T)z = -C_{\Psi}\Psi + C_J (I_{\Psi J} + MVg) \quad (4-69)$$

It is convenient to define

$$B = (I_{\Psi\Psi} + MVM^T)^{-1} \quad (4-70a)$$

$$C = (I_{\Psi J} + MVg) \quad (4-70b)$$

Substitution of Eq. (4-70) into Eq. (4-69) and solution for z yields

$$z = B(-C_{\Psi}\Psi + C_J C) \quad (4-71)$$

Substitution of Eq. (4-71) into Eq. (4-65) yields

$$\delta u = U(-C_J H_u^T + G^T \Lambda_1 B(-C_{\Psi}\Psi + C_J C)) \quad (4-72a)$$

$$\delta v = -C_J Vg + VM^T B(-C_{\Psi}\Psi + C_J C) \quad (4-72b)$$

Reordering of terms in Eq. (4-72) leads to

$$\delta u = U(-C_{\Psi} G^T \Lambda_1 B \Psi - C_J (H_u^T - G^T \Lambda_1 B C)) \quad (4-73a)$$

$$\delta v = -C_{\Psi} VM^T B \Psi - C_J (Vg - VM^T B C) \quad (4-73b)$$

An equation defining the value of C_J is necessary. Since it is also necessary to control the magnitude of the desired improvement in cost on any iteration in order to assure the validity of the first order approximations already used, it is appropriate to mathematically

tie the value of C_J to the gradient equations and some suitable cost variation (a measure of step size). One therefore defines a specified cost variation dJ_s .

Using Eq. (4-73) and (4-57a) one gets

$$dJ_s = \int_{\tau}^0 H_u U (-C_\psi G^T \Lambda_1 B \Psi - C_J (H_u^T - G^T \Lambda_1 BC)) dt + g^T (-C_\psi V M^T B \Psi - C_J (Vg - V M^T BC)) \quad (4-74)$$

Reordering terms in Eq. (4-74) yields

$$dJ_s = -C_\psi \left(\int_{\tau}^0 H_u U G^T \Lambda_1 B \Psi dt + g^T V M^T B \Psi \right) - C_J \left(\int_{\tau}^0 (H_u U H_u^T - H_u U G^T \Lambda_1 BC) dt + g^T (Vg - V M^T BC) \right) \quad (4-75)$$

It is convenient to define a new function

$$I_{JJ} = \int_{\tau}^0 H_u U H_u^T dt \quad (4-76)$$

Substitution of Eqs. (4-76) and (4-68b) into Eq. (4-75) yields

$$dJ_s = -C_\psi (I_{\psi J}^T B \Psi + g^T V M^T B \Psi) - C_J (I_{JJ} - I_{\psi J}^T BC + g^T Vg - g^T V M^T BC) \quad (4-77)$$

Solving Eq. (4-77) for C_J one gets

$$C_J = - \frac{dJ_s + C_\psi (I_{\psi J}^T B \Psi + g^T V M^T B \Psi)}{I_{JJ} - I_{\psi J}^T BC + g^T Vg - g^T V M^T BC} \quad (4-78)$$

With dJ_s somehow specified, use of Eqs. (4-78) and (4-73) permits one to evaluate δu and δv providing C_ψ is computable. C_ψ , however,

is simply a value used to establish a rate at which the Ψ vector violations are reduced. Starting with a small positive value ($0 < C_\Psi \leq 0.2$) when the violations of Ψ are large, and increasing C_Ψ towards 1.0 as the violations diminish, permits stable convergence and suits the linear approximations used throughout.

CHAPTER V

SPECIFIC FUNCTIONAL, DERIVATIVE, AND BOUNDARY CONDITION RELATIONS

Use of the optimization algorithm outlined in Chapter IV requires definition of the cost function terms, choice of initial state boundary conditions, specification of equality constraints and the state integration cutoff conditions, computation of derivative terms, and evaluation of boundary conditions on adjoined functions.

5.1 The Cost Function

Equation (4-2) specifies a mathematical cost function to define the measure of optimal system behavior. The cost consists of two components, one evaluated at the terminal state condition, the other distributed over the entire trajectory.

Three quantities: fuel consumption, dynamic pressure, and specific force, are chosen as a minimum set of elements required to characterize optimal system performance. Fuel consumption is a quantity which ought to be minimized. Dynamic pressure and specific force (the acceleration exclusive of gravity) are quantities which ought to be constrained to fall within bounds determined by structural failure loads, and payload or crew load tolerances.

The terminal state cost function term may be viewed as the quantity to be minimized, which is total fuel mass consumed in the example under study.

This leads to the following definition

$$\phi(x(\tau)) = x_5(\tau) + x_6(\tau) + x_7(\tau) = m_1(\tau) + m_2(\tau) + m_3(\tau) \quad (5-1)$$

Thus, the terminal cost element is the sum of fuel used for all propulsive modes combined.

The distributed cost function term may be viewed as a collection of penalty terms to increase resultant system cost for the violation of desired bounds on inequality constrained quantities. Dynamic pressure and specific force can be penalized in this manner when they exceed design limits.

This gives

$$L(x(t), u(t), p) = L_1(x(t)) + L_2(x(t), u(t), p) \quad (5-2)$$

where

L_1 = penalty term on dynamic pressure

L_2 = penalty term on specific force

A proper choice of L_1 and L_2 requires that no penalty be assessed when the dynamic pressure and specific force remain within desired bounds, that penalties be assessed at increasing rates as the bound violations increase, and that no discontinuities in the penalty term should exist at the bounds. A reasonable choice of penalty terms is

$$L_1 = Q(q - q_d)^2 u_0(q - q_d) \quad (5-3a)$$

$$L_2 = C_A(F_{sp} - a_d)^2 u_0(F_{sp} - a_d) \quad (5-3b)$$

where

Q = a constant to be chosen that weights dynamic pressure bound violation penalties

C_A = a constant to be chosen that weights specific force bound violation penalties

q = dynamic pressure

q_d = desired dynamic pressure bound

F_{sp} = specific force

a_d = desired acceleration bound (excluding gravity)

$u_0(q - q_d)$ = a unit step function with the step at $q = q_d$

$u_0(F_{sp} - a_d)$ = a unit step function with the step at $F_{sp} = a_d$

Note that

$$q = \rho \left(\frac{\dot{r}^2 + r^2 (\dot{\theta} - \omega_e)^2}{2} \right) = \rho \left(\frac{x_2^2 + x_1^2 (x_4 - \omega_e)^2}{2} \right) \quad (5-4a)$$

$$F_{sp} = \frac{\sqrt{(F_r - F_g)^2 + F_\theta^2}}{m} \quad (5-4b)$$

where

$\rho = \rho(r) = \rho(x_1)$ = atmospheric density model, assumed a function of altitude only

F_r = net radial force on the vehicle

F_g = net gravitational force on the vehicle

F_θ = net tangential force on the vehicle

m = net vehicle mass

Substitution of Eqs. (5-3) and (5-2) into Eq. (4-2) yields

$$J(\tau) = m_1(\tau) + m_2(\tau) + m_3(\tau) + \int_{\tau}^0 [Q(q - q_d)^2 u_0(q - q_d) + C_A (F_{sp} - a_d)^2 u_0(F_{sp} - a_d)] dt \quad (5-5)$$

5.2 The Initial State Boundary Condition

The initial state is specified as the desired orbital state of the launch vehicle. (With the terminal state locating the launch conditions). The primary function of any vehicle in the space shuttle class is to deliver payloads to low earth orbit, so a representative low earth orbit is chosen as a basis of evaluation of the air-breathing vehicle performance. The choice of a seventy-five mile circular orbit seems simplest and appropriate since it represents the fringe of the sensible atmosphere.

The use of a circular reference orbit makes the desired radial velocity vanish, and the desired angular velocity independent of position. The angular position can be chosen on the basis of a convenient reference value. One gets

$$\mathbf{x}(0) = \begin{pmatrix} r(0) \\ \dot{r}(0) \\ \theta(0) \\ \dot{\theta}(0) \\ m_1(0) \\ m_2(0) \\ m_3(0) \end{pmatrix} = \begin{pmatrix} R_e + h_0 \\ 0 \\ 0 \\ \omega_0 \\ 0 \\ 0 \\ 0 \end{pmatrix} \quad (5-6)$$

where

R_e = earth radius

h_0 = orbital altitude

ω_0 = orbital angular rate

The propellant should be totally consumed at orbit insertion leading to the zero value for propellant mass at $t = 0$. Since angular position is an arbitrary reference, it is chosen to be zero.

Elementary orbital mechanics yield^[32]

$$\omega_0 = \sqrt{\frac{GM_e}{r^3}} \quad (5-7)$$

making $\dot{\theta}(0)$ an explicit function of specified orbit altitude.

5.3 The Equality Constraints and the State Integration Cutoff Condition

The equality constraints were formulated as a method of handling the desired terminal state conditions on vehicle parameters, desired position and velocity, and propellant quantity.

Of the four position and velocity states only three require constraint since the angular position can be tied to an arbitrary initial state angular position reference. This leaves a requirement for constraint of radial position as well as radial and tangential velocity.

The optimization algorithm allows specification of parameter-dependent constraints. Since it is desired to match propellant tank

capacity with propellant requirements, a set of propellant mass constraints are derived, one for each propellant type.

Equation (4-7) specifies a function required for state integration cutoff. (The function locates the terminal time.) The cutoff function must come from the list of possible equality constraint functions, and should have an unambiguous zero crossing to assure proper choice of cutoff time.

The most promising candidate for the cutoff function is angular velocity since the entire desired velocity component for a horizontal takeoff would be tangential, and is likely to be a well defined minimum value. This defines

$$\Omega(x(t)) = x_4(t) - \dot{\theta}_d = \dot{\theta} - \dot{\theta}_d \quad (5-8)$$

where

$$\dot{\theta}_d = \text{desired angular velocity at takeoff}$$

Equation (5-8) eliminates one of the equality constraints leaving

$$\Psi = 0 = \begin{pmatrix} r - R_e \\ \dot{r} \\ m_1 - M_1 \\ m_2 - M_2 \\ m_3 - M_3 \end{pmatrix} = \begin{pmatrix} x_1 - R_e \\ x_2 \\ x_5 - M_1 \\ x_6 - M_2 \\ x_7 - M_3 \end{pmatrix} \quad (5-9)$$

where

$$M_1 = \text{turbojet propellant tank mass capacity}$$

$$M_2 = \text{scramjet propellant tank mass capacity}$$

$$M_3 = \text{rocket propellant tank mass capacity}$$

The constraints imply takeoff from the earth's surface, with horizontal velocity only at takeoff, and with no excess tank capacity.

5.4 The Derivative Terms

Two partial derivative matrices require evaluation at each integration step in the implementation of the optimization algorithm. These are F and K defined in Eqs. (4-15) and (4-20b).

Differentiation of Eq. (3-7) yields

$$F = \begin{pmatrix} 0 & 1 & 0 & 0 & 0 & 0 & 0 \\ \left(\dot{\dot{r}}^2 + \frac{1}{m} \frac{\partial F_r}{\partial r} \right) & \frac{1}{m} \frac{\partial F_r}{\partial r} & 0 & \left(2r\dot{\dot{\theta}} + \frac{1}{m} \frac{\partial F_r}{\partial \dot{\theta}} \right) & \left(-\frac{F_r}{m^2} + \frac{1}{m} \frac{\partial F_r}{\partial m_1} \right) & \left(-\frac{F_r}{m^2} + \frac{1}{m} \frac{\partial F_r}{\partial m_2} \right) & \left(-\frac{F_r}{m^2} + \frac{1}{m} \frac{\partial F_r}{\partial m_3} \right) \\ 0 & 0 & 0 & 1 & 0 & 0 & 0 \\ \left(\frac{2r\dot{\dot{\theta}}}{r} - \frac{F_\theta}{mr} + \frac{1}{mr} \frac{\partial F_\theta}{\partial r} \right) & \left(-\frac{2r\dot{\dot{\theta}}}{r} + \frac{1}{mr} \frac{\partial F_\theta}{\partial r} \right) & 0 & \left(-\frac{2r\dot{\dot{\theta}}}{r} + \frac{1}{mr} \frac{\partial F_\theta}{\partial \dot{\theta}} \right) & \left(-\frac{F_\theta}{m^2 r} + \frac{1}{mr} \frac{\partial F_\theta}{\partial m_1} \right) & \left(-\frac{F_\theta}{m^2 r} + \frac{1}{mr} \frac{\partial F_\theta}{\partial m_2} \right) & \left(-\frac{F_\theta}{m^2 r} + \frac{1}{mr} \frac{\partial F_\theta}{\partial m_3} \right) \\ \frac{\partial \dot{m}_1}{\partial r} & \frac{\partial \dot{m}_1}{\partial r} & 0 & \frac{\partial \dot{m}_1}{\partial \dot{\theta}} & \frac{\partial \dot{m}_1}{\partial m_1} & \frac{\partial \dot{m}_1}{\partial m_2} & \frac{\partial \dot{m}_1}{\partial m_3} \\ \frac{\partial \dot{m}_2}{\partial r} & \frac{\partial \dot{m}_2}{\partial r} & 0 & \frac{\partial \dot{m}_2}{\partial \dot{\theta}} & \frac{\partial \dot{m}_2}{\partial m_1} & \frac{\partial \dot{m}_2}{\partial m_2} & \frac{\partial \dot{m}_2}{\partial m_3} \\ \frac{\partial \dot{m}_3}{\partial r} & \frac{\partial \dot{m}_3}{\partial r} & 0 & \frac{\partial \dot{m}_3}{\partial \dot{\theta}} & \frac{\partial \dot{m}_3}{\partial m_1} & \frac{\partial \dot{m}_3}{\partial m_2} & \frac{\partial \dot{m}_3}{\partial m_3} \end{pmatrix}$$

(5-10a)

and

$$K = \begin{pmatrix} 0 \\ \frac{1}{m} \frac{\partial F_r}{\partial p} - \frac{F_r}{m^2} \frac{\partial m}{\partial p} \\ 0 \\ \frac{1}{mr} \frac{\partial F_\theta}{\partial p} - \frac{F_\theta}{m^2 r} \frac{\partial m}{\partial p} \\ \frac{\partial \dot{m}_1}{\partial p} \\ \frac{\partial \dot{m}_2}{\partial p} \\ \frac{\partial \dot{m}_3}{\partial p} \end{pmatrix}$$

(5-10b)

The partial derivatives contained in Eq. (5-10) are not readily evaluated directly, so expressions for each must be derived in terms of numerically computable quantities.

Prior to generation of the derivative expressions, it is necessary to evaluate the forces involved in the dynamics Eq. (3-7).

Another requirement is to remove the constraint implied by the quantity ϕ in Eq. (2-20) where

$$0 < \phi \leq 1 \quad (5-11)$$

since the optimization algorithm requires a control quantity without constraints. A simple mathematical transformation yields

$$\phi = \frac{1}{1 + u_f^2} \quad (5-12)$$

where

u_f = an unbounded fuel flow function

Use of Eq. (5-12) and geometric considerations yield

$$F_r = (T + P) \sin \delta + N \cos \delta - \frac{GM_e m}{r^2} \quad (5-13a)$$

$$F_\theta = (T + P) \cos \delta - N \sin \delta \quad (5-13b)$$

$$\dot{m}_1 = -\rho_1 u_1 A_T r_{f_T} / (1 + u_f^2) \quad (5-13c)$$

$$\dot{m}_2 = -\rho_1 u_1 A_S r_{f_S} m_{CR} / (1 + u_f^2) \quad (5-13d)$$

$$\dot{m}_3 = -T_R / [I_{spR} g_0 (1 + u_f^2)] \quad (5-13e)$$

$$\delta = \tan^{-1} \left(\frac{\dot{r}}{r(\dot{\theta} - \omega_e)} \right) + \alpha \quad (5-13f)$$

where

$T = T_T + T_S + T_R$ = the total vehicle thrust, constrained to be in the body x-axis direction

$P = L \sin \alpha - D \cos \alpha =$ the aerodynamic force parallel
to the body x-axis and of the same
sign convention as the thrust

 $N = L \cos \alpha + D \sin \alpha =$ the aerodynamic force normal to the
body x-axis

also

$\delta =$ the body x-axis angle relative to the local horizontal
 $\rho_1 =$ density of air at propulsion system inlet
 $u_1 =$ velocity of air at propulsion system inlet
 $I_{spR} =$ rocket specific impulse

Differentiation of Eq. (5-13) yields the desired partial derivative relations in terms of computable quantities

$$\frac{\partial F_r}{\partial r} = \left(\frac{\partial T}{\partial r} + \frac{\partial P}{\partial r} - N \frac{\partial \delta}{\partial r} \right) \sin \delta + \left(\frac{\partial N}{\partial r} + (T + P) \frac{\partial \delta}{\partial r} \right) \cos \delta + \frac{2GM_e m}{r^3} \quad (5-14a)$$

$$\frac{\partial F_r}{\partial \dot{r}} = \left(\frac{\partial T}{\partial \dot{r}} + \frac{\partial P}{\partial \dot{r}} - N \frac{\partial \delta}{\partial \dot{r}} \right) \sin \delta + \left(\frac{\partial N}{\partial \dot{r}} + (T + P) \frac{\partial \delta}{\partial \dot{r}} \right) \cos \delta \quad (5-14b)$$

$$\frac{\partial F_r}{\partial \dot{\theta}} = \left(\frac{\partial T}{\partial \dot{\theta}} + \frac{\partial P}{\partial \dot{\theta}} - N \frac{\partial \delta}{\partial \dot{\theta}} \right) \sin \delta + \left(\frac{\partial N}{\partial \dot{\theta}} + (T + P) \frac{\partial \delta}{\partial \dot{\theta}} \right) \cos \delta \quad (5-14c)$$

$$\frac{\partial F_r}{\partial m_i} = - \frac{GM_e}{r^2} \quad (5-14d)$$

$$\frac{\partial F_r}{\partial p} = \left(\frac{\partial T}{\partial p} + \frac{\partial P}{\partial p} \right) \sin \delta + \frac{\partial N}{\partial p} \cos \delta - \frac{GM_e}{r^2} \frac{\partial m}{\partial p} \quad (5-14e)$$

$$\frac{\partial F_\theta}{\partial r} = \left(\frac{\partial T}{\partial r} + \frac{\partial P}{\partial r} - N \frac{\partial \delta}{\partial r} \right) \cos \delta - \left(\frac{\partial N}{\partial r} + (T + P) \frac{\partial \delta}{\partial r} \right) \sin \delta \quad (5-15a)$$

$$\frac{\partial F_\theta}{\partial \dot{r}} = \left(\frac{\partial T}{\partial \dot{r}} + \frac{\partial P}{\partial \dot{r}} - N \frac{\partial \delta}{\partial \dot{r}} \right) \cos \delta - \left(\frac{\partial N}{\partial \dot{r}} + (T + P) \frac{\partial \delta}{\partial \dot{r}} \right) \sin \delta \quad (5-15b)$$

$$\frac{\partial F_\theta}{\partial \dot{\theta}} = \left(\frac{\partial T}{\partial \dot{\theta}} + \frac{\partial P}{\partial \dot{\theta}} - N \frac{\partial \delta}{\partial \dot{\theta}} \right) \cos \delta - \left(\frac{\partial N}{\partial \dot{\theta}} + (T + P) \frac{\partial \delta}{\partial \dot{\theta}} \right) \sin \delta \quad (5-15c)$$

$$\frac{\partial F_\theta}{\partial m_i} = 0 \quad (5-15d)$$

$$\frac{\partial F_\theta}{\partial p} = \left(\frac{\partial T}{\partial p} + \frac{\partial P}{\partial p} \right) \cos \delta - \frac{\partial N}{\partial p} \sin \delta \quad (5-15e)$$

$$\frac{\partial \dot{m}_1}{\partial r} = -A_{r f_T} \frac{\partial (\rho_1 u_1)}{\partial r} / (1 + u_f^2) \quad (5-16a)$$

$$\frac{\partial \dot{m}_1}{\partial \dot{r}} = -A_{T r f_T} \frac{\partial (\rho_1 u_1)}{\partial \dot{r}} / (1 + u_f^2) \quad (5-16b)$$

$$\frac{\partial \dot{m}_1}{\partial \dot{\theta}} = -A_{T r f_T} \frac{\partial (\rho_1 u_1)}{\partial \dot{\theta}} / (1 + u_f^2) \quad (5-16c)$$

$$\frac{\partial \dot{m}_1}{\partial m_i} = 0 \quad (5-16d)$$

$$\frac{\partial \dot{m}_1}{\partial p} = -r_{f_T} \frac{\partial (\rho_1 u_1 A_T)}{\partial p} / (1 + u_f^2) \quad (5-16e)$$

$$\frac{\partial \dot{m}_2}{\partial r} = -A_{S r f_S} \frac{\partial (\rho_1 u_1^{m_{CR}})}{\partial r} / (1 + u_f^2) \quad (5-17a)$$

$$\frac{\partial \dot{m}_2}{\partial \dot{r}} = -A_{S r f_S} \frac{\partial (\rho_1 u_1^{m_{CR}})}{\partial \dot{r}} / (1 + u_f^2) \quad (5-17b)$$

$$\frac{\partial \dot{m}_2}{\partial \dot{\theta}} = -A_S r_{f_S} \frac{\partial (\rho_1 u_1 m_{CR})}{\partial \dot{\theta}} / (1 + u_f^2) \quad (5-17c)$$

$$\frac{\partial \dot{m}_2}{\partial m_i} = 0 \quad (5-17d)$$

$$\frac{\partial \dot{m}_2}{\partial p} = -r_{f_S} \frac{\partial (\rho_1 u_1 m_{CR} A_S)}{\partial p} / (1 + u_f^2) \quad (5-17e)$$

$$\frac{\partial \dot{m}_3}{\partial r} = 0 \quad (5-18a)$$

$$\frac{\partial \dot{m}_3}{\partial \dot{r}} = 0 \quad (5-18b)$$

$$\frac{\partial \dot{m}_3}{\partial \dot{\theta}} = 0 \quad (5-18c)$$

$$\frac{\partial \dot{m}_3}{\partial m_i} = 0 \quad (5-18d)$$

$$\frac{\partial \dot{m}_3}{\partial p} = - \frac{\partial T_R}{\partial p} / (I_{sp_R} g_0 [1 + u_f^2]) \quad (5-18e)$$

Also, differentiation of Eq. (5-13f) yields

$$\frac{\partial \delta}{\partial r} = - \frac{\dot{r}(\dot{\theta} - \omega_e)}{r^2(\dot{\theta} - \omega_e)^2 + \dot{r}^2} \quad (5-19a)$$

$$\frac{\partial \delta}{\partial \dot{r}} = \frac{r(\dot{\theta} - \omega_e)}{r^2(\dot{\theta} - \omega_e)^2 + \dot{r}^2} \quad (5-19b)$$

$$\frac{\partial \delta}{\partial \dot{\theta}} = - \frac{r\dot{r}}{r^2(\dot{\theta} - \omega_e)^2 + \dot{r}^2} \quad (5-19c)$$

5.5 The Boundary Conditions of the Adjoined Functions

In Chapter IV, Eqs. (4-32) and (4-53) specified boundary condition relations on the required adjoint functions. The terms ϕ_x , Ω_x , Ψ_x , and Ψ_p are required along with f and L at terminal time.

Differentiation of Eq. (5-1) with respect to states yields

$$\phi_x = (0 \ 0 \ 0 \ 0 \ 1 \ 1 \ 1) \quad (5-20)$$

Differentiation of Eq. (5-8) with respect to states yields

$$\Omega_x = (0 \ 0 \ 0 \ 1 \ 0 \ 0 \ 0) \quad (5-21)$$

Differentiation of Eq. (5-9) with respect to states yields

$$\Psi_x = \begin{pmatrix} 1 & 0 & 0 & 0 & 0 & 0 & 0 \\ 0 & 1 & 0 & 0 & 0 & 0 & 0 \\ 0 & 0 & 0 & 0 & 1 & 0 & 0 \\ 0 & 0 & 0 & 0 & 0 & 1 & 0 \\ 0 & 0 & 0 & 0 & 0 & 0 & 1 \end{pmatrix} \quad (5-22)$$

Differentiation of Eq. (5-9) with respect to parameters yields

$$\Psi_p = \begin{pmatrix} 0 \\ 0 \\ -\frac{\partial M_1}{\partial p} \\ -\frac{\partial M_2}{\partial p} \\ -\frac{\partial M_3}{\partial p} \end{pmatrix} \quad (5-23)$$

where the rows of Eq. (5-23) are row vectors of the same dimension as the parameter vector p .

Substitution of Eqs. (5-21), (5-20), (5-3), (5-2), and (3-7) into Eq. (4-32) yields

$$\lambda^T(\tau) = (0 \ 0 \ 0 \ \lambda_4 \ -1 \ -1 \ -1) \quad (5-24a)$$

where

$$\lambda_4 = \left[\frac{r}{\frac{F_\theta}{m} - 2\dot{r}\dot{\theta}} (\dot{m}_1 + \dot{m}_2 + \dot{m}_3 - Q(q - q_d)^2 u_0 (q - q_d) - C_A (F_{sp} - a_d)^2 u_0 (F_{sp} - a_d)) \right] \Big|_{t=\tau} \quad (5-24b)$$

Substitution of Eqs. (5-23), (5-22), (5-21), and (3-7) into Eq. (4-53) yields

$$\Lambda_1^T(\tau) = \begin{pmatrix} -1 & 0 & 0 & (\Lambda_0 \dot{r}) & 0 & 0 & 0 \\ 0 & -1 & 0 & \left(\Lambda_0 (r\dot{\theta}^2 + \frac{F_r}{m}) \right) & 0 & 0 & 0 \\ 0 & 0 & 0 & (\Lambda_0 \dot{m}_1) & -1 & 0 & 0 \\ 0 & 0 & 0 & (\Lambda_0 \dot{m}_2) & 0 & -1 & 0 \\ 0 & 0 & 0 & (\Lambda_0 \dot{m}_3) & 0 & 0 & -1 \end{pmatrix} \Big|_{t=\tau} \quad (5-25a)$$

where

$$\Lambda_0 = \left[\frac{r}{\frac{F_\theta}{m} - 2\dot{r}\dot{\theta}} \right] \Big|_{t=\tau} \quad (5-25b)$$

$$\Lambda_2^T(\tau) = \begin{pmatrix} 0 \\ 0 \\ \frac{\partial M_1}{\partial p} \\ \frac{\partial M_2}{\partial p} \\ \frac{\partial M_3}{\partial p} \end{pmatrix} \quad (5-25c)$$

CHAPTER VI

NUMERICAL DIFFICULTIES AND THEIR RESOLUTION

6.1 An Overview

As anyone experienced with computer implementation of complex mathematical algorithms would expect, a number of difficult numerical problems arose in applying the technique described in Chapter IV to the air-breathing launch vehicle optimization. These numerical problems originate from idiosyncrasies of the algorithm, nonlinearities of the system dynamics and constraints, and machine data manipulation effects. To minimize frustration and wasted effort for anyone who chooses to apply the techniques contained in this dissertation, these problems are discussed, and their resolutions are characterized below.

6.2 Loss of Significant Information

The gradient type optimization techniques characteristically have sums and differences of numbers with similar magnitude. The differences lead to a decrease in the number of significant digits in the information due to the finite truncation of all information manipulated by a computer. The interpolation of tabulated data to obtain gradient information compounds the effect. The iterative techniques used to evaluate some quantities contained in the dynamics equations can further accumulate the errors.

Double precision computation of all key variables, and double precision storage of all important data seems essential to prevent complete loss of necessary information.

6.3 Equality Constraint Effect on Stability of Convergence

The optimization algorithm described in Chapter IV includes the capability to contribute to the control vector variation a quantity associated with terminal state and parameter equality constraint violations. The initial size of the violations can influence the stability

of the algorithmic convergence to an extremal point. To understand the effect, it is best to consider an unconstrained example.

Suppose one chooses to find an extremal point in a problem where the cost is a function of a single scalar quantity (see Figure VI-1). There may be local minima or maxima, but no absolute extremal value. In a simple physical example, this may imply a local minimum exists for fuel consumption as a function of positive fuel flow, but the absolute minimum might require an unrealizable negative fuel flow setting.

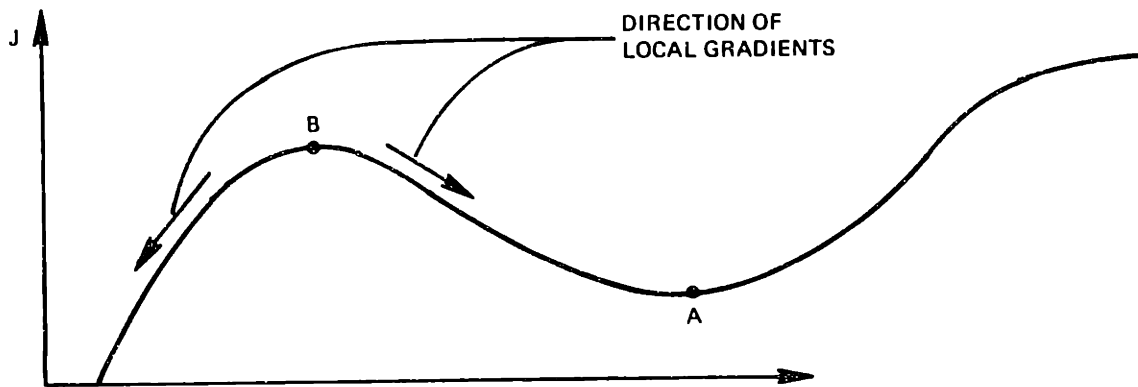


Figure VI-1.

Referring to Figure VI-1, one can see that point A represents a local minimum, point B a local maximum. In a minimization problem, convergence to point A will only result if one starts to the right of point B. To the left of point B the cost gradient points in a direction without solution.

Similar curve "bumpiness" and "over the hill" effects can be expected for equality constraint convergence—particularly when there are several interacting constraints. Too large an initial constraint violation is almost sure to push one over at least one multidimensional "hill". The result is that an initial set of controls, parameters, and transition times must be chosen to lead to an approximation of a physically realizable configuration, although suboptimal.

To judge how large a constraint violation can be tolerated which does not prevent constraint convergence, several rules of thumb, combined with a little trial and error can help.

First, the violations must be small enough such that nonlinearities in the dynamics do not direct the constraint related contributions in an entirely wrong direction.

Second, for state related constraints, energy considerations may be used to judge the relative magnitudes of upper bounds of constraint violations.

Third, the initial violations must have a scale far smaller than the natural scales of the problem.

In the air-breathing vehicle example, the rules lead to the following conclusions.

The atmosphere properties vary nonlinearly with altitude when viewed over intervals of more than a few thousand feet. The thrust of an air-breathing vehicle will superimpose that effect with its own Mach number related nonlinearities. The first rule suggests an upper bound in an altitude constraint violation of a few thousand feet.

If the equality constraints are applied at the ground end of flight, altitude provides a measure of vehicle potential energy increase, while velocity provides a measure of kinetic energy increase from ground state. The two are additive to obtain system energy changes. The potential energy is approximately linear in altitude over a few thousand feet. The kinetic energy is quadratic in velocity. Using the second rule, assuming the tolerable constraint violations can be comparable in energy measure, the maximum velocity constraint violations will be several tens of feet per second.

For parameter related constraints the third rule must be applied. Specifically, to match propellant consumed to propellant tank capacity, the initial constraint violations ought not be more than several percent of the expected fuel requirement.

Once the above listed conditions are met, constraint induced stability problems are not likely. Failure to satisfy the above conditions generally results in convergence in most constraints with divergence in at least one. (Often, the altitude constraint diverges in the air-breathing launch vehicle case.)

Finding an initial guess of a vehicle and trajectory that satisfies the equality constraint violation bounds established above is not a simple task. It can be done, however, through the iterative use of a

forward time vehicle flight simulation combined with a forward time optimization routine which treats only equality constraint violations of states at the desired orbit.

The forward time simulation consists of a vehicle dynamics model, and a guessed set of parameters and controls. The air-breathing part of the flight is "flown" to fuel depletion, automatically satisfying propellant consumption/tank volume matching constraints. The rocket trajectory can then be experimentally "flown", with multiple control histories, to burnout to establish the feasible range of orbits for the configuration used in the guess. If the energy of the achievable orbits is higher than is desired, the entire configuration should be scaled down accordingly. If the energy of the achievable orbits is lower than is desired, scale the configuration up. When the desired energy level seems possible with a given configuration, experimentally find a control history that results in an orbital velocity very close to the desired value, with large altitude errors permissible. (At orbital velocities, small velocity changes have the same system energy effect as large altitude changes.)

The configuration obtained by the process just detailed is used as an initial guess for a forward time optimization. The optimization routine is the forward time equivalent of the method detailed in Chapter IV except that no performance measure is included ($\phi=L=0$). Only equality constraints on the terminal orbital states are applied as a basis for choosing control variations.

The result of applying the forward time constraint violation reduction algorithm for a few iterations is a suitable configuration for the backwards time optimization technique. Even after roundoff errors introduced in inverting the time varying control histories, an initial guess with suitably small equality constraint violations is likely to result.

6.4 Choosing Metrics

Step size scaling within the various elements of the control vector from one iteration of the optimization algorithm to the next is accomplished through the use of the matrices U and V, referred to as metrics.

The metric V weights the variations of the parameters p and the transition times t_s , which are all time invariant. Consequently, the elements of V are time invariant.

The metric U weights the variations of the time varying control histories, and consequently should be time varying.

The rate of convergence to the extremal points is highly sensitive to the choice of U and V . In fact, the effect of the metrics on the convergence may be seen as a reflection of the nonuniformity of the performance function constant cost contours' curvature with respect to each of the control elements in the locality of the current control values. This leads to the conclusion that the best choice of U and V requires a good estimate of the nature of the second derivatives of the performance function geometry.

Since it is often difficult to discern much detail of the likely second order behavior prior to applying an optimization technique, some more "rules of thumb" must be used to get an initial set of metrics. Some experimentation with the values arrived at by these rules is suggested.

A desirable goal is to assure that the step taken in the direction of each control element leads to unit changes in performance. For the parameters, a good starting point is to assume that the curvature effects are approximately proportional to the initial value of the parameter.

The V matrix includes cross coupling terms in the off diagonal, and single element terms on the diagonal. Little is likely to be known, a priori, about interaction between parameters or transition times. Consequently, one should choose a diagonal matrix whose parameter associated elements are proportional to the square of the parameter values. (The square requirement results from the metric appearing in a quadratic term of control variations to control step size.) For the transition times, the characteristic dimension to judge metric size should be a substantial fraction of the total flight time.

The U matrix includes cross coupling terms which ought to be set to zero for reasons similar to those used in assigning off diagonal elements of the V matrix (i.e., ignorance of anything better to do). The diagonal elements are more difficult to select than for the V matrix, however. A magnitude is needed, and a shape is needed as a function of time.

The time integrated magnitude of the diagonal elements of U may be chosen by evaluating the time integrated magnitude of the corresponding controls over the entire flight, using these values as the characteristic

dimension in a fashion similar to that used when selecting the V matrix diagonal values.

The shape as a function of time of the U matrix ought to reflect time dependent behavior of the performance function constant cost contour curvature which is very difficult to fathom without analytical formulation of all the dynamics equations. Experimental variation of the shape must be attempted to judge the effect on algorithmic convergence rates.

To avoid too much complexity without good physical justification, it is recommended that the shape function be no more complex than a linear function of time.

6.5 Choosing a Penalty Function Weighting Factor

The inequality constraints are accommodated through the use of quadratic penalties outside the constraint bounds. The weight assigned to the penalty functions influences the relative rate of reduction of the penalty terms and the fuel performance terms. The effect is not as strong as the metric values on resulting step size, but it does have an effect on how closely the constraint bounds are satisfied. It is probably not desirable to apply the full force of the penalties initially. The penalty coefficient's initial value should be chosen so that the cost contribution is comparable to, or a low multiple of, the expected non-penalty performance improvement, with optimization allowed to proceed until most of the initial penalty contribution is small. The penalty gain should be boosted and the process repeated until the desired convergence is achieved toward the inequality constraint bounds. The precise weighting factor should be chosen realizing that the bounds in the optimal solution will be slightly violated, since pushing them to zero is offset by cost increases in other terms. If the bound requirement is very rigid, a final gain ten to one hundred times higher is desirable than for loose bound requirements.

6.6 Choosing a Specified Cost Improvement

The quantity dJ_s , the specified cost improvement, determines the overall step size of the optimization algorithm perturbations in all dimensions at once. It clearly can force the step to range from nearly linear to highly nonlinear changes in the performance function of a system with nonlinear dynamics. A non-linear step may prevent stable algorithm convergence.

Choosing a proper value for a specified cost improvement requires that one decrease its magnitude as the extremal point is approached to prevent the larger and larger control element variations that would be required to satisfy the specified quantity. To fail to change the specified improvement results in increasingly nonlinear, and possibly destabilizing, performance measure changes. If one has a rough estimate of the cost improvement still possible, the specified cost improvement should never exceed 15-20% of that value, and should probably only be a few percent of the expected improvement when starting the optimization process. Stability of equality constraint violations should be monitored during convergence of cost to assure that the specified cost improvement is in fact small enough.

CHAPTER VII

COMPUTER RESULTS

7.1 An Overview

A software implementation of the algorithm specified in Chapter IV with the dynamics and boundary conditions specified in Chapters II, III, and V was developed and used to evaluate the characteristics of the optimal air-breathing vehicle geometry, propulsion history, and trajectory as a function of different bounds on the inequality constraints. (The software listing is provided in the appendix.)

Cases were run fixing the specific force bound while varying the dynamic pressure bound. Cases were also run fixing the dynamic pressure bound while varying the specific force bound. The details of the cases run, the results of the optimizations, and some physical interpretations are presented below.

7.2 Details of Computer Cases

All cases run imposed the same orbit and ground boundary conditions. The orbit chosen was a 75 mile circular orbit. This represents the delivery of a payload to an orbit at the outer fringe of the sensible atmosphere where a small propulsive device similar to the space shuttle orbital maneuvering system would be capable of transferring the vehicle to the desired low earth orbit parameters. The ground conditions chosen represent horizontal sea level takeoff at an air speed of 250 miles per hour. The takeoff speed was chosen as a compromise between low takeoff speed to keep runway requirements down, and a lift requirement from the vehicle first stage to achieve flight with minimum wing size.

All cases run assumed equatorial launch to equatorial orbit, allowing use of two-dimensional orbital mechanics. A consequence of these assumptions is also minimal energy required to achieve orbit.

(The launch was assumed to be due East.) The results therefore shed the most favorable light on the potential of the air-breathing vehicle.

The specific inequality constraints used in each case are provided in Table VII-1. The dynamic pressure bounds were chosen to cover the range of values considered reasonable for air-breathing vehicles in a wide range of studies. The specific force bounds were chosen to keep g loads endurable on any passengers who may fly the vehicle (the space shuttle limits are close to 600 psf and 3 g's). The initial guess used for all runs was the same, and consistently quite different from the converged solutions. Convergence was assumed to occur when the gradient magnitude on any iteration was less than two orders of magnitude smaller than that of the initial iteration.

Table VII-1. Inequality constraints on computer runs.

Case	Dynamic Pressure Bound lbf/ft ²	Specific Force Bound g's
I	1000	3.0
II	800	3.0
III	600	3.0
IV	800	2.5

7.3 Optimization Data

The data from the optimization runs is presented tabularly and in plots. Tables VII-2 through VII-5 present the parameters, transition point times, relevant states at the transition points, and fuel consumption data for the cases run. Figures VII-1 through VII-20 present the interesting time dependent variables including controls or control-dependent functions, inequality constrained variables, two state related functions, and Mach number.

Table VII-2 presents the parameters in units of radians, feet, slugs, and pounds force. The meaning of each parameter is labeled.

Table VII-3 presents transition point times and other relevant flight times in seconds from ground takeoff. The significance of each time is labeled in Table VII-3.

Table VII-4 presents some relevant state variable related data at the transition points for each case run in feet, radians, and seconds.

Table VII-2. Parameter values.

Parameter	Physical Variable	Case			
		I	II	III	IV
P ₁	Nose Angle	0.01925	0.01909	0.01879	0.01912
P ₂	Fuselage Width	34.3	35.2	35.7	34.9
P ₃	Scramjet Inlet Height	14.56	15.80	16.66	15.53
P ₄	Turbojet Inlet Height	9.66	10.25	10.74	9.92
P ₅	Wing Span	323	293	271	308
P ₆	Delta Wing Angle	1.340	1.272	1.344	1.313
P ₇	TJ/SCRJ Tank Volume Ratio	0.417	0.417	0.418	0.417
P ₈	Fuselage Length	151.6	150.9	149.5	151.0
P ₉	Rocket Fuel Capacity	3.16×10^4	3.16×10^4	3.15×10^4	3.15×10^4
P ₁₀	Maximum Rocket Thrust	1.724×10^6	1.738×10^6	1.820×10^6	1.726×10^6

Table VII-3. Transition and flight times.

Time	Physical Meaning	Case			
		I	II	III	IV
t _{s1}	Scramjet Ignition	42.4	55.3	65.3	47.8
t _{s2}	Turbojet Shutdown	161.7	169.9	183.3	167.5
t _{s3}	Staging	179.0	190.9	213.2	179.6
τ	Total Flight Time	512	521	532	513
τ-t _{s3}	Rocket Flight Time	333	331	319	333

Table VII-4. Transition point state functions.

	Transition Point	Altitude	Radial Velocity	Angular Velocity	Tangential Air Speed
Case	t_{s_i}	$r \times 10^4$	\dot{r}	$\dot{\theta} \times 10^{-4}$	$(r+R_e) (\dot{\theta} - \omega_e) \times 10^3$
I	1	2.77	781	1.291	1.175
II	1	3.49	634	1.356	1.313
III	1	3.94	573	1.347	1.293
IV	1	3.24	702	1.301	1.196
I	2	7.82	136	2.31	3.32
II	2	7.55	103	2.32	3.33
III	2	7.48	43.1	2.30	3.30
IV	2	7.01	2.92	2.35	3.39
I	3	7.99	186	2.30	3.29
II	3	7.72	231	2.31	3.32
III	3	7.72	306	2.30	3.30
IV	3	7.18	344	2.33	3.36

Table VII-5. Ground value of propellant masses.

	Turbojet Fuel	Scramjet Fuel	Rocket Fuel
Case	$m_1 \times 10^3$	$m_2 \times 10^2$	$m_3 \times 10^4$
I	3.16	4.42	3.16
II	3.20	4.45	3.16
III	3.14	4.36	3.15
IV	3.17	4.43	3.15

Table VII-5 presents total fuel consumption for each propulsive mode in slugs. The first mode is the turbojet using a hydrocarbon fuel. The second mode is the scramjet using liquid hydrogen. The third mode is the rocket using liquid hydrogen and liquid oxygen.

Figures VII-1 through VII-20 are plots of the interesting time dependent variables, and are divided into two groups. The first group, Figures VII-1 through VII-10, are plots of the cases with the specific force bound held at 3.0 g's and the dynamic pressure bound varied. The second group, Figures VII-11 through VII-20, are plots of the cases with the dynamic pressure bound held at 800 lbf/ft² and the specific force bound varied.

Within each group of ten plots, the first four show control functions. The first two plots show angle of attack on different time scales (early flight/entire flight). The third and fourth plots show throttle setting on the same two time scales. By expanding the time scale in early flight, more detail is visible in the plots.

The fifth through seventh plots in each group show constrained variables. The first of these is dynamic pressure, plotted only in the range where the atmosphere is dense enough to cause the constraint to affect the vehicle. The other two plots show specific force on the same two time scales as the control variables.

The eighth through tenth plots in each group present variables plotted through first stage flight which show interesting structure in that flight phase only. The radial velocity and tangential air speed are plotted to show energy, velocity, and constraint tradeoff effects. The Mach number is presented to correlate other first stage effects with Mach number, and to show staging Mach number similarities.

7.4 Physical Effects in Optimal Results

A wide variety of physical effects influencing the optimization results are apparent upon inspection of the results of the different cases run. These include effects resulting from the dynamic differences in the two stages, effects resulting from aerodynamic properties of the first stage, and effects resulting from the influence of the inequality constraints.

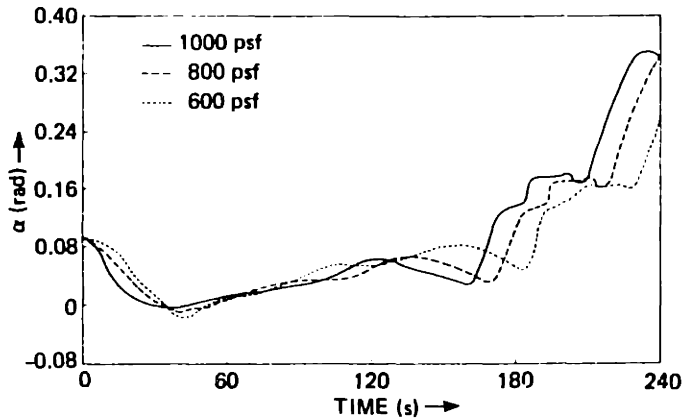


Figure VII-1. Angle of attack α vs. t . First 240 seconds. Specific force bound = 3 g's. Dynamic pressure bound varied.

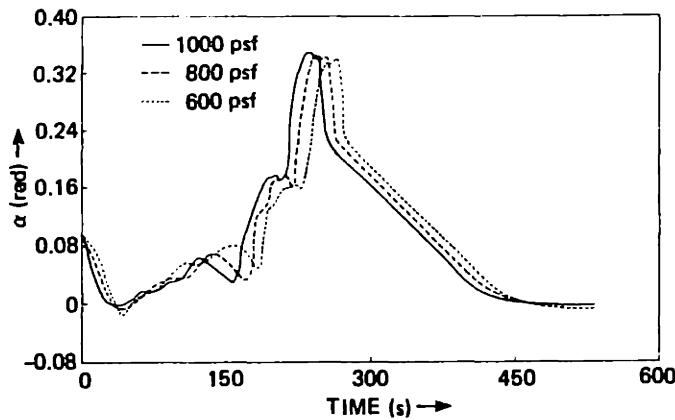


Figure VII-2. Angle of attack α vs. t . Full flight time. Specific force bound = 3 g's. Dynamic pressure bound varied.

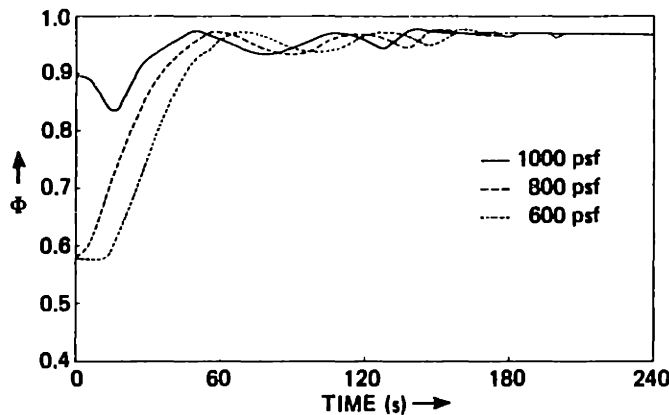


Figure VII-3. Throttle setting ϕ vs. t . First 240 seconds. Specific force bound = 3 g's. Dynamic pressure bound varied.

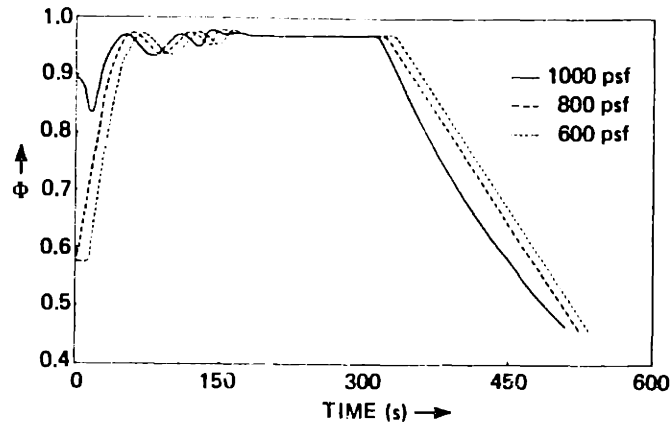


Figure VII-4. Throttle setting ϕ vs. t . Full flight time. Specific force bound = 3 g's. Dynamic pressure bound varied.

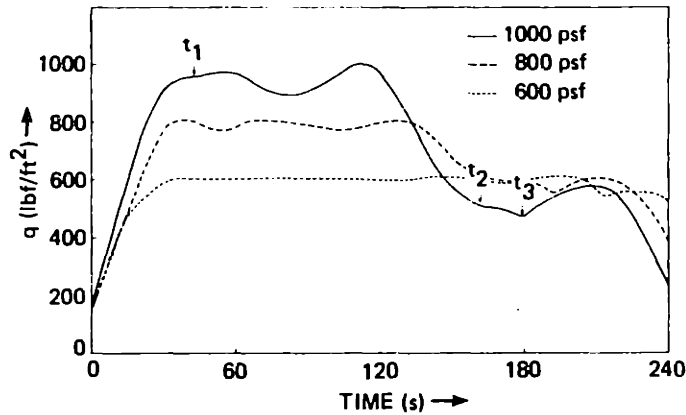


Figure VII-5. Dynamic pressure q vs. t . Through dense atmosphere. Specific force bound = 3 g's. Dynamic pressure bound varied.

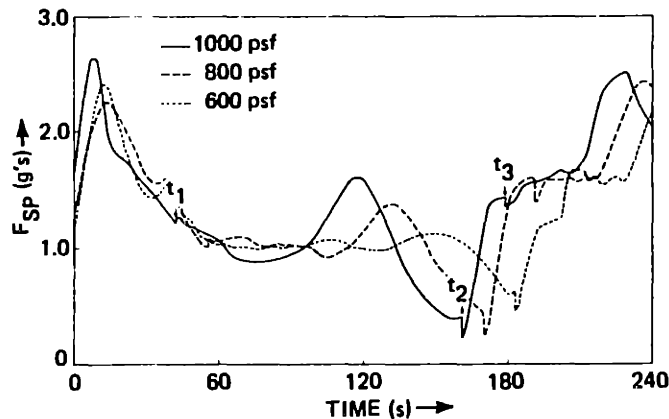


Figure VII-6. Specific force F_{sp} vs. t . First 240 seconds. Specific force bound = 3 g's. Dynamic pressure bound varied.

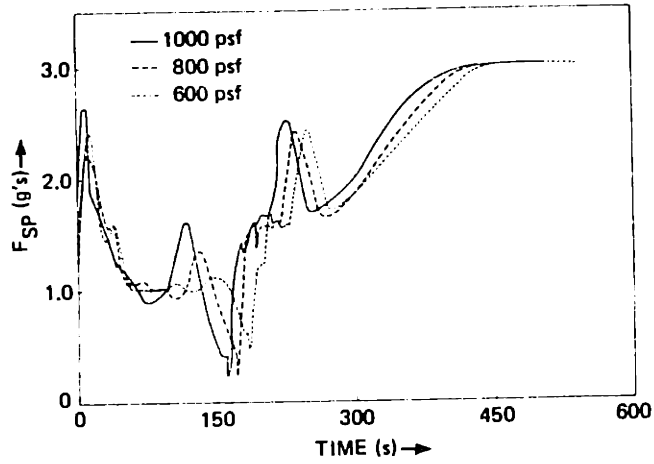


Figure VII-7. Specific force F_{SP} vs. t . Full flight time. Specific force bound = 3 g's. Dynamic pressure bound varied.

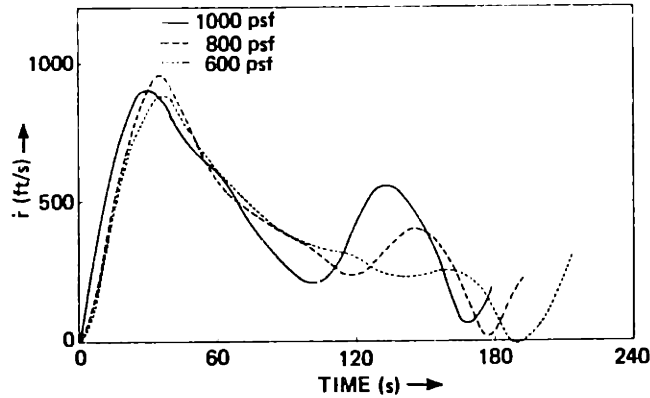


Figure VII-8. Radial velocity \dot{r} vs. t . Through first stage flight. Specific force bound = 3 g's. Dynamic pressure bound varied.

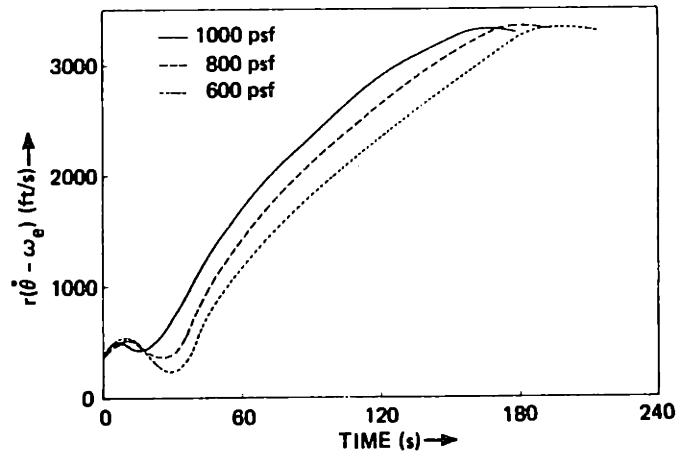


Figure VII-9. Tangential air speed $r(\dot{\theta} - \omega_e)$ vs. t . Through first stage flight. Specific force bound = 3 g's. Dynamic pressure bound varied.

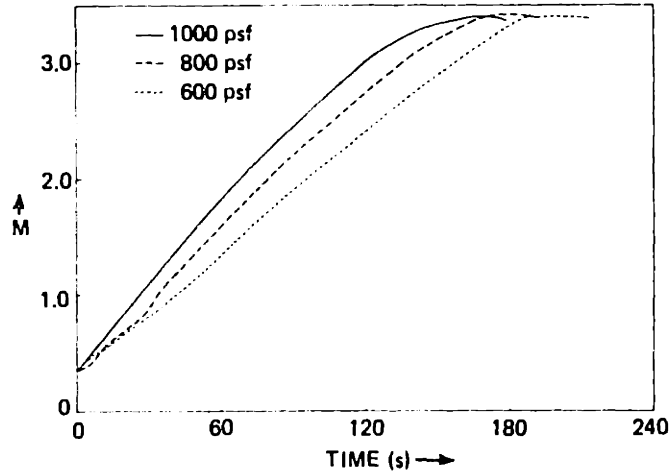


Figure VII-10. Mach number M vs. t . Through first stage flight. Specific force bound = 3 g's. Dynamic pressure bound varied.

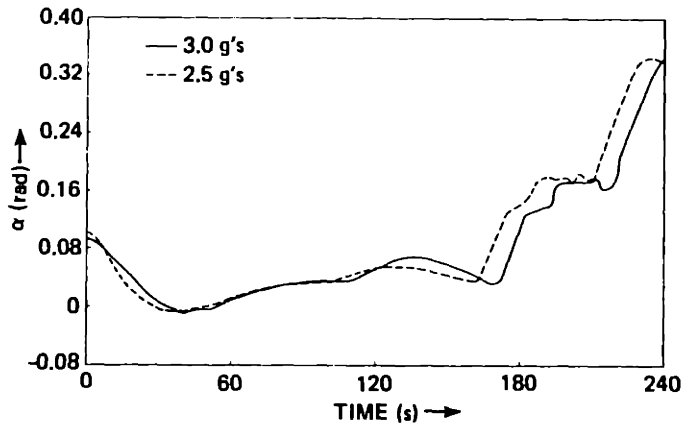


Figure VII-11. Angle of attack α vs. t . First 240 seconds. Dynamic pressure bound = 800 psf. Specific force bound varied.

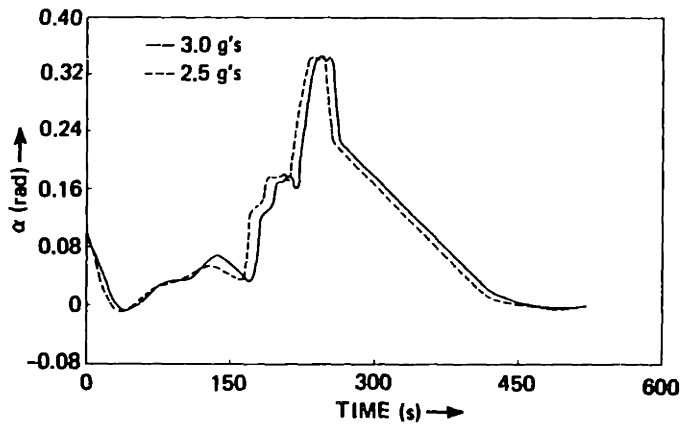


Figure VII-12. Angle of attack α vs. t . Full flight time. Dynamic pressure bound = 800 psf. Specific force bound varied.

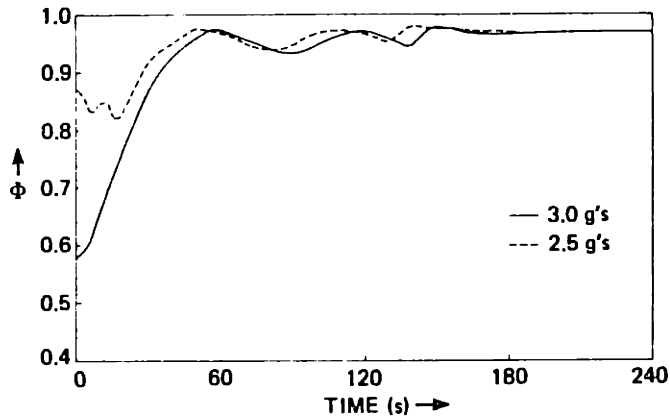


Figure VII-13. Throttle setting ϕ vs. t . First 240 seconds. Dynamic pressure bound = 800 psf. Specific force bound varied.

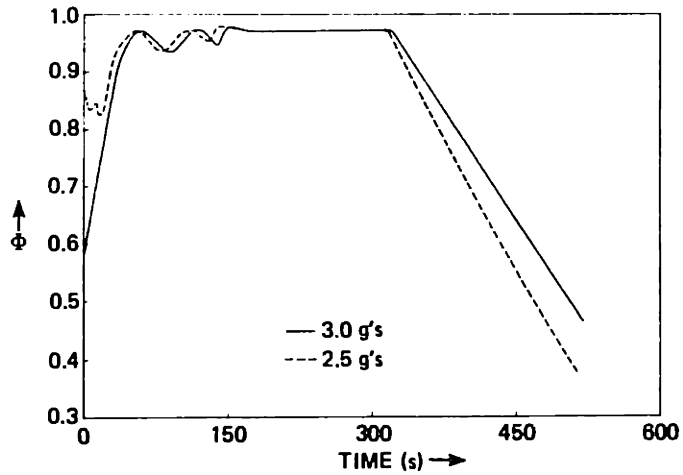


Figure VII-14. Throttle setting ϕ vs. t . Full flight time. Dynamic pressure bound = 800 psf. Specific force bound varied.

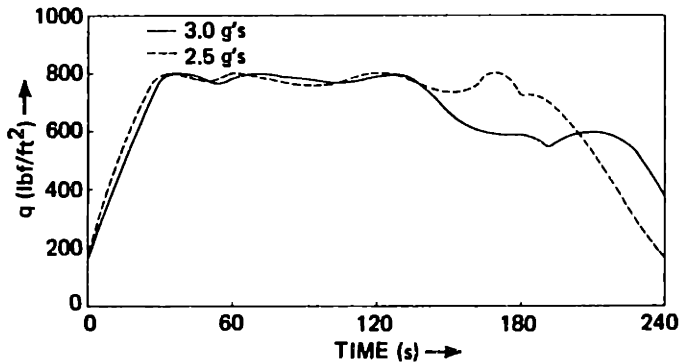


Figure VII-15. Dynamic pressure q vs. t . Through dense atmosphere. Dynamic pressure bound = 800 psf. Specific force bound varied.

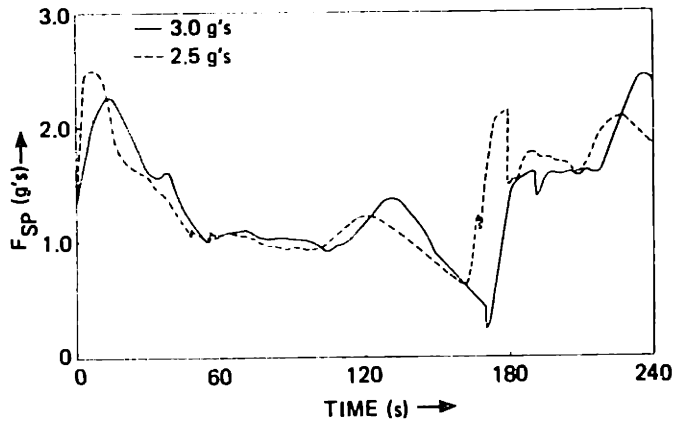


Figure VII-16. Specific force F_{SP} vs. t . First 240 seconds. Dynamic pressure bound = 800 psf. Specific force bound varied.

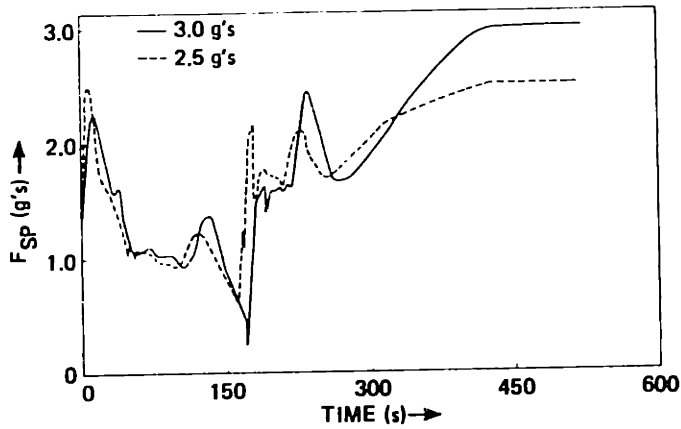


Figure VII-17. Specific force F_{SP} vs. t . Full flight time. Dynamic pressure bound = 800 psf. Specific force bound varied.

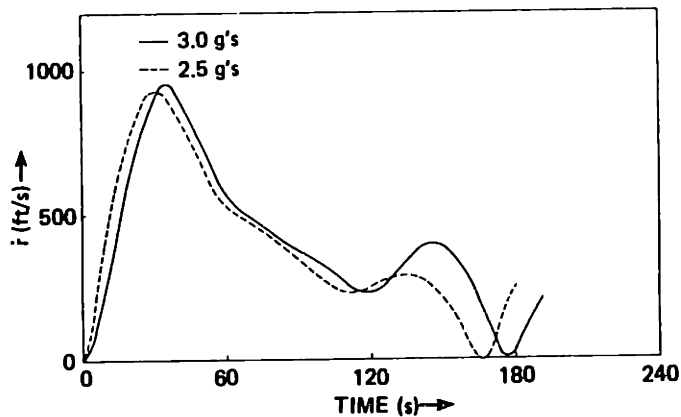


Figure VII-18. Radial velocity \dot{r} vs. t . Through first stage flight. Dynamic pressure bound = 800 psf. Specific force bound varied.

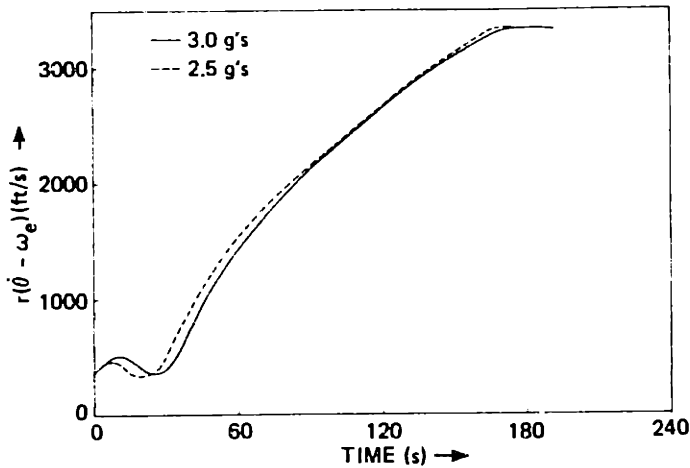


Figure VII-19. Tangential air speed. $r(\dot{\theta} - \omega_e)$ vs. t . Through first stage flight. Dynamic pressure bound = 800 psf. Specific force bound varied.

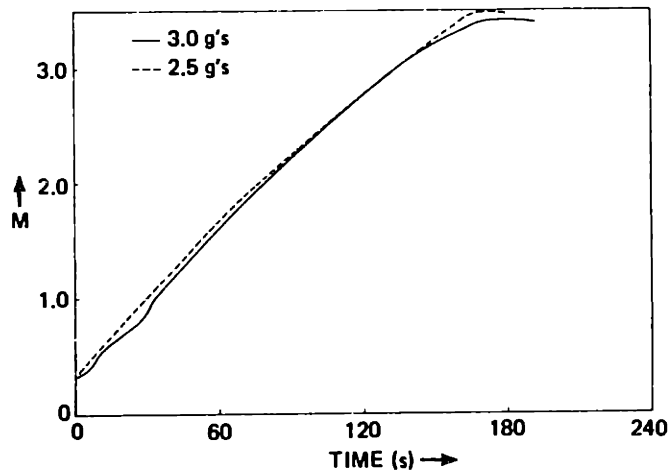


Figure VII-20. Mach number M vs. t . Through first stage flight. Dynamic pressure bound = 800 psf. Specific force bound varied.

Some trends are common to all cases run, indicating their association with the equality constraints and fuel performance cost function contributions. Other trends are apparent only upon variation of one of the inequality constraints, indicating a tradeoff between vehicle solution character and inequality constraint bounds.

7.4.1 Universal Solution Properties

A variety of state, trajectory, and propellant properties are apparent in all cases run, indicating their association with the specifics of vehicle dynamics as well as state and propellant constraints.

The most striking similarity in all cases run is seen in Table VII-5. The fuel consumption is only weakly associated with the inequality constraint bounds used. In fact, given the slow terminal convergence of gradient algorithms, the difference in the propellant consumption numbers can be attributed as much to small differences in the degree of optimality achieved at the cutoff of the optimization algorithm as it can be associated with genuine physical effects. In spite of simultaneous application of both inequality bounds, and substantial variation in each bound in the different cases run on the computer, it seems that within the range of inequality constraint bounds studied, fuel consumption effects of constraint-bound variations can be offset by vehicle configuration and trajectory changes.

Referring to Table VII-5 it is apparent that the high specific impulse of the air-breathing system when compared to the rocket leads to the vast bulk of the propellant consumption occurring during rocket flight in spite of the substantial velocity contributions of the first stage. (Data in Table VII-4 can be used to show air speed ranges between 3300 and 3400 feet per second at staging.) This implies that the air-breathing propulsion is very desirable, since a large gain in system energy is achieved with a relatively small fuel expenditure when compared to expected "first stage" rocket fuel usage rates on the space shuttle. It also suggests that significant air-breathing system improvements will only marginally improve overall system fuel usage.

Further reference to Table VII-4 shows that the general altitude range at the transition points is similar in all cases, with the altitude changing little between turbojet shutdown and staging. Table VII-3 shows a consistent time lapse of less than 20 seconds between these last two transition points.

Inspection of Figures VII-1 and VII-11 show consistent early angle-of-attack patterns during air-breathing flight. All cases start with relatively high angle of attack to achieve necessary lift for takeoff. The angle of attack subsequently undergoes a continuous decline in the first 35-45 seconds to a slightly negative value. The

nadir of the angle-of-attack plots compared with the Mach number plots in Figures VII-10 and VII-20 consistently occur in the transonic region (between $M = 1.0$ and $M = 1.2$) where the drag coefficient peaks. This is the consequence of the utilization of stored potential energy (altitude) combined with thrust to rapidly go through the most dissipative aerodynamic flight region. An angle-of-attack increase follows to achieve climb, it peaks, then declines again as air-breathing thrust capability diminishes with altitude. The angle of attack bottoms out again at about the time when the turbojet shuts down. (t_{s_2} in Table VII-3 provides the shutdown time.) A pullup maneuver is then executed under scramjet power alone. The pullup orients the vehicle for effective use of the rocket power at staging. Since the rocket uses fuel much more rapidly than the air-breathing engines, improper rocket orientation can lead to inefficient use of rocket fuel to achieve a substantial change in flight path angle. The likely reason for scramjet power only in a primarily aerodynamic maneuver is the continued high specific impulse available to that propulsive mode under conditions where the turbojet specific impulse has dropped considerably. The dominance of the aerodynamic effect on the pullup is apparent upon inspection of the staging Mach number in Figures VII-10 and VII-20. Staging consistently occurs between $M = 3.3$ and $M = 3.5$. At these low Mach numbers the scramjet has low mass capture and therefore low power.

The consistency of the staging Mach number is itself an extremely important effect. Its value suggests that the scramjet provides little net benefit while contributing a high dry mass penalty to the first stage. Recalling that the scramjet mass model is based on the high mass of a system capable of tolerating the heat soak of high Mach numbers, this conclusion may in part be a consequence of design conservatism.

Figures VII-2 and VII-12 plot the angle-of-attack histories for the entire flight, consistently showing a large peak in the early phase of rocket flight followed by a dropoff to near zero. This effect is a consequence of the need to achieve a substantial radial velocity component in order to obtain the desired altitude at rocket burnout. The dropoff in angle of attack near the flight end is a consequence of an increasing use of gravity turning prior to orbit insertion.

Figures VII-3, VII-4, VII-13, and VII-14 all plot fuel throttle settings. They show a characteristic throttled-down setting at takeoff to prevent excessive vehicle loading that could result from the

high mass capture rate and high lift that the dense atmosphere and high angle of attack induce. The throttle setting increases subsequently to achieve high thrust through the dissipative transonic region, followed by a slight throttling down in the less dissipative supersonic environment, and then a move toward maximum thrust is made (hence maximum acceleration) until specific force effects dominate in the late phases of rocket flight. The failure to achieve full throttle settings ($\phi = 0.97$ rather than $\phi = 1.00$) is a consequence of the slow terminal convergence of the gradient algorithm to the optimum and the optimization algorithm cutoff point.

In Figures VII-8 and VII-18 radial velocity through first stage flight is plotted showing a persistent double peak effect and pre-staging climb out. The second peak is affected by constraints which are discussed later. The first peak is a consequence of the transonic negative angle of attack followed by a need to stay in a sufficiently dense atmosphere to hold turbojet thrust levels high, permitting continued tangential velocity acceleration. The second peak seems to be a consequence of Mach number associated gains in rate of mass capture, permitting higher altitude flight with continued acceleration. The pullup, as discussed earlier, permits good vehicle orientation for rocket ignition.

Figures VII-9 and VII-19, the tangential air speed through first stage flight, show consistent acceleration except early and late in flight. The acceleration demonstrates that the main orbital energy benefit from the first stage comes in the tangential velocity component. The late velocity dropoff is a consequence of a combination of atmospheric rarefaction, reducing thrust, and finally an aerodynamic energy transfer to radial velocity to achieve vehicle pullup. The early flight tangential velocity dip is associated with a preferential early radial velocity gain to permit a subsequent altitude gain while accelerating. This effect permits vehicle load relief discussed later in more detail.

7.4.2 Dynamic Pressure Constraint Effects

A variety of trends in the vehicle geometric parameters, transition times, and time dependent behavior are apparent upon variation of the dynamic pressure inequality constraint bound. Three cases were run with the specific force bound held at 3.0 g's and the dynamic pressure

bound set at 1000, 800, and 600 pounds force per square foot. Tables VII-2 through VII-5 and Figures VII-1 through VII-10 present the results of optimization with these bounds. (Table VII-1 specifies which bounds apply to each case run.)

Table VII-2 shows definite dynamic pressure related trends in the parameters p_1 through p_5 , p_8 , and p_{10} . Parameters p_2 through p_4 all define inlet areas for the air-breathing propulsion systems, and all grow with a decline in dynamic pressure bound. Comparison of altitudes at the first transition point in Table VII-4 shows a steady altitude increase for this point with the decrease in dynamic pressure bound. These effects taken together permit the vehicle to hold down the dynamic pressure due to the lower air density at higher altitude while keeping reasonable levels of air-breathing thrust as a result of larger propulsion system intake. Table VII-5 shows fuel consumption to be relatively constant during air-breathing flight for all cases run. An increase in p_2 combined with the constraint that demands the propellant volume to match the tank volume requires a decline in other fuselage dimensions. Thus, parameters p_1 and p_8 decrease. A secondary effect of increasing air-breathing propulsion system inlet size is to increase available thrust at takeoff, permitting somewhat reduced wing lift capability for the vehicle. A decline in p_5 , the wing span, results with reduced dynamic pressure bound reflecting the lower lift requirements when combined with the delta wing sweep angle, p_6 , and the dc_L/da data in Table II-1. The increase in p_{10} , maximum rocket thrust, with declining dynamic pressure bound has an effect apparent in the bottom entry of Table VII-3, a decline in rocket flight time. With the staging states very similar, as seen in Table VII-4, the cause of the rocket thrust effect is obscure.

The time dependent variable plots show a great deal of dynamic pressure bound related structure. Figure VII-5 shows the dynamic pressure plotted through dense atmospheric flight. The most obvious effect is the close tracking of the dynamic pressure bounds, in all cases, until the decline in atmospheric density reduces the value below the bound for the remainder of flight. With less stringent constraints the bound is less precisely tracked. This is a result of the vehicle's ability to more closely approximate the desired unconstrained behavior. As the bound is decreased more time is spent near the limit, which is a consequence of greater constraints on acceleration. The increasing

acceleration limits are seen in Tables VII-3 and VII-4 which show increasing amounts of time spent in air-breathing flight in spite of very similar staging states. The dynamic pressure plots also all show a temporary rise in dynamic pressure after staging as a result of velocity increase effects initially exceeding the atmospheric density decrease with altitude when the vehicle begins the high rate of rocket acceleration.

The angle-of-attack histories seen in Figures VII-1 and VII-2 all show similar structure. It is interesting, however, to note the differences in the pairs of air-breathing flight angle of attack valleys, the magnitudes of which are secondary effects of reduced wing lift capability. In the transonic negative angle of attack region a more negative angle of attack is permitted for tighter dynamic pressure bounds. The result is similar net negative lift, and similar first peak radial velocity behavior, seen in Figure VII-8, eventually leading to similar terminal first stage states. The second angle of attack valley is just prior to pre-rocket ignition pullup. Reduced wing lift capability results in a somewhat greater angle of attack to help keep up the net lift for the flight phase immediately preceding the aerodynamic pullup maneuver. In spite of the higher angle of attack, net lift does decline with wing span in the flight region before the second radial velocity peak. The reduced lift also pulls down the magnitude of the second peak, and causes lower radial velocities just before the aerodynamic pullup.

Figure VII-6, specific force during early flight, shows one significant dynamic pressure bound dependent structure. The second peak declines with decreases in the bound. This effect is strictly aerodynamic, being a consequence of reduced lift from the reduced wing size, with inadequate increases in the angle of attack to compensate for the smaller wing.

The first stage tangential air speed, plotted in Figure VII-9, also shows one significant dynamic pressure bound related effect in early flight. The velocity component declines once in early flight in all cases run, with the decline becoming more pronounced as the dynamic pressure bound is reduced. The vehicle with a reduced bound needs to achieve higher altitude early in flight to keep air density down, controlling the dynamic pressure magnitude. The radial velocity component is given preference to achieve the altitude increase. Therefore, as the bound is reduced, greater emphasis is put on the radial

component, leading to less energy being fed into the tangential component. The result, when aerodynamic dissipation is included, is a greater dip in magnitude of the tangential air speed.

7.4.3 Specific Force Constraint Effects

There are some physical phenomena apparent in the optimization results that are clearly a consequence of the specific force bounds. There is, however, more limited data from cases run in which the specific force bound was varied, making it necessary to be more cautious on conclusions drawn about the subtler effects.

Table VII-2 shows a trend in p_2 through p_4 , the air-breathing propulsion system inlet sizing parameters. A decline in the specific force bound from Case II to Case IV results in a small but consistent decrease in all three parameters. Figure VII-16, the plot of specific force versus time in early flight shows that with the more constrained case the bound is reached in early air-breathing flight. The influence of the constraint would be expected to hold down the propulsion system size since acceleration is limited by the bound. Since this specific force peak precedes initiation of scramjet use the effect is principally on p_2 and p_4 , the turbojet inlet dimensions. The effect on p_3 may be a consequence of reduced system dry mass with the decline in the turbojet size. The parameters p_1 and p_8 would be expected to show a small increase with a decline in p_2 due to the nearly constant fuel consumption figures of Table VII-5, combined with the propellant volume/tank volume matching constraint, which is in fact seen to be true, though it is a very small effect.

There is a significant increase in p_5 , the wing span, with the decline in specific force bound. This effect, combined with the increase in p_6 and the effect on $dc_L/d\alpha$ given in Table II-1, actually has little effect on wing lift capability. Therefore, no trends can be extracted from the phenomena.

Figure VII-14 shows the most obvious effects of the specific force bound on time varying flight controls, the continuous decline in throttle setting in the later phase of rocket flight. The reason for the effect is clearly seen in Figure VII-17, the need to stay within the specific force bound as the rocket mass declines. Figure VII-14 shows that the lower specific force bound results in a steeper and greater decline in throttle setting, a consequence of similar rocket stage mass properties

and maximum rocket thrust magnitudes, with substantially reduced acceleration bounds.

Figure VII-15 shows a more extended time spent near the dynamic pressure bound for the lower specific force bound case. This effect is a consequence of the lower staging altitude combined with high rocket acceleration in the denser atmosphere, pushing the dynamic pressure back up temporarily. The lower staging altitude also causes the higher specific force during the prestaging aerodynamic pullup maneuver, as seen in Figure VII-16. The higher atmospheric density generates more lift, leading to the higher specific force.

7.4.4 Conflict Between Inequality Constraints

There are circumstances under which application of stringent constraints in both specific force and dynamic pressure can force substantial changes in solution character making it difficult to satisfy both bounds while still matching the requirements of the terminal equality constraints. A case was run where this effect was evident.

A run with a dynamic pressure bound of 2.0 g's was attempted. Table VII-6 and Figures VII-21 through VII-23 present some relevant results.

Table VII-6. Data from 2.0 g's, 800 psf bound case.
(Not a fully converged solution.)

Data Type	Value	Transition Point	Time (s)	Altitude (10 ³ ft)
Fuselage Width	35.1 ft	Scramjet Ignition	27.1	22.9
Scramjet Height	16.21 ft.	Turbojet Shutdown	171.9	73.2
Turbojet Height	9.76 ft	Staging	173.7	73.4
Max. Rocket Thrust	1.679×10 ⁶ lbf			
Staging Mach No.	3.56			
Rocket Flight Time	348 s			

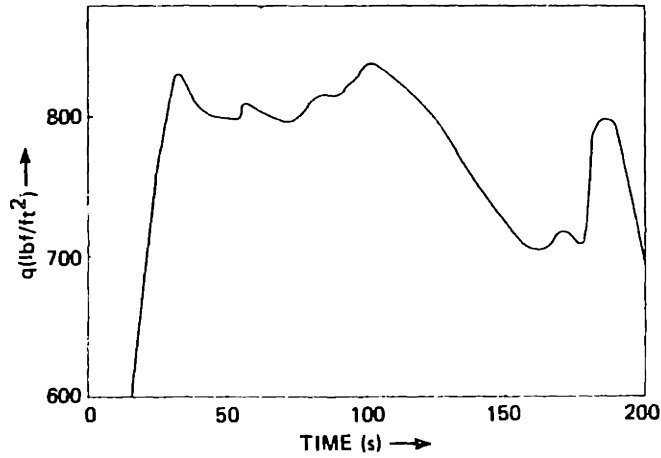


Figure VII-21. Dynamic pressure q vs. t . Bound violation region. Specific force bound = 2 g's. Dynamic pressure bound = 800 psf.

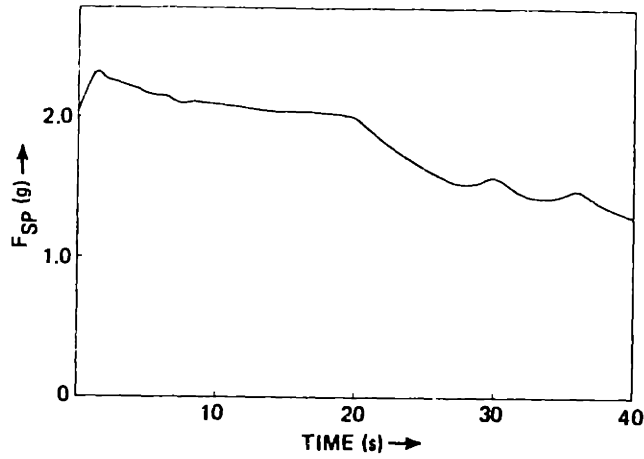


Figure VII-22. Specific force F_{sp} vs. t . Early flight. Specific force bound = 2 g's. Dynamic pressure bound = 800 psf.

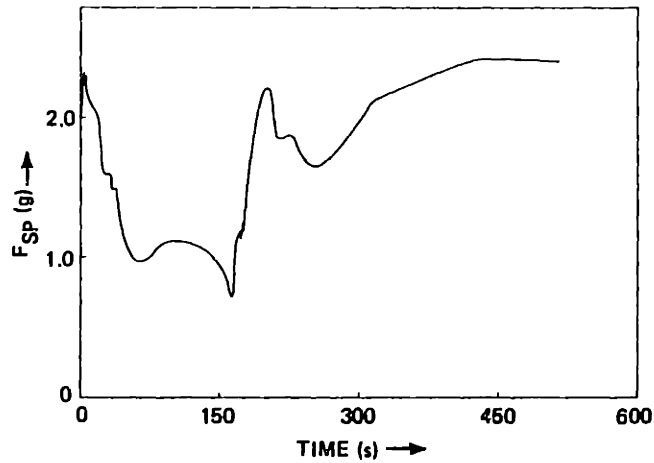


Figure VII-23. Specific force F_{sp} vs. t . Full flight time. Specific force bound = 2 g's. Dynamic pressure bound = 800 psf.

As one would expect with reduced specific force bounds, both the rocket and turbojet thrust capabilities decline, though slightly. The maximum rocket thrust is less than both cases II and IV, and the turbojet thrust capability, proportional to the product of the fuselage width and turbojet height, is less than both cases II and IV. However, inspection of Figure VII-21, the dynamic pressure in the high q range, and Figures VII-22 and VII-23, the specific force plots, show substantial violation of both bounds in spite of configuration and trajectory adjustments.

Comparison of Figures VII-21 and VII-22 show that the early flight specific force bound violations overlap the first peak in the dynamic pressure bound violations. Also, the dynamic pressure peak in rocket flight, at the right of Figure VII-21, hits the dynamic pressure bound at the same time as the second specific force bound violation peak occurs in Figure VII-23. This demonstrates that a conflict exists between the two bounds. The violation of the specific force bound in late rocket flight, seen at the right in Figure VII-23, is probably indirectly the result of the earlier time-bound difficulties combined with the continued requirement to satisfy the terminal equality constraints.

As a consequence of the overlapping violations, attempted satisfaction of one bound can adversely affect the magnitude of the violation of the other. The relative violation in the two different constraints depends on how heavily each violation is penalized.

The root of the problem is apparent upon inspection of the altitude of the first transition point. Comparison with cases II and IV show the altitude at scramjet ignition to decline with specific force bound. A lower altitude profile for the entire air-breathing flight, until near the staging point, results. With a similar staging altitude and Mach number to the other cases, higher Mach number flight at the lower altitudes results. The higher atmospheric density at the lower altitudes affects both dynamic pressure and specific force. Large changes in the early flight profile are likely to be necessary to get a suitable solution. The second order effects are likely to undergo major changes as well. This affects the choice of the metrics U and V , and makes the task of achieving convergence difficult.

7.5 Some Comments About the Scramjet

The low staging Mach number in all cases run on the computer provides little support for use of a scramjet in a vehicle with the flight

profile and configuration studied. However, this should not be interpreted as a universal condemnation of the supersonic combustion propulsion system.

The turbojet system model includes a rapid dropoff of specific impulse near the staging Mach number. When this effect is coupled with the dynamic pressure constraint, thrust diminishes rapidly. The scramjet mass capture ratio remains well below unity, limiting its thrust contribution, and forcing vehicle staging to sustain acceleration under rocket power.

Several changes in the vehicle design considerations could change the scramjet contributions.

Use of a rocket in the first stage, or a single-stage-to-orbit vehicle, which could overlap with air-breathing propulsion, could drive the vehicle to a Mach number range where the scramjet thrust could sustain vehicle acceleration to a considerably higher Mach number.

Development of a higher temperature tolerant turbojet system, with the resulting higher impulse, could accelerate the vehicle to the Mach number range where scramjet thrust propagates the air-breathing flight to higher velocities.

Reduction in scramjet system mass by development of light weight high temperature tolerant materials (i.e., ceramics) could sufficiently reduce first stage dry mass to permit the diminished low Mach number scramjet thrust to continue to accelerate the vehicle to the higher scramjet thrust Mach number range, again permitting the continuation of air-breathing flight until the scramjet impulse declines, and atmospheric density is insufficient to permit much thrust.

7.6 Summary

A variety of physical effects are evident as a result of the optimization cases run. The effects are seen to depend both marginally and heavily on the inequality constraint bounds.

Fuel consumption is very weakly associated with the magnitude of the inequality constraint bounds within the ranges studied.

Staging consistently occurs near Mach 3.4 for all cases studied implying little if any gain from scramjet propulsion, though this could be partly the consequence of the conservatively high scramjet mass model.

Air-breathing propulsion fuel consumption is small for the substantial velocity gain that results.

Throttling capability is essential to stay within specific force bounds at both takeoff and in late rocket flight. The slope in the throttle history plots during rocket flight is a function of the bound.

The altitude and time of the first transition point, and the times of the second and third transition points are strongly tied to dynamic pressure bounds. The air-breathing propulsion inlets are also a function of the dynamic pressure constraints. Lower air density at higher altitude, and larger inlets to retain sufficient mass capture combine to meet increasingly stringent dynamic pressure bounds.

The relative rate of energy gain in the two velocity components is a function of constraints, and affects the structure of the plots in first stage flight.

Finally, the angle of attack plots show effects from physical influences of the environment. Required lift for takeoff results in a high angle of attack in early flight, with dissipation properties in transonic flight forcing it negative. An aerodynamic turn preceding rocket ignition causes an increase, and radial velocity requirements after staging result in a sharp peak. Gravity turning then permits the angle of attack to approach zero at powered flight completion. The size of the effects in air-breathing flight are bound-dependent.

CHAPTER VIII

CONCLUSIONS AND SUGGESTIONS FOR FUTURE RESEARCH

8.1 An Overview

A gradient type algorithm for two-point boundary value optimization problems, permitting evaluation of optimal parameter values, optimal dynamic discontinuity locations, and optimal history of time varying controls, has been developed and applied to a two-staged air-breathing launch vehicle concept. Mathematical peculiarities of the algorithm, and physical characteristics of the air-breathing launch vehicle have been evaluated. Many interesting conclusions can be drawn from the work already done. Some significant research areas have been identified which, if pursued, could significantly expand the capabilities of this approach to flight vehicle design analysis.

8.2 Conclusions

It has been demonstrated that a gradient-type algorithm incorporating several classes of controls, including time varying control histories, time invariant design parameters, and locations of dynamic discontinuities, and permitting application of equality and inequality constraints can be derived and successfully applied to a design problem involving complex system dynamics.

The stability and rate of algorithm convergence are highly sensitive to several factors. An initial guess at the solution is necessary and will violate the equality constraints to some degree. A gradient correction term for the violations is included, but excessive initial constraint violations will destabilize the algorithm. The algorithm incorporates weighting matrices for each control vector element, referred to as metrics, whose element magnitudes strongly affect convergence rates. Guesses at system second derivative properties provide a basis for good selection of the metric elements. The algorithm step size is tied to a desired improvement in performance per iteration, and inappropriate assignment of the specified improvement can also adversely influence convergence rates.

The algorithm can in principle handle any system with any number of elements in the control vector or constraint set, though practical considerations limit this. The computation time grows rapidly with system dimension, and resolution of the numerical problems listed above becomes much more difficult with growth in system complexity.

The algorithm has been successfully implemented on a digital computer and applied to a hypothetical two staged launch vehicle with an air-breathing first stage and rocket second stage.

The most significant conclusion about the proposed launch vehicle concept is that overall fuel consumption to deliver a space shuttle sized payload to low earth orbit is relatively insensitive to substantial variations in the inequality constraint bounds on dynamic pressure and specific force when vehicle geometry modifications, propulsion mode change time modifications, and trajectory changes are all allowed to accommodate the constraint-bound variations.

In all cases run, the staging Mach number, the transition from air-breathing flight to rocket flight, occurred between $M = 3.3$ and $M = 3.5$. The relatively low staging Mach number in spite of the availability of a supersonic combustion ramjet, implies that little is gained from an air-breathing system suited to high Mach number flight. Turbojet power alone in the first stage, followed by rocket flight, is likely to provide similar performance with a less complex system. These effects may, however, be propulsion system mass model dependent.

Highly variable throttle settings in the propulsion systems are necessary to accommodate the specific force bounds imposed on the vehicle. The effect is particularly obvious in the later stages of rocket flight when the bound is followed in spite of declining system mass.

Reducing the dynamic pressure bound expands the air-breathing propulsion system inlets and raises the early low Mach number flight altitude, though staging states are very similar.

There is no reason to suppose that application of other inequality constraints will produce results any less interesting. The general approach seems to work well with definite trends apparent after a limited number of optimization cases are run to completion.

8.3 Suggested Future Research

The material presented in this dissertation may be perceived as a demonstration of a design technique on the simplest possible mathematical model of an air-breathing launch vehicle. This was done to keep computer software complexity within reasonable limits. It is clear that a number of research extensions would be worthwhile in characterizing the detailed behavior and physical properties of the desired launch vehicle. Some of these areas are suggested below, and active investigation of each is encouraged.

8.3.1 Rollout Fuel Consumption

A factor contributing to fuel consumption of the air-breathing launch vehicle not considered in the dissertation is fuel consumed in accelerating to takeoff speed. Due to the high thrust nature of the vehicle, and short flight time of the air-breathing stage, this acceleration may have a non-negligible effect on performance. It would be worthwhile to incorporate it into the dynamics model. Also, an optimal takeoff speed would result, eliminating the effect of fixing it as was done in the dissertation research.

8.3.2 Booster Flyback

A fully reuseable launch vehicle will require first stage flyback with corresponding fuel consumption and aerodynamic effects. The algorithm has not been designed to treat two separate vehicle trajectories simultaneously as would be required to track the booster stage after separation. Extension of the technique to handle the flyback booster problem would be enormously useful.

8.3.3 Scramjet Removal

The low staging Mach number and high scramjet structural weight suggest marginal benefit of a propulsion system that will require large economic investment to develop. Investigation of the comparative performance of a vehicle with turbojet and rocket propulsion only would be useful.

8.3.4 Better Wing Models

Development of a software package allowing greater wing shape flexibility and characterizing fuselage wing interaction explicitly would lead to more realistic configuration conclusions.

8.3.5 Aerodynamic Interaction Between Stages

Aerodynamic interaction between stages in the noted configuration was ignored. The drag contributions due to interference effects are probably not negligible. Though modelling these effects is complicated it would be a worthwhile endeavor.

8.3.6 Variable Rocket Fuel Mix

Work has been done elsewhere^[33,34] evaluating methods of mixing fuel types or changing fuel/oxidizer ratios in rockets to improve launch performance. Applying these techniques to the rocket flight portion of the air-breathing launch vehicle may result in some performance improvement. To permit comparison of the air-breathing vehicle to the pure rocket configurations incorporating these technologies requires variable rocket propulsion models to be included in the analysis.

8.3.7 Interactive Design

Many design considerations are not easily expressed mathematically, but can be perceived by an experienced engineer upon inspection. Permitting interactive optimization via CRT monitored results and plotting, and allowing interactive constraint adjustment may lead to rapid prototype design development. While improved computer processing rates may be necessary to make this technique effective, development of interactive software packages and CRT driver routines would be worthwhile.

8.3.8 Adaptive Metrics

Convergence of the optimization routine is not generally uniform in all dimensions, leading to the need to adjust the metrics to accommodate changing second derivative properties in the different control elements as the extremal point is approached. Devising a method to automatically adjust the metrics on a per iteration basis would be useful and would save substantial computer processing time.

8.3.9 Higher Fidelity Vehicle Dynamics Model

A variety of improvements to the dynamics model of the vehicle already studied can be applied to permit study of more detailed system behavior.

System rotational dynamics could be included, requiring aerodynamic pressure distributions as well as vehicle inertial properties. This would clearly affect the rate of change allowed in angle of attack.

Three dimensional orbital mechanics could be included, allowing study of the effects of inclined orbits and crossrange requirements on system behavior and performance.

Internal modeling of air-breathing propulsion dynamics could be developed to permit separate optimization of turbine and compressor sizing as well as inlet diffuser and outlet expansion nozzle shape. More accurate system dry mass properties would result.

The consequence of all the improvements mentioned above is a considerably higher control vector dimension, more state variables, and more constraints resulting in greatly expanded computer processing time requirements.

8.3.10 Single Stage to Orbit with Air-Breathing Propulsion

Some work has been done on single-stage-to-orbit launch vehicles including air-breathing propulsion in the lower Mach number flight regions.^[35] Optimization efforts could lead to interesting conclusions, particularly with the possibility of overlapping air-breathing and rocket power.

8.3.11 Less Conservative Scramjet Mass Models

The low staging Mach numbers obtained in the cases shown in Chapter VII suggest that the scramjet mass models may have been based on too high a heat flux tolerance. Comparison of results with cases using a more optimistic dry mass model would be useful to judge the true scramjet launch vehicle potential.

APPENDIX

OPTIMIZATION SOFTWARE PROGRAM

The following material is a compilation listing of the software implementation of the algorithm in Chapter IV with the dynamics and boundary conditions given in Chapters II, III, and V. All system-dependent references and debugging routines have been extracted.

The code is HAL, a language developed for use in the space shuttle program, and should be easily read. A few notes on how to read some keys in the code, how to recognize certain mathematical operands, and how to use the cross reference are useful.

Within the code listing, on the left, one will note statement numbers followed by the letters C, E, M, or S. The letter C simply denotes a nonexecutable comment. The other three letters specify the type of code line to the right. E represents the exponent line, if any, to operate on the M line representing the middle or main code line. S represents subscripts, and can occur more than once in a given statement if subscripts are nested.

To the right, after each statement, is a note of the procedure in which the statement is contained.

At the end of each procedure a listing of variables used within, but defined outside, is given. The mention of a compool is a reference to the HAL equivalent of a common block, found at the beginning of the listing in RUN_POOL.

Most mathematical operations are self-evident, but the notation for different multiplication routines may not be obvious.

For a scalar multiple of any function, a space is used. For vectors, the inner product uses a period (the "dot" product), the outer product uses a space, and the cross product uses a single asterisk. Matrix/vector multiples use a space. Division uses a slash.

The cross reference contains much useful information. For each variable, a specification to type of usage in each statement is given to the left of the statement number. The key is at the top of the cross reference. Multiple types of usages in a single statement add together in the key. At the end of the cross reference is a listing of preprogrammed function calls. This includes normal math functions. Some nonstandard functions are also included. These are Modulo Counters ("MOD"), scalar-to-integer roundup and round down functions ("CEILING" and "FLOOR"), scalar to integer truncation ("TRUNCATE") and matrix transposition ("TRANSPOSE").

STMT	SOURCE	CURRENT SCOPE
24+M	.0507, .0518, .0521, .0516, .047, .0378, .0327, .0295, .0263, .0261;	RUN_POOL
25+M	DECLARE MCR_MAX_INDEX INTEGER CONSTANT(5);	RUN_POOL
26+M	DECLARE MCR_M_ARRAY(MCR_MAX_INDEX) SCALAR DOUBLE CONSTANT(.5, 3.5, 5., 5.5, 8.);	RUN_POOL
27+M	DECLARE MCR_C_ARRAY(MCR_MAX_INDEX) SCALAR DOUBLE CONSTANT(.35, .6, .9, .65, .95);	RUN_POOL
28+M	DECLARE MAX_FS_AR_INDEX INTEGER CONSTANT(5);	RUN_POOL
29+M	DECLARE MAX_FS_M_INDEX INTEGER CONSTANT(10);	RUN_POOL
30+M	DECLARE FS_CD_MAT MATRIX(MAX_FS_AR_INDEX, MAX_FS_M_INDEX) DOUBLE CONSTANT(.77, .79, .80, .86, .69, .92, 1.0, 1.1, 1.45, 2.0, .47, .48, .42, .39, .41, .43, .58, .69, 1.1, 1.99, .30, .30, .27, .24, .26, .27, .34, .48, 1.0, 1.99, .25, .25, .23, .21, .22, .24, .31, .46, 1.0, 1.99, .22, .22, .21, .195, .21, .22, .28, .45, 1.0, 1.99);	RUN_POOL
31+M	DECLARE FS_CL_MAT MATRIX(MAX_FS_AR_INDEX, MAX_FS_M_INDEX) DOUBLE CONSTANT(.012, .013, .014, .0145, .0155, .015, .0145, .014, .012, .0075, .020, .033, .025, .028, .030, .028, .034, .015, .0075, .040, .044, .048, .053, .068, .062, .053, .039, .0175, .0075, .053, .059, .063, .072, .087, .074, .062, .042, .018, .0075, .065, .070, .073, .081, .098, .080, .070, .044, .019, .0075);	RUN_POOL
32+M	DECLARE FS_M_VAL ARRAY(MAX_FS_M_INDEX) SCALAR DOUBLE CONSTANT(.25, .6, .7, .9, 1.1, 1.2, 1.5, 2., 4., 8.);	RUN_POOL
33+M	DECLARE FS_A_VAL ARRAY(MAX_FS_AR_INDEX) SCALAR DOUBLE CONSTANT(.5, 1., 2., 3., 4.);	RUN_POOL
34+M	DECLARE DELIVERED_MASS SCALAR DOUBLE CONSTANT(6500.);	RUN_POOL
35+M	DECLARE DELIVERED_PLANFORM_AREA SCALAR DOUBLE CONSTANT(4000.);	RUN_POOL
36+M	DECLARE MAX_SS_ANGLE_INDEX INTEGER CONSTANT(5);	RUN_POOL
37+M	DECLARE MAX_SS_M_INDEX INTEGER CONSTANT(16);	RUN_POOL
38+M	DECLARE SS_CL_MAT MATRIX(MAX_SS_ANGLE_INDEX, MAX_SS_M_INDEX) DOUBLE CONSTANT(-.4974, -.5239, -.5734, -.6094, -.6373, -.6308, -.6263, -.6034, -.5550, -.4784, -.3735, -.3011, -.2390, -.2073, -.1860, -.1300, -.0393, -.0469, -.0501, -.0292, -.0257, -.0197, -.0118, -.0168, -.0348, -.0422, -.0595, -.0578, -.0529, -.0520, .4281, .4383, .4419, .4521, .5123, .5458, .5417, .5236, .4993, .4335, .3281, .2114, .1674, .1399, .1069, .1010, 1.0001, .9432, .8956, .8770, .9360, 1.0163, .9958, .9585, .9269, .8433, .6792, .5118, .4505, .4180, .3733, .3621, 1.1420,	RUN_POOL

STMT	SOURCE	CURRENT SCOPE
65*H	DECLARE PSI_START SCALAR DOUBLE CONSTANT(1.1);	RUN_FPOOL
66*H	DECLARE MAX_CUTOFF_ITERATIONS INTEGER CONSTANT(30);	RUN_FPOOL
67*H	DECLARE NEG_TIME_STEP ARRAY(NUM_TRANS_PTS) SCALAR DOUBLE INITIAL(.375, .375, .001);	RUN_FPOOL
68*H	DECLARE POS_TIME_STEP ARRAY(NUM_TRANS_PTS) SCALAR DOUBLE INITIAL(.125, .125, .499);	RUN_FPOOL
69*H	DECLARE W ARRAY((STEP_DIM + 2) / 2) MATRIX(NUM_CONTROLS, NUM_CONTROLS) DOUBLE;	RUN_FPOOL
70*H	DECLARE OMEGA_I_TIME ARRAY(NUM_TRANS_PTS) INTEGER;	RUN_FPOOL
71*H	DECLARE ITERATION INTEGER;	RUN_FPOOL
72*H	DECLARE FIRST_PSI_MAG SCALAR DOUBLE;	RUN_FPOOL
73*H	DECLARE L_FILE INTEGER;	RUN_FPOOL
74*H	DECLARE FIRST_ITERATION_FLAG BIT(1);	RUN_FPOOL
75*H	DECLARE P VECTOR(NUM_CONSTANT_PARAMETERS) DOUBLE;	RUN_FPOOL
76*H	DECLARE U_ACTIVE ARRAY(STEP_DIM + 1) VECTOR(NUM_CONTROLS) DOUBLE;	RUN_FPOOL
77*H	DECLARE U_TIME_KEEP ARRAY((STEP_DIM + 2) / 2) SCALAR DOUBLE;	RUN_FPOOL
78*H	DECLARE J_SCALE_FACTOR SCALAR DOUBLE INITIAL(3.);	RUN_FPOOL
79*H	DECLARE PSI_SCALE_FACTOR SCALAR DOUBLE INITIAL(2.);	RUN_FPOOL
80*H	DECLARE DELTA_COST_CHECK SCALAR DOUBLE INITIAL(-50.);	RUN_FPOOL
81*H	DECLARE DELTA_COST_SHRINK SCALAR DOUBLE INITIAL(.8);	RUN_FPOOL
82*H	DECLARE THETA_DOT_INITIAL SCALAR DOUBLE INITIAL(9.05E-05);	RUN_FPOOL
83*H	DECLARE CAP_Q SCALAR DOUBLE INITIAL(1.);	RUN_FPOOL
84*H	DECLARE Q_D SCALAR DOUBLE INITIAL(600.);	RUN_FPOOL
85*H	DECLARE CAP_CA SCALAR DOUBLE INITIAL(10.);	RUN_FPOOL
86*H	DECLARE G_D SCALAR DOUBLE INITIAL(2.0);	RUN_FPOOL
87*H	DECLARE STEP_SCALE_PSI SCALAR DOUBLE INITIAL(1.);	RUN_FPOOL
88*H	DECLARE STEP_SCALE_J SCALAR DOUBLE INITIAL(1.);	RUN_FPOOL
89*H	DECLARE PSI_COST_MIX SCALAR DOUBLE INITIAL(.04);	RUN_FPOOL
90*H	DECLARE MIN_PSI_THRESHOLD SCALAR DOUBLE INITIAL(.04);	RUN_FPOOL
91*H	DECLARE MAX_STEP_I INTEGER INITIAL(4);	RUN_FPOOL
92*H	DECLARE MIN_COST_ROOT SCALAR DOUBLE INITIAL(.1);	RUN_FPOOL

```

STMT          SOURCE          CURRENT SCOPE
93+M1  DECLARE MIN_PSI_RGHT SCALAR DOUBLE INITIAL(2.E03);      | RUN_POOL
94+M1  DECLARE DJS_INIT SCALAR DOUBLE INITIAL(-4000.);        | RUN_POOL
95+M1  DECLARE MAX_ITERATIONS INTEGER INITIAL(1341);          | RUN_POOL
96+M1  DECLARE PSI_CHECK SCALAR DOUBLE INITIAL(4.E-06);       | RUN_POOL
97+M1  DECLARE R_CUTOFF_CHECK SCALAR DOUBLE INITIAL(2500.);    | RUN_POOL
98+M1  DECLARE X_STORE ARRAY(STEP_DIM + 1) VECTOR(NUM_STATES) DOUBLE;
99+M1  DECLARE U_OLD_TIME ARRAY(STEP_DIM + 1) SCALAR DOUBLE;
100+M1  DECLARE FINAL_STEP INTEGER;
101+M1  CLOSE;

```

```

+D1 VERSION 1
*****END OF INCLUDED MEMBER, RVL 00, CATENATION NUMBER 1*****

```

STMT	SOURCE	CURRENT SCOPE
102 M	AIR_BREATHER_OPTIMIZATION:	AIR_BREATHER_OPTIMIZAT
102 M	PROCEDURE;	AIR_BREATHER_OPTIMIZAT
103 M	DECLARE DYNAMIC_PO SCALAR DOUBLE STATIC;	AIR_BREATHER_OPTIMIZAT
104 M	DECLARE STAGE_SEP_BIT(1) STATIC;	AIR_BREATHER_OPTIMIZAT
105 M	DECLARE H2_TANK_VOL SCALAR DOUBLE STATIC;	AIR_BREATHER_OPTIMIZAT
106 M	DECLARE HC_TANK_VOL SCALAR DOUBLE STATIC;	AIR_BREATHER_OPTIMIZAT
107 M	DECLARE TJ_FUEL_FLOW SCALAR DOUBLE STATIC;	AIR_BREATHER_OPTIMIZAT
108 M	DECLARE SS_FUEL_FLOW SCALAR DOUBLE STATIC;	AIR_BREATHER_OPTIMIZAT
109 M	DECLARE SCRJ_FUEL_FLOW SCALAR DOUBLE STATIC;	AIR_BREATHER_OPTIMIZAT
110 M	DECLARE NET_R_FORCE SCALAR DOUBLE STATIC;	AIR_BREATHER_OPTIMIZAT
111 M	DECLARE NET_THETA_FORCE SCALAR DOUBLE STATIC;	AIR_BREATHER_OPTIMIZAT
112 M	DECLARE N_AERO SCALAR DOUBLE STATIC;	AIR_BREATHER_OPTIMIZAT
113 M	DECLARE P_AERO SCALAR DOUBLE STATIC;	AIR_BREATHER_OPTIMIZAT
114 M	DECLARE SCRAMJET_THRUST SCALAR DOUBLE STATIC;	AIR_BREATHER_OPTIMIZAT
115 M	DECLARE TURSOJET_THRUST SCALAR DOUBLE STATIC;	AIR_BREATHER_OPTIMIZAT
116 M	DECLARE ROCKET_THRUST SCALAR DOUBLE STATIC;	AIR_BREATHER_OPTIMIZAT
117 M	DECLARE FIRST_STAGE_DRY_MASS SCALAR DOUBLE STATIC;	AIR_BREATHER_OPTIMIZAT
118 M	DECLARE TURBOJET_POWER_BIT(1) STATIC;	AIR_BREATHER_OPTIMIZAT
119 M	DECLARE SCRAMJET_POWER_BIT(1) STATIC;	AIR_BREATHER_OPTIMIZAT
120 M	DECLARE SS_DRY_MASS SCALAR DOUBLE STATIC;	AIR_BREATHER_OPTIMIZAT
121 M	DECLARE I_TIME INTEGER STATIC;	AIR_BREATHER_OPTIMIZAT
122 M	DECLARE RESHAPE_FLAG_BIT(1) STATIC;	AIR_BREATHER_OPTIMIZAT
123 M	DECLARE RO_0 SCALAR DOUBLE STATIC;	AIR_BREATHER_OPTIMIZAT
124 M	DECLARE RO_2 SCALAR DOUBLE STATIC;	AIR_BREATHER_OPTIMIZAT
125 M	DECLARE U2 SCALAR DOUBLE STATIC;	AIR_BREATHER_OPTIMIZAT
126 M	DECLARE DRO_DR SCALAR DOUBLE STATIC;	AIR_BREATHER_OPTIMIZAT
127 M	DECLARE CAP_PHI SCALAR DOUBLE STATIC;	AIR_BREATHER_OPTIMIZAT
128 M	DECLARE SCRJ_MASS_CAPTURE_RATIO SCALAR DOUBLE STATIC;	AIR_BREATHER_OPTIMIZAT

STMT

SOURCE

CURRENT SCOPE

```

109 M| DECLARE SCRAHJET_MASS SCALAR DOUBLE STATIC; | AIR_BREATHER_OPTIMIZAT
130 M| DECLARE M0 SCALAR DOUBLE STATIC; | AIR_BREATHER_OPTIMIZAT
131 M| DECLARE VEHICLE_ANGLE SCALAR DOUBLE STATIC; | AIR_BREATHER_OPTIMIZAT
132 M| DECLARE G_LOAD SCALAR DOUBLE STATIC; | AIR_BREATHER_OPTIMIZAT
133 M| DECLARE STATE_INTEGRATION_FLAG BIT(1) STATIC; | AIR_BREATHER_OPTIMIZAT
134 M| DECLARE L_TIME INTEGER STATIC; | AIR_BREATHER_OPTIMIZAT
135 M| DECLARE M0_2 SCALAR DOUBLE STATIC; | AIR_BREATHER_OPTIMIZAT
136 M| DECLARE T0 SCALAR DOUBLE STATIC; | AIR_BREATHER_OPTIMIZAT
137 M| DECLARE M2 SCALAR DOUBLE STATIC; | AIR_BREATHER_OPTIMIZAT
138 M| DECLARE BETA_NOSE_SHOCK SCALAR DOUBLE STATIC; | AIR_BREATHER_OPTIMIZAT
139 M| DECLARE THETA_NOSE SCALAR DOUBLE STATIC; | AIR_BREATHER_OPTIMIZAT
140 M| DECLARE TURBOJET_ISP SCALAR DOUBLE STATIC; | AIR_BREATHER_OPTIMIZAT
141 M| DECLARE SCRAHJET_ISP SCALAR DOUBLE STATIC; | AIR_BREATHER_OPTIMIZAT
142 M| DECLARE WING_AREA SCALAR DOUBLE STATIC; | AIR_BREATHER_OPTIMIZAT
143 M| DECLARE SS_PLANFORM_AREA SCALAR DOUBLE STATIC; | AIR_BREATHER_OPTIMIZAT
144 M| DECLARE LIFT SCALAR DOUBLE STATIC; | AIR_BREATHER_OPTIMIZAT
145 M| DECLARE DRAG SCALAR DOUBLE STATIC; | AIR_BREATHER_OPTIMIZAT
146 M| DECLARE MD_MASS SCALAR DOUBLE STATIC; | AIR_BREATHER_OPTIMIZAT
147 M| DECLARE NET_X_FORCE SCALAR DOUBLE STATIC; | AIR_BREATHER_OPTIMIZAT
148 M| DECLARE T2 SCALAR DOUBLE STATIC; | AIR_BREATHER_OPTIMIZAT
149 M| DECLARE OSLIRJE_SHOCK_FLAG BIT(1) STATIC; | AIR_BREATHER_OPTIMIZAT
150 M| DECLARE NORMAL_SHOCK_FLAG BIT(1) STATIC; | AIR_BREATHER_OPTIMIZAT
*** 151 M| DECLARE EXPANSION_FLAG BIT(1) STATIC; | AIR_BREATHER_OPTIMIZAT
152 M| DECLARE SUBSONIC_FLAG BIT(1) STATIC; | AIR_BREATHER_OPTIMIZAT
153 M| DECLARE DTO_DR SCALAR DOUBLE STATIC; | AIR_BREATHER_OPTIMIZAT
154 M| DECLARE DMCR_DM2 SCALAR DOUBLE STATIC; | AIR_BREATHER_OPTIMIZAT
*** 155 M| DECLARE DCL1_DM0 SCALAR DOUBLE STATIC; | AIR_BREATHER_OPTIMIZAT
156 M| DECLARE DCL2_DM0 SCALAR DOUBLE STATIC; | AIR_BREATHER_OPTIMIZAT

```

STMT	SOURCE	CURRENT SCOPE
157 MI	DECLARE DCD1_DMO SCALAR DOUBLE STATIC;	AIR_BREATHER_OPTIMIZAT
158 MI	DECLARE DCD2_DMO SCALAR DOUBLE STATIC;	AIR_BREATHER_OPTIMIZAT
159 MI	DECLARE DCL1_DAR SCALAR DOUBLE STATIC;	AIR_BREATHER_OPTIMIZAT
160 MI	DECLARE DCD1_DAR SCALAR DOUBLE STATIC;	AIR_BREATHER_OPTIMIZAT
161 MI	DECLARE CL SCALAR DOUBLE STATIC;	AIR_BREATHER_OPTIMIZAT
162 MI	DECLARE CD SCALAR DOUBLE STATIC;	AIR_BREATHER_OPTIMIZAT
163 MI	DECLARE SS_CL SCALAR DOUBLE STATIC;	AIR_BREATHER_OPTIMIZAT
164 MI	DECLARE SS_CD SCALAR DOUBLE STATIC;	AIR_BREATHER_OPTIMIZAT
165 MI	DECLARE SIN_VEHICLE_ANGLE SCALAR DOUBLE STATIC;	AIR_BREATHER_OPTIMIZAT
166 MI	DECLARE COS_VEHICLE_ANGLE SCALAR DOUBLE STATIC;	AIR_BREATHER_OPTIMIZAT
167 MI	DECLARE G SCALAR DOUBLE STATIC;	AIR_BREATHER_OPTIMIZAT
168 MI	DECLARE DCL2_DUAL SCALAR DOUBLE STATIC;	AIR_BREATHER_OPTIMIZAT
169 MI	DECLARE DCD2_DUAL SCALAR DOUBLE STATIC;	AIR_BREATHER_OPTIMIZAT
170 MI	DECLARE DCL_DALPHA SCALAR DOUBLE STATIC;	AIR_BREATHER_OPTIMIZAT
171 MI	DECLARE DCD_DCL2 SCALAR DOUBLE STATIC;	AIR_BREATHER_OPTIMIZAT

STMT	SOURCE	CURRENT SCORE
172 MI	MODEL_DRIVER:	MODEL_DRIVER
172 MI	PROCEDURE:	MODEL_DRIVER
CI	THE THRUST IS ALWAYS ASSUMED IN PLANE WITH THE X BODY AXIS.	MODEL_DRIVER
173 MI	DECLARE ROCKET_MAX_T SCALAR DOUBLE STATIC;	MODEL_DRIVER
174 MI	DECLARE NOSE_ANGLE SCALAR DOUBLE STATIC;	MODEL_DRIVER
175 MI	DECLARE H_SCRJ SCALAR DOUBLE STATIC;	MODEL_DRIVER
176 MI	DECLARE H_C SCALAR DOUBLE STATIC;	MODEL_DRIVER
177 MI	DECLARE H_C_TJ SCALAR DOUBLE STATIC;	MODEL_DRIVER
178 MI	DECLARE WING_SPAN SCALAR DOUBLE STATIC;	MODEL_DRIVER
179 MI	DECLARE DELTA_ANGLE SCALAR DOUBLE STATIC;	MODEL_DRIVER
180 MI	DECLARE HC_TANK_VOL_FRACTION SCALAR DOUBLE STATIC;	MODEL_DRIVER
181 MI	DECLARE FIRST_STAGE_LENGTH SCALAR DOUBLE STATIC;	MODEL_DRIVER
182 MI	DECLARE SS_MAX_FUEL_LOAD SCALAR DOUBLE STATIC;	MODEL_DRIVER
183 MI	DECLARE MAX_ROCKET_THRUST SCALAR DOUBLE STATIC;	MODEL_DRIVER
184 MI	DECLARE P0 SCALAR DOUBLE STATIC;	MODEL_DRIVER
185 MI	DECLARE U0 SCALAR DOUBLE STATIC;	MODEL_DRIVER
186 MI	DECLARE M1 SCALAR DOUBLE STATIC;	MODEL_DRIVER
187 MI	DECLARE P1 SCALAR DOUBLE STATIC;	MODEL_DRIVER
189 MI	DECLARE RO_1 SCALAR DOUBLE STATIC;	MODEL_DRIVER
189 MI	DECLARE T1 SCALAR DOUBLE STATIC;	MODEL_DRIVER
190 MI	DECLARE U1 SCALAR DOUBLE STATIC;	MODEL_DRIVER
191 MI	DECLARE F1 SCALAR DOUBLE AUTOMATIC;	MODEL_DRIVER
192 MI	DECLARE F2 SCALAR DOUBLE AUTOMATIC;	MODEL_DRIVER
193 MI	DECLARE F3 SCALAR DOUBLE AUTOMATIC;	MODEL_DRIVER
194 MI	DECLARE F4 SCALAR DOUBLE AUTOMATIC;	MODEL_DRIVER
195 MI	DECLARE F5 SCALAR DOUBLE AUTOMATIC;	MODEL_DRIVER
196 MI	DECLARE I_BETA INTEGER AUTOMATIC;	MODEL_DRIVER
197 MI	DECLARE R_NEW_BOUND SCALAR DOUBLE AUTOMATIC;	MODEL_DRIVER

SHT	SOURCE	CURRENT SCOPE
198 MI	DECLARE BETA_UPPER_BOUND SCALAR DOUBLE AUTOMATIC;	MODEL_DRIVER
199 MI	DECLARE BETA_LOWER_BOUND SCALAR DOUBLE AUTOMATIC;	MODEL_DRIVER
200 MI	DECLARE L_BETA SCALAR DOUBLE AUTOMATIC;	MODEL_DRIVER
201 MI	DECLARE BETA_NEW_BOUND SCALAR DOUBLE AUTOMATIC;	MODEL_DRIVER
202 MI	DECLARE M1_2 SCALAR DOUBLE AUTOMATIC;	MODEL_DRIVER
203 MI	DECLARE NU0 SCALAR DOUBLE AUTOMATIC;	MODEL_DRIVER
204 MI	DECLARE NU1 SCALAR DOUBLE AUTOMATIC;	MODEL_DRIVER
205 MI	DECLARE LOW_M_2 SCALAR DOUBLE AUTOMATIC;	MODEL_DRIVER
206 MI	DECLARE HIGH_M_2 SCALAR DOUBLE AUTOMATIC;	MODEL_DRIVER
207 MI	DECLARE M_2_FLAG BIT(1) AUTOMATIC;	MODEL_DRIVER
208 MI	DECLARE HIGH_NU SCALAR DOUBLE AUTOMATIC;	MODEL_DRIVER
209 MI	DECLARE MID_M_2 SCALAR DOUBLE AUTOMATIC;	MODEL_DRIVER
210 MI	DECLARE MID_NU SCALAR DOUBLE AUTOMATIC;	MODEL_DRIVER
211 MI	DECLARE EXTREMAL_ARRAY ARRAY(2) SCALAR DOUBLE AUTOMATIC;	MODEL_DRIVER
212 MI	DECLARE SIN_BETA_THETA_MAX SCALAR DOUBLE AUTOMATIC;	MODEL_DRIVER
213 MI	DECLARE BETA_THETA_MAX SCALAR DOUBLE AUTOMATIC;	MODEL_DRIVER
214 MI	DECLARE TAN_THETA_MAX SCALAR DOUBLE AUTOMATIC;	MODEL_DRIVER
215 MI	DECLARE THETA_MAX SCALAR DOUBLE AUTOMATIC;	MODEL_DRIVER
216 MI	DECLARE ANGLE_OF_ATTACK SCALAR DOUBLE STATIC;	MODEL_DRIVER
217 MI	DECLARE R SCALAR DOUBLE STATIC;	MODEL_DRIVER
218 MI	DECLARE U_R SCALAR DOUBLE STATIC;	MODEL_DRIVER
219 MI	DECLARE U_THETA SCALAR DOUBLE STATIC;	MODEL_DRIVER
220 MI	DECLARE U_T_AIR SCALAR DOUBLE STATIC;	MODEL_DRIVER
221 MI	DECLARE FS_LIFT SCALAR DOUBLE STATIC;	MODEL_DRIVER
222 MI	DECLARE FS_DRAG SCALAR DOUBLE STATIC;	MODEL_DRIVER
223 MI	DECLARE SS_LIFT SCALAR DOUBLE STATIC;	MODEL_DRIVER
224 MI	DECLARE SS_DRAG SCALAR DOUBLE STATIC;	MODEL_DRIVER

STMT	SOURCE	CURRENT SCOPE
225 MI	VEHICLE:	VEHICLE
225 MI	PROCEDURE:	VEHICLE
226 MI	DECLARE HIGH_M INTEGER AUTOMATIC;	VEHICLE
227 MI	DECLARE LOW_M INTEGER AUTOMATIC;	VEHICLE
228 MI	DECLARE I_SEARCH INTEGER AUTOMATIC;	VEHICLE
229 MI	DECLARE HIGH_CD SCALAR DOUBLE AUTOMATIC;	VEHICLE
230 MI	DECLARE LOW_CD SCALAR DOUBLE AUTOMATIC;	VEHICLE
231 MI	DECLARE HIGH_CL SCALAR DOUBLE AUTOMATIC;	VEHICLE
232 MI	DECLARE LOW_CL SCALAR DOUBLE AUTOMATIC;	VEHICLE
233 MI	DECLARE M_FIND BIT(1) AUTOMATIC;	VEHICLE

STMT	SOURCE	CURRENT SCOPE
234 MI	FIRST_STAGE;	FIRST_STAGE
234 MI	PROCEDURE;	FIRST_STAGE
235 MI	DECLARE CDO SCALAR DOUBLE STATIC;	FIRST_STAGE
236 MI	DECLARE ASPECT_RATIO SCALAR DOUBLE STATIC;	FIRST_STAGE
237 MI	DECLARE TURBOJET_MASS SCALAR DOUBLE AUTOMATIC;	FIRST_STAGE
238 MI	DECLARE FUSELAGE_SURFACE_AREA SCALAR DOUBLE AUTOMATIC;	FIRST_STAGE
239 MI	DECLARE BODY_MING_MASS SCALAR DOUBLE AUTOMATIC;	FIRST_STAGE
240 MI	DECLARE HC_TANK_MASS SCALAR DOUBLE AUTOMATIC;	FIRST_STAGE
241 MI	DECLARE H2_TANK_MASS SCALAR DOUBLE AUTOMATIC;	FIRST_STAGE
242 MI	DECLARE FIND_FLAG BIT(1) AUTOMATIC;	FIRST_STAGE
243 MI	DECLARE I_ZLD INTEGER AUTOMATIC;	FIRST_STAGE
244 MI	DECLARE LOW_CDO SCALAR DOUBLE AUTOMATIC;	FIRST_STAGE
245 MI	DECLARE LOW_M_S SCALAR DOUBLE AUTOMATIC;	FIRST_STAGE
246 MI	DECLARE HIGH_CDO SCALAR DOUBLE AUTOMATIC;	FIRST_STAGE
247 MI	DECLARE HIGH_M_S SCALAR DOUBLE AUTOMATIC;	FIRST_STAGE
248 MI	DECLARE I_MCR INTEGER AUTOMATIC;	FIRST_STAGE
249 MI	DECLARE MCR_FLAG BIT(1) AUTOMATIC;	FIRST_STAGE
250 MI	DECLARE A_FIND BIT(1) AUTOMATIC;	FIRST_STAGE
251 MI	DECLARE LOW_A INTEGER AUTOMATIC;	FIRST_STAGE
252 MI	DECLARE HIGH_A INTEGER AUTOMATIC;	FIRST_STAGE
253 MI	DECLARE DRY_TANK_VOLUME SCALAR DOUBLE AUTOMATIC;	FIRST_STAGE
254 MI	DECLARE FUSELAGE_VOLUME SCALAR DOUBLE AUTOMATIC;	FIRST_STAGE
255 MI	DECLARE DDCD_DCL2_DAR SCALAR DOUBLE AUTOMATIC;	FIRST_STAGE
256 MI	DECLARE DDCD_DCL2_DMO SCALAR DOUBLE AUTOMATIC;	FIRST_STAGE
257 MI	DECLARE DDCD_DMO SCALAR DOUBLE AUTOMATIC;	FIRST_STAGE
EI		
253 MI	IF RESHAPE_FLAG = ON THEN	FIRST_STAGE
259 MI	DO;	FIRST_STAGE

STMT	SOURCE	CURRENT SCOPE
C	THIS BRANCH COMPUTES GEOMETRY DEPENDENT FIRST STAGE PROPERTIES	FIRST_STAGE
C	ALL UNITS ARE MASS=SLUGS,LENGTH=FEET,TIME=SECONDS	FIRST_STAGE
260 M 1	SCRAMJET_MASS = (15.2 H_C) - (4.6 / H_C);	FIRST_STAGE
261 M 1	IF SCRAMJET_MASS < MIN_SCRJ_MASS_PER_FT THEN	FIRST_STAGE
262 M 1	SCRAMJET_MASS = MIN_SCRJ_MASS_PER_FT;	FIRST_STAGE
263 M 1	SCRAMJET_MASS = SCRAMJET_MASS W_SCRJ;	FIRST_STAGE
C	FOR THE BASIS OF THE SCRAMJET MASS MODEL	FIRST_STAGE
C	SEE FIG. 16 AND TABLE I OF 'SCRAMJET PERFORMANCE CHARACTERISTICS'	FIRST_STAGE
C	THE LOWER BOUND MASS IS BASED ON NON-PROPULSIVE SYSTEMS REQUIRED	FIRST_STAGE
C	TO OPERATE THE SCRAMJET	FIRST_STAGE
264 M 1	TURBOJET_MASS = 5. W_SCRJ H_C T_J;	FIRST_STAGE
C	THE MODEL FOR THE TURBOJET MASS IS	FIRST_STAGE
C	BASED ON GE CFA-6 DATA (JP-121 NOTES)	FIRST_STAGE
C	SCALED BY 2/3 FOR ADVANCED ENGINES	FIRST_STAGE
265 M 1	WING_AREA = (WING_SPAN WING_SPAN) / (4. TAN(DELTA_ANGLE));	FIRST_STAGE
C	TO KEEP THE NUMBER OF PARAMETERS TO A MINIMUM, THE ENGINE WIDTH IS	FIRST_STAGE
C	ASSUMED EQUAL TO THE FUSELAGE WIDTH	FIRST_STAGE
266 M 1	FUSELAGE_VOLUME = (FIRST_STAGE_LENGTH FIRST_STAGE_LENGTH W_SCRJ SIN(NOSE_ANGLE) SIN(FIRST_STAGE
266 M 1	NOZZLE_ANGLE)) / (SIN(ANGLE + NOZZLE_ANGLE) 2.);	FIRST_STAGE
267 M 1	FUSELAGE_SURFACE_AREA = (FIRST_STAGE_LENGTH (1. + ((SIN(ANGLE) + SIN(ANGLE) + SIN(ANGLE) /	FIRST_STAGE
267 M 1	SIN(ANGLE + NOZZLE_ANGLE))) W_SCRJ) + ((2. FUSELAGE_VOLUME) / W_SCRJ);	FIRST_STAGE
268 M 1	BODY_WING_MASS = .25 (FUSELAGE_SURFACE_AREA + WING_AREA);	FIRST_STAGE
C	THE BASIS OF THE BODY AND WING HEIGHT MODEL IS	FIRST_STAGE
C	EQ. 2.60 MARTIN MS THESIS	FIRST_STAGE
269 M 1	DRY_TANK_VOLUME = .8 FUSELAGE_VOLUME;	FIRST_STAGE
270 M 1	HC_TANK_VOL = DRY_TANK_VOLUME HC_TANK_VOL_FRACTION;	FIRST_STAGE
271 M 1	HC_TANK_MASS = .01 HYDROCARBON_DENSITY HC_TANK_VOL;	FIRST_STAGE
C	THE HYDROCARBON TANK MASS IS	FIRST_STAGE
C	BASED ON SCALED DCRN H2 TANK VALUE SINCE HC IS NOT CRYOGENIC	FIRST_STAGE
272 M 1	H2_TANK_VOL = DRY_TANK_VOLUME (1. - HC_TANK_VOL_FRACTION);	FIRST_STAGE
273 M 1	H2_TANK_MASS = .25 H2_DENSITY H2_TANK_VOL;	FIRST_STAGE
C	THE HYDROGEN TANK MASS IS	FIRST_STAGE
C	BASED ON H2/O2 PHI=1.6 TANKS=.05 FUEL HEIGHT SCALED TO H2 ONLY	FIRST_STAGE

```

SOURCE
CURRENT SCOPE
274 M 1 FIRST_STAGE_DRY_MASS = SCRANJET_MASS + TURBOJET_MASS + BODY_WING_MASS + HC_TANK_MASS + FIRST_STAGE
274 M 1 HC_TANK_MASS; FIRST_STAGE
275 M END; FIRST_STAGE
276 M ELSE FIRST_STAGE
276 M DO; FIRST_STAGE
C) THIS BRANCH COMPUTES MACH NUMBER, ALTITUDE, AND ANGLE OF ATTACK
C) DEPENDENT FIRST STAGE PROPERTIES
E)
277 M 1 IF ((M2 > 1.) AND (SCRANJET_FCHER = ON)) THEN FIRST_STAGE
DO;
278 M 1 IF M2 > MCR_M MCR_MAX_INDEX THEN FIRST_STAGE
S)
280 M 2 SCRJ_MASS_CAPTURE_RATIO = MCR_C MCR_MAX_INDEX;
S)
281 M 2 ELSE FIRST_STAGE
281 M 2 DO; FIRST_STAGE
E) MCR_FLAG = ON; FIRST_STAGE
282 M 3 DO FOR I_MCR = 2 TO MCR_MAX_INDEX WHILE MCR_FLAG = ON; FIRST_STAGE
E)
283 M 3 IF ((M2 < MCR_M I_MCR) OR (M2 = MCR_M I_MCR)) THEN FIRST_STAGE
S)
284 M 4 DO; FIRST_STAGE
E) MCR_FLAG = OFF; FIRST_STAGE
285 M 5 HIGH_M = I_MCR; FIRST_STAGE
286 M 5 END; FIRST_STAGE
287 M 4 LOW_M = HIGH_M - 1; FIRST_STAGE
288 M 3 SCRJ_MASS_CAPTURE_RATIO = MCR_C LOW_M + (((M2 - MCR_M LOW_M) (MCR_C HIGH_M -
S) MCR_C LOW_M) / (MCR_M HIGH_M - MCR_M LOW_M)); FIRST_STAGE
289 M 3 S) FIRST_STAGE

```



```

STMT
292 M| 3      DMCR_DM2 = (MCR_C      HIGH_M      - MCR_C      LOW_M      ) / (MCR_M      HIGH_M      - MCR_M      LOW_M      );
SI
293 M| 2      END;
294 M| 2      IF SCRJ_MASS_CAPTURE_RATIO < 0. THEN
295 M| 2      DO;
296 M| 3          SCRJ_MASS_CAPTURE_RATIO = 0.;
297 M| 3          DMCR_DM2 = 0.;
298 M| 2      END;
299 M| 1      ELSE
300 M| 1
301 M| 1      SCRJ_MASS_CAPTURE_RATIO = 0.;
302 M| 1      TURBOJET_ISP = 3800. - (300. M2) - (100. M2 M2);
EI
303 M| 1      SCRANJET_ISP = 15000. (M21.6) EXP(-1.73 (M2.52));
CI THE INSTALLED SPECIFIC IMPULSE EQUATIONS GIVEN ABOVE ARE BASED ON
CI A CURVE FIT.
CI SEE JONES AND HUEER 'AIRFRAME INTEGRATED PROPULSION SYSTEM FOR
CI HYPERSONIC CRUISE VEHICLES'
EI
304 M| 1      IF TURBOJET_FOXR = OFF THEN
305 M| 1      TURBOJET_THRUST = 0.;
EI
306 M| 1      IF SCRANJET_FOXR = OFF THEN
307 M| 1      SCRANJET_THRUST = 0.;
EI
308 M| 1      TURBOJET_THRUST = RO_2 U2 W_SCRJ H_C_TJ T_J_MAX_FUEL_AIR_RATIO 60 TURBOJET_ISP CAP_PHI;
EI
309 M| 1      SCRANJET_THRUST = RO_2 U2 W_SCRJ H_C_SCRJ_MASS_CAPTURE_RATIO SCRJ_MAX_FUEL_AIR_RATIO 60
EI
310 M| 1      SCRANJET_ISP CAP_PHI;
EI
311 M| 1      ASPECT_RATIO = (WING_SPAN WING_SPAN) / WING_AREA;

```

```

SOURCE
CURRENT SCOPE
310 MI 1  IF ((ASPECT_RATIO = FS_A_VAL             ) OR (ASPECT_RATIO > FS_A_VAL
SI         MAX_FS_AR_INDEX                         MAX_FS_AR_INDEX )) | FIRST_STAGE
310 MI 1  THEN | FIRST_STAGE
311 MI 1  HIGH_A = MAX_FS_AR_INDEX; | FIRST_STAGE
312 MI 1  ELSE | FIRST_STAGE
312 MI 1  DO; | FIRST_STAGE
313 MI 2  A_FIND = ON; | FIRST_STAGE
314 MI 2  DO FOR I_SEARCH = 2 TO MAX_FS_AR_INDEX WHILE A_FIND = ON; | FIRST_STAGE
315 MI 3  IF FS_A_VAL > ASPECT_RATIO THEN | FIRST_STAGE
SI         I_SEARCH
316 MI 3  DO; | FIRST_STAGE
317 MI 4  HIGH_A = I_SEARCH; | FIRST_STAGE
318 MI 4  A_FIND = OFF; | FIRST_STAGE
319 MI 3  END; | FIRST_STAGE
320 MI 2  END; | FIRST_STAGE
321 MI 1  LOW_A = HIGH_A - 1; | FIRST_STAGE
322 MI 1  IF ((M0 = FS_M_VAL             ) OR (M0 > FS_M_VAL
SI         MAX_FS_M_INDEX                         MAX_FS_M_INDEX )) THEN | FIRST_STAGE
324 MI 1  HIGH_M = MAX_FS_M_INDEX; | FIRST_STAGE
325 MI 1  ELSE | FIRST_STAGE
325 MI 1  DO; | FIRST_STAGE
326 MI 2  M_FIND = ON; | FIRST_STAGE
327 MI 2  DO FOR I_SEARCH = 2 TO MAX_FS_M_INDEX WHILE M_FIND = ON; | FIRST_STAGE
328 MI 3  IF FS_M_VAL > M0 THEN | FIRST_STAGE
SI         I_SEARCH
329 MI 3  DO; | FIRST_STAGE

```

```

SOURCE
STRT
330 MI 4                    HIGH_M = I_SEARCH;                    | FIRST_STAGE
EI
331 MI 4                    M_FIND = OFF;                         | FIRST_STAGE
332 MI 3                    END;                                     | FIRST_STAGE
333 MI 2                    END;                                     | FIRST_STAGE
334 MI 1                    END;                                     | FIRST_STAGE
335 MI 1                    LOW_M = HIGH_M - 1;                    | FIRST_STAGE
336 MI 1                    F1 = (M0 - FS_M_VAL                    | FIRST_STAGE
                              LOW_M                    HIGH_M                    - FS_M_VAL                    LOW_M);
337 MI 1                    LOW_CL = FS_CL_MAT                    | FIRST_STAGE
                              LCH_A,LOW_M                    + (F1 (FS_CL_MAT                    LOW_A,HIGH_M                    - FS_CL_MAT                    LOW_A,LOW_M));
338 MI 1                    LOW_CD = FS_CD_MAT                    | FIRST_STAGE
                              LOW_A,LOW_M                    + (F1 (FS_CD_MAT                    LOW_A,HIGH_M                    - FS_CD_MAT                    LOW_A,LOW_M));
339 MI 1                    HIGH_CL = FS_CL_MAT                    | FIRST_STAGE
                              HIGH_A,LOW_M                    + (F1 (FS_CL_MAT                    HIGH_A,HIGH_M                    - FS_CL_MAT                    HIGH_A,LOW_M));
340 MI 1                    HIGH_CD = FS_CD_MAT                    | FIRST_STAGE
                              HIGH_A,LOW_M                    + (F1 (FS_CD_MAT                    HIGH_A,HIGH_M                    - FS_CD_MAT                    HIGH_A,LOW_M));
341 MI 1                    F1 = (ASPECT_RATIO - FS_A_VAL                    | FIRST_STAGE
                              LCH_A                    / (FS_A_VAL                    HIGH_A                    - FS_A_VAL                    LOW_A));
342 MI 1                    IF ASPECT_RATIO > FS_A_VAL                    | FIRST_STAGE
                              MAX_FS_AR_INDEX                    THEN
343 MI 1                    DCD_DCL2 = HIGH_CD;                    | FIRST_STAGE
344 MI 1                    ELSE                                     | FIRST_STAGE
344 MI 1                    DCD_DCL2 = LOW_CD + (F1 (HIGH_CD - LOW_CD));                    | FIRST_STAGE
345 MI 1                    DCL_DALPHA = LCH_CL + (F1 (HIGH_CL - LOW_CL));                    | FIRST_STAGE
346 MI 1                    CL = DCL_DALPHA ANGLE_OF_ATTACK DEGREES_PER_RADIAN;                    | FIRST_STAGE
347 MI 1                    DCL1_DAR = ((HIGH_CL - LOW_CL) / (FS_A_VAL                    | FIRST_STAGE
                              HIGH_A                    - FS_A_VAL                    LOW_A)) (ANGLE_OF_ATTACK                    DEGREES_PER_RADIAN);                    | FIRST_STAGE
348 MI 1                    IF ASPECT_RATIO > FS_A_VAL                    | FIRST_STAGE
                              MAX_FS_AR_INDEX                    THEN
349 MI 1                    DDCD_DCL2_DAR = 0.;                    | FIRST_STAGE
350 MI 1                    ELSE                                     | FIRST_STAGE

```

```

SOURCE
STMT
350 MI 1          DDCD_DCL2_DAR = (HIGH_CD - LOW_CD) / (FS_A_VAL          HIGH_A - FS_A_VAL          LOW_A          );
SI
351 MI 1          DCD1_DAR = (DDCD_DCL2_DAR CL CL) + (.2. DCD_DCL2 CL DCL1_DAR);
352 MI 1          LOW_CL = FS_CL_MAT          LOW_A,LOW_M          + (F1 (FS_CL_MAT          HIGH_A,LOW_M          - FS_CL_MAT          LOW_A,LOW_M          ));
SI
353 MI 1          LOW_CD = FS_CD_MAT          LOW_A,LOW_M          + (F1 (FS_CD_MAT          HIGH_A,LOW_M          - FS_CD_MAT          LOW_A,LOW_M          ));
SI
354 MI 1          HIGH_CL = FS_CL_MAT          LOW_A,HIGH_M          + (F1 (FS_CL_MAT          HIGH_A,HIGH_M          - FS_CL_MAT          LOW_A,HIGH_M          ));
SI
355 MI 1          HIGH_CD = FS_CD_MAT          LOW_A,HIGH_M          + (F1 (FS_CD_MAT          HIGH_A,HIGH_M          - FS_CD_MAT          LOW_A,HIGH_M          ));
SI
356 MI 1          DCL1_DM0 = ((HIGH_CL - LOW_CL) / (FS_M_VAL          HIGH_M          - FS_M_VAL          LOW_M          )) (ANGLE_OF_ATTACK);
SI
357 MI 1          DEGREES_PER_RADIAN);
SI
358 MI 1          DDCD_DCL2_DM0 = (HIGH_CD - LOW_CD) / (FS_M_VAL          HIGH_M          - FS_M_VAL          LOW_M          );
SI
359 MI 1          IF ((M0 < M_ZLD ) OR (M0 = M_ZLD )) THEN
360 MI 1          C00 = ZLD ;
SI
361 MI 1          ELSE
362 MI 2          IF M0 ` M_ZLD          MAX_ZLD_INDEX          THEN
SI
363 MI 2          C00 = ZLD          MAX_ZLD_INDEX          ;
SI
364 MI 2          ELSE
365 MI 3          FIND_FLAG = OFF;
SI
366 MI 3          DO FOR I_ZLD = 2 TO MAX_ZLD_INDEX WHILE FIND_FLAG = OFF;
SI
367 MI 4          IF ((M0 < M_ZLD          ) OR (M0 = M_ZLD          )) THEN
SI

```

```

STMT          SOURCE          CURRENT SCOPE
368 M| 4      DO;              | FIRST_STAGE
369 M| 5      LOW_CDO = ZLD      | FIRST_STAGE
      S|        I_ZLD-1;
370 M| 5      LOW_M_S = M_ZLD    | FIRST_STAGE
      S|        I_ZLD-1;
371 M| 5      HIGH_CDO = ZLD     | FIRST_STAGE
      S|        I_ZLD;
372 M| 5      HIGH_M_S = M_ZLD   | FIRST_STAGE
      S|        I_ZLD;
      E|
373 M| 5      FIND_FLAG = ON;    | FIRST_STAGE
374 M| 4      END;              | FIRST_STAGE
375 M| 3      END;              | FIRST_STAGE
376 M| 3      CDO = LOW_CDO + ((HO - LOW_M_S) (HIGH_CDO - LOW_CDO)) / (HIGH_M_S - LOW_M_S); | FIRST_STAGE
377 M| 3      ;
378 M| 2      DCDO_DM0 = (HIGH_CDO - LOW_CDO) / (HIGH_M_S - LOW_M_S); | FIRST_STAGE
379 M| 1      END;              | FIRST_STAGE
380 M| 1      CD = (DCD_DCL2 CL CL) + CDO; | FIRST_STAGE
381 M| 1      DCD1_DM0 = (DCD_DCL2_DM0 CL CL) + DCDO_DM0 + (2. DCD_DCL2 CL DCL1_DM0); | FIRST_STAGE
382 M| 1      FI = SQRT(L_D_SCALE_FACTOR); | FIRST_STAGE
383 M| 1      CD = CD / FI;      | FIRST_STAGE
384 M| 1      CL = CL FI;       | FIRST_STAGE
385 M| 1      DCD1_DM0 = DCD1_DM0 / FI; | FIRST_STAGE
386 M| 1      DCL1_DM0 = DCL1_DM0 FI; | FIRST_STAGE
387 M| 1      DCD1_DAR = DCD1_DAR / FI; | FIRST_STAGE
388 M| 1      DCL1_DAR = DCL1_DAR FI; | FIRST_STAGE
      E|
389 M| 1      DCD_DCL2 = DCD_DCL2 / (FI ); | FIRST_STAGE
390 M| 1      DCL_DALPHA = DCL_DALPHA FI; | FIRST_STAGE
      E|
      CI FI IS A LIFT AND DRAG SCALING FACTOR TO PERMIT USING EXISTING DATA | FIRST_STAGE

```

133

```

STRT
SOURCE
CURRENT SCOPE
C| WHILE ASSUMING IMPROVED WING DESIGN
391 M| 1      FS_LIFT = CL 'WING_AREA DYNAMIC_PO;      | FIRST_STAGE
392 M| 1      FS_DRAG = CD WING_AREA DYNAMIC_PO;      | FIRST_STAGE
393 M| 1      IF FS_DRAG < 0. THEN      | FIRST_STAGE
394 M| 1      DO;      | FIRST_STAGE
395 M| 2      FS_DRAG = 0.;      | FIRST_STAGE
396 M| 2      CD = 0.;      | FIRST_STAGE
397 M| 2      DCDL_DMO = 0.;      | FIRST_STAGE
398 M| 2      DCDL_DAR = 0.;      | FIRST_STAGE
399 M| 2      DCD_DCL2 = 0.;      | FIRST_STAGE
400 M| 1      END;      | FIRST_STAGE
401 M|      END;      | FIRST_STAGE
402 M| CLOSE FIRST_STAGE;      | FIRST_STAGE

```

*** B L O C K S J M H A R Y ***

CONFOL VARIABLES USED

MIN_SCRJ_MASS_PER_FT, NOZZLE_ANGLE, HYDROCARBON_DENSITY, H2_DENSITY, MCR_MAX_INDEX, MCR_M, MCR_C, T_J_MAX_FUEL_AIR_RATIO, GO_SCRJ_MAX_FUEL_AIR_RATIO, MAX_FS_AR_INDEX, FS_A_VAL, MAX_FS_M_INDEX, FS_M_VAL, FS_CL_MAT, FS_CD_MAT, DEGRES_PER_RADIAN, M_ZLD_ZLD, MAX_ZLD_INDEX, L_D_SCALE_FACTOR

OUTER VARIABLES USED
 RESHAPE_FLAG, SCRAMJET_MASS, H_C, SCRAMJET_MASS, M_SCRJ, H_C_TJ, WING_AREA, WING_SPAN, DELTA_ANGLE, FIRST_STAGE_LENGTH
 NOSE_ANGLE, WING_AREA, HC_TANK_VOL, HC_TANK_VOL_FRACTION, HC_TANK_VOL, H2_TANK_VOL, H2_TANK_VOL, FIRST_STAGE_DRY_MASS, M2
 SCRAMJET_POWER, SCRJ_MASS_CAPTURE_RATIO, HIGH_M2, LOW_M2, HIGH_M, LOW_M, DTHR_DTHR, SCRJ_MASS_CAPTURE_RATIO, TURBOJET_ISP*
 SCRAMJET_ISP, TURBOJET_FCR, TURBOJET_THRUST, RO2, US, TURBOJET_ISP, CAP_PHI, SCRAMJET_THRUST, SCRAMJET_ISP, I_SEARCH*
 I_SEARCH, M0, M_FIND, M_FIND, FL, LCH_CL, HIGH_CD, HIGH_CD, OGD_DCL2, HIGH_CD, LOH_CD, DCL_DALPHA, LCH_CL
 HIGH_CL, CL, DCL_DALPHA, ANGLE_OF_ATTACK, DCLL_DAR, DCDL_DAR, CL, DCD_DCL2, DCLL_DAR, DCLL_DMO, CD, DCDL_DMO, DCLL_DMO, CD

```

SYMT          SOURCE          CURRENT SCOPE
403 MI SCND_STAGE:          | SCND_STAGE
403 MI PROCEDURE;          | SCND_STAGE
404 MI DECLARE ANG_FIND BIT(1) AUTOMATIC;          | SCND_STAGE
405 MI DECLARE LOW_ANGLE INTEGER AUTOMATIC;          | SCND_STAGE
406 MI DECLARE HIGH_ANGLE INTEGER AUTOMATIC;          | SCND_STAGE
407 MI DECLARE NO_FLAG BIT(1) AUTOMATIC;          | SCND_STAGE
EI
408 MI IF RESHAPE_FLAG = ON THEN          | SCND_STAGE
409 MI DO;          | SCND_STAGE
CI ALL UNITS ARE MASS=SLUGS,LENGTH=FEET,TIME=SECONDS          | SCND_STAGE
410 MI I SS_DRY_MASS = DELIVERED_MASS + (.04 SS_MAX_FUEL_LOAD) + (MAX_ROCKET_THRUST / 3220.);          | SCND_STAGE
CI THE ROCKET PROPELLANT TANK MASS MODEL IS          | SCND_STAGE
CI BASED ON TANK MASS=.04 FUEL MASS          | SCND_STAGE
EI
411 MI I SS_PLANFORM_AREA = DELIVERED_PLANFORM_AREA ((1. + (.0000334 SS_MAX_FUEL_LOAD))          | SCND_STAGE
        .6667          | SCND_STAGE
CI THE PLANFORM AREA IS DERIVED FROM A VOLUME/AREA SCALING LAW          | SCND_STAGE
CI BASED ON PHI=1.6          | SCND_STAGE
CI AVAILABLE VOLUME FOR FUEL=.8 TANK VOLUME          | SCND_STAGE
CI VOLUME DELIVERED=59000 CU. FT.          | SCND_STAGE
CI PLANFORM AREA PROPORTIONAL TO TANK VOLUME          | SCND_STAGE
CI LO2 DENSITY=2.223          | SCND_STAGE
CI LH2 DENSITY=.1357          | SCND_STAGE
412 MI END;          | SCND_STAGE
413 MI ELSE          | SCND_STAGE
413 MI DO;          | SCND_STAGE
414 MI I IF ((ANGLE_OF_ATTACK = SS_ANGLE_OF_ATTACK_VAL          | SCND_STAGE
SI          | SCND_STAGE
        MAX_SS_ANGLE_INDEX          | SCND_STAGE
        ) OR (ANGLE_OF_ATTACK >          | SCND_STAGE
        MAX_SS_ANGLE_INDEX          | SCND_STAGE
        )) THEN          | SCND_STAGE
SI          | SCND_STAGE
        SS_ANGLE_OF_ATTACK_VAL          | SCND_STAGE
        MAX_SS_ANGLE_INDEX          | SCND_STAGE
415 MI I HIGH_ANGLE = MAX_SS_ANGLE_INDEX;          | SCND_STAGE
416 MI I ELSE          | SCND_STAGE
SI          | SCND_STAGE
        DO;          | SCND_STAGE
416 MI I          | SCND_STAGE
SI          | SCND_STAGE
        ANG_FIND = ON;          | SCND_STAGE
417 MI 2          | SCND_STAGE
SI          | SCND_STAGE
        ANG_FIND = ON;          | SCND_STAGE

```

```

STMT          SOURCE          CURRENT SCOPE
-----
418 M| 2      E|              | SCND_STAGE
419 M| 3      S|              | SCND_STAGE
420 M| 3      DO;              | SCND_STAGE
421 M| 4              HIGH_ANGLE = I_SEARCH; | SCND_STAGE
422 M| 4      E|              | SCND_STAGE
423 M| 3      S|              | SCND_STAGE
424 M| 2      END;              | SCND_STAGE
425 M| 1      END;              | SCND_STAGE
426 M| 1      LOW_ANGLE = HIGH_ANGLE - 1; | SCND_STAGE
427 M| 1      IF M0 < SS_M_VAL THEN | SCND_STAGE
428 M| 1      S|              | SCND_STAGE
429 M| 2      DO;              | SCND_STAGE
430 M| 2      S|              | SCND_STAGE
431 M| 2      S|              | SCND_STAGE
432 M| 2      S|              | SCND_STAGE
433 M| 1      END;              | SCND_STAGE
434 M| 1      IF ((M0 = SS_M_VAL | SCND_STAGE
435 M| 1      S|              | SCND_STAGE
436 M| 2      S|              | SCND_STAGE
437 M| 2      S|              | SCND_STAGE
438 M| 2      S|              | SCND_STAGE

```



```

STMT          SOURCE          CURRENT SCOPE
439 M| 2      HIGH_CD = SS_CD_MAT      SCND_STAGE
   S|          HIGH_ANGLE,MAX_SS_M_INDEX
440 M| 1      END;                   SCND_STAGE
   E|
441 M| 1      MO_FLAG = OFF;          SCND_STAGE
442 M| 1      IF (((MO = SS_M_VAL_1) OR (MO > SS_M_VAL_1) AND (MO < SS_M_VAL_1
   S|          MAX_SS_M_INDEX)) THEN
443 M| 1      DO;                   SCND_STAGE
   E|
444 M| 2      M_FIND = ON;           SCND_STAGE
   E|
445 M| 2      DO FOR I_SEARCH = 2 TO MAX_SS_M_INDEX WHILE M_FIND = ON;
446 M| 3      IF SS_M_VAL_I_SEARCH > MO THEN
   S|
447 M| 3      DO;
448 M| 4      HIGH_M = I_SEARCH;
449 M| 4      M_FIND = OFF;
450 M| 3      END;
451 M| 2      END;
452 M| 2      LOW_M = HIGH_M - 1;
453 M| 2      F1 = (MO - SS_M_VAL_LOW_M) / (SS_M_VAL_HIGH_M - SS_M_VAL_LOW_M);
   S|
454 M| 2      LOW_CL = SS_CL_MAT_LOW_M + (F1 (SS_CL_MAT_LOW_ANGLE,HIGH_M
   S|          - SS_CL_MAT_LOW_ANGLE,HIGH_M));
454 M| 2      LOW_ANGLE,LOW_M
   S|
455 M| 2      LOW_CD = SS_CD_MAT_LOW_M + (F1 (SS_CD_MAT_LOW_ANGLE,HIGH_M
   S|          - SS_CD_MAT_LOW_ANGLE,HIGH_M));
455 M| 2      LOW_ANGLE,LOW_M
   S|
456 M| 2      HIGH_CL = SS_CL_MAT_LOW_M + (F1 (SS_CL_MAT_LOW_ANGLE,HIGH_M
   S|          - SS_CL_MAT_LOW_ANGLE,HIGH_M));
456 M| 2      HIGH_ANGLE,LOW_M
   S|

```

```

STMT          SOURCE          CURRENT SCOPE
457 M| 2      HIGH_CD = SS_CD_MAT + (F1 (SS_CD_MAT - SS_CD_MAT
SI           HIGH_ANGLE,LOW_M HIGH_ANGLE,HIGH_M
457 M| 2      HIGH_ANGLE,LOW_M
SI
EI
458 M| 2      MO_FLAG = ON;
SI
459 M| 1      END;
SI
460 M| 1      F1 = (ANGLE_OF_ATTACK - SS_ANGLE_OF_ATTACK_VAL LOW_ANGLE
SI           LOW_ANGLE) / (SS_ANGLE_OF_ATTACK_VAL
460 M| 1      HIGH_ANGLE - SS_ANGLE_OF_ATTACK_VAL LOW_ANGLE);
SI           LOW_ANGLE
461 M| 1      SS_CL = LOW_CL + (F1 (HIGH_CL - LOW_CL));
SI
462 M| 1      SS_CD = LOW_CD + (F1 (HIGH_CD - LOW_CD));
SI
463 M| 1      DCCL2_DUAL = (HIGH_CL - LOW_CL) / (SS_ANGLE_OF_ATTACK_VAL HIGH_ANGLE -
SI           HIGH_ANGLE)
463 M| 1      SS_ANGLE_OF_ATTACK_VAL LOW_ANGLE);
SI           LOW_ANGLE
464 M| 1      DCCL2_DUAL = (HIGH_CD - LOW_CD) / (SS_ANGLE_OF_ATTACK_VAL HIGH_ANGLE -
SI           HIGH_ANGLE)
464 M| 1      SS_ANGLE_OF_ATTACK_VAL LOW_ANGLE);
SI           LOW_ANGLE
EI
465 M| 1      IF MO_FLAG = ON THEN
SI
466 M| 1      DO:
SI
467 M| 2      LOW_CL = SS_CL_MAT LOW_ANGLE,LOW_M + (F1 (SS_CL_MAT HIGH_ANGLE,LOW_M - SS_CL_MAT
SI           LOW_ANGLE,LOW_M));
467 M| 2      LOW_ANGLE,LOW_M
SI
468 M| 2      LOW_CD = SS_CD_MAT LOW_ANGLE,LOW_M + (F1 (SS_CD_MAT HIGH_ANGLE,LOW_M - SS_CD_MAT
SI           LOW_ANGLE,LOW_M));
468 M| 2      LOW_ANGLE,LOW_M
SI
469 M| 2      HIGH_CL = SS_CL_MAT LOW_ANGLE,HIGH_M + (F1 (SS_CL_MAT HIGH_ANGLE,HIGH_M - SS_CL_MAT
SI           LOW_ANGLE,HIGH_M));
469 M| 2      LOW_ANGLE,HIGH_M
SI

```

```

ST:T
470 MI 2 HIGH_CD = SS_CD_MAT LOW_ANGLE,HIGH_M + (F1 (SS_CD_MAT HIGH_ANGLE,HIGH_M - SS_CD_MAT
SI
470 MI 2 LOW_ANGLE,HIGH_M ));
SI
471 MI 2 DCL2_DM0 = ((HIGH_CL - LOW_CL) / (SS_M_VAL HIGH_M - SS_M_VAL LOW_M ));
SI
472 MI 2 DCD2_DM0 = ((HIGH_CD - LOW_CD) / (SS_M_VAL HIGH_M - SS_M_VAL LOW_M ));
SI
473 MI 1 END;
474 MI 1 ELSE
474 MI 1 DO;
475 MI 2 DCL2_DM0 = 0.;
476 MI 2 DCD2_DM0 = 0.;
477 MI 1 END;
478 MI 1 F1 = SQRT(L_D_SCALE_FACTOR);
479 MI 1 SS_CL = SS_CL F1;
480 MI 1 SS_CD = SS_CD / F1;
481 MI 1 DCL2_DM0 = DCL2_DM0 F1;
482 MI 1 DCD2_DM0 = DCD2_DM0 / F1;
483 MI 1 DCL2_DUA1 = DCL2_DUA1 F1;
484 MI 1 DCD2_DUA1 = DCD2_DUA1 / F1;
C1 THE SCALING FACTOR (SQRT(F1)) IS TO ALLOW SHUTTLE LIFT/DRAG VALUES
C1 TO BE USED WHILE ASSUMING IMPROVED AERODYNAMICS OF A VEHICLE IN THE
C1 FUTURE
485 MI 1 SS_LIFT = SS_CL SS_PLANFORM_AREA DYNAMIC_P0;
486 MI 1 SS_DRAG = SS_CD SS_PLANFORM_AREA DYNAMIC_P0;
487 MI 1 IF SS_DRAG < 0. THEN
488 MI 1 DO;
489 MI 2 SS_DRAG = 0.;
490 MI 2 SS_CD = 0.;
491 MI 2 DCD2_DM0 = 0.;

```

```

STMT          SOURCE          CURRENT SCOPE
-----
492 M| 2      DCD2_DUAL = 0.;          | SCND_STAGE
493 M| 1      END;                    | SCND_STAGE
494 M|        END;                    | SCND_STAGE
495 M| CLOSE SCND_STAGE;              | SCND_STAGE

```

**** B L O C K S U M M A R Y ****

CCPOOL VARIABLES USED
DELIVERED_MASS, DELIVERED_PLANFORM_AREA, MAX_SS_ANGLE_INDEX, SS_ANGLE_OF_ATTACK_VAL, SS_M_VAL, SS_CL_MAT, SS_CD_MAT
MAX_SS_M_INDEX, L_D_SCALE_FACTOR

OUTER VARIABLES USED
RESHAPE_FLAG, SS_DRY_MASS*, SS_MAX_FUEL_LOAD, MAX_ROCKET_THRUST, SS_PLANFORM_AREA*, ANGLE_OF_ATTACK, I_SEARCH, MO
LOW_CL*, LOW_CD*, HIGH_CL*, HIGH_CD*, M_FIND*, M_FIND*, HIGH_M*, HIGH_M*, LOW_M*, LOW_M*, LC:LH, FL, SS_CL*, LOW_CL, HIGH_CL, SS_CD*
LCM_CD, HIGH_CD, DCL2_DUAL*, DCD2_DUAL*, DCL2_DHO*, DCD2_DHO*, SS_CL, SS_CD, DCL2_DUAL, DCL2_DUAL, DCD2_DUAL, SS_LIFT*
SS_PLANFORM_AREA, DYNAMIC_PO, SS_DRAG*, SS_DRAG

STMT	SOURCE	CURRENT SCOPE
EI		
496 MI	IF RESHAPE_FLAG = OFF THEN	VEHICLE
497 MI	DO;	VEHICLE
C	THIS IS CALLED TO COMPUTE VEHICLE FORCES, MAXIMUM THRUST, AND	VEHICLE
C	MAXIMUM FUEL FLOW	VEHICLE
EI		
498 MI	IF STAGE_SEP = OFF THEN	VEHICLE
499 MI	CALL FIRST_STAGE;	VEHICLE
500 MI	CALL SCND_STAGE;	VEHICLE
501 MI	END;	VEHICLE
502 MI	ELSE	VEHICLE
502 MI	DO;	VEHICLE
C	THIS IS CALLED IF THE VEHICLE GEOMETRY IS TO BE COMPUTED ALONG	VEHICLE
C	WITH EMPTY FUEL TANK VEHICLE MASS PROPERTIES	VEHICLE
503 MI	CALL FIRST_STAGE;	VEHICLE
504 MI	CALL SCND_STAGE;	VEHICLE
EI		
505 MI	RESHAPE_FLAG = OFF;	VEHICLE
506 MI	END;	VEHICLE
507 MI	CLOSE VEHICLE;	VEHICLE

**** B L O C K S U M M A R Y ****
 OUTER VARIABLES USED
 RESHAPE_FLAG, STAGE_SEP, RESHAPE_FLAG*

```

STMT              SOURCE              CURRENT SCOPE
508 M1 ENVIRONMENT:                    | ENVIRONMENT
509 M1 PROCEDURE;                      | ENVIRONMENT
510 M1 DECLARE LOW_ALT INTEGER AUTOMATIC; | ENVIRONMENT
511 M1 DECLARE HIGH_ALT INTEGER AUTOMATIC; | ENVIRONMENT
512 M1 DECLARE ALTITUDE SCALAR DOUBLE AUTOMATIC; | ENVIRONMENT
513 M1 DECLARE REL_RO SCALAR DOUBLE AUTOMATIC; | ENVIRONMENT
514 M1 ALTITUDE = X_STORE / (FEET_PER_METER ALT_METER_INTERVAL); | ENVIRONMENT
515 M1 I_TIME:1
516 M1 LOW_ALT = FLOOR(ALTITUDE) + 1;    | ENVIRONMENT
517 M1 IF LOW_ALT > MAX_ALT THEN       | ENVIRONMENT
518 M1 DO:                              | ENVIRONMENT
519 M1 WRITE(6) SKIP(2), COLUMN(30), 'ALTITUDE IS TOO HIGH', SKIP(2); | ENVIRONMENT
520 M1 REL_RO = ATH_DENS * MAX_ALT+1;  | ENVIRONMENT
521 M1 T0 = ATH_TEMP * 1.8;           | ENVIRONMENT
522 M1 DO:                              | ENVIRONMENT
523 M1 IF LOW_ALT < 1 THEN              | ENVIRONMENT
524 M1 T0 = ATH_TEMP * 1.8;           | ENVIRONMENT
525 M1 REL_RO = ATH_DENS * T0;        | ENVIRONMENT
526 M1 END;                             | ENVIRONMENT
527 M1 ELSE                             | ENVIRONMENT
528 M1 DO:                              | ENVIRONMENT

```

```

STMT          SOURCE          CURRENT SCOPE
528 M| 2      HIGH_ALT = LOW_ALT + 1;          | ENVIRONMENT
529 M| 2      T0 = (ATH_TEMP LOW_ALT         | ENVIRONMENT
    S|         + ((ALTITUDE - LOW_ALT + 1) (ATH_TEMP HIGH_ALT
529 M| 2      )) ) 1.0;                      | ENVIRONMENT
    S|         LOW_ALT
530 M| 2      DTO_DR = ((ATH_TEMP HIGH_ALT   | ENVIRONMENT
    S|         - ATH_TEMP LOW_ALT         ) 1.0) / (FEET_PER_METER
530 M| 2      ALT_METER_INTERVAL);          | ENVIRONMENT
531 M| 2      F1 = LOG(ATH_DENS LOW_ALT     | ENVIRONMENT
    S|         / ATH_DENS HIGH_ALT
532 M| 2      F2 = ATH_DENS LOW_ALT     EXP(F1 (LOW_ALT - 1)); | ENVIRONMENT
    S|
533 M| 2      REL_RO = F2 EXP(-F1 ALTITUDE); | ENVIRONMENT
C| THE DENSITY IS COMPUTED FROM AN EXPONENTIAL INTERPOLATION SCHEME
534 M| 2      DRO_DR = -(F1 REL_RO GROUND_RO) / (FEET_PER_METER ALT_METER_INTERVAL); | ENVIRONMENT
535 M| 1      END;                          | ENVIRONMENT
536 M|         END;                          | ENVIRONMENT
537 M|         RO_0 = REL_RO GROUND_RO;      | ENVIRONMENT
538 M|         PO = RO_0 R_0 T0;            | ENVIRONMENT
539 M|         MO = U0 / SQR(TGAPHA0 R_0 T0); | ENVIRONMENT
540 M|         G = (UNIVERSAL_G_CONSTANT EARTH_MASS) / (R R); | ENVIRONMENT
541 M| CLOSE ENVIRONMENT;                  | ENVIRONMENT

```

```

**** B L O C K   S U M M A R Y ****
COMPOC VARIABLES USED
X_STORE, FEET_PER_METER, ALT_METER_INTERVAL, MAX_ALT, ATH_DENS, ATH_TEMP, GROUND_RO, R_0, GAPHA0, UNIVERSAL_G_CONSTANT
EARTH_MASS
OUTER VARIABLES USED
I_TIME, TG*, DTO_DR*, F1*, F2*, DRO_DR*, RO_0*, PO*, R_0, TO, MO*, U0, G*, R

```

STMT	SOURCE	CURRENT SCOPE
542 M S	NOSE_ANGLE = P ; 1	MODEL_DRIVER
543 M S	H_SCRJ = P ; 2	MODEL_DRIVER
544 M S	H_C = P ; 3	MODEL_DRIVER
545 M S	H_C_TJ = P ; 4	MODEL_DRIVER
546 M S	WING_SPAN = P ; 5	MODEL_DRIVER
547 M S	DELTA_ANGLE = P ; 6	MODEL_DRIVER
548 M S	HC_TANK_VOL_FRACTION = P ; 7	MODEL_DRIVER
549 M S	FIRST_STAGE_LENGTH = P ; 8	MODEL_DRIVER
550 M S	SS_MAX_FUEL_LOAD = P ; 9	MODEL_DRIVER
551 M S	MAX_ROCKET_THRUST = P ; 10	MODEL_DRIVER
E		
552 M	IF RESHAPE_FLAG = ON THEN	MODEL_DRIVER
553 M	CALL VEHICLE;	MODEL_DRIVER
554 M	ELSE	MODEL_DRIVER
554 M	DO:	MODEL_DRIVER
E		
555 M 1	OBLIQUE_SHOCK_FLAG = OFF;	MODEL_DRIVER
E		
556 M 1	NORMAL_SHOCK_FLAG = OFF;	MODEL_DRIVER
E		
557 M 1	EXPANSION_FLAG = OFF;	MODEL_DRIVER
E		
558 M 1	SUBSONIC_FLAG = OFF;	MODEL_DRIVER
559 M 1	DCL_DALPHA = 0.;	MODEL_DRIVER
560 M 1	DCO_DCL2 = 0.;	MODEL_DRIVER


```

STMT                                SOURCE                                CURRENT SCOPE
561 M| 1 CL = 0.;                    | MODEL_DRIVER
562 M| 1 CD = 0.;                    | MODEL_DRIVER
563 M| 1 DCL1_DM0 = 0.;              | MODEL_DRIVER
564 M| 1 DCL2_DM0 = 0.;              | MODEL_DRIVER
565 M| 1 DCD1_DM0 = 0.;              | MODEL_DRIVER
566 M| 1 DCD2_DM0 = 0.;              | MODEL_DRIVER
567 M| 1 DCL1_DAR = 0.;              | MODEL_DRIVER
568 M| 1 DCD1_DAR = 0.;              | MODEL_DRIVER
569 M| 1 DMCR_DM2 = 0.;              | MODEL_DRIVER
570 M| 1 DTO_DR = 0.;               | MODEL_DRIVER
571 M| 1 DRO_DR = 0.;               | MODEL_DRIVER
572 M| 1 R = X_STORE + EARTH_RADIUS; | MODEL_DRIVER
    S| I_TIME:1
573 M| 1 U_R = X_STORE ;              | MODEL_DRIVER
    S| I_TIME:2
574 M| 1 U_THETA = R X_STORE ;        | MODEL_DRIVER
    S| I_TIME:4
575 M| 1 IF STATE_INTEGRATION_FLAG = ON THEN | MODEL_DRIVER
576 M| 1 DO;                          | MODEL_DRIVER
577 M| 2 ANGLE_OF_ATTACK = U_ACTIVE ;  | MODEL_DRIVER
    S| I_TIME:1
578 M| 2 CAP_PHI = 1. / (1. + (U_ACTIVE | MODEL_DRIVER
    S| I_TIME:2 U_ACTIVE I_TIME:2));
579 M| 1 END;                          | MODEL_DRIVER
580 M| 1 ELSE                          | MODEL_DRIVER
581 M| 2 ANGLE_OF_ATTACK = U_ACTIVE ;  | MODEL_DRIVER
    S| I_TIME:1
582 M| 2 CAP_PHI = 1. / (1. + (U_ACTIVE | MODEL_DRIVER
    S| I_TIME:2 U_ACTIVE I_TIME:2));
583 M| 1 END;                          | MODEL_DRIVER

```

STMT

SOURCE

CURRENT SCOPE

```

594 M1 1 M2 = 0.; MODEL_DRIVER
585 M1 1 RO_2 = 0.; MODEL_DRIVER
586 M1 1 U2 = 0.; MODEL_DRIVER
587 M1 1 T2 = 0.; MODEL_DRIVER
588 M1 1 U_T_AIR = U_THETA - (R EARTH_CHEGA); MODEL_DRIVER
C1 IT IS ASSUMED THAT THE ATMOSPHERE MOVES WITH THE EARTH'S SURFACE MODEL_DRIVER
589 M1 1 VEHICLE_ANGLE = ARCTAN(U_R / U_T_AIR) + ANGLE_OF_ATTACK; MODEL_DRIVER
590 M1 1 U0 = SQRT((U_R U_R) + (U_T_AIR U_T_AIR)); MODEL_DRIVER
591 M1 1 CALL ENVIRONMENT; MODEL_DRIVER
592 M1 1 DYNAMIC_PO = (RO_0 U0 U0) / 2.; MODEL_DRIVER
E1
593 M1 1 IF STAGE_SEP = OFF THEN MODEL_DRIVER
594 M1 1 DO; MODEL_DRIVER
595 M1 2 IF M0 < 1. THEN MODEL_DRIVER
596 M1 2 DO; MODEL_DRIVER
C1 THE CHANGE IN FLOW PROPERTIES FOR SUBSONIC FLOW IS IGNORED DUE TO MODEL_DRIVER
C1 THE SMALL EXPECTED FLOW DIRECTION CHANGES MODEL_DRIVER
E1
597 M1 3 SUBSONIC_FLAG = ON; MODEL_DRIVER
598 M1 3 P1 = P0; MODEL_DRIVER
599 M1 3 RO_1 = RO_0; MODEL_DRIVER
600 M1 3 T1 = T0; MODEL_DRIVER
601 M1 3 M1 = M0; MODEL_DRIVER
602 M1 3 U1 = U0; MODEL_DRIVER
END; MODEL_DRIVER
603 M1 2 ELSE MODEL_DRIVER
604 M1 2 DO; MODEL_DRIVER
605 M1 3 M0_2 = M0 M0; MODEL_DRIVER
E1
C1 THETA_NOSE, THE NOSE TURNING ANGLE IS SET EQUAL TO THE SUM OF THE MODEL_DRIVER
C1 ANGLE OF ATTACK AND VEHICLE CENTER LINE NOSE ANGLE. IF THETA_NOSE MODEL_DRIVER

```

STMT

SOURCE

CURRENT SCOPE

C1 IS GREATER THAN ZERO, AND THE FREE STREAM MACH NUMBER IS GREATER
 C1 THAN ONE, THEN A SEARCH IS MADE FOR A WEAK SHOCK SOLUTION. IF A
 C1 SOLUTION EXISTS, THEN IT IS FOUND. OTHERWISE NORMAL SHOCK
 C1 THEORY AND/OR SUBSONIC FLOW THEORY IS USED.

```

606 M1 3      THETA_NOSE = ANGLE_OF_ATTACK + NOSE_ANGLE;
607 M1 3      IF THETA_NOSE > 0. THEN
608 M1 3          DO;
C1 THE FOLLOWING IS FOR SHOCKED FLOW
609 M1 4          SIN_BETA_THETA_MAX = SORT(((GAM2 MO_2) - 4. + SQRT((GAM2 ((GAM2 MO_2 MO_2
609 M1 4          ) + (8. GAM3 MO_2) + 16.))) / (4. GAMMAO MO_2));
610 M1 4          BETA_THETA_MAX = ARCSIN(SIN_BETA_THETA_MAX);
611 M1 4          TAN_THETA_MAX = (2. ((MO_2 SIN_BETA_THETA_MAX SIN_BETA_THETA_MAX) - 1.)) /
611 M1 4          / (TAN(BETA_THETA_MAX) ((MO_2 (GAMMAO + COS(2. BETA_THETA_MAX))) + 2.));
612 M1 4          THETA_MAX = ARCTAN(TAN_THETA_MAX);
613 M1 4          IF ((THETA_NOSE < THETA_MAX) OR (THETA_NOSE = THETA_MAX)) THEN
614 M1 4              DO;
C1 THE FOLLOWING IS FOR OBLIQUE SHOCKS
E1
615 M1 5          OBLIQUE_SHOCK_FLAG = ON;
616 M1 5          EXTREMAL_ARRAY = THETA_NOSE;
S1
617 M1 5          EXTREMAL_ARRAY = ARCSIN(1. / MO);
S1
618 M1 5          BETA_LOWER_BOUND = MAX([EXTREMAL_ARRAY]);
619 M1 5          BETA_UPPER_BOUND = BETA_THETA_MAX;
620 M1 5          L_BETA = TAN(THETA_NOSE);
DO FOR I_BETA = 1 TO MAX_BETA_CYCLES;
621 M1 5          BETA_NEW_BOUND = (BETA_UPPER_BOUND + BETA_LOWER_BOUND) / 2.;
622 M1 6          R_NEW_BOUND = (2. ((MO_2 (SIN(BETA_NEW_BOUND)) - 1.)) / (TAN(
623 M1 6          BETA_NEW_BOUND) ((MO_2 (GAMMAO + COS(2. BETA_NEW_BOUND))) + 2.)) /
624 M1 6          BETA_NEW_BOUND)

```

```

STMT          SOURCE          CURRENT SCOPE
623 MI 6      );          | MODEL_DRIVER
624 MI 6      IF R_NEW_BOUND > L_BETA THEN | MODEL_DRIVER
625 MI 6      BETA_UPPER_BOUND = BETA_NEW_BOUND; | MODEL_DRIVER
626 MI 6      ELSE          | MODEL_DRIVER
627 MI 6      BETA_LOWER_BOUND = BETA_NEW_BOUND; | MODEL_DRIVER
628 MI 5      END;          | MODEL_DRIVER
              BETA_NOISE_SHOCK = (BETA_LOWER_BOUND + BETA_UPPER_BOUND) / 2.;
629 MI 5      F4 = SIN(BETA_NOISE_SHOCK) / 2.; | MODEL_DRIVER
630 MI 5      M1_2 = (1. + (GAM1 M0_2 F4)) / (((GAMMA0 M0_2 F4) - GAM1) (SIN( | MODEL_DRIVER
              BETA_NOISE_SHOCK - THETA_NOISE)) / 2.); | MODEL_DRIVER
631 MI 5      P1 = (1. + ((2. GAMMA0 ((M0_2 F4) - 1.)) / GAM2)) P0; | MODEL_DRIVER
632 MI 5      T1 = (1. + ((2. GAM3 ((M0_2 F4) - 1.)) ((GAMMA0 M0_2 F4) + 1.)) / ( | MODEL_DRIVER
              GAM2 GAM2 M0_2 F4)) T0; | MODEL_DRIVER
633 MI 4      END;          | MODEL_DRIVER
634 MI 4      ELSE          | MODEL_DRIVER
634 MI 4      DO;          | MODEL_DRIVER
              CI THE FOLLOWING IS FOR NORMAL SHOCKS
635 MI 5      NORMAL_SHOCK_FLAG = ON; | MODEL_DRIVER
636 MI 5      M1_2 = (1. + (GAM1 M0_2)) / ((GAMMA0 M0_2) - GAM1); | MODEL_DRIVER
637 MI 5      P1 = (1. + ((2. GAMMA0 (M0_2 - 1.)) / GAM2)) P0; | MODEL_DRIVER
638 MI 5      T1 = (1. + ((2. GAM3 ((GAMMA0 M0_2) + 1.)) (M0_2 - 1.)) / (GAM2 | MODEL_DRIVER
              GAM2 M0_2)) T0; | MODEL_DRIVER
639 MI 4      END;          | MODEL_DRIVER
640 MI 3      END;          | MODEL_DRIVER
641 MI 3      ELSE          | MODEL_DRIVER
641 MI 3      DO;          | MODEL_DRIVER

```



```

SOURCE
665 M| 4                    M1_2 = MID_M_2;                    | MODEL_DRIVER
666 M| 4                    T1 = (1. + (GAM1 M0_2)) / (1. + (GAM1 M1_2));                    | MODEL_DRIVER
E|
667 M| 4                    P1 = (T1                    GAM1_0/GAM3                    ) P0;                    | MODEL_DRIVER
668 M| 4                    T1 = T1 T0;                    | MODEL_DRIVER
669 M| 3                    END;                    | MODEL_DRIVER
670 M| 3                    M1 = SQRT(M1_2);                    | MODEL_DRIVER
671 M| 3                    RO_1 = P1 / (R_0 T1);                    | MODEL_DRIVER
672 M| 3                    U1 = M1 SQRT(GAM1_0 R_0 T1);                    | MODEL_DRIVER
673 M| 2                    END;                    | MODEL_DRIVER
C| THE CHANGES IN FLOW PROPERTIES IN THE SUBSONIC FLOW PAST THE
C| VEHICLE NOSE ARE IGNORED
674 M| 2                    M2 = M1;                    | MODEL_DRIVER
675 M| 2                    U2 = U1;                    | MODEL_DRIVER
676 M| 2                    RO_2 = RO_1;                    | MODEL_DRIVER
677 M| 2                    T2 = T1;                    | MODEL_DRIVER
C| IT IS ASSUMED NO FLOW FIELD INTERACTIONS AFFECT FLUID PROPERTIES
C| BETWEEN THE VEHICLE NOSE AND PROPULSION INLETS
678 M| 1                    END;                    | MODEL_DRIVER
679 M| 1                    SIN_VEHICLE_ANGLE = SIN(VEHICLE_ANGLE);                    | MODEL_DRIVER
680 M| 1                    COS_VEHICLE_ANGLE = COS(VEHICLE_ANGLE);                    | MODEL_DRIVER
681 M| 1                    CALL VEHICLE;                    | MODEL_DRIVER
E|
682 M| 1                    IF STAGE_SEP = OFF THEN                    | MODEL_DRIVER
683 M| 1                    ROCKET_MAX_T = 0.;                    | MODEL_DRIVER
ELSE
684 M| 1                    DO;                    | MODEL_DRIVER
ROCKET_MAX_T = MAX_ROCKET_THRUST;
685 M| 2                    SCRAMJET_THRUST = 0.;                    | MODEL_DRIVER
686 M| 2                    TURBOJET_THRUST = 0.;                    | MODEL_DRIVER
687 M| 2                    | MODEL_DRIVER

```

```

SOURCE
STMT          CURRENT SCOPE
688 M| 2      FS_LIFT = 0.;          | MODEL_DRIVER
689 M| 2      FS_DRAG = 0.;         | MODEL_DRIVER
690 M| 2      SCRJ_MASS_CAPTURE_RATIO = 0.; | MODEL_DRIVER
691 M| 1      END;                   | MODEL_DRIVER
692 M| 1      LIFT = FS_LIFT + SS_LIFT; | MODEL_DRIVER
693 M| 1      DRAG = FS_DRAG + SS_DRAG; | MODEL_DRIVER
694 M| 1      F1 = SIN(ANGLE_OF_ATTACK); | MODEL_DRIVER
695 M| 1      F2 = COS(ANGLE_OF_ATTACK); | MODEL_DRIVER
696 M| 1      P_AERO = (LIFT F1) - (DRAG F2); | MODEL_DRIVER
697 M| 1      N_AERO = (LIFT F2) + (DRAG F1); | MODEL_DRIVER
C| P_AERO AND N_AERO CONSTITUTE THE AERODYNAMIC FORCES IN BODY X AND Y
C| AXES RESPECTIVELY
698 M| 1      MD_MASS = SS_DRY_MASS + X_STORE I_TIME:5 + X_STORE I_TIME:6 + X_STORE I_TIME:7;
S|
E|
699 M| 1      IF STAGE_SEP = OFF THEN | MODEL_DRIVER
700 M| 1      MD_MASS = MD_MASS + FIRST_STAGE_DRY_MASS; | MODEL_DRIVER
701 M| 1      ROCKET_THRUST = CAP_PHI ROCKET_MAX_T; | MODEL_DRIVER
E|
702 M| 1      IF STAGE_SEP = OFF THEN | MODEL_DRIVER
703 M| 1      DO: | MODEL_DRIVER
704 M| 2      TJ_FUEL_FLOW = TURBOJET_THRUST / (TURBOJET_ISP GO); | MODEL_DRIVER
705 M| 2      SCRJ_FUEL_FLOW = SCRANJET_THRUST / (SCRANJET_ISP GO); | MODEL_DRIVER
706 M| 1      END; | MODEL_DRIVER
E|
707 M| 1      ELSE | MODEL_DRIVER
707 M| 1      DO: | MODEL_DRIVER
708 M| 2      TJ_FUEL_FLOW = 0.; | MODEL_DRIVER
709 M| 2      SCRJ_FUEL_FLOW = 0.; | MODEL_DRIVER
E|
710 M| 1      END; | MODEL_DRIVER
E|
711 M| 1      SS_FUEL_FLOW = ROCKET_THRUST / (ROCKET_ISP GO); | MODEL_DRIVER

```

```

SOURCE
CURRENT SCOPE
712 MI 1 NET_X_FORCE = TURBOJET_THRUST + SCRAJNET_THRUST + ROCKET_THRUST + P_AERO; | MODEL_DRIVER
713 MI 1 NET_R_FORCE = (NET_X_FORCE SIN_VEHICLE_ANGLE) + (N_AERO COS_VEHICLE_ANGLE) - (MD_MASS G); | MODEL_DRIVER
714 MI 1 NET_THETA_FORCE = (NET_X_FORCE COS_VEHICLE_ANGLE) - (N_AERO SIN_VEHICLE_ANGLE); | MODEL_DRIVER
715 MI 1 G_LOAD = SQRT((NET_X_FORCE + (N_AERO N_AERO)) / (MD_MASS G)); | MODEL_DRIVER
716 MI END; | MODEL_DRIVER
717 MI CLOSE MODEL_DRIVER; | MODEL_DRIVER

```

**** B L O C K S U M M A R Y ****

COMPOOL VARIABLES USED

P, X_STORE, EARTH_RADIUS, U_ACTIVE, EARTH_OMEGA, GAM2, GAM3, GAMMA0, MAX_BETA_CYCLES, GAMI, R_0, G0, ROCKET_ISP

OUTER VARIABLES USED

RESHAPE_FLAG, OBLIQUE_SHOCK_FLAG*, NORMAL_SHOCK_FLAG*, EXPANSION_FLAG*, DCL_DALPHA*, DCD_DCLC*, CL*, CD*
 DCL1_DM0*, DCL2_DM0*, DCD1_DM0*, DCD2_DM0*, DCHR_DM2*, DTD_DR*, DRO_DR*, I_TIME, STATE_INTEGRATION_FLAG
 CAP_PHI*, L_TIME, M2*, RO_2*, U2*, T2*, VEHICLE_ANGLE, DYNAMIC_PO*, RO_0, STAGE_SEP, H0, T0, H0_2*, THETA_NOSE*, THETA_NOSE
 H0_2, BETA_NOSE_SHOCK*, BETA_NOSE_SHOCK, SIN_VEHICLE_ANGLE*, VEHICLE_ANGLE, COS_VEHICLE_ANGLE*, SCRAJNET_THRUST*
 TURBOJET_THRUST*, SCRJ_MASS_CAPTURE_RATIO*, LIFT*, DRAG*, P_AEROM*, LIFT, DRAG, N_AEROC*, MD_MASS*, SS_DRY_MASS, MD_MASS
 FIRST_STAGE_DRY_MASS, ROCKET_THRUST*, CAP_PHI, TJ_FUEL_FLOW*, TURBOJET_THRUST, TURBOJET_ISP, SCRJ_FUEL_FLOW*, SCRAJNET_THRUST
 SCRAJNET_ISP, SS_FUEL_FLOW*, ROCKET_THRUST, NET_X_FORCE*, P_AERO, NET_R_FORCE*, NET_X_FORCE, SIN_VEHICLE_ANGLE, N_AERO
 COS_VEHICLE_ANGLE, G, NET_THETA_FORCE*, G_LOAD*


```

SOURCE
716 MI THESIS_ALGORITHM:      CURRENT SCOPE
716 MI PROCEDURE:      | THESIS_ALGORITHM
719 MI    DECLARE I_FD INTEGER STATIC:      | THESIS_ALGORITHM
720 MI    DECLARE FIRST_DERIV_FLAG BIT(1) STATIC:      | THESIS_ALGORITHM
721 MI    DECLARE PARTIAL_DERIV_FLAG BIT(1) STATIC:      | THESIS_ALGORITHM
722 MI    DECLARE DP_DUA VECTOR(NUM_CONTROLS) DOUBLE STATIC:      | THESIS_ALGORITHM
723 MI    DECLARE DN_DUA VECTOR(NUM_CONTROLS) DOUBLE STATIC:      | THESIS_ALGORITHM
724 MI    DECLARE RK_VAL_N MATRIX(10, NUM_CONSTRAINTS) DOUBLE STATIC:      | THESIS_ALGORITHM
725 MI    DECLARE RK_VAL_N_PLUS_1 MATRIX(10, NUM_CONSTRAINTS) DOUBLE STATIC:      | THESIS_ALGORITHM
C1    THE ABOVE TWO VARIABLES HAVE THE NUMBER OF ROWS EQUAL MAXI
C1    NUM_STATES+1,NUM_CONSTANT_PARAMETERS,NUM_CONSTRAINTS);      | THESIS_ALGORITHM
C1    THE ABOVE VARIABLES REQUIRE AN INITIALIZE/DIMENSION MATCH      | THESIS_ALGORITHM
726 MI    DECLARE NET_MASS ARRAY(STEP_DIM + 1) SCALAR DOUBLE STATIC:      | THESIS_ALGORITHM
727 MI    DECLARE L_X_STCRE ARRAY(STEP_DIM + 1) VECTOR(NUM_STATES) DOUBLE STATIC:      | THESIS_ALGORITHM
728 MI    DECLARE DM_DP ARRAY(NUM_CONSTANT_PARAMETERS) SCALAR DOUBLE STATIC:      | THESIS_ALGORITHM
729 MI    DECLARE H_SUB_U ARRAY((STEP_DIM + 2) / 2) VECTOR(NUM_CONTROLS) DOUBLE STATIC:      | THESIS_ALGORITHM
730 MI    DECLARE DELTA_U ARRAY((STEP_DIM + 2) / 2) VECTOR(NUM_CONTROLS) DOUBLE STATIC:      | THESIS_ALGORITHM
731 MI    DECLARE DELTA_V VECTOR(NUM_CONSTANT_PARAMETERS + NUM_TRANS_PTS) DOUBLE STATIC:      | THESIS_ALGORITHM
732 MI    DECLARE G_MAT ARRAY((STEP_DIM + 2) / 2) MATRIX(NUM_STATES, NUM_CONTROLS) DOUBLE STATIC:      | THESIS_ALGORITHM
733 MI    DECLARE CAP_LAMBDA_1 ARRAY((STEP_DIM + 2) / 2) MATRIX(NUM_STATES, NUM_CONSTRAINTS) DOUBLE STATIC:      | THESIS_ALGORITHM
733 MI    ;      | THESIS_ALGORITHM
734 MI    DECLARE CAP_LAMBDA_2 MATRIX(NUM_CONSTANT_PARAMETERS, NUM_CONSTRAINTS) DOUBLE STATIC:      | THESIS_ALGORITHM
735 MI    DECLARE PSI VECTOR(NUM_CONSTRAINTS) DOUBLE STATIC:      | THESIS_ALGORITHM
736 MI    DECLARE I_PSI_PSI MATRIX(NUM_CONSTRAINTS, NUM_CONSTRAINTS) DOUBLE STATIC:      | THESIS_ALGORITHM
737 MI    DECLARE DELTA_OMEGA_I_TIME ARRAY(NUM_TRANS_PTS) INTEGER STATIC:      | THESIS_ALGORITHM
738 MI    DECLARE I_PSI_J VECTOR(NUM_CONSTRAINTS) DOUBLE STATIC:      | THESIS_ALGORITHM
739 MI    DECLARE X_DOT VECTOR(NUM_STATES) DOUBLE STATIC:      | THESIS_ALGORITHM
740 MI    DECLARE F MATRIX(NUM_STATES, NUM_STATES) DOUBLE STATIC:      | THESIS_ALGORITHM
741 MI    DECLARE K MATRIX(NUM_STATES, NUM_CONSTANT_PARAMETERS) DOUBLE STATIC:      | THESIS_ALGORITHM

```

STMT	SOURCE	CURRENT SCOPE
742 MI	DECLARE LAMBDA_DOT VECTOR(NUM_STATES) DOUBLE STATIC;	THESIS_ALGORITHM
743 MI	DECLARE CAP_LAMBDA_1_DOT MATRIX(NUM_STATES, NUM_CONSTRAINTS) DOUBLE STATIC;	THESIS_ALGORITHM
744 MI	DECLARE CAP_LAMBDA_2_DOT MATRIX(NUM_CONSTANT_PARAMETERS, NUM_CONSTRAINTS) DOUBLE STATIC;	THESIS_ALGORITHM
745 MI	DECLARE I_PSI_J_DOT VECTOR(NUM_CONSTRAINTS) DOUBLE STATIC;	THESIS_ALGORITHM
746 MI	DECLARE I_PSI_FSI_DOT MATRIX(NUM_CONSTRAINTS, NUM_CONSTRAINTS) DOUBLE STATIC;	THESIS_ALGORITHM
747 MI	DECLARE SGV_DOT VECTOR(NUM_CONSTANT_PARAMETERS) DOUBLE STATIC;	THESIS_ALGORITHM
748 MI	DECLARE LAMBDA_ARRAY(1001) VECTOR(NUM_STATES) DOUBLE STATIC;	THESIS_ALGORITHM
749 MI	DECLARE M MATRIX(NUM_CONSTRAINTS, NUM_CONSTANT_PARAMETERS + NUM_TRANSPTS) DOUBLE STATIC;	THESIS_ALGORITHM
750 MI	DECLARE SMALL_G_VEC VECTOR(NUM_CONSTANT_PARAMETERS + NUM_TRANSPTS) DOUBLE STATIC;	THESIS_ALGORITHM
751 MI	DECLARE U_J_OLD_TIME ARRAY((STEP_DIM + 2) / 2) SCALAR DOUBLE STATIC;	THESIS_ALGORITHM
752 MI	DECLARE U_NEW_TIME ARRAY(STEP_DIM + 1) SCALAR DOUBLE STATIC;	THESIS_ALGORITHM
753 MI	DECLARE TIME_STEP SCALAR DOUBLE STATIC;	THESIS_ALGORITHM
754 MI	DECLARE FINAL_TIME_STEP SCALAR DOUBLE STATIC;	THESIS_ALGORITHM
755 MI	DECLARE TIME_INTERVAL SCALAR DOUBLE STATIC;	THESIS_ALGORITHM
756 MI	DECLARE C_SUB_PSI SCALAR DOUBLE STATIC;	THESIS_ALGORITHM
757 MI	DECLARE DELTA_CCST SCALAR DOUBLE STATIC;	THESIS_ALGORITHM
758 MI	DECLARE OJS SCALAR DOUBLE STATIC;	THESIS_ALGORITHM
759 MI	DECLARE I_J_J SCALAR DOUBLE STATIC;	THESIS_ALGORITHM
760 MI	DECLARE I_J_J_DOT SCALAR DOUBLE STATIC;	THESIS_ALGORITHM
761 MI	DECLARE LAMBDA_FLAG BIT(1) STATIC;	THESIS_ALGORITHM
762 MI	DECLARE CAP_LAMBDA_1_FLAG BIT(1) STATIC;	THESIS_ALGORITHM
763 MI	DECLARE CAP_LAMBDA_2_FLAG BIT(1) STATIC;	THESIS_ALGORITHM
764 MI	DECLARE SGV_FLAG BIT(1) STATIC;	THESIS_ALGORITHM
765 MI	DECLARE I_J_J_FLAG BIT(1) STATIC;	THESIS_ALGORITHM
766 MI	DECLARE I_PSI_J_FLAG BIT(1) STATIC;	THESIS_ALGORITHM
767 MI	DECLARE I_PSI_PSI_FLAG BIT(1) STATIC;	THESIS_ALGORITHM
768 MI	DECLARE RK_ROWS INTEGER STATIC;	THESIS_ALGORITHM
769 MI	DECLARE RK_COLUMNS INTEGER STATIC;	THESIS_ALGORITHM

STMT	SOURCE	CURRENT SCOPE
770 M	DECLARE CONFIG_INDEX INTEGER STATIC;	THESIS_ALGORITHM
771 M	DECLARE MASS_FLOW_FINAL_STEP_SCALAR DOUBLE STATIC;	THESIS_ALGORITHM
772 M	DECLARE M1_FLOW_FINAL_STEP_SCALAR DOUBLE STATIC;	THESIS_ALGORITHM
773 M	DECLARE M2_FLOW_FINAL_STEP_SCALAR DOUBLE STATIC;	THESIS_ALGORITHM
774 M	DECLARE M3_FLOW_FINAL_STEP_SCALAR DOUBLE STATIC;	THESIS_ALGORITHM
775 M	DECLARE I_LOOP INTEGER STATIC;	THESIS_ALGORITHM
776 M	DECLARE I_STORE INTEGER STATIC;	THESIS_ALGORITHM
777 M	DECLARE J_STORE INTEGER STATIC;	THESIS_ALGORITHM
778 M	DECLARE PSI_MAG_SCALAR DOUBLE STATIC;	THESIS_ALGORITHM
779 M	DECLARE ITER_FLAG BIT(1) STATIC;	THESIS_ALGORITHM
780 M	DECLARE IIT INTEGER STATIC;	THESIS_ALGORITHM
781 M	DECLARE COST_SCALAR DOUBLE STATIC;	THESIS_ALGORITHM
782 M	DECLARE OVER_ITER_FLAG BIT(1) STATIC;	THESIS_ALGORITHM
783 M	DECLARE I_TIME_STORE INTEGER STATIC;	THESIS_ALGORITHM
784 M	DECLARE OVER_STEP BIT(1) STATIC;	THESIS_ALGORITHM
785 M	DECLARE J_TIME INTEGER STATIC;	THESIS_ALGORITHM
786 M	DECLARE FD_COURT INTEGER STATIC;	THESIS_ALGORITHM
787 M	DECLARE INTEG_L_SCALAR DOUBLE STATIC;	THESIS_ALGORITHM
788 M	DECLARE L_FINAL_SCALAR DOUBLE STATIC;	THESIS_ALGORITHM
789 M	DECLARE I_CL INTEGER STATIC;	THESIS_ALGORITHM
790 M	DECLARE FD_FLAG BIT(1) STATIC;	THESIS_ALGORITHM
791 M	DECLARE PRESENT_TIME_STEP_SCALAR DOUBLE STATIC;	THESIS_ALGORITHM
792 M	DECLARE OIT_FLAG BIT(1) STATIC;	THESIS_ALGORITHM
793 M	DECLARE T_FLAG BIT(1) AUTOMATIC;	THESIS_ALGORITHM
794 M	DECLARE HELD_FS_MASS_SCALAR DOUBLE STATIC;	THESIS_ALGORITHM
795 M	DECLARE U_TIME INTEGER STATIC;	THESIS_ALGORITHM
796 M	DECLARE U_MATRIX(NUM_CONTROLS, NUM_CONTROLS) DOUBLE STATIC;	THESIS_ALGORITHM
797 M	DECLARE DJS_SCALE_SCALAR DOUBLE STATIC;	THESIS_ALGORITHM

STMT	SOURCE	CURRENT SCOPE
798 HI	DECLARE HOLD_X ARRAY(STEP_DIM + 1) VECTOR(NUM_STATES) DOUBLE STATIC;	THESIS_ALGORITHM
799 HI	DECLARE HOLD_M ARRAY(STEP_DIM + 1) SCALAR DOUBLE STATIC;	THESIS_ALGORITHM
800 HI	DECLARE HOLD_L_X ARRAY(STEP_DIM + 1) VECTOR(NUM_STATES) DOUBLE STATIC;	THESIS_ALGORITHM
801 HI	DECLARE HOLD_P VECTOR(NUM_CONSTANT_PARAMETERS) DOUBLE STATIC;	THESIS_ALGORITHM
802 HI	DECLARE HOLD_U_T ARRAY(STEP_DIM + 1) SCALAR DOUBLE STATIC;	THESIS_ALGORITHM
803 HI	DECLARE HOLD_T ARRAY(NUM_TRANSPTS) INTEGER STATIC;	THESIS_ALGORITHM
804 HI	DECLARE HOLD_U ARRAY(STEP_DIM + 1) VECTOR(NUM_CONTROLS) DOUBLE STATIC;	THESIS_ALGORITHM
805 HI	DECLARE HOLD_POS_TIME ARRAY(NUM_TRANSPTS) SCALAR DOUBLE STATIC;	THESIS_ALGORITHM
806 HI	DECLARE HOLD_NEG_TIME ARRAY(NUM_TRANSPTS) SCALAR DOUBLE STATIC;	THESIS_ALGORITHM
807 HI	DECLARE STEP_I INTEGER STATIC;	THESIS_ALGORITHM
808 HI	DECLARE FIRST_PASS_PSI_MAG SCALAR DOUBLE STATIC;	THESIS_ALGORITHM
809 HI	DECLARE L_SUB_U_1 VECTOR(NUM_CONTROLS) DOUBLE STATIC;	THESIS_ALGORITHM
810 HI	DECLARE L_SUB_U_3 VECTOR(NUM_CONTROLS) DOUBLE STATIC;	THESIS_ALGORITHM
811 HI	DECLARE L_SUB_U_L VECTOR(NUM_CONTROLS) DOUBLE STATIC;	THESIS_ALGORITHM

```

SOURCE
CURRENT SCOPE
812 M| U_COMPUTE: | U_COMPUTE
812 M| PROCEDURE: | U_COMPUTE
813 M| DECLARE U_A INTEGER AUTOMATIC; | U_COMPUTE
814 M| DECLARE U_B INTEGER AUTOMATIC; | U_COMPUTE
815 M| DECLARE U_I INTEGER AUTOMATIC; | U_COMPUTE
816 M| DECLARE U_SET BIT(1) AUTOMATIC; | U_COMPUTE
817 M| DECLARE U_VAL SCALAR DOUBLE AUTOMATIC; | U_COMPUTE
818 M| U_I = (2 NUM_TRANSPTS) + 3; | U_COMPUTE
819 M| U_A = U_TIME - U_I; | U_COMPUTE
820 M| IF U_A < 2 THEN | U_COMPUTE
821 M|     U_A = 2; | U_COMPUTE
822 M| U_B = U_TIME + U_I; | U_COMPUTE
823 M| IF U_B > FLOOR((FINAL_STEP + 2) / 2) THEN | U_COMPUTE
824 M|     U_B = FLOOR((FINAL_STEP + 2) / 2); | U_COMPUTE
825 M| U_SET = ON; | U_COMPUTE
826 M| DO FOR U_I = U_A TO U_B WHILE U_SET = ON; | U_COMPUTE
827 M| 1 IF ((U_TIME_KEEP > U_J_OLD_TIME) OR (U_TIME_KEEP = U_J_OLD_TIME)) THEN | U_COMPUTE
827 M| S| U_I | U_I
828 M| 1 DO; | U_COMPUTE
829 M| 2 U_SET = OFF; | U_COMPUTE
830 M| 2 U_VAL = (U_TIME_KEEP - U_J_OLD_TIME) / (U_TIME_KEEP - U_I - 1); | U_COMPUTE
830 M| S| U_I - 1 | U_I - 1
831 M| 2 U = W + ((W - W) * U_I - 1) / (U_I - 1); | U_COMPUTE
831 M| S| U_I - 1:1,1 | U_I - 1:1,1
832 M| 2 U = W + ((W - W) * U_I - 2) / (U_I - 2); | U_COMPUTE
832 M| S| U_I - 1:2,2 | U_I - 1:2,2
833 M| 1 END; | U_COMPUTE
834 M| END; | U_COMPUTE

```

HAL/S 360-23.05

INTERMETRICS, INC.

MARCH 7, 1980

6:29:25.65

PAGE 46

STMT

SOURCE

CURRENT SCOPE

835 MI CLOSE U_COMPUTE;

U_COMPUTE

**** B L O C K S U M M A R Y ****

COMPOOL VARIABLES USED

NUM_TRANS_PTS, FINAL_STEP, U_TIME_KEEP, M

OUTER VARIABLES USED

U_TIME, U_J_OLD_TIME, U*

```

      STMT                SOURCE                CURRENT SCOPE
836 M| STATE_DERIVS:    | STATE_DERIVS
836 M| PROCEDURE:       | STATE_DERIVS
837 M| DECLARE VEHICLE_MASS SCALAR DOUBLE AUTOMATIC; | STATE_DERIVS
838 M| DECLARE X_R SCALAR DOUBLE AUTOMATIC;         | STATE_DERIVS
839 M| VEHICLE_MASS = X_STORE I_TIME:5 + X_STORE I_TIME:6 + SS_DRY_MASS; | STATE_DERIVS
      SI
      EI
840 M| IF STAGE_SEP = OFF THEN                    | STATE_DERIVS
841 M|     VEHICLE_MASS = VEHICLE_MASS + FIRST_STAGE_DRY_MASS; | STATE_DERIVS
842 M|     X_R = X_STORE I_TIME:1 + EARTH_RADIUS;    | STATE_DERIVS
      SI
843 M|     X_DOT = X_STORE I_TIME:2;                | STATE_DERIVS
      SI
844 M|     X_DOT = (X_R X_STORE I_TIME:4 X_STORE I_TIME:4) + (NET_R_FORCE / VEHICLE_MASS); | STATE_DERIVS
      SI
845 M|     X_DOT = X_STORE I_TIME:3;                | STATE_DERIVS
      SI
846 M|     X_DOT = ((-2. X_STORE I_TIME:2 X_STORE I_TIME:4) + (NET_THETA_FORCE / (VEHICLE_MASS X_R))); | STATE_DERIVS
      SI
847 M|     X_DOT = -TJ_FUEL_FLOW;                   | STATE_DERIVS
      SI
848 M|     X_DOT = -SCRJ_FUEL_FLOW;                  | STATE_DERIVS
      SI
849 M|     X_DOT = -SS_FUEL_FLOW;                    | STATE_DERIVS
      SI
850 M| CLOSE STATE_DERIVS;                          | STATE_DERIVS

```

```

**** B L O C K   S U M M A R Y ****

```

```

COMPOD VARIABLES USED
  X_STORE, EARTH_RADIUS

```

```

OUTER VARIABLES USED

```

```

  I_TIME, SS_DRY_MASS, STAGE_SEP, FIRST_STAGE_DRY_MASS, X_DOT*, NET_R_FORCE, NET_THETA_FORCE, TJ_FUEL_FLOW, SCRJ_FUEL_FLOW,
  SS_FUEL_FLOW

```

STMT	SOURCE	CURRENT SCOPE
851 MI	HAM_SUB_U:	HAM_SUB_U
851 MI	PROCEDURE:	HAM_SUB_U
852 MI	IF I_TIME = 1 THEN	HAM_SUB_U
853 MI	DO:	HAM_SUB_U
854 MI	IF I_CL = 1 THEN	HAM_SUB_U
855 MI	H_SUB_U = (LAMBDA G_MAT * J_TIME) + L_SUB_U_1:	HAM_SUB_U
856 MI	ELSE	HAM_SUB_U
856 MI	H_SUB_U = (LAMBDA G_MAT * J_TIME) + L_SUB_U_3:	HAM_SUB_U
857 MI	END:	HAM_SUB_U
858 MI	ELSE	HAM_SUB_U
858 MI	H_SUB_U = (LAMBDA G_MAT * J_TIME) + L_SUB_U_1:	HAM_SUB_U
859 MI	CLOSE HAM_SUB_U:	HAM_SUB_U

*** B L O C K S U M M A R Y ***

OUTER VARIABLES USED
I_TIME, I_CL, J_TIME, H_SUB_U, LAMBDA, G_MAT, L_SUB_U_1, L_SUB_U_3, L_SUB_U_1


```

SHTT          SOURCE          CURRENT SCOPE
860 MI DELTA_U_V_CALC:      | DELTA_U_V_CALC
860 MI PROCEDURE:          | DELTA_U_V_CALC
861 MI DECLARE B MATRIX(NUM_CONSTRAINTS, NUM_CONSTRAINTS) DOUBLE STATIC;
862 MI DECLARE I_VEC_1 VECTOR(NUM_CONSTRAINTS) DOUBLE STATIC;
863 MI DECLARE I_VEC_2 VECTOR(NUM_CONSTRAINTS) DOUBLE STATIC;
864 MI DECLARE I_VEC_3 VECTOR(NUM_CONSTRAINTS) DOUBLE STATIC;
865 MI DECLARE I_MAT MATRIX(NUM_CONSTANT_PARAMETERS + NUM_TRANSPTS, NUM_CONSTRAINTS) DOUBLE STATIC;
866 MI DECLARE J_MAT MATRIX(NUM_CONTROLS, NUM_CONSTRAINTS) DOUBLE STATIC;
867 MI DECLARE C_SUB_J SCALAR DOUBLE STATIC;
868 MI DECLARE PSI_VAL SCALAR DOUBLE AUTOMATIC;
869 MI DECLARE J_DU INTEGER STATIC;
870 MI DECLARE IN_I INTEGER AUTOMATIC;
871 MI DECLARE IN_J INTEGER AUTOMATIC;
872 MI DECLARE IN_K INTEGER AUTOMATIC;
873 MI DECLARE C_SUB_PSI_KEEP SCALAR DOUBLE STATIC;
874 MI DECLARE B_INT_1 ARRAY(NUM_CONSTRAINTS) SCALAR DOUBLE AUTOMATIC;
875 MI DECLARE B_INT_2 ARRAY(NUM_CONSTRAINTS) SCALAR DOUBLE AUTOMATIC;
876 MI DECLARE MAX_B SCALAR DOUBLE AUTOMATIC;
877 MI DECLARE B_HOLD SCALAR DOUBLE AUTOMATIC;
878 MI IF STEP_I = 1 THEN
879 MI DO;
880 MI 1      * * * * *
      B = I_PSI_PSI + (M V TRANSPOSE(M));
881 MI 1      DO FOR IN_K = 1 TO NUM_CONSTRAINTS;
882 MI 2      B_INT_1 IN_K = IN_K;
883 MI 2      B_INT_2 IN_K = IN_K;
884 MI 2      MAX_B = B IN_K, IN_K;

```

```

STMT SOURCE CURRENT SCOPE
895 MI 2 DO FOR IN_I = IN_K TO NUM_CONSTRAINTS; | DELTA_U_V_CALC
896 MI 3 DO FOR IN_J = IN_K TO NUM_CONSTRAINTS; | DELTA_U_V_CALC
897 MI 4 IF ABS(MAX_B) < ABS(B | DELTA_U_V_CALC
SI IN_I,IN_J ) THEN
898 MI 4 DO; | DELTA_U_V_CALC
899 MI 5 MAX_B = B | DELTA_U_V_CALC
SI IN_I,IN_J ;
900 MI 5 B_INT_1 = IN_I; | DELTA_U_V_CALC
SI IN_K IN_K
901 MI 5 B_INT_2 = IN_J; | DELTA_U_V_CALC
SI IN_K
902 MI 4 END; | DELTA_U_V_CALC
903 MI 3 END; | DELTA_U_V_CALC
904 MI 2 IN_J = B_INT_1 | DELTA_U_V_CALC
SI IN_K ;
905 MI 2 IF B_INT_1 | DELTA_U_V_CALC
SI IN_K > IN_K THEN
906 MI 2 DO FOR IN_I = 1 TO NUM_CONSTRAINTS; | DELTA_U_V_CALC
SI B_HOLD = -B | DELTA_U_V_CALC
IN_K,IN_I ;
907 MI 3 B | DELTA_U_V_CALC
SI IN_K,IN_I = B | DELTA_U_V_CALC
IN_J,IN_I ;
908 MI 3 B | DELTA_U_V_CALC
SI IN_J,IN_I = B_HOLD; | DELTA_U_V_CALC
909 MI 2 END; | DELTA_U_V_CALC
SI IN_I = B_INT_2 | DELTA_U_V_CALC
IN_K ;
910 MI 2 IF B_INT_2 | DELTA_U_V_CALC
SI IN_K > IN_K THEN
911 MI 2 DO FOR IN_J = 1 TO NUM_CONSTRAINTS; | DELTA_U_V_CALC
SI B_HOLD = -B | DELTA_U_V_CALC
IN_J,IN_K ;
912 MI 3 END; | DELTA_U_V_CALC
SI IN_J,IN_K

```


HAL/S 360-23.05 INTERMETRICS, INC. MARCH 7, 1980 6:29:25.65 PAGE 54

STMT SOURCE CURRENT SCOPE

OUTER PROCEDURES CALLED
U_COMPUTE

COMPOOL VARIABLES USED
NUM_CONSTRAINTS, NUM_CONSTANT_PARAMETERS, NUM_TRANS_PTS, NUM_CONTROLS, V, ITERATION, PSI_START, FIRST_PSI_MAG, STEP_SCALE_PSI
STEP_SCALE_J, PSI_CCST_HEX, FINAL_STEP

OUTER VARIABLES USED
STEP_I, I_PSI_PSI, M, PSI_MAG, PSI, SMALL_C_VEC, I_PSI_J, C_SUB_PSI*, DJS_SCALE*, DJS, FIRST_PASS_PSI_MAG, DJS_SCALE, C_SUB_PSI
I_J, G_HAT, CAP_LAMBDA_I, U_TIME*, DELTA_U*, U, H_SUB_U, DELTA_V*

STMT	SOURCE	CURRENT SCOPE
971 MI	RUNGE_KUTTA:	RUNGE_KUTTA
971 MI	PROCEDURE;	RUNGE_KUTTA
972 MI	DECLARE K0 MATRIX(10, NUM_CONSTRAINTS) DOUBLE STATIC;	RUNGE_KUTTA
973 MI	DECLARE K1 MATRIX(10, NUM_CONSTRAINTS) DOUBLE STATIC;	RUNGE_KUTTA
974 MI	DECLARE K2 MATRIX(10, NUM_CONSTRAINTS) DOUBLE STATIC;	RUNGE_KUTTA
975 MI	DECLARE K3 MATRIX(10, NUM_CONSTRAINTS) DOUBLE STATIC;	RUNGE_KUTTA
976 MI	DECLARE FIRST_RK_VAL_N MATRIX(10, NUM_CONSTRAINTS) DOUBLE STATIC;	RUNGE_KUTTA
	C THE ABOVE VARIABLES HAVE THE NUMBER OF ROWS EQUAL MAX(RUNGE_KUTTA
	C NUM_STATES+1,NUM_CONSTANT_PARAMETERS,NUM_CONSTRAINTS)	RUNGE_KUTTA
977 MI	DECLARE F1 MATRIX(NUM_STATES, NUM_STATES) DOUBLE STATIC;	RUNGE_KUTTA
978 MI	DECLARE F2 MATRIX(NUM_STATES, NUM_STATES) DOUBLE STATIC;	RUNGE_KUTTA
979 MI	DECLARE F3 MATRIX(NUM_STATES, NUM_STATES) DOUBLE STATIC;	RUNGE_KUTTA
980 MI	DECLARE F4 MATRIX(NUM_STATES, NUM_STATES) DOUBLE STATIC;	RUNGE_KUTTA
981 MI	DECLARE F5 MATRIX(NUM_STATES, NUM_STATES) DOUBLE STATIC;	RUNGE_KUTTA
982 MI	DECLARE KA MATRIX(NUM_STATES, NUM_CONSTANT_PARAMETERS) DOUBLE STATIC;	RUNGE_KUTTA
983 MI	DECLARE KB MATRIX(NUM_STATES, NUM_CONSTANT_PARAMETERS) DOUBLE STATIC;	RUNGE_KUTTA
984 MI	DECLARE KC MATRIX(NUM_STATES, NUM_CONSTANT_PARAMETERS) DOUBLE STATIC;	RUNGE_KUTTA
985 MI	DECLARE KD MATRIX(NUM_STATES, NUM_CONSTANT_PARAMETERS) DOUBLE STATIC;	RUNGE_KUTTA
986 MI	DECLARE KE MATRIX(NUM_STATES, NUM_CONSTANT_PARAMETERS) DOUBLE STATIC;	RUNGE_KUTTA
987 MI	DECLARE M_1 MATRIX(NUM_CONSTRAINTS, NUM_CONTROLS) DOUBLE AUTOMATIC;	RUNGE_KUTTA
988 MI	DECLARE I_RK INTEGER STATIC;	RUNGE_KUTTA
989 MI	DECLARE J_RK INTEGER STATIC;	RUNGE_KUTTA
990 MI	DECLARE RK_D_VAL SCALAR DOUBLE STATIC;	RUNGE_KUTTA
991 MI	DECLARE RK_STEP INTEGER STATIC;	RUNGE_KUTTA
992 MI	DECLARE VAL_1 INTEGER STATIC;	RUNGE_KUTTA
993 MI	DECLARE START_RK_COLUMNS INTEGER STATIC;	RUNGE_KUTTA

STMT	SOURCE	CURRENT SCOPE
994 MI	RK_DERIV:	RK_DERIV
994 MI	PROCEDURE:	RK_DERIV
995 MI	DECLARE L_SUB_X VECTOR(NUM_STATES) DOUBLE STATIC;	RK_DERIV
996 MI	DECLARE L_SUB_P VECTOR(NUM_CONSTANT_PARAMETERS) DOUBLE STATIC;	RK_DERIV
997 MI	DECLARE L_SUB_P_1 VECTOR(NUM_CONSTANT_PARAMETERS) DOUBLE STATIC;	RK_DERIV
998 MI	DECLARE L_SUB_P_3 VECTOR(NUM_CONSTANT_PARAMETERS) DOUBLE STATIC;	RK_DERIV
999 MI	DECLARE L_SUB_P_5 VECTOR(NUM_CONSTANT_PARAMETERS) DOUBLE STATIC;	RK_DERIV
1000 MI	DECLARE DFR_DP ARRAY(NUM_CONSTANT_PARAMETERS) SCALAR DOUBLE STATIC;	RK_DERIV
1001 MI	DECLARE DFTHETA_DP ARRAY(NUM_CONSTANT_PARAMETERS) SCALAR DOUBLE STATIC;	RK_DERIV
1002 MI	DECLARE DM1DOT_DP ARRAY(NUM_CONSTANT_PARAMETERS) SCALAR DOUBLE STATIC;	RK_DERIV
1003 MI	DECLARE DM2DOT_DP ARRAY(NUM_CONSTANT_PARAMETERS) SCALAR DOUBLE STATIC;	RK_DERIV
1004 MI	DECLARE DM3DOT_DP ARRAY(NUM_CONSTANT_PARAMETERS) SCALAR DOUBLE STATIC;	RK_DERIV
1005 MI	DECLARE DP_DP ARRAY(NUM_CONSTANT_PARAMETERS) SCALAR DOUBLE STATIC;	RK_DERIV
1006 MI	DECLARE DN_DP ARRAY(NUM_CONSTANT_PARAMETERS) SCALAR DOUBLE STATIC;	RK_DERIV
1007 MI	DECLARE DT_DP ARRAY(NUM_CONSTANT_PARAMETERS) SCALAR DOUBLE STATIC;	RK_DERIV
1008 MI	DECLARE DMASSFLUX_DP1 ARRAY(NUM_CONSTANT_PARAMETERS) SCALAR DOUBLE STATIC;	RK_DERIV
1009 MI	DECLARE DMASSFLUX_DP2 ARRAY(NUM_CONSTANT_PARAMETERS) SCALAR DOUBLE STATIC;	RK_DERIV
1010 MI	DECLARE DFR_DR SCALAR DOUBLE STATIC;	RK_DERIV
1011 MI	DECLARE DFTHETA_DR SCALAR DOUBLE STATIC;	RK_DERIV
1012 MI	DECLARE DM1DOT_DR SCALAR DOUBLE STATIC;	RK_DERIV
1013 MI	DECLARE DM2DOT_DR SCALAR DOUBLE STATIC;	RK_DERIV
1014 MI	DECLARE DP_DR SCALAR DOUBLE STATIC;	RK_DERIV
1015 MI	DECLARE DN_DR SCALAR DOUBLE STATIC;	RK_DERIV
1016 MI	DECLARE DT_DR SCALAR DOUBLE STATIC;	RK_DERIV
1017 MI	DECLARE DMASSFLUX_DR1 SCALAR DOUBLE STATIC;	RK_DERIV
1018 MI	DECLARE DMASSFLUX_DR2 SCALAR DOUBLE STATIC;	RK_DERIV
1019 MI	DECLARE DP_DUR SCALAR DOUBLE STATIC;	RK_DERIV
1020 MI	DECLARE DN_DUR SCALAR DOUBLE STATIC;	RK_DERIV

STMT	SOURCE	CURRENT SCOPE
1021 MI	DECLARE DT_DUR SCALAR DOUBLE STATIC;	RK_DERIV
1022 MI	DECLARE DMASSFLUX_DUR1 SCALAR DOUBLE STATIC;	RK_DERIV
1023 MI	DECLARE DMASSFLUX_DUR2 SCALAR DOUBLE STATIC;	RK_DERIV
1024 MI	DECLARE DFR_DMI SCALAR DOUBLE STATIC;	RK_DERIV
1025 MI	DECLARE DFR_DUR SCALAR DOUBLE STATIC;	RK_DERIV
1026 MI	DECLARE DFTHETA_DUR SCALAR DOUBLE STATIC;	RK_DERIV
1027 MI	DECLARE DM1DOT_DUR SCALAR DOUBLE STATIC;	RK_DERIV
1028 MI	DECLARE DM2DOT_DUR SCALAR DOUBLE STATIC;	RK_DERIV
1029 MI	DECLARE DFR_DTDOT SCALAR DOUBLE STATIC;	RK_DERIV
1030 MI	DECLARE DFTHETA_DTDOT SCALAR DOUBLE STATIC;	RK_DERIV
1031 MI	DECLARE DM1DOT_DTDOT SCALAR DOUBLE STATIC;	RK_DERIV
1032 MI	DECLARE DM2DOT_DTDOT SCALAR DOUBLE STATIC;	RK_DERIV
1033 MI	DECLARE DP_DTDOT SCALAR DOUBLE STATIC;	RK_DERIV
1034 MI	DECLARE DN_DTDOT SCALAR DOUBLE STATIC;	RK_DERIV
1035 MI	DECLARE DT_DTDOT SCALAR DOUBLE STATIC;	RK_DERIV
1036 MI	DECLARE DMASSFLUX_DTDOT1 SCALAR DOUBLE STATIC;	RK_DERIV
1037 MI	DECLARE DMASSFLUX_DTDOT2 SCALAR DOUBLE STATIC;	RK_DERIV
1038 MI	DECLARE DDELTA_DR SCALAR DOUBLE STATIC;	RK_DERIV
1039 MI	DECLARE DDELTA_DUR SCALAR DOUBLE STATIC;	RK_DERIV
1040 MI	DECLARE DDELTA_DTDOT SCALAR DOUBLE STATIC;	RK_DERIV
1041 MI	DECLARE S2 SCALAR DOUBLE STATIC;	RK_DERIV
1042 MI	DECLARE S3 SCALAR DOUBLE STATIC;	RK_DERIV
1043 MI	DECLARE S5 SCALAR DOUBLE STATIC;	RK_DERIV
1044 MI	DECLARE S6 SCALAR DOUBLE STATIC;	RK_DERIV
1045 MI	DECLARE COS_DELTA SCALAR DOUBLE STATIC;	RK_DERIV
1046 MI	DECLARE SIN_DELTA SCALAR DOUBLE STATIC;	RK_DERIV
1047 MI	DECLARE S6 SCALAR DOUBLE STATIC;	RK_DERIV
1048 MI	DECLARE L_CONST SCALAR DOUBLE STATIC;	RK_DERIV

CURRENT SCOPE

SOURCE

STMT

```

1049 MI DECLARE LAMSDA_HOLD VECTOR(NUM_STATES) DOUBLE STATIC;
1050 MI DECLARE CAP_LAMSDA_I_HOLD MATRIX(NUM_STATES, NUM_CONSTRAINTS) DOUBLE STATIC;
1051 MI DECLARE KEEP_MASS SCALAR DOUBLE STATIC;
1052 MI DECLARE SR SCALAR DOUBLE STATIC;
1053 MI DECLARE K_RK INTEGER STATIC;
1054 MI DECLARE L_RK INTEGER AUTOMATIC;
1055 MI DECLARE I_FK INTEGER STATIC;
1056 MI DECLARE T_VAL SCALAR DOUBLE STATIC;
1057 MI DECLARE SPEED_OF_SOUND_2 SCALAR DOUBLE STATIC;
1058 MI DECLARE DHO_DR SCALAR DOUBLE STATIC;
1059 MI DECLARE DHO_DUR SCALAR DOUBLE STATIC;
1060 MI DECLARE DHO_DTDOT SCALAR DOUBLE STATIC;
1061 MI DECLARE DH2_DPBETA SCALAR DOUBLE STATIC;
1062 MI DECLARE DT2_DPBETA SCALAR DOUBLE STATIC;
1063 MI DECLARE DRO2_DPBETA SCALAR DOUBLE STATIC;
1064 MI DECLARE DU2_DH2 SCALAR DOUBLE STATIC;
1065 MI DECLARE DU2_DT2 SCALAR DOUBLE STATIC;
1066 MI DECLARE SIN_BETA SCALAR DOUBLE STATIC;
1067 MI DECLARE COS_BETA SCALAR DOUBLE STATIC;
1068 MI DECLARE SIN_2_BETA SCALAR DOUBLE STATIC;
1069 MI DECLARE SIN_B_T SCALAR DOUBLE STATIC;
1070 MI DECLARE COS_B_T SCALAR DOUBLE STATIC;
1071 MI DECLARE OSC1 SCALAR DOUBLE STATIC;
1072 MI DECLARE DT2_DHO SCALAR DOUBLE STATIC;
1073 MI DECLARE DT2_DTO SCALAR DOUBLE STATIC;
1074 MI DECLARE DRO2_DHO SCALAR DOUBLE STATIC;
1075 MI DECLARE DRO2_PRO_0 SCALAR DOUBLE STATIC;
1076 MI DECLARE DBETA_DR SCALAR DOUBLE STATIC;

```

::

STMT	SOURCE	CURRENT SCOPE
1077 MI	DECLARE DBETA_DUR SCALAR DOUBLE STATIC;	RK_DERIV
1078 MI	DECLARE DBETA_DTDOT SCALAR DOUBLE STATIC;	RK_DERIV
1079 MI	DECLARE DM2_DR SCALAR DOUBLE STATIC;	RK_DERIV
1080 MI	DECLARE DM2_DUR SCALAR DOUBLE STATIC;	RK_DERIV
1081 MI	DECLARE DM2_DTDOT SCALAR DOUBLE STATIC;	RK_DERIV
1082 MI	DECLARE DT2_DR SCALAR DOUBLE STATIC;	RK_DERIV
1083 MI	DECLARE DT2_DUR SCALAR DOUBLE STATIC;	RK_DERIV
1084 MI	DECLARE DT2_DTDOT SCALAR DOUBLE STATIC;	RK_DERIV
1085 MI	DECLARE DU2_DR SCALAR DOUBLE STATIC;	RK_DERIV
1086 MI	DECLARE DU2_DUR SCALAR DOUBLE STATIC;	RK_DERIV
1087 MI	DECLARE DU2_DTDOT SCALAR DOUBLE STATIC;	RK_DERIV
1088 MI	DECLARE DRO2_DR SCALAR DOUBLE STATIC;	RK_DERIV
1089 MI	DECLARE DRO2_DUR SCALAR DOUBLE STATIC;	RK_DERIV
1090 MI	DECLARE DRO2_DTDOT SCALAR DOUBLE STATIC;	RK_DERIV
1091 MI	DECLARE DISP1_DM2 SCALAR DOUBLE STATIC;	RK_DERIV
1092 MI	DECLARE DISP2_DM2 SCALAR DOUBLE STATIC;	RK_DERIV
1093 MI	DECLARE DT1_DR SCALAR DOUBLE STATIC;	RK_DERIV
1094 MI	DECLARE DT1_DUR SCALAR DOUBLE STATIC;	RK_DERIV
1095 MI	DECLARE DT1_DTDOT SCALAR DOUBLE STATIC;	RK_DERIV
1096 MI	DECLARE DTH2_DR SCALAR DOUBLE STATIC;	RK_DERIV
1097 MI	DECLARE DTH2_DUR SCALAR DOUBLE STATIC;	RK_DERIV
1098 MI	DECLARE DTH2_DTDOT SCALAR DOUBLE STATIC;	RK_DERIV
1099 MI	DECLARE DCL1_DR SCALAR DOUBLE STATIC;	RK_DERIV
1100 MI	DECLARE DCL2_DR SCALAR DOUBLE STATIC;	RK_DERIV
1101 MI	DECLARE DCD1_DR SCALAR DOUBLE STATIC;	RK_DERIV
1102 MI	DECLARE DCD2_DR SCALAR DOUBLE STATIC;	RK_DERIV
1103 MI	DECLARE DCL1_DUR SCALAR DOUBLE STATIC;	RK_DERIV
1104 MI	DECLARE DCL2_DUR SCALAR DOUBLE STATIC;	RK_DERIV

STRT	SOURCE	CURRENT SCOPE
1105 MI	DECLARE DCD1_DUR SCALAR DOUBLE STATIC;	RK_DERIV
1106 MI	DECLARE DCD2_DUR SCALAR DOUBLE STATIC;	RK_DERIV
1107 MI	DECLARE DCL1_DTDOT SCALAR DOUBLE STATIC;	RK_DERIV
1108 MI	DECLARE DCL2_DTDOT SCALAR DOUBLE STATIC;	RK_DERIV
1109 MI	DECLARE DCD1_RTCOT SCALAR DOUBLE STATIC;	RK_DERIV
1110 MI	DECLARE DCD2_DTDOT SCALAR DOUBLE STATIC;	RK_DERIV
1111 MI	DECLARE V0_2 SCALAR DOUBLE STATIC;	RK_DERIV
1112 MI	DECLARE DL_DR SCALAR DOUBLE STATIC;	RK_DERIV
1113 MI	DECLARE DL_DUR SCALAR DOUBLE STATIC;	RK_DERIV
1114 MI	DECLARE DL_DTDOT SCALAR DOUBLE STATIC;	RK_DERIV
1115 MI	DECLARE DD_DR SCALAR DOUBLE STATIC;	RK_DERIV
1116 MI	DECLARE DD_DUR SCALAR DOUBLE STATIC;	RK_DERIV
1117 MI	DECLARE DD_DTDOT SCALAR DOUBLE STATIC;	RK_DERIV
1118 MI	DECLARE SIN_A SCALAR DOUBLE STATIC;	RK_DERIV
1119 MI	DECLARE COS_A SCALAR DOUBLE STATIC;	RK_DERIV
1120 MI	DECLARE DT2_DM2 SCALAR DOUBLE STATIC;	RK_DERIV
1121 MI	DECLARE DRO2_DM2 SCALAR DOUBLE STATIC;	RK_DERIV
1122 MI	DECLARE DBETA_DM0 SCALAR DOUBLE STATIC;	RK_DERIV
1123 MI	DECLARE DM2_DM0 SCALAR DOUBLE STATIC;	RK_DERIV
1124 MI	DECLARE M2_2 SCALAR DOUBLE STATIC;	RK_DERIV
1125 MI	DECLARE DAR_DPI VECTOR(NUM_CONSTANT_PARAMETERS) DOUBLE STATIC;	RK_DERIV
1126 MI	DECLARE DAH1_DPI VECTOR(NUM_CONSTANT_PARAMETERS) DOUBLE STATIC;	RK_DERIV
1127 MI	DECLARE DAH2_DPI VECTOR(NUM_CONSTANT_PARAMETERS) DOUBLE STATIC;	RK_DERIV
1128 MI	DECLARE DTH1_DPI VECTOR(NUM_CONSTANT_PARAMETERS) DOUBLE STATIC;	RK_DERIV
1129 MI	DECLARE DTH2_DPI VECTOR(NUM_CONSTANT_PARAMETERS) DOUBLE STATIC;	RK_DERIV
1130 MI	DECLARE DTH3_DPI VECTOR(NUM_CONSTANT_PARAMETERS) DOUBLE STATIC;	RK_DERIV
1131 MI	DECLARE DAE1_DPI VECTOR(NUM_CONSTANT_PARAMETERS) DOUBLE STATIC;	RK_DERIV
1132 MI	DECLARE DAE2_DPI VECTOR(NUM_CONSTANT_PARAMETERS) DOUBLE STATIC;	RK_DERIV

```

SOURCE
CURRENT SCOPE
1133 MI DECLARE DG_DPI VECTOR(NUM_CONSTANT_PARAMETERS) DOUBLE STATIC; | RK_DERIV
1134 MI DECLARE DR02_DPI SCALAR DOUBLE STATIC; | RK_DERIV
1135 MI DECLARE DETA_DPI SCALAR DOUBLE STATIC; | RK_DERIV
1136 MI DECLARE DT2_DPI SCALAR DOUBLE STATIC; | RK_DERIV
1137 MI DECLARE DM2_DPI SCALAR DOUBLE STATIC; | RK_DERIV
1138 MI DECLARE DISP1_DPI SCALAR DOUBLE STATIC; | RK_DERIV
1139 MI DECLARE DISP2_DPI SCALAR DOUBLE STATIC; | RK_DERIV
1140 MI DECLARE DKCR_DPI SCALAR DOUBLE STATIC; | RK_DERIV
1141 MI DECLARE DU2_DPI SCALAR DOUBLE STATIC; | RK_DERIV
1142 MI DECLARE DL_DPI SCALAR DOUBLE AUTOMATIC; | RK_DERIV
1143 MI DECLARE DD_DPI SCALAR DOUBLE AUTOMATIC; | RK_DERIV
1144 MI DECLARE DM1DOT_DUA VECTOR(NUM_CONTROLS) DOUBLE STATIC; | RK_DERIV
1145 MI DECLARE DM2DOT_DUA VECTOR(NUM_CONTROLS) DOUBLE STATIC; | RK_DERIV
1146 MI DECLARE DM3DOT_DUA VECTOR(NUM_CONTROLS) DOUBLE STATIC; | RK_DERIV
1147 MI DECLARE DFR_DUA VECTOR(NUM_CONTROLS) DOUBLE STATIC; | RK_DERIV
1148 MI DECLARE DFTHETA_DUA VECTOR(NUM_CONTROLS) DOUBLE STATIC; | RK_DERIV
1149 MI DECLARE DT_DUA VECTOR(NUM_CONTROLS) DOUBLE STATIC; | RK_DERIV
1150 MI DECLARE L_SUB_U VECTOR(NUM_CONTROLS) DOUBLE STATIC; | RK_DERIV
1151 MI DECLARE DL_DUA1 SCALAR DOUBLE STATIC; | RK_DERIV
1152 MI DECLARE DD_DUA1 SCALAR DOUBLE STATIC; | RK_DERIV
1153 MI DECLARE DPHI_DUA2 SCALAR DOUBLE STATIC; | RK_DERIV
1154 MI DECLARE NET_THRUST SCALAR DOUBLE STATIC; | RK_DERIV
...
1155 MI IF STATE_INTEGRATION_FLAG = ON THEN | RK_DERIV
1156 MI DO; | RK_DERIV
1157 MI 1 IF I_RK = (NUM_STATES + 1) THEN | RK_DERIV
1158 MI 1 DO; | RK_DERIV
1159 MI 2 RK_D_VAL = 0.; | RK_DERIV

```

CURRENT SCOPE

SOURCE

```

STHT
1160 MI 2      IF DYNAMIC_PO > Q_D THEN
EI
1161 MI 2      RK_D_VAL = CAP_Q ((DYNAMIC_F0 - Q_D) )2
1162 MI 2      IF G_LOAD > G_D THEN
EI
1163 MI 2      RK_D_VAL = RK_D_VAL + (CAP_CA (((G_LOAD - G_D) G0) )2);
1164 MI 1      END;
1165 MI 1      ELSE
1165 MI 1      RK_D_VAL = X_DOT2 ;
SI              I_RK
1166 MI       END;
1167 MI       ELSE
1167 MI       DO;
1168 MI 1      RK_STEP = RK_STEP + 1;
EI
1169 MI 1      IF FIRST_DERIV_FLAG = ON THEN
1170 MI 1      DO;
EI
1171 MI 2      FIRST_DERIV_FLAG = OFF;
EI
1172 MI 2      IF (LAMBDA_FLAG OR CAP_LAMBDA_I_FLAG) = ON THEN
1173 MI 2      DO FOR K_RK = 1 TO NUM_STATES;
EI
1174 MI 3      IF LAMBDA_FLAG = ON THEN
1175 MI 3      LAMBDA_HOLD = RK_VAL_NK_RK ;
SI              K_RK
1176 MI 3      ELSE
1176 MI 3      DO FOR L_RK = 1 TO NUM_CONSTRAINTS;
1177 MI 4      CAP_LAMBDA_I_HOLD = RK_VAL_NK_RK,L_RK ;
SI              K_RK,L_RK
1178 MI 3      END;
1179 MI 2      END;

```

```

SOURCE
CURRENT SCOPE
STMT
E|
1180 M| 2 IF PARTIAL_DERIV_FLAG = ON THEN
1181 M| 2 DO;
E|
1182 M| 3 PARTIAL_DERIV_FLAG = OFF;
1183 M| 3 IF RK_STEP > VAL_1 THEN
1184 M| 3 DO;
E|
1185 M| 4 IF (LAMBDA_FLAG OR CAP_LAMBDA_1_FLAG OR CAP_LAMBDA_2_FLAG) = ON THEN
1186 M| 4 I_TIME = I_TIME - 1;
1187 M| 4 ELSE
1188 M| 4 I_TIME = I_TIME - 2;
1189 M| 4 J_TIME = FLOOR((I_TIME + 2) / 2);
E|
C| COSTATE DERIVATIVES FOLLOW
E|
1190 M| 3 IF LAMBDA_FLAG = ON THEN
1191 M| 3 DO;
E|
1192 M| 4 IF ((I_CL = 2) AND (FD_FLAG = ON)) THEN
E|
1193 M| 4 FD_FLAG = OFF;
1194 M| 4 ELSE
1195 M| 4 DO;
S| SR = X_STORE + EARTH_RADIUS;
1196 M| 5 I_TIME = I_TIME - 1;
1197 M| 5 IF L_TIME = 0 THEN
1198 M| 5 L_TIME = 1;
E|
1199 M| 5 OIT_FLAG = OFF;

```

STMT	SOURCE	CURRENT SCOPE
EI 1200 MI 5	T_FLAG = OFF;	RK_DERIV
1201 MI 5	IF MOD(I_TIME, 4) = 1 THEN	RK_DERIV
1202 MI 5	DO FOR I_FK = 1 TO NUM_TRANSPTS;	RK_DERIV
1203 MI 6 SI	IF OMEGA_I_TIME = I_TIME THEN I_FK	RK_DERIV
1204 MI 6	DO;	RK_DERIV
EI 1205 MI 7	T_FLAG = ON;	RK_DERIV
1206 MI 7 SI	IF OMEGA_I_TIME = I_TIME STORE THEN I_FK	RK_DERIV
EI 1207 MI 7	OIT_FLAG = ON;	RK_DERIV
1208 MI 6	END;	RK_DERIV
1209 MI 5	END;	RK_DERIV
EI 1210 MI 5	IF (T_FLAG AND NOT OIT_FLAG) = ON THEN	RK_DERIV
1211 MI 5	L_TIME = I_TIME;	RK_DERIV
EI 1212 MI 5	L_SUB_X = 0.;	RK_DERIV
EI 1213 MI 5	L_SUB_P = 0.;	RK_DERIV
1214 MI 5	CALL MODEL_DRIVER;	RK_DERIV
1215 MI 5	NET_THRUST = TURBOJET_THRUST + SCRAJET_THRUST + ROCKET_THRUST;	RK_DERIV
1216 MI 5	L_CONST = 2. CAP_CA (G_LOAD - G_D) GO GO;	RK_DERIV
1217 MI 5	FD_COUNT = FD_COUNT + 1;	RK_DERIV
1218 MI 5	IF FD_COUNT = 5 THEN	RK_DERIV
1219 MI 5	FD_COUNT = 0;	RK_DERIV
EI 1220 MI 5 SI	IF ((I_TIME = OMEGA_I_TIME) AND (OIT_FLAG = ON)) THEN	RK_DERIV
1221 MI 5	DO;	RK_DERIV


```

      STMT          SOURCE          CURRENT SCOPE
1222 MI 6          KEEP_MASS = NET_MASS          | RK_DERIV
      SI           I_TIME                       |
1223 MI 6          NET_MASS = NET_MASS          | RK_DERIV
      SI           I_TIME - HELD_FS_MASS;       |
1224 MI 5          END;                        | RK_DERIV
1225 MI 5          IF G_LOAD > G_D THEN        | RK_DERIV
1226 MI 5          DO FOR I_FK = 5 TO 7;       | RK_DERIV
1227 MI 6          L_SUB_X = -(G_LOAD L_CONST) / MD_MASS;
      SI           I_FK                       | RK_DERIV
1228 MI 5          END;                        | RK_DERIV
1229 MI 5          MO_2 = MO MO;              | RK_DERIV
1230 MI 5          T_VAL = X_STORE            - EARTH_OMEGA;
      SI           I_TIME:4                   | RK_DERIV
1231 MI 5          SPEED_OF_SOUND_2 = GAMMAO R_0 T0;
1232 MI 5          DM0_DR = ((SR T_VAL T_VAL) / (MO SPEED_OF_SOUND_2)) - ((MO DT0_DR)
      SI           / (2. T0));                | RK_DERIV
1233 MI 5          DM0_DUR = X_STORE          / (MO SPEED_OF_SOUND_2);
      SI           I_TIME:2                   | RK_DERIV
1234 MI 5          DM0_DTCOT = (SR SR T_VAL) / (MO SPEED_OF_SOUND_2);
1235 MI 5          DM2_DBETA = 0.;
1236 MI 5          DT2_DBETA = 0.;
1237 MI 5          DROT_DBETA = 0.;
1238 MI 5          DT2_DM2 = 0.;
1239 MI 5          DROT_DM2 = 0.;
1240 MI 5          DBETA_DM0 = 0.;
1241 MI 5          DM2_DM0 = 0.;
      SI
1242 MI 5          IF STAGE_SEP = OFF THEN
1243 MI 5          DO;
      SI
      SI           DU2_DM2 = SQRT(GAMMAO R_0 T2);
1244 MI 6          IF T2 == 0. THEN
1245 MI 6          | RK_DERIV

```

```

      STMT          SOURCE          CURRENT SCOPE
1246 M| 6          DU2_DT2 = (M2 DU2_DM2) / (2. T2);          | RK_DERIV
      E|
1247 M| 6          IF OBLIQUE_SHOCK_FLAG = CN THEN          | RK_DERIV
1248 M| 6          DO;          | RK_DERIV
1249 M| 7          SIN_DELTA = SIN(BETA_NOSE_SHOCK);          | RK_DERIV
1250 M| 7          COS_BETA = COS(BETA_NOSE_SHOCK);          | RK_DERIV
1251 M| 7          SIN_2_BETA = SIN_BETA SIN_BETA;          | RK_DERIV
1252 M| 7          SIN_B_T = SIN(BETA_NOSE_SHOCK - THETA_NOSE); | RK_DERIV
1253 M| 7          COS_B_T = COS(BETA_NOSE_SHOCK - THETA_NOSE); | RK_DERIV
1254 M| 7          OSC1 = SQRT(((GAMMA0 M0_2 SIN_2_BETA) - GAM1) / (1. + | RK_DERIV
1255 M| 7          (GAM1 M0_2 SIN_2_BETA)));          | RK_DERIV
1256 M| 7          DBETA_DM0 = (2. M0 GAM2 SIN_BETA COS_BETA) / ((M0_2 | RK_DERIV
1257 M| 7          M0_2 SIN_2_BETA ((2. GAMMA0 SIN_2_BETA) - GAM2)) + ( | RK_DERIV
1258 M| 7          M0_2 ((4. SIN_2_BETA) - GAM2)) - 2.);          | RK_DERIV
1259 M| 7          IF SIN_B_T /= 0. THEN          | RK_DERIV
1260 M| 7          DO;          | RK_DERIV
1261 M| 7          DM2_DBETA = (- (GAM2 GAM2 M0_2 SIN_BETA COS_BETA | RK_DERIV
1262 M| 7          OSC1) / (4. SIN_B_T ((GAMMA0 M0_2 SIN_2_BETA) - | RK_DERIV
1263 M| 7          GAM1) )) - (COS_B_T / (SIN_B_T SIN_B_T OSC1));          | RK_DERIV
1264 M| 7          DM2_DM0 = - (GAM2 GAM2 M0 SIN_2_BETA OSC1) / (4. | RK_DERIV
1265 M| 7          SIN_B_T ((GAMMA0 M0_2 SIN_2_BETA) - GAM1) ));          | RK_DERIV
1266 M| 7          END;          | RK_DERIV
1267 M| 7          IF ((SIN_2_BETA /= 0.) OR (SIN_BETA /= 0.)) THEN          | RK_DERIV
1268 M| 7          DT2_DBETA = (4. T0 GAM3 COS_BETA ((GAMMA0 M0_2 M0_2 | RK_DERIV
1269 M| 7          SIN_2_BETA SIN_2_BETA) + 1.)) / (GAM2 GAM2 M0_2 | RK_DERIV
1270 M| 7          SIN_2_BETA SIN_BETA);          | RK_DERIV
1271 M| 7          IF COS_BETA /= 0. THEN          | RK_DERIV

```

```

SOURCE                                CURRENT SCOPE
-----                                -
1264 M| 7 DT2_DMO = (DT2_DBETA SIN_BETA) / (COS_BETA MO); | RK_DERIV
1265 M| 7 DT2_DTO = T2 / T0; | RK_DERIV
1266 M| 7 DR02_DBETA = (4. RO_0 GAM2 MO_2 SIN_BETA COS_BETA) / ( | RK_DERIV
      E| ((GAM3 MO_2 SIN_2_BETA) + 2.)) ; |
1266 M| 7 ((GAM3 MO_2 SIN_2_BETA) + 2.)) ; | RK_DERIV
1267 M| 7 IF COS_BETA ^= 0. THEN | RK_DERIV
1268 M| 7 DR02_DMO = (DR02_DBETA SIN_BETA) / (COS_BETA MO); | RK_DERIV
1269 M| 7 DR02_DRO_0 = RO_2 / RO_0; | RK_DERIV
1270 M| 6 END; | RK_DERIV
      E|
1271 M| 6 IF NORMAL_SHOCK_FLAG = ON THEN |
1272 M| 6 DO; | RK_DERIV
1273 M| 7 DM2_DMO = -(GAM2 GAM2 MO SQRT(((GAMMA0 MO_2) - GAM1) / | RK_DERIV
      E| (1. + (GAM1 MO_2))) / (4. (((GAMMA0 MO_2) - GAM1) )); | RK_DERIV
1274 M| 7 DT2_DMO = (4. T0 GAM3 ((GAMMA0 MO_2 MO_2) + 1.)) / ( | RK_DERIV
1274 M| 7 GAM2 GAM2 MO_2 MO); | RK_DERIV
1275 M| 7 DT2_DTO = T2 / T0; | RK_DERIV
      E|
1276 M| 7 DR02_DMO = (4. RO_0 GAM2 MO) / (((GAM3 MO_2) + 2.)) ; | RK_DERIV
1277 M| 7 DR02_DRO_0 = RO_2 / RO_0; | RK_DERIV
1278 M| 6 END; | RK_DERIV
      E|
1279 M| 6 IF ((EXPANSION_FLAG = ON) AND ((M2_2 - 1.) > 0.)) THEN |
      E| DO; | RK_DERIV
1280 M| 6 M2_2 = M2 M2; | RK_DERIV
1281 M| 7 DM2_DMO = SQRT((MO_2 - 1.) / (M2_2 - 1.)) (M2 / MO) ( | RK_DERIV
1282 M| 7 2. + (GAM3 M2_2)) / (2. + (GAM3 MO_2)); | RK_DERIV
      E|
1283 M| 7 DT2_DMO = (T0 GAM3 MO) / (1. + (GAM1 M2_2)); | RK_DERIV
1284 M| 7 DT2_DTO = T2 / T0; | RK_DERIV

```

STMT	SOURCE	CURRENT SCOPE
1265 MI 7	DRO2_DM0 = (RO_2 M0) / (1. + (GAM1 M0_2));	RK_DERIV
1286 MI 7	DRO2_DRO_0 = RO_2 / RO_0;	RK_DERIV
1287 MI 7	DT2_DM2 = -(T2 GAM3 M2) / (1. + (GAM1 M2_2));	RK_DERIV
1288 MI 7	DRO2_DM2 = -(RO_2 M2) / (1. + (GAM1 M2_2));	RK_DERIV
1289 MI 6	END;	RK_DERIV
EI		
1290 MI 6	IF SUBSONIC_FLAG = ON THEN	RK_DERIV
1291 MI 6	DO;	RK_DERIV
1292 MI 7	DM2_DM0 = 1.;	RK_DERIV
1293 MI 7	DT2_DM0 = 0.;	RK_DERIV
1294 MI 7	DT2_DT0 = 1.;	RK_DERIV
1295 MI 7	DRO2_DM0 = 0.;	RK_DERIV
1296 MI 7	DRO2_DRO_0 = 1.;	RK_DERIV
1297 MI 6	END;	RK_DERIV
1298 MI 6	DBETA_DR = DBETA_DM0 DM0_DR;	RK_DERIV
1299 MI 6	DBETA_DUR = DBETA_DM0 DM0_DUR;	RK_DERIV
1300 MI 6	DBETA_DTDOT = DBETA_DM0 DM0_DTDOT;	RK_DERIV
1301 MI 6	DM2_DR = (DM2_DM0 DM0_DR) + (DM2_DBETA DBETA_DR);	RK_DERIV
1302 MI 6	DM2_DUR = (DM2_DM0 DM0_DUR) + (DM2_DBETA DBETA_DUR);	RK_DERIV
1303 MI 6	DM2_DTDOT = (DM2_DM0 DM0_DTDOT) + (DM2_DBETA DBETA_DTDOT);	RK_DERIV
1304 MI 6	DT2_DR = (DT2_DM0 DM0_DR) + (DT2_DBETA DBETA_DR) + (DT2_DT0	RK_DERIV
1304 MI 6	DT0_DR) + (DT2_DM2 DM2_DR);	RK_DERIV
1305 MI 6	DT2_DUR = (DT2_DM0 DM0_DUR) + (DT2_DBETA DBETA_DUR) + (RK_DERIV
1305 MI 6	DT2_DM2 DM2_DUR);	RK_DERIV
1306 MI 6	DT2_DTDOT = (DT2_DM0 DM0_DTDOT) + (DT2_DBETA DBETA_DTDOT) +	RK_DERIV
1306 MI 6	(DT2_DM2 DM2_DTDOT);	RK_DERIV
1307 MI 6	DU2_DR = (DU2_DM2 DM2_DR) + (DU2_DT2 DT2_DR);	RK_DERIV
1308 MI 6	DU2_DUR = (DU2_DM2 DM2_DUR) + (DU2_DT2 DT2_DUR);	RK_DERIV

```

STM1
1309 M1 6          SOURCE
DU2_DTDOT = (DU2_DM2 DM2_DTDOT) + (DU2_DT2 DT2_DTDOT);          | RK_DERIV
1310 M1 6          DRO2_DR = (DRO2_DM0 DM0_DR) + (DRO2_DBETA DBETA_DR) + (          | RK_DERIV
1311 M1 6          DRO2_DRO_0 DRO_DR) + (DRO2_DM2 DM2_DR);          | RK_DERIV
1312 M1 6          DRO2_DUR = (DRO2_DM0 DM0_DUR) + (DRO2_DSETA DSETA_DUR) + (          | RK_DERIV
1313 M1 6          DRO2_DM2 DM2_DUR);          | RK_DERIV
1314 M1 6          DRO2_DTDOT = (DRO2_DM0 DM0_DTDOT) + (DRO2_DBETA DBETA_DTDOT) | RK_DERIV
+ (DRO2_DM2 DM2_DTDOT);          | RK_DERIV
1315 M1 6          DISP1_DM2 = -300. - (200. M2);          | RK_DERIV
IF M2 > 0. THEN          | RK_DERIV
DISP2_DM2 = EXP(-1.73 (M2.52)) ((24000. (M2.6)) - (13494.          |
(M21.12)));          | RK_DERIV
1316 M1 5          END;          | RK_DERIV
1317 M1 5          IF ((RO_2 ~= 0.) AND (U2 ~= 0.)) THEN          | RK_DERIV
DO;          | RK_DERIV
1318 M1 6          IF ((TURBOJET_POWER = ON) AND (TURBOJET_ISP ~= 0.)) THEN          |
DO;          | RK_DERIV
1319 M1 7          DT1_DR = TURBOJET_THRUST ((DRO2_DR / RO_2) + (DM2_DR /          |
U2) + ((DISP1_DM2 DM2_DR) / TURBOJET_ISP));          | RK_DERIV
1320 M1 7          DT1_DUR = TURBOJET_THRUST ((DRO2_DUR / RO_2) + (          |
DU2_DUR / U2) + ((DISP1_DM2 DM2_DUR) / TURBOJET_ISP));          | RK_DERIV
1321 M1 7          DT1_DTDOT = TURBOJET_THRUST ((DRO2_DTDOT / RO_2) + (          |
DU2_DTDOT / U2) + ((DISP1_DM2 DM2_DTDOT) /          |
TURBOJET_ISP));          | RK_DERIV
1322 M1 6          END;          | RK_DERIV
1323 M1 6          ELSE          | RK_DERIV
DO;          | RK_DERIV
1324 M1 6
1325 M1 6
1326 M1 6

```

```

STMT          SOURCE          CURRENT SCOPE
1326 M| 7      DT1_DR = 0.;      | RK_DERIV
1327 M| 7      DT1_DUR = 0.;      | RK_DERIV
1328 M| 7      DT1_DTDOT = 0.;    | RK_DERIV
1329 M| 6      END;              | RK_DERIV
      EI
1330 M| 6      IF ((SCRAMJET_POWER = ON) AND (SCRAMJET_ISP /= 0.) AND (
1330 M| 6          SCRJ_MASS_CAPTURE_RATIO > 0.)) THEN      | RK_DERIV
1331 M| 6      DO;                | RK_DERIV
1332 M| 7          S2 = (SCRAMJET_THRUST DMCR_DM2) /      | RK_DERIV
1332 M| 7          SCRJ_MASS_CAPTURE_RATIO;              | RK_DERIV
1333 M| 7          DTH2_DR = (SCRAMJET_THRUST ((DR02_DR / RO_2) + (DU2_DR
1333 M| 7          / U2) + ((DISP2_DM2 DM2_DR) / SCRAMJET_ISP))) + (S2      | RK_DERIV
1333 M| 7          DM2_DR);                                  | RK_DERIV
1334 M| 7          DTH2_DUR = (SCRAMJET_THRUST ((DR02_DUR / RO_2) + (
1334 M| 7          DU2_DUR / U2) + ((DISP2_DM2 DM2_DUR) / SCRAMJET_ISP)); | RK_DERIV
1334 M| 7          + (S2 DM2_DUR);                          | RK_DERIV
1335 M| 7          DTH2_DTDOT = (SCRAMJET_THRUST ((DR02_DTDOT / RO_2) + (
1335 M| 7          DU2_DTDOT / U2) + ((DISP2_DM2 DM2_DTDOT) /
1335 M| 7          SCRAMJET_ISP))) + (S2 DM2_DTDOT);        | RK_DERIV
1336 M| 6      END;                | RK_DERIV
      ELSE
1337 M| 6      DO;                | RK_DERIV
1337 M| 6          DTH2_DR = 0.;      | RK_DERIV
1339 M| 7          DTH2_DUR = 0.;      | RK_DERIV
1340 M| 7          DTH2_DTDOT = 0.;    | RK_DERIV
1341 M| 6      END;                | RK_DERIV
1342 M| 5      DCL1_DR = DCL1_DM0 DM0_DR;
1343 M| 5

```

```

SOURCE
1344 MI 5 DCL2_DR = DCL2_DMO DMO_DR; | RK_DERIV
1345 MI 5 DCD1_DR = DCD1_DMO DMO_DR; | RK_DERIV
1346 MI 5 DCD2_DR = DCD2_DMO DMO_DR; | RK_DERIV
1347 MI 5 DCL1_DUR = DCL1_DMO DMO_DUR; | RK_DERIV
1348 MI 5 DCL2_DUR = DCL2_DMO DMO_DUR; | RK_DERIV
1349 MI 5 DCD1_DUR = DCD1_DMO DMO_DUR; | RK_DERIV
1350 MI 5 DCD2_DUR = DCD2_DMO DMO_DUR; | RK_DERIV
1351 MI 5 DCL1_DTDOT = DCL1_DMO DMO_DTDOT; | RK_DERIV
1352 MI 5 DCL2_DTDOT = DCL2_DMO DMO_DTDOT; | RK_DERIV
1353 MI 5 DCD1_DTDOT = DCD1_DMO DMO_DTDOT; | RK_DERIV
1354 MI 5 DCD2_DTDOT = DCD2_DMO DMO_DTDOT; | RK_DERIV
EI
1355 MI 5 V0_2 = (X_STORE X_STORE ) + ((SR T_VAL) ); | RK_DERIV
SI I_TIME:2 I_TIME:2
1356 MI 5 DL_DR = (LIFT ((DRO_DR / RO_C) + ((2. SR T_VAL T_VAL) / V0_2))) + | RK_DERIV
((DCL1_DR WING_AREA) + (DCL2_DR SS_PLANFORM_AREA)) DYNAMIC_PO; | RK_DERIV
1357 MI 5 DL_DUR = ((2. X_STORE LIFT) / V0_2) + ((DCL1_DUR | RK_DERIV
SI I_TIME:2 I_TIME:2
1357 MI 5 WING_AREA) + (DCL2_DUR SS_PLANFORM_AREA)) DYNAMIC_PO; | RK_DERIV
1358 MI 5 DL_DTDOT = ((2. SR SR T_VAL LIFT) / V0_2) + ((DCL1_DTDOT | RK_DERIV
1358 MI 5 WING_AREA) + (DCL2_DTDOT SS_PLANFORM_AREA)) DYNAMIC_PO; | RK_DERIV
1359 MI 5 DD_DR = (DRAG ((DRO_DR / RO_0) + ((2. SR T_VAL T_VAL) / V0_2))) + | RK_DERIV
((DCD1_DR WING_AREA) + (DCD2_DR SS_PLANFORM_AREA)) DYNAMIC_PO; | RK_DERIV
1360 MI 5 DD_DUR = ((2. X_STORE DRAG) / V0_2) + ((DCD1_DUR | RK_DERIV
SI I_TIME:2 I_TIME:2
1360 MI 5 WING_AREA) + (DCD2_DUR SS_PLANFORM_AREA)) DYNAMIC_PO; | RK_DERIV
1361 MI 5 DD_DTDOT = ((2. SR SR T_VAL DRAG) / V0_2) + ((DCD1_DTDOT | RK_DERIV
1361 MI 5 WING_AREA) + (DCD2_DTDOT SS_PLANFORM_AREA)) DYNAMIC_PO; | RK_DERIV
1362 MI 5 SIN_A = SIN(U_ACTIVE L_TIME:1 | RK_DERIV
SI L_TIME:1

```

```

SOURCE
STMT
1363 MI 5 COS_A = COS(U_ACTIVE_L_TIME:1);          | RK_DERIV
SI
1364 MI 5 DP_DR = (DL_DR SIN_A) - (DD_DR COS_A);   | RK_DERIV
1365 MI 5 DP_DUR = (DL_DUR SIN_A) - (DD_DUR COS_A); | RK_DERIV
1366 MI 5 DP_DTDOT = (DL_DTDOT SIN_A) - (DD_DTDOT COS_A); | RK_DERIV
1367 MI 5 DN_DR = (DL_DR COS_A) + (DD_DR SIN_A);   | RK_DERIV
1368 MI 5 DN_DUR = (DL_DUR COS_A) + (DD_DUR SIN_A); | RK_DERIV
1369 MI 5 DN_DTDOT = (DL_DTDOT COS_A) + (DD_DTDOT SIN_A); | RK_DERIV
EI
1370 MI 5 IF STAGE_SEP = OFF THEN
1371 MI 5 DO;
1372 MI 6 DMASSFLUX_DR1 = (DRO2_DR U2) + (RO_2 DU2_DR);
1373 MI 6 DMASSFLUX_DUR1 = (DRO2_DUR U2) + (RO_2 DU2_DUR);
1374 MI 6 DMASSFLUX_DTDOT1 = (DRC2_DTDOT U2) + (RO_2 DU2_DTDOT);
1375 MI 6 DMASSFLUX_DR2 = (DRO2_DR U2 SCRJ_MASS_CAPTURE_RATIO) + (RO_2 | RK_DERIV
DU2_DR SCRJ_MASS_CAPTURE_RATIO) + (RO_2 U2 DMCR_DM2_DR); | RK_DERIV
1376 MI 6 DMASSFLUX_DUR2 = (DRO2_DUR U2 SCRJ_MASS_CAPTURE_RATIO) + ( | RK_DERIV
RO_2 DU2_DUR SCRJ_MASS_CAPTURE_RATIO) + (RO_2 U2 DMCR_DM2 | RK_DERIV
DM2_DUR);
1377 MI 6 DMASSFLUX_DTDOT2 = (DRO2_DTDOT U2 SCRJ_MASS_CAPTURE_RATIO) + | RK_DERIV
(RO_2 DU2_DTDOT SCRJ_MASS_CAPTURE_RATIO) + (RO_2 U2 DMCR_DM2 | RK_DERIV
DM2_DTDOT);
1378 MI 5 END;
EI
1379 MI 5 OSC1 = L_CONST / (G_LOAD ((MD_MASS GO) ** 2));
1380 MI 5 DT_DR = DT1_DR + DTH2_DR;
1381 MI 5 DT_DUR = DT1_DUR + DTH2_DUR;
1382 MI 5 DT_DTDOT = DT1_DTDOT + DTH2_DTDOT;
1383 MI 5 IF G_LOAD > G_D THEN
| RK_DERIV

```



```

STMT          SOURCE          CURRENT SCOPE
1384 M| 5      DO;                | RK_DERIV
1395 M| 6      L_SUB_X_1 = OSC1 ((NET_X_FORCE (DT_DR + DP_DR)) + (N_AERO | RK_DERIV
S|          DN_DR));                |
1385 M| 6      L_SUB_X_2 = OSC1 ((NET_X_FORCE (DT_DUR + DP_DUR)) + (N_AERO | RK_DERIV
S|          DN_DUR));                |
1386 M| 6      L_SUB_X_4 = OSC1 ((NET_X_FORCE (DT_DTDOT + DP_DTDOT)) + ( | RK_DERIV
S|          N_AERO DN_DTDOT));        |
1387 M| 6      END;                | RK_DERIV
1388 M| 5      OG_DPI = 0.;          | RK_DERIV
E|          DAR_DPI = 0.;          |
1389 M| 5      DAW1_DPI = 0.;       | RK_DERIV
E|          DAW2_DPI = 0.;       |
1390 M| 5      DTH1_DPI = 0.;       | RK_DERIV
E|          DTH2_DPI = 0.;       |
1391 M| 5      DTH3_DPI = 0.;       | RK_DERIV
E|          DAE1_DPI = 0.;       |
1392 M| 5      DAE2_DPI = 0.;       | RK_DERIV
E|          [DMASSFLUX_DP1] = 0.; |
1393 M| 5      [DMASSFLUX_DP2] = 0.; |
E|          DO FOR I_FK = 1 TO HUM_CONSTANT_PARAMETERS;
1394 M| 5      IF I_FK = 9 THEN
1395 M| 5          IF I_FK = 9 THEN
1396 M| 5          IF I_FK = 9 THEN
1397 M| 5          IF I_FK = 9 THEN
1398 M| 5          IF I_FK = 9 THEN
1399 M| 5          IF I_FK = 9 THEN
1400 M| 5          IF I_FK = 9 THEN
1401 M| 6          IF I_FK = 9 THEN

```



```

SOURCE                                CURRENT SCOPE
-----                                -
E|
1415 M| 9      GAMMA0 M0_2 SIN_2 BETA - GAM1))2); | RK_DERIV
1416 M| 9      IF ((SIN_2_BETA == 0.) AND (SIN_BETA == 0.)) | RK_DERIV
1416 M| 9      THEN | RK_DERIV
1417 M| 9      DT2_DPI = (4. TO GAM3 DBETA_DPI COS_BETA ( | RK_DERIV
1417 M| 9      (GAMMA0 M0_2 M0_2 SIN_2 BETA SIN_2 BETA) + | RK_DERIV
1417 M| 9      1.)) / (GAM2 GAM2 M0_2 SIN_2 BETA SIN_BETA | RK_DERIV
1417 M| 9      ); | RK_DERIV
1418 M| 8      END; | RK_DERIV
E|
1419 M| 8      IF EXPANSION_FLAG = ON THEN |
1420 M| 8      DO; | RK_DERIV
1421 M| 9      IF (M2_2 - 1.) > 0. THEN | RK_DERIV
1422 M| 9      DM2_DPI = -(M2 (GAM2 + (GAM3 (M2_2 - 1.))) | RK_DERIV
1422 M| 9      ) / (2. SQRT(M2_2 - 1.)); | RK_DERIV
1423 M| 9      DT2_DPI = -(T2 GAM3 M2 DM2_DPI) / (1. + (GAM1 | RK_DERIV
1423 M| 9      M2_2)); | RK_DERIV
1424 M| 9      DRO2_DPI = -(RO_2 M2 DM2_DPI) / (1. + (GAM1 | RK_DERIV
1424 M| 9      M2_2)); | RK_DERIV
1425 M| 8      END; | RK_DERIV
1426 M| 8      DISPI_DPI = DISPI_DM2 DM2_DPI; | RK_DERIV
1427 M| 8      DISP2_DPI = DISP2_DM2 DM2_DPI; | RK_DERIV
1428 M| 8      DMCR_DPI = DMCR_DM2 DM2_DPI; | RK_DERIV
1429 M| 8      DU2_DPI = (DU2_DM2 DM2_DPI) + (DU2_DT2 DT2_DPI); | RK_DERIV
E|
1430 M| 8      IF ((TURBOJET_POWER = ON) AND (RO_2 == 0.) AND (U2 | RK_DERIV
1430 M| 8      == 0.) AND (TURBOJET_ISP == 0.)) THEN | RK_DERIV
1431 M| 8      DTH1_DPI = TURBOJET_THRUST ((DRO2_DPI / RO_2) + | RK_DERIV
1431 M| 8      S |
1431 M| 8      (DU2_DPI / U2) + (DISPI_DPI / TURBOJET_ISP)); | RK_DERIV

```

```

SOURCE                                CURRENT SCORE
STHT
1432 MI 8                               | RK_DERIV
EI                                     |
1432 MI 8                               | RK_DERIV
1432 MI 8                               | RK_DERIV
1432 MI 8                               | RK_DERIV
1433 MI 8                               | RK_DERIV
SI                                     |
1433 MI 8                               | RK_DERIV
1433 MI 8                               | RK_DERIV
1434 MI 8                               | RK_DERIV
SI                                     |
1434 MI 8                               | RK_DERIV
1435 MI 8                               | RK_DERIV
SI                                     |
1435 MI 8                               | RK_DERIV
1436 MI 7                               | RK_DERIV
1437 MI 7                               | RK_DERIV
1438 MI 7                               | RK_DERIV
1439 MI 8                               | RK_DERIV
SI                                     |
1440 MI 8                               | RK_DERIV
SI                                     |
1441 MI 7                               | RK_DERIV
1442 MI 7                               | RK_DERIV
1443 MI 7                               | RK_DERIV
SI                                     |
1444 MI 7                               | RK_DERIV
1445 MI 7                               | RK_DERIV
SI                                     |
1446 MI 7                               | RK_DERIV

```

```

STMT          SOURCE          CURRENT SCOPE
1447 MI 7     DAH1_DPI = (2. WING_AREA) / P ;      | RK_DERIV
SI 5
1448 MI 7     IF I_FK = 6 THEN                    | RK_DERIV
1449 MI 7     DO;                          | RK_DERIV
1450 MI 8     DAR_DPI = 4. / (COS(P) ) ;      | RK_DERIV
SI 6
1451 MI 8     E1                             | RK_DERIV
SI 6
1452 MI 7     END;                          | RK_DERIV
1453 MI 7     IF TURBOJET_POWER = ON THEN    | RK_DERIV
1454 MI 7     DTH1_DPI = DTH1_DPI + ((TURBOJET_THRUST | RK_DERIV
SI I_FK
1454 MI 7     DAE1_DPI ) / (P P) ) ;      | RK_DERIV
SI I_FK 2 4
1455 MI 7     E1                             | RK_DERIV
1456 MI 7     IF SCRAMJET_POWER = ON THEN    | RK_DERIV
1456 MI 7     DTH2_DPI = DTH2_DPI + ((SCRAMJET_THRUST | RK_DERIV
SI I_FK
1456 MI 7     DAE2_DPI ) / (P P) ) ;      | RK_DERIV
SI I_FK 2 3
1457 MI 7     DMASSFLUX_DPI = DMASSFLUX_DPI + (RO_2 U2 DAE1_DPI | RK_DERIV
SI I_FK
1457 MI 7     I_FK );                       | RK_DERIV
SI I_FK
1458 MI 7     DMASSFLUX_DP2 = DMASSFLUX_DP2 + (RO_2 U2 | RK_DERIV
SI I_FK
1458 MI 7     SCRJ_MASS_CAPTURE_RATIO DAE2_DPI ) ; | RK_DERIV
SI I_FK
1459 MI 6     END;                          | RK_DERIV
1460 MI 6     ELSE IF I_FK = 10 THEN         | RK_DERIV
1461 MI 6     DTH3_DPI = CAP_PHI;          | RK_DERIV
SI 10

```

```

SOURCE
CURRENT SCOPE
1452 M| 6 DT_DP = DTH1_DPI + DTH2_DPI + DTH3_DPI ; RK_DERIV
S| I_FK I_FK I_FK
1463 M| 6 DL_DPI = DYNAMIC_PO ((DCL1_DAR DAR_DPI WING_AREA) + (CL RK_DERIV
S| I_FK I_FK I_FK
1463 M| 6 DAH1_DPI ) + (SS_CL DAM2_DPI )); RK_DERIV
S| I_FK I_FK
1464 M| 6 DD_DPI = DYNAMIC_PO ((DCD1_DAR DAR_DPI WING_APEA) + (CD RK_DERIV
S| I_FK I_FK
1464 M| 6 DAH1_DPI ) + (SS_CD DAM2_DPI )); RK_DERIV
S| I_FK I_FK
1465 M| 6 DP_DP = (DL_DPI SIN_A) - (DD_DPI COS_A); RK_DERIV
S| I_FK
1466 M| 6 DN_DP = (DL_DPI COS_A) + (DD_DPI SIN_A); RK_DERIV
S| I_FK
E|
1467 M| 6 IF ((STAGE_SEP = OFF) OR (I_FK > FS_FIXED_PARAMETERS)) THEN RK_DERIV
1468 M| 6 DG_DP = (((NET_THRUST + P_AERO) (DT_DP + DP_DP I_FK
S| I_FK I_FK
)) + (N_AERO DN_DP )) / (G_LOAD ((MD_MASS GO )2)) - (( RK_DERIV
E| I_FK
1468 M| 6 G_LOAD DM_DP ) / MD_MASS); RK_DERIV
S| I_FK
1469 M| 6 IF G_LOAD > G_D THEN RK_DERIV
1470 M| 6 L_SUB_P = DG_DPI L_CONST; RK_DERIV
S| I_FK I_FK
1471 M| 5 END; RK_DERIV
E|
1472 M| 5 DM1DOT_DUA = 0.; RK_DERIV
E|
1473 M| 5 DM2DOT_DUA = 0.; RK_DERIV
E|
1474 M| 5 DM3DOT_DUA = 0.; RK_DERIV
E|
1475 M| 5 DT_DUA = DT_DP ; RK_DERIV
S| I_1
E|
1476 M| 5 DPHI_DUA2 = -2. U_ACTIVE CAP_PHI CAP_PHI; RK_DERIV
S| L_TIME:2

```

```

STMT          SOURCE          CURRENT SCOPE
1477 MI 5     DT_DUA_2 = (NET_THRUST DPHI_DUA2) / CAP_PHI;          | RK_DERIV
SI
1478 MI 5     DL_DUA1 = DYNAMIC_PO ((DCL_DALPHA DEGREES_PER_RADIAN WING_AREA) + | RK_DERIV
1478 MI 5     (DCL2_DUAL SS_PLANFORM_AREA));          | RK_DERIV
1479 MI 5     CD_DUA1 = DYNAMIC_PO ((2. CL DCD_DCL2 DCL_DALPHA          | RK_DERIV
1479 MI 5     DEGREES_PER_RADIAN WING_AREA) + (DCD2_DUAL SS_PLANFORM_AREA)); | RK_DERIV
1480 MI 5     DP_DUA_1 = (DL_DUAL SIN_A) - (DD_DUAL COS_A) + N_AERO;    | RK_DERIV
SI
1481 MI 5     DN_DUA_1 = (DD_DUAL SIN_A) + (DL_DUAL COS_A) - P_AERO;  | RK_DERIV
SI
EI
1482 MI 5     IF STAGE_SEP = OFF THEN
1483 MI 5     DO;
EI
1484 MI 6     IF ((TURBOJET_POMER = ON) AND (TURBOJET_ISP == 0.)) THEN
1485 MI 6     DO;
1486 MI 7     DM1DOT_DUA_1 = ((TURBOJET_THRUST DISPL_DM2_DM2_DPI) / ( | RK_DERIV
SI
1486 MI 7     TURBOJET_ISP TURBOJET_ISP GO)) - (DTH1_DPI_1 / ( | RK_DERIV
SI
1486 MI 7     TURBOJET_ISP GO));
1487 MI 7     DM1DOT_DUA_2 = -(TURBOJET_THRUST DPHI_DUA2) / ( | RK_DERIV
SI
1487 MI 7     TURBOJET_ISP GO CAP_PHI);
1488 MI 6     END;
EI
1489 MI 6     IF ((SCRAMJET_POMER = ON) AND (SCRAMJET_ISP == 0.)) THEN
1490 MI 6     DO;
1491 MI 7     DM2DOT_DUA_1 = ((SCRAMJET_THRUST DISP2_DM2_DM2_DPI) / ( | RK_DERIV
SI
1491 MI 7     SCRAMJET_ISP SCRAMJET_ISP GO)) - (DTH2_DPI_1 / ( | RK_DERIV
SI
1491 MI 7     SCRAMJET_ISP GO));
SI

```

```

SOURCE
CURRENT SCOPE
1492 MI 7 DM2DOT_DUA = -(SCRAMJET_THRUST DPHI_DUA2) / (
SI 2 | RK_DERIV
1492 MI 7 SCRAMJET_ISP 60 CAP_PHI); | RK_DERIV
1493 MI 6 END; | RK_DERIV
1494 MI 5 END; | RK_DERIV
1495 MI 5 ELSE | RK_DERIV
1495 MI 5 DM3DOT_DUA = -(ROCKET_THRUST DPHI_DUA2) / (ROCKET_ISP 60 | RK_DERIV
SI 2 |
1495 MI 5 CAP_PHI); | RK_DERIV
1496 MI 5 E |
SI ( (SR T_VAL) ) + (X_STORE X_STORE I_TIME:2 I_TIME:2); | RK_DERIV
1497 MI 5 DDELTA_DR = -(X_STORE T_VAL) / S3; | RK_DERIV
SI I_TIME:2 |
1498 MI 5 DDELTA_DUR = (SR T_VAL) / S3; | RK_DERIV
1499 MI 5 DDELTA_DTDOT = -(SR X_STORE I_TIME:2) / S3; | RK_DERIV
SI I_TIME:2 |
1500 MI 5 S2 = ARCTAN(X_STORE I_TIME:2 / (SR T_VAL)) + U_ACTIVE L_TIME:1 |
SI I_TIME:2 |
1501 MI 5 COS_DELTA = COS(S2); | RK_DERIV
1502 MI 5 SIN_DELTA = SIN(S2); | RK_DERIV
1503 MI 5 S6 = (UNIVERSAL_G_CONSTANT EARTH_MASS) / (SR SR); | RK_DERIV
1504 MI 5 DFR_DPHI = -S6; | RK_DERIV
1505 MI 5 S5 = DT_DR + DP_DR - (N_AERO DDELTA_DR); | RK_DERIV
1506 MI 5 S6 = DN_DR + ((NET_THRUST + P_AERO) DDELTA_DR); | RK_DERIV
1507 MI 5 DFR_DR = (S5 SIN_DELTA) + (S6 COS_DELTA) + ((2. S6 NET_MASS I_TIME |
SI I_TIME |
1507 MI 5 / SR); | RK_DERIV
1508 MI 5 DFTHETA_DR = (S5 COS_DELTA) - (S6 SIN_DELTA); | RK_DERIV
1509 MI 5 S5 = DT_DUR + DP_DUR - (N_AERO DDELTA_DUR); | RK_DERIV
1510 MI 5 S6 = DN_DUR + ((NET_THRUST + P_AERO) DDELTA_DUR); | RK_DERIV
1511 MI 5 DFR_DUR = (S5 SIN_DELTA) + (S6 COS_DELTA); | RK_DERIV

```



```

SOURCE
CURRENT SCOPE
-----
1512 M| 5 DFTHETA_DUR = (S5 COS_DELTA) - (S6 SIN_DELTA); | RK_DERIV
1513 M| 5 S5 = DT_DTDOT + DP_DTDOT - (N_AERO ODELTA_DTDOT); | RK_DERIV
1514 M| 5 S6 = DN_DTDOT + ((NET_THRUST + P_AERO) DDELTA_DTDOT); | RK_DERIV
1515 M| 5 DFR_DTDOT = (S5 SIN_DELTA) + (S6 COS_DELTA); | RK_DERIV
1516 M| 5 DFTHETA_DTDOT = (S5 COS_DELTA) - (S6 SIN_DELTA); | RK_DERIV
1517 M| 5 IF STAGE_SEP = OFF THEN | RK_DERIV
1518 M| 5 DO: | RK_DERIV
1519 M| 6 IF TURBOJET_POWER = ON THEN | RK_DERIV
1520 M| 6 DO: | RK_DERIV
1521 M| 7 S5 = -P P T J MAX_FUEL_AIR_RATIO CAP_PHI; | RK_DERIV
1522 M| 7 DM1DOT_DR = S5 DMASSFLUX_DR1; | RK_DERIV
1523 M| 7 DM1DOT_DUR = S5 DMASSFLUX_DUR1; | RK_DERIV
1524 M| 7 DM1DOT_DTDOT = S5 DMASSFLUX_DTDOT1; | RK_DERIV
1525 M| 5 END; | RK_DERIV
1526 M| 6 ELSE | RK_DERIV
1527 M| 6 DO: | RK_DERIV
1528 M| 7 DM1DOT_DR = 0.; | RK_DERIV
1529 M| 7 DM1DOT_DUR = 0.; | RK_DERIV
1530 M| 6 DM1DOT_DTDOT = 0.; | RK_DERIV
1531 M| 6 END; | RK_DERIV
1532 M| 6 IF SCRAMJET_POWER = ON THEN | RK_DERIV
1533 M| 7 DO: | RK_DERIV
1534 M| 7 S5 = -P P SCRJ_MAX_FUEL_AIR_RATIO CAP_PHI; | RK_DERIV
1535 M| 7 DM2DOT_DR = S5 DMASSFLUX_DR2; | RK_DERIV
1536 M| 7 DM2DOT_DUR = S5 DMASSFLUX_DUR2; | RK_DERIV

```

```

STMT          SOURCE          CURRENT SCOPE
1536 MI 7     DM2DOT_DTDOT = S5 DM2SSFLUX_DTDOT2;      | RK_DERIV
1537 MI 6     END;                                       | RK_DERIV
1539 MI 6     ELSE                                       | RK_DERIV
1539 MI 6     DO;                                       | RK_DERIV
1539 MI 7     DM2DOT_DR = 0.;                          | RK_DERIV
1540 MI 7     DM2DOT_DUR = 0.;                      | RK_DERIV
1541 MI 7     DM3DOT_DTDOT = 0.;                 | RK_DERIV
1542 MI 6     END;                                       | RK_DERIV
1543 MI 5     END;                                       | RK_DERIV
1544 MI 5     ELSE                                       | RK_DERIV
1544 MI 5     DO;                                       | RK_DERIV
1545 MI 6     DM1DOT_DR = 0.;                      | RK_DERIV
1546 MI 6     DM1DOT_DUR = 0.;                      | RK_DERIV
1547 MI 6     DM1DOT_DTDOT = 0.;                 | RK_DERIV
1548 MI 6     DM2DOT_DR = 0.;                      | RK_DERIV
1549 MI 6     DM2DOT_DUR = 0.;                      | RK_DERIV
1550 MI 6     DM3DOT_DTDOT = 0.;                 | RK_DERIV
1551 MI 5     END;                                       | RK_DERIV
1552 MI 5     * F = 0;                                       | RK_DERIV
1553 MI 5     F = 1.;                                       | RK_DERIV
1554 MI 5     F      1,2;                                       |
1554 MI 5     F      3,4;                                       |
1555 MI 5     F = (X_STORE X_STORE ) + (DFR_DR / NET_MASS | RK_DERIV
1555 MI 5     I_TIME:4 I_TIME:4);
1555 MI 5     I_TIME);
1556 MI 5     F = DFR_CUR / NET_MASS I_TIME | RK_DERIV
1556 MI 5     I_TIME;
1556 MI 5     F      2,2;

```

STMT	SOURCE	CURRENT SCOPE
1557 MI 5 SI	F = (2. SR X_STORE) + (DFR_DTDOT / NET_MASS I_TIME:4	RK_DERIV
1558 MI 5 SI	F = (DFR_OHI - (NET_R_FORCE / NET_MASS I_TIME:4	RK_DERIV
1559 MI 5 SI	F = F ;	RK_DERIV
1560 MI 5 SI	F = F ;	RK_DERIV
1561 MI 5 SI	F = (((2. X_STORE X_STORE I_TIME:2 - (NET_THETA_FORCE	RK_DERIV
1562 MI 5 SI	/ NET_MASS I_TIME:4) / SR) + (DFTHETA_DR / NET_MASS I_TIME	RK_DERIV
1563 MI 5 SI	F = ((DFTHETA_DUR / NET_MASS I_TIME:4) - (2. X_STORE I_TIME:4	RK_DERIV
1564 MI 5 SI	SR;	RK_DERIV
1565 MI 5 SI	F = (DFTHETA_DTDOT / (NET_MASS I_TIME:4 SR)) - ((2. X_STORE I_TIME:4	RK_DERIV
1566 MI 5 SI) / SR);	RK_DERIV
1567 MI 5 SI	F = -NET_THETA_FORCE / (NET_MASS I_TIME:4 NET_MASS SR);	RK_DERIV
1568 MI 5 SI	F = F ;	RK_DERIV
1569 MI 5 SI	F = F ;	RK_DERIV
1570 MI 5 SI	F = DM1DOT_DR;	RK_DERIV
1571 MI 5 SI	F = DM1DOT_DUR;	RK_DERIV
1572 MI 5 SI	F = DM1DOT_DTDOT;	RK_DERIV
1573 MI 5 SI	F = DM2DOT_DR;	RK_DERIV
1574 MI 5 SI	F = DM2DOT_DUR;	RK_DERIV

```

STMT          SOURCE          CURRENT SCOPE
1572 MI 5     F = DM2DOT_DTDOT;      | RK_DERIV
SI           6,4
1573 MI 5     *
EI           K = 0.;
1574 MI 5     DO FOR I_FK = 1 TO NUM_CONSTANT_PARAMETERS;
1575 MI 6     IF ((STAGE_SEP = OFF) OR (I_FK > FS_FIXED_PARAMETERS)) THEN
EI           DO;
1576 MI 6     SS = DT_DP
SI           I_FK + OP_DP
1577 MI 7     I_FK
SI           I_FK;
1578 MI 7     DFR_DP
SI           I_FK = (SS SIN_DELTA) + (DN_DP
I_FK COS_DELTA) - (SG
I_FK
1578 MI 7     DM_DP
SI           I_FK);
1579 MI 7     OFTHETA_DP
SI           I_FK = (SS COS_DELTA) - (DN_DP
I_FK SIN_DELTA);
1580 MI 6     END;
1581 MI 6     ELSE
1581 MI 6     DO;
1582 MI 7     DFR_DP
SI           I_FK = 0.;
1583 MI 7     OFTHETA_DP
SI           I_FK = 0.;
1584 MI 6     END;
1585 MI 6     IF STAGE_SEP = OFF THEN
1586 MI 6     DO;
--          EI
1587 MI 7     IF TURBOJET_POKER = ON THEN
1588 MI 7     DM1DOT_DP
SI           I_FK = -TJ_MAX_FUEL_AIR_RATIO CAP_PHI
1588 MI 7     DMASSFLUX_DP1
SI           I_FK;
--          EI
1589 MI 7     ELSE

```

```

STMT          SOURCE          CURRENT SCOPE
1589 MI 7     DM1DOT_DP      RK_DERIV
SI           I_FK = 0.;
1590 MI 7     IF SCRAMJET_POWER = ON THEN
EI
1591 MI 7     DM2DOT_DP      RK_DERIV
SI           I_FK = -SCRJ_MAX_FUEL_AIR_RATIO CAP_PHI
1591 MI 7     DMASSFLUX_DP2   RK_DERIV
SI           I_FK
1592 MI 7     ELSE
1592 MI 7     DM2DOT_DP      RK_DERIV
SI           I_FK = 0.;
1593 MI 7     DM3DOT_DP      RK_DERIV
SI           I_FK = 0.;
1594 MI 6     END;
1595 MI 6     ELSE
1595 MI 6     DO;
1596 MI 7     DM1DOT_DP      RK_DERIV
SI           I_FK = 0.;
1597 MI 7     DM2DOT_DP      RK_DERIV
SI           I_FK = 0.;
1598 MI 7     IF I_FK = 10 THEN
1599 MI 7     DM3DOT_DP      RK_DERIV
SI           I_FK = -CAP_PHI / (ROCKET_ISP GO);
1600 MI 7     ELSE
1600 MI 7     DM3DOT_DP      RK_DERIV
SI           I_FK = 0.;
1601 MI 6     END;
1602 MI 6     IF ((STAGE_SEP = OFF) OR (I_FK > FS_FIXED_PARAMETERS)) THEN
EI
1603 MI 6     DO;
1604 MI 7     K = (DFR_DP      RK_DERIV
SI           I_FK - ((NET_R_FORCE DM_DP      RK_DERIV
SI           I_FK) /
NET_MASS I_TIME) / NET_MASS I_TIME;
1604 MI 7     NET_MASS I_TIME
SI

```

```

SOURCE                                CURRENT SCOPE
-----                                -
1605 MI 7                             K      = (DFTHETA_DP      - ((NET_THETA_FORCE DM_DP      ) ) ) / RK_DERIV
SI      4,I_FK                          I_FK
1605 MI 7                             / NET_MASS      ) / (NET_MASS      SR);
SI      I_TIME
1606 MI 7                             K      = DM1DOT_DP      ;
SI      5,I_FK                          I_FK
1607 MI 7                             K      = DM2DOT_DP      ;
SI      6,I_FK                          I_FK
1608 MI 7                             K      = DM3DOT_DP      ;
SI      7,I_FK                          I_FK
1609 MI 6                             END;
1610 MI 5                             END;
1611 MI 5                             DFR_DUA      = ((DT_DUA      + DP_DUA      ) SIN_VEHICLE_ANGLE) + (DN_DUA      )
SI      1                               1
1611 MI 5                             COS_VEHICLE_ANGLE) + NET_THETA_FORCE;
1612 MI 5                             DFTHETA_DUA      = ((DT_DUA      + DP_DUA      ) COS_VEHICLE_ANGLE) - (DN_DUA      )
SI      1                               1
1612 MI 5                             SIN_VEHICLE_ANGLE) - NET_R_FORCE - (NET_MASS      I_TIME G);
SI
1613 MI 5                             DFR_DUA      = DT_DUA      SIN_VEHICLE_ANGLE;
SI      2
1614 MI 5                             DFTHETA_DUA      = DT_DUA      COS_VEHICLE_ANGLE;
SI      2
1615 MI 5                             IF ((FD_COUNT = 1) OR (FD_COUNT = 3) OR (I_TIME = 1)) THEN
1616 MI 5                             DO:
1617 MI 6                             DO FOR I_FK = 1 TO NUM_CONTROLS;
1618 MI 7                             G_MAT      = DFR_DUA      / NET_MASS      ;
SI      J_TIME:2,I_FK                  I_FK      I_TIME
1619 MI 7                             G_MAT      = DFTHETA_DUA      / (NET_MASS      SR
SI      J_TIME:4,I_FK                  I_FK      I_TIME
1619 MI 7                             );
1620 MI 7                             G_MAT      = DM1DOT_DUA      ;
SI      J_TIME:5,I_FK                  I_FK
1621 MI 7                             G_MAT      = DM2DOT_DUA      ;
SI      I_TIME:6,I_FK                  I_FK

```

```

SOURCE
CURRENT SCOPE
1622 MI 7 G_MAT J_TIME:7,I_FK = DH3DOT_DUA ; RK_DERIV
SI I_FK
1623 MI 7 IF G_LOAD > G_D THEN RK_DERIV
1624 MI 7 L_SUB_U I_FK = (((DT_DUA I_FK + DP_DUA I_FK) (NET_THRUST I_FK) (NET_THRUST I_FK)
SI I_FK + P_AERO)) + (DN_DUA I_FK N_AERO)) L_CONST) / (G_LOAD ( RK_DERIV
EI (NET_MASS I_TIME ) ) ) ;
SI I_TIME
1625 MI 7 ELSE RK_DERIV
1626 MI 6 L_SUB_U I_FK = 0.; RK_DERIV
1627 MI 5 END; RK_DERIV
1628 MI 5 IF FD_COUNT = 1 THEN RK_DERIV
1629 MI 5 DO; RK_DERIV
* * RK_DERIV
F1 = F; RK_DERIV
* * RK_DERIV
KA = K; RK_DERIV
L_SUB_P_1 = L_SUB_P; RK_DERIV
L_SUB_U_1 = L_SUB_U; RK_DERIV
END; RK_DERIV
1635 MI 5 IF FD_COUNT = 2 THEN RK_DERIV
1636 MI 5 DO; RK_DERIV
* * RK_DERIV
F2 = F; RK_DERIV
* * RK_DERIV
KB = K; RK_DERIV
END; RK_DERIV
1639 MI 5 IF FD_COUNT = 3 THEN RK_DERIV
1640 MI 5

```


STMT	SOURCE	CURRENT SCOPE
1662 MI 4	END;	RK_DERIV
1663 MI 3	END;	RK_DERIV
1664 MI 2	END;	RK_DERIV
1665 MI 2	IF LAMSDA_FLAG = ON THEN	RK_DERIV
1666 MI 2	LAMSDA_DOT = -(TRANSPPOSE(F) LAMSDA_HOLD) - L_X_STORE I_TIME; - L_SUS_X;	RK_DERIV
1667 MI 2	IF CAP_LAMSDA_1_FLAG = ON THEN	RK_DERIV
1668 MI 2	DO;	RK_DERIV
1669 MI 3	IF I_FD = 1 THEN	RK_DERIV
1670 MI 3	CAP_LAMSDA_1_DOT = -TRANSPPOSE(F1) CAP_LAMSDA_1_HOLD;	RK_DERIV
1671 MI 3	IF I_FD = 2 THEN	RK_DERIV
1672 MI 3	CAP_LAMSDA_1_DOT = -TRANSPPOSE(F2) CAP_LAMSDA_1_HOLD;	RK_DERIV
1673 MI 3	IF I_FD = 3 THEN	RK_DERIV
1674 MI 3	CAP_LAMSDA_1_DOT = -TRANSPPOSE(F3) CAP_LAMSDA_1_HOLD;	RK_DERIV
1675 MI 3	IF I_FD = 4 THEN	RK_DERIV
1676 MI 3	CAP_LAMSDA_1_DOT = -TRANSPPOSE(F4) CAP_LAMSDA_1_HOLD;	RK_DERIV
1677 MI 3	IF I_FD = 5 THEN	RK_DERIV
1678 MI 3	CAP_LAMSDA_1_DOT = -TRANSPPOSE(F5) CAP_LAMSDA_1_HOLD;	RK_DERIV
1679 MI 2	END;	RK_DERIV
1680 MI 2	IF CAP_LAMSDA_2_FLAG = ON THEN	RK_DERIV
1681 MI 2	DO;	RK_DERIV
1682 MI 3	IF I_FD = 1 THEN	RK_DERIV
1683 MI 3	CAP_LAMSDA_2_DOT = -TRANSPPOSE(KA) CAP_LAMSDA_1_J_TIME;	RK_DERIV
1683 MI 3	SI	RK_DERIV

STMT	SOURCE	CURRENT SCOPE
1701 MI 2	END;	RK_DERIV
EI		
1702 MI 2	IF (I_J_J_FLAG OR I_PSI_J_FLAG OR I_PSI_FLAG) = ON THEN	RK_DERIV
1703 MI 2	DO;	RK_DERIV
1704 MI 3	U_TIME = J_TIME;	RK_DERIV
1705 MI 3	CALL U_CCHPUTE;	RK_DERIV
EI		
1706 MI 3	IF I_J_J_FLAG = ON THEN	RK_DERIV
EI		
1707 MI 3	I_J_J_DOT = (H_SUB_U * U) . H_SUB_U	RK_DERIV
SI	J_TIME:	
EI		
1708 MI 3	IF I_PSI_J_FLAG = ON THEN	RK_DERIV
EI		
1709 MI 3	I_PSI_J_DOT = (TRANPOSE(CAP_LAMBDA_I * J_TIME) G_MAT * (U H_SUB_U	RK_DERIV
SI	J_TIME: J_TIME:	
1709 MI 3);	RK_DERIV
SI		
EI		
1710 MI 3	IF I_PSI_FLAG = ON THEN	RK_DERIV
1711 MI 3	DO;	RK_DERIV
EI		
1712 MI 4	* M_1 = TRANPOSE(CAP_LAMBDA_I * J_TIME) G_MAT * J_TIME;	RK_DERIV
SI		
EI		
1713 MI 4	I_PSI_PSI_DOT = (M_1 U) TRANPOSE(M_1);	RK_DERIV
1714 MI 3	END;	RK_DERIV
1715 MI 2	END;	RK_DERIV
1716 MI 1	END;	RK_DERIV
CI	COSTATE DERIVATIVE COMPUTATIONS END HERE	RK_DERIV
EI		
1717 MI 1	IF LAMBDA_FLAG = ON THEN	RK_DERIV
1718 MI 1	RK_D_VAL = LAMBDA_DOT I_RK	RK_DERIV
SI		

```

SYMT SOURCE CURRENT SCOPE
E|
1719 HI 1 IF CAP_LAM3DA_1_FLAG = ON THEN | RK_DERIV
1720 HI 1 RK_D_VAL = CAP_LAM3DA_1_DOT | RK_DERIV
SI I_RK,J_RK
E|
1721 HI 1 IF CAP_LAM3DA_2_FLAG = ON THEN | RK_DERIV
1722 HI 1 RK_D_VAL = CAP_LAM3DA_2_DOT | RK_DERIV
SI I_RK,J_RK
E|
1723 HI 1 IF SGV_FLAG = ON THEN | RK_DERIV
1724 HI 1 RK_D_VAL = SGV_DOT | RK_DERIV
SI I_RK
E|
1725 HI 1 IF I_J_J_FLAG = ON THEN | RK_DERIV
1726 HI 1 RK_D_VAL = I_J_J_DOT | RK_DERIV
E|
1727 HI 1 IF I_PSI_J_FLAG = ON THEN | RK_DERIV
1728 HI 1 RK_D_VAL = I_PSI_J_DOT | RK_DERIV
SI I_RK
E|
1729 HI 1 IF I_PSI_PSI_FLAG = ON THEN | RK_DERIV
1730 HI 1 RK_D_VAL = I_PSI_PSI_DOT | RK_DERIV
SI I_RK,J_RK
1731 HI END;
1732 HI CLOSE RK_DERIV;

```

**** B L O C K S U M M A R Y ****

OUTER PROCEDURES CALLED
MODEL_DRIVER, U_COMPUTE

COMPOOL VARIABLES USED

NUM_STATES, NUM_CONSTANT_PARAMETERS, NUM_CONSTRAINTS, NUM_CONTROLS, Q_D, CAP_Q, G_D, CAP_CA, GO, X_STORE, EARTH_RADIUS
 NUM_TRANSPTS, CHESS_I_TIME, EARTH_CHESSA, GAMMA_0, R_0, GAM1, GAM2, GAM3, U_ACTIVE, DELIVERED_PLANTFORM_AREA, P
 FS_FIXED_PARAMETERS, DEGREES_PER_RADIAN, ROCKET_ISP, UNIVERSAL_G_CONSTANT, EARTH_MASS, TJ_MAX_FUEL_AIR_RATIO
 SCRJ_MAX_FUEL_AIR_RATIO

OUTER VARIABLES USED

STATE_INTEGRATION_FLAG, I_EK, RK_D_VAL*, DYNAMIC_PO, G_LOAD, RK_D_VAL, X_DOT, RK_STEP*, RK_STEP, FIRST_DERIV_FLAG
 FIRST_DERIV_FLAG*, LAM3DA_FLAG, CAP_LAM3DA_1_FLAG, RK_VAL_N, PARTIAL_DERIV_FLAG, PARTIAL_DERIV_FLAG*, VAL_1, CAP_LAM3DA_2_FLAG
 I_TIME*, I_TIME, J_TIME*, I_GL, FD_FLAG, FD_FLAG, L_TIME*, L_TIME*, L_TIME*, L_TIME*, I_TIME_STORE, I_FLAG, OIT_FLAG


```

SOURCE
CURRENT SCOPE
1754 MI 3      RK_VAL_N      I_RK,J_RK      = CAP_LAMBDA_1      J_TIME:I_RK,J_RK      ;
SI
| RUNGE_KUTTA
1755 MI 2      END;
| RUNGE_KUTTA
1756 MI 1      END;
| RUNGE_KUTTA
EI
1757 MI 1      IF CAP_LAMBDA_2_FLAG = ON THEN
| RUNGE_KUTTA
1758 MI 1      DO FOR I_RK = 1 TO NUM_CONSTANT_PARAMETERS;
| RUNGE_KUTTA
1759 MI 2      DO FOR J_RK = 1 TO NUM_CONSTRAINTS;
| RUNGE_KUTTA
1760 MI 3      RK_VAL_N      I_RK,J_RK      = CAP_LAMBDA_2      I_RK,J_RK      ;
SI
| RUNGE_KUTTA
1761 MI 2      END;
| RUNGE_KUTTA
1762 MI 1      END;
| RUNGE_KUTTA
EI
1763 MI 1      IF SGV_FLAG = ON THEN
| RUNGE_KUTTA
1764 MI 1      DO FOR I_RK = 1 TO NUM_CONSTANT_PARAMETERS;
| RUNGE_KUTTA
1765 MI 2      RK_VAL_N      I_RK,1      = SMALL_G_VEC      I_RK      ;
SI
| RUNGE_KUTTA
1766 MI 1      END;
| RUNGE_KUTTA
EI
1767 MI 1      IF I_J_J_FLAG = ON THEN
| RUNGE_KUTTA
1768 MI 1      RK_VAL_N      I_RK,1      = I_J_J;
SI
| RUNGE_KUTTA
EI
1769 MI 1      IF I_PSI_J_FLAG = ON THEN
| RUNGE_KUTTA
1770 MI 1      DO FOR I_RK = 1 TO NUM_CONSTRAINTS;
| RUNGE_KUTTA
1771 MI 2      RK_VAL_N      I_RK,1      = I_PSI_J      I_RK      ;
SI
| RUNGE_KUTTA
1772 MI 1      END;
| RUNGE_KUTTA
EI
1773 MI 1      IF I_PSI_PSI_FLAG = ON THEN
| RUNGE_KUTTA
1774 MI 1      DO FOR I_RK = 1 TO NUM_CONSTRAINTS;
| RUNGE_KUTTA
1775 MI 2      DO FOR J_RK = I_RK TO NUM_CONSTRAINTS;
| RUNGE_KUTTA

```



```

STMT
1842 MI 1      DO FOR I_RK = 1 TO NUM_STATES;
1843 MI 2      X_STORE
SI            I_TIME:I_RK      = RK_VAL_N_PLUS_1 I_RK,1
1844 MI 1      END;
1845 MI 1      INTEG_L = RK_VAL_N_PLUS_1
SI            NUM_STATES+1,1 ;
1846 MI 1      NET_MASS
SI            I_TIME      = X_STORE I_TIME:5 + X_STORE I_TIME:6 + SS_DRY_MASS;
EI
1847 MI 1      IF ((STAGE_SEP = OFF) OR (OMEGA_I_TIME = I_TIME)) THEN
SI
1848 MI 1      NET_MASS
SI            I_TIME      = NET_MASS I_TIME + FIRST_STAGE_DRY_MASS;
1849 MI 1      END;
1850 MI 1      CLOSE RUNGE_KUTTA;

```

CURRENT SCOPE

- | RUNGE_KUTTA
- | RUNGE_KUTTA
- | RUNGE_KUTTA
- | RUNGE_KUTTA
- | RUNGE_KUTTA
- | RUNGE_KUTTA
- | RUNGE_KUTTA
- | RUNGE_KUTTA
- | RUNGE_KUTTA
- | RUNGE_KUTTA

*** B L O C K S U M M A R Y ***
 OUTER PROCEDURES CALLED
 STATE_DERIVS

COMFOOL VARIABLES USED
 NUM_STATES, X_STORE, NUM_CONSTRAINTS, NUM_CONSTANT_PARAMETERS, X_STORE*, OMEGA_I_TIME
 OUTER VARIABLES USED
 STATE_INTEGRATION_FLAG, TIME_INTERVAL*, TIME_STEP, RK_VAL_N*, I_TIME, INTEG_L, LAMBDA_FLAG, CAP_LAMBDA_1_FLAG, CAP_LAMBDA_2_FLAG
 J_TIME, LAMBDA_1, CAP_LAMBDA_1, CAP_LAMBDA_2, SGV_FLAG, SMALL_G_VEC, I_J_J_FLAG, I_J_J_FLAG, I_PSI_J_FLAG, I_PSI_PSI_FLAG
 I_PSI_PSI, RK_COLS, RK_COLS, I_FD, I_FD*, FIRST_DERIV_FLAG*, PARTIAL_DERIV_FLAG*, TIME_INTERVAL, RK_VAL_N, RK_VAL_N_PLUS_1*
 I_TIME*, RK_VAL_N_PLUS_1, INTEG_L*, NET_MASS*, SS_DRY_MASS, STAGE_SEP, NET_MASS, FIRST_STAGE_DRY_MASS

```

SOURCE                                CURRENT SCOPE
-----                                -
1852 MI TIME_SET:                     | TIME_SET
1851 MI PROCEDURE:                    | TIME_SET
1852 MI DECLARE TSI INTEGER AUTOMATIC; | TIME_SET
1853 MI PRESENT_TIME_STEP = NORM_TIME_STEP; | TIME_SET
1854 MI DO FOR TSI = 1 TO NUM_TRANS_PTS; | TIME_SET
E|
1855 MI 1 IF STATE_INTEGRATION_FLAG = ON THEN | TIME_SET
1856 MI 1 DO; | TIME_SET
1857 MI 2 IF ((OMEGA_I_TIME > (I_TIME - 4)) AND ((OMEGA_I_TIME < I_TIME) OR (OMEGA_I_TIME | TIME_SET
SI |
1857 MI 2 = I_TIME))) THEN | TIME_SET
SI |
1858 MI 2 PRESENT_TIME_STEP = NEG_TIME_STEP ; | TIME_SET
SI |
1859 MI 2 IF ((OMEGA_I_TIME > I_TIME) AND ((OMEGA_I_TIME < (I_TIME + 4)) OR (OMEGA_I_TIME | TIME_SET
SI |
1859 MI 2 = (I_TIME + 4)))) THEN | TIME_SET
SI |
1860 MI 2 PRESENT_TIME_STEP = POS_TIME_STEP ; | TIME_SET
SI |
1861 MI 1 END; | TIME_SET
1862 MI 1 ELSE | TIME_SET
1862 MI 1 DO; | TIME_SET
1863 MI 2 IF (((OMEGA_I_TIME > (I_TIME - 4)) OR (OMEGA_I_TIME = (I_TIME - 4))) AND ( | TIME_SET
SI |
1863 MI 2 OMEGA_I_TIME < I_TIME)) THEN | TIME_SET
SI |
1864 MI 2 PRESENT_TIME_STEP = NEG_TIME_STEP ; | TIME_SET
SI |
1865 MI 2 IF (((OMEGA_I_TIME > I_TIME) OR (OMEGA_I_TIME = I_TIME)) AND (OMEGA_I_TIME < ( | TIME_SET
SI |
1865 MI 2 I_TIME + 4))) THEN | TIME_SET
SI |
1866 MI 2 PRESENT_TIME_STEP = POS_TIME_STEP ; | TIME_SET
SI |

```

```

SOURCE
1867 MI 1      END;          I TIME_SET
1868 MI      END;          I TIME_SET
1869 MI CLOSE TIME_SET;    I TIME_SET

```

*** B L O C K S U M M A R Y ***

```

COMPOOL VARIABLES USED
  NORM_TIME_STEP, NUM_TRANS_PTS, OMEGA_I_TIME, NEG_TIME_STEP, POS_TIME_STEP
OUTER VARIABLES USED
  PRESENT_TIME_STEP*, STATE_INTEGRATION_FLAG, I_TIME

```

STMT	SOURCE	CURRENT SCOPE
1870 MI	ITERATION_DRIVER:	ITERATION_DRIVER
1870 MI	PROCEDURE:	ITERATION_DRIVER
1871 MI	DECLARE CHECK1 SCALAR DOUBLE AUTOMATIC;	ITERATION_DRIVER
1872 MI	DECLARE TANK1 SCALAR DOUBLE AUTOMATIC;	ITERATION_DRIVER
1873 MI	DECLARE TANK2 SCALAR DOUBLE AUTOMATIC;	ITERATION_DRIVER
1874 MI	DECLARE I_INIT INTEGER AUTOMATIC;	ITERATION_DRIVER
1875 MI	DECLARE I_XDOT VECTOR(NUM_STATES) DOUBLE STATIC;	ITERATION_DRIVER
1876 MI	DECLARE H_VEC VECTOR(NUM_CONSTRAINTS) DOUBLE STATIC;	ITERATION_DRIVER
1877 MI	DECLARE DELTA_U_NEW ARRAY((STEP_DIH + 2) / 2) VECTOR(NUM_CONTROLS) DOUBLE AUTOMATIC;	ITERATION_DRIVER
1878 MI	DECLARE I_RCP INTEGER AUTOMATIC;	ITERATION_DRIVER
1879 MI	DECLARE J_RCP INTEGER AUTOMATIC;	ITERATION_DRIVER
1880 MI	DECLARE J_TIME_STORE INTEGER STATIC;	ITERATION_DRIVER
1881 MI	DECLARE I_U INTEGER STATIC;	ITERATION_DRIVER
1882 MI	DECLARE J_U INTEGER AUTOMATIC;	ITERATION_DRIVER
1883 MI	DECLARE J_OMEGA INTEGER STATIC;	ITERATION_DRIVER
1884 MI	DECLARE I_OMEGA INTEGER STATIC;	ITERATION_DRIVER
1885 MI	DECLARE TIME_SIGN SCALAR DOUBLE STATIC;	ITERATION_DRIVER
1886 MI	DECLARE SC1 SCALAR DOUBLE STATIC;	ITERATION_DRIVER
1887 MI	DECLARE SC2 SCALAR DOUBLE STATIC;	ITERATION_DRIVER
1888 MI	DECLARE SC3 SCALAR DOUBLE STATIC;	ITERATION_DRIVER
1889 MI	DECLARE SC4 SCALAR DOUBLE STATIC;	ITERATION_DRIVER
1890 MI	DECLARE DFP3 SCALAR DOUBLE AUTOMATIC;	ITERATION_DRIVER
1891 MI	DECLARE S9 SCALAR DOUBLE STATIC INITIAL(1.0001);	ITERATION_DRIVER
1892 MI	DECLARE PAST_INTEG_L SCALAR DOUBLE STATIC;	ITERATION_DRIVER
1893 MI	DECLARE LI4 INTEGER AUTOMATIC;	ITERATION_DRIVER
1894 MI	DECLARE LI5 INTEGER AUTOMATIC;	ITERATION_DRIVER
1895 MI	DECLARE LI_FLAG BIT(1) AUTOMATIC;	ITERATION_DRIVER
1896 MI	DECLARE OLD_SC3 SCALAR DOUBLE AUTOMATIC;	ITERATION_DRIVER

```

SOURCE
1897 MI  DECLARE T_MASS SCALAR DOUBLE STATIC;
1898 MI  DECLARE OLD_FINAL_STEP INTEGER STATIC;
1899 MI  DECLARE FINAL_U_STORE ARRAY(4) VECTOR(NUM_CONTROLS) DOUBLE STATIC;
1900 MI  DECLARE STEP_I_FLAG BIT(1) STATIC;
1901 MI  DECLARE U_KEEP VECTOR(NUM_CONTROLS) DOUBLE AUTOMATIC;
1902 MI  DECLARE HOLD_PSI VECTOR(NUM_CONSTRAINTS) DOUBLE STATIC;
1903 MI  DECLARE U_NEW ARRAY(1001) VECTOR(NUM_CONTROLS) DOUBLE AUTOMATIC;
1904 MI  DECLARE UV1 SCALAR DOUBLE AUTOMATIC;

CURRENT SCOPE
| ITERATION_DRIVER
| ITERATION_DRIVER
| ITERATION_DRIVER
| ITERATION_DRIVER
| ITERATION_DRIVER
| ITERATION_DRIVER
| ITERATION_DRIVER
| ITERATION_DRIVER
| ITERATION_DRIVER

```

STMT	SOURCE	CURRENT SCOPE
1905 M	STATE_INTEGRATION::	STATE_INTEGRATION
1905 M	PROCEDURE;	STATE_INTEGRATION
E		STATE_INTEGRATION
1906 M	LAMBDA_FLAG = OFF;	STATE_INTEGRATION
E		STATE_INTEGRATION
1907 M	CAP_LAMBDA_1_FLAG = OFF;	STATE_INTEGRATION
E		STATE_INTEGRATION
1908 M	CAP_LAMBDA_2_FLAG = OFF;	STATE_INTEGRATION
E		STATE_INTEGRATION
1909 M	SGV_FLAG = OFF;	STATE_INTEGRATION
E		STATE_INTEGRATION
1910 M	I_J_FLAG = OFF;	STATE_INTEGRATION
E		STATE_INTEGRATION
1911 M	I_PSI_J_FLAG = OFF;	STATE_INTEGRATION
E		STATE_INTEGRATION
1912 M	I_PSI_PSI_FLAG = OFF;	STATE_INTEGRATION
1913 M	RK_ROWS = NUM_STATES + 1;	STATE_INTEGRATION
1914 M	RK_COLUMNS = 1;	STATE_INTEGRATION
1915 M	I_TIME = 1;	STATE_INTEGRATION
E		STATE_INTEGRATION
1916 M	STAGE_SEP = ON;	STATE_INTEGRATION
E		STATE_INTEGRATION
1917 M	TURBOJET_POWER = OFF;	STATE_INTEGRATION
E		STATE_INTEGRATION
1918 M	SCRAMJET_POWER = OFF;	STATE_INTEGRATION
E		STATE_INTEGRATION
1919 M	STATE_INTEGRATION_FLAG = ON;	STATE_INTEGRATION
--1920 M	X_STORE = ALT_FINAL;	STATE_INTEGRATION
S	1:1	STATE_INTEGRATION
1921 M	X_STORE = U_R_FINAL;	STATE_INTEGRATION
S	1:2	STATE_INTEGRATION
1922 M	X_STORE = THETA_FINAL;	STATE_INTEGRATION
S	1:3	STATE_INTEGRATION
--1923 M	X_STORE = U_THETA_FINAL / (ALT_FINAL + EARTH_RADIUS);	STATE_INTEGRATION
S	1:4	STATE_INTEGRATION


```

SOURCE
1944 M 1 TIME_STEP = PRESENT_TIME_STEP;          STATE_INTEGRATION
1945 M 1 CALL RUNGE_KUTTA;                       STATE_INTEGRATION
1946 M 1 IF MOD(I_TIME, 4) = 1 THEN             STATE_INTEGRATION
1947 M 1 DO;                                     STATE_INTEGRATION
1948 M 2 IF ((X_STORE(I_TIME:4) < THETA_DOT_INITIAL) AND (X_STORE(I_TIME:1) < R_CUTOFF_CHECK)) THEN STATE_INTEGRATION
S1
1949 M 2 DO;                                     STATE_INTEGRATION
1950 M 3 I_TIME = I_TIME - 4;                   STATE_INTEGRATION
1951 M 3 DO FOR I_OMEGA = 1 TO 4;              STATE_INTEGRATION
E1
1952 M 4 FINAL_U_STORE(I_OMEGA) = U_ACTIVE(I_TIME+I_OMEGA); STATE_INTEGRATION
S1
1953 M 3 END;                                   STATE_INTEGRATION
1954 M 3 SC2 = 2. NORH_TIME_STEP;              STATE_INTEGRATION
1955 M 3 CALL TIME_SET;                        STATE_INTEGRATION
1956 M 3 DO FOR I_OMEGA = 1 TO MAX_CUTOFF_ITERATIONS; STATE_INTEGRATION
1957 M 4 INTEG_L = PAST_INTEG_L;              STATE_INTEGRATION
1958 M 4 IF I_OMEGA = 1 THEN                   STATE_INTEGRATION
1959 M 4 TIME_STEP = (PRESENT_TIME_STEP / 2.); STATE_INTEGRATION
1960 M 4 DO FOR J_OMEGA = 1 TO 4;              STATE_INTEGRATION
1961 M 5 CALL MODEL_DRIVER;                   STATE_INTEGRATION
1962 M 5 CALL RUNGE_KUTTA;                    STATE_INTEGRATION
1963 M 5 IF I_OMEGA = MAX_CUTOFF_ITERATIONS THEN STATE_INTEGRATION
1964 M 5 DO;                                   STATE_INTEGRATION
1965 M 6 IF DYNAMIC_PO -> Q_D THEN             STATE_INTEGRATION
E1
1966 M 6 L_X_STORE(I_TIME) = 0.;              STATE_INTEGRATION
S1
1967 M 6 ELSE                                  STATE_INTEGRATION
1967 M 6 DO;                                   STATE_INTEGRATION

```

```

SOURCE                                CURRENT SCOPE
-----                                -
1968 MI 7                               SCI = 2. CAP_Q (DYNAMIC_PO - Q_D); | STATE_INTEGRATION
1969 MI 7                               L_X_STORE = ((RO_0 (X_STORE + EARTH_RADIUS) ( | STATE_INTEGRATION
SI I_TIME:1                               I_TIME:1
1969 MI 7                               X_STORE - EARTH_OMEGA) ) + ((DYNAMIC_PO DRO_DR) / RO_0 | STATE_INTEGRATION
SI I_TIME:4                               I_TIME:4
1969 MI 7                               )) SCI; | STATE_INTEGRATION
1970 MI 7                               L_X_STORE = RO_0 X_STORE I_TIME:2 SCI; | STATE_INTEGRATION
SI I_TIME:2                               I_TIME:2
1971 MI 7                               L_X_STORE = RO_0 ((X_STORE I_TIME:4 + EARTH_RADIUS) ) ( | STATE_INTEGRATION
SI I_TIME:4                               I_TIME:1
1971 MI 7                               X_STORE - EARTH_OMEGA) SCI; | STATE_INTEGRATION
SI I_TIME:4                               I_TIME:4
1972 MI 6                               END; | STATE_INTEGRATION
1973 MI 5                               END; | STATE_INTEGRATION
1974 MI 4                               END; | STATE_INTEGRATION
1975 MI 4                               IF X_STORE < THETA_DOT_INITIAL THEN | STATE_INTEGRATION
SI I_TIME:4                               I_TIME:4
1976 MI 4                               TIME_SIGN = -1.; | STATE_INTEGRATION
1977 MI 4                               ELSE | STATE_INTEGRATION
1977 MI 4                               TIME_SIGN = 1.; | STATE_INTEGRATION
1978 MI 4                               IF I_OMEGA /= MAX_CUTOFF_ITERATIONS THEN | STATE_INTEGRATION
1979 MI 4                               DO; | STATE_INTEGRATION
1980 MI 5                               TIME_STEP = TIME_STEP + ((TIME_SIGN PRESENT_TIME_STEP) / (2. | STATE_INTEGRATION
SI I_TIME - 4;                               I_TIME:1));
1981 MI 5                               I_TIME = I_TIME - 4; | STATE_INTEGRATION
1982 MI 5                               DO FOR J_OMEGA = 1 TO 4; | STATE_INTEGRATION
1983 MI 6                               SCI = TIME_STEP J_OMEGA; | STATE_INTEGRATION
1984 MI 6                               IF SCI < SCI THEN | STATE_INTEGRATION
SI I_TIME+J_OMEGA:                               I_TIME:2
1985 MI 6                               U_ACTIVE = U_ACTIVE + ((FINAL_U_STORE - | STATE_INTEGRATION
SI I_TIME+J_OMEGA:                               I_TIME:2

```

```

STMT          SOURCE          CURRENT SCOPE
-----
1955 MI 6     U_ACTIVE      I_TIME:      ( SCI / SCC2 ) ;      STATE_INTEGRATION
SI
1985 MI 6     ELSE
1986 MI 6     U_ACTIVE      I_TIME+J_OMEGA:  = FINAL_U_STORE 2:  + ((FINAL_U_STORE 4:  -
SI
1987 MI 5     FINAL_U_STORE 2:  ( SCI - SCC2 ) / SCC2 ;      STATE_INTEGRATION
SI
1988 MI 4     END;
1989 MI 3     END;
1990 MI 3     FINAL_TIME_STEP = TIME_STEP;
1991 MI 3     DO FOR I_OMEGA = 1 TO 4;
1992 MI 4     U_OLD_TIME      I_TIME-4+I_OMEGA      = U_OLD_TIME      I_TIME-4      + ( I_OMEGA FINAL_TIME_STEP ) ;      STATE_INTEGRATION
SI
1993 MI 3     END;
1994 MI 3     DO FOR I_OMEGA = 1 TO I_TIME;
1995 MI 4     IF MOD(I_TIME, 2) = 1 THEN
1996 MI 4     U_J_OLD_TIME      CEILING(I_OMEGA/2)      = U_OLD_TIME      I_OMEGA      ;      STATE_INTEGRATION
SI
1997 MI 3     END;
1998 MI 3     L_FINAL = 0.;
1999 MI 3     IF DYNAMIC_PO > Q_D THEN
2000 MI 3     L_FINAL = CAP_Q ((DYNAMIC_PO - Q_D) ) ;      STATE_INTEGRATION
SI
2001 MI 3     IF G_LOAD > G_D THEN
2002 MI 3     L_FINAL = L_FINAL + (CAP_CA (((G_LOAD - G_D) G0) ) ) ;      STATE_INTEGRATION
SI
2003 MI 3     STATE_INTEGRATION_FLAG = OFF;
2004 MI 3     FINAL_STEP = I_TIME;
SI

```

```

STMT                                     SOURCE                                CURRENT SCOPE
2005 MI 2                               END;                                     | STATE_INTEGRATION
2006 MI 1                               END;                                     | STATE_INTEGRATION
EI
2007 MI 1                               IF STATE_INTEGRATION_FLAG = ON THEN    | STATE_INTEGRATION
2008 MI 1                               DO;                                     | STATE_INTEGRATION
CI IT IS ASSUMED THAT EITHER THE SCRAMJET ONLY OR THE SCRAMJET AND
CI TURBOJET BOTH WILL BE ON AT STAGING BUT NOT JUST THE TURBOJET
2009 MI 2                               IF MOD(I_TIME, 4) = 1 THEN            | STATE_INTEGRATION
2010 MI 2                               DO;                                     | STATE_INTEGRATION
EI
2011 MI 3                               IF STAGE_SEP = ON THEN                | STATE_INTEGRATION
2012 MI 3                               DO;                                     | STATE_INTEGRATION
2013 MI 4                               IF I_TIME = OMEGA_I_TIME THEN        | STATE_INTEGRATION
SI
2014 MI 4                               DO;                                     | STATE_INTEGRATION
EI
2015 MI 5                               STAGE_SEP = OFF;                       | STATE_INTEGRATION
EI
2016 MI 5                               SCRAMJET_POWER = ON;                   | STATE_INTEGRATION
2017 MI 4                               END;                                     | STATE_INTEGRATION
2018 MI 4                               IF I_TIME = OMEGA_I_TIME THEN        | STATE_INTEGRATION
SI
2019 MI 4                               DO;                                     | STATE_INTEGRATION
EI
2020 MI 5                               TURBOJET_POWER = ON;                   | STATE_INTEGRATION
2021 MI 5                               IF I_TIME = OMEGA_I_TIME THEN        | STATE_INTEGRATION
SI
...
2022 MI 5                               SCRAMJET_POWER = OFF;                 | STATE_INTEGRATION
2023 MI 4                               END;                                     | STATE_INTEGRATION
2024 MI 3                               END;                                     | STATE_INTEGRATION
...
2025 MI 3                               ELSE                                     | STATE_INTEGRATION
2025 MI 3                               DO;                                     | STATE_INTEGRATION

```

```

STMT          SOURCE          CURRENT SCOPE
2026 M| 4     IF I_TIME = OMEGA_I_TIME THEN          | STATE_INTEGRATION
S|
E|
2027 M| 4     TURSOJET_POWER = ON;                   | STATE_INTEGRATION
E|
2028 M| 4     IF I_TIME = OMEGA_I_TIME THEN          | STATE_INTEGRATION
S|
E|
2029 M| 4     SCRAMJET_POWER = OFF;                  | STATE_INTEGRATION
E|
2030 M| 3     END;                                    | STATE_INTEGRATION
E|
2031 M| 3     PAST_INTEG_L = INTEG_L;                | STATE_INTEGRATION
E|
2032 M| 2     END;                                    | STATE_INTEGRATION
E|
2033 M| 2     IF I_TIME > STEP_DIM THEN              | STATE_INTEGRATION
E|
2034 M| 2     OVER_STEP = ON;                          | STATE_INTEGRATION
E|
2035 M| 1     END;                                    | STATE_INTEGRATION
E|
2036 M| 1     END;                                    | STATE_INTEGRATION
E|
2037 M| 1     IF OVER_STEP = OFF THEN                 | STATE_INTEGRATION
E|
2038 M| 1     DO:                                     | STATE_INTEGRATION
S|
2039 M| 1     PSI = X_STORE I_TIME:1;                 | STATE_INTEGRATION
S|
2040 M| 1     PSI = X_STORE I_TIME:2;                 | STATE_INTEGRATION
S|
2041 M| 1     PSI = X_STORE - (HC_TANK_VOL HYDROCARBON_DENSITY); | STATE_INTEGRATION
S|
2042 M| 1     PSI = X_STORE - (H2_TANK_VOL H2_DENSITY); | STATE_INTEGRATION
S|
2043 M| 1     PSI = X_STORE I_TIME:7 - P;             | STATE_INTEGRATION
S|
E|
2044 M| 1     PSI_MAG = PSI * (PSI_HEIGHT PSI);       | STATE_INTEGRATION
E|
2045 M| 1     END;                                    | STATE_INTEGRATION
E|
2046 M| 1     CLOSE STATE_INTEGRATION;                | STATE_INTEGRATION

```

STMT SOURCE CURRENT SCOPE

**** B L O C K S U M M A R Y ****

OUTER PROCEDURES CALLED
MODEL_DRIVER, TIME_SET, RUNGE_KUTTA

COMPOOL VARIABLES USED

NUM_STATES, X_STORE*, ALT_FINAL, U_R_FINAL, THETA_FINAL, U_THETA_FINAL, EARTH_RADIUS, M1_FINAL, M2_FINAL, M3_FINAL, Q_D, CAP_Q
X_STORE, EARTH_OMEGA, THETA_DOT_INITIAL, R_CUTOFF_CHECK, U_ACTIVE, NORH_TIME_STEP, MAX_CUTOFF_ITERATIONS, U_ACTIVE*, U_OLD_TIME*
U_OLD_TIME, G_D, CAP_CA, GO, FINAL_STEP*, OMEGA_I_TIME, STEP_DIM, HYDROCARBON_DENSITY, H2_DENSITY, P, PSI_WEIGHT

OUTER VARIABLES USED

LAMBDA_FLAG*, CAP_LAMBDA_1_FLAG*, CAP_LAMBDA_2_FLAG*, SGV_FLAG*, I_J_FLAG*, I_PSI_PSI_FLAG*, RK_RCHS*
RK_COLUMNS*, I_TIME*, STAGE_SEP*, TURBOJET_PORER*, SCRAJET_PORER*, STATE_INTEGRATION_FLAG*, INTEG_L*, PAST_INTEG_L*
RESHAPE_FLAG*, NET_MASS*, SS_DRY_MASS, HELD_FS_MASS*, FIRST_STAGE_DRY_MASS, L_X_STORE*, STATE_INTEGRATION_FLAG, OVER_STEP
DYNAMIC_PO, SCI*, I_TIME, RO_0, DRO_DR, SCI, TIME_STEP*, PRESENT_TIME_STEP, I_OMEGA, FINAL_U_STORE*, SC2*
PAST_INTEG_L, J_OMEGA*, TIME_SIGN*, TIME_STEP, TIME_SIGN, J_OMEGA, SC2, FINAL_U_STORE, FINAL_TIME_STEP*, FINAL_TIME_STEP
U_J_OLD_TIME*, L_FINAL*, G_LOAD, L_FINAL, STAGE_SEP, INTEG_L, OVER_STEP*, PSI*, HC_TANK_VOL, H2_TANK_VOL, PSI_MAG*, PSI

STMT

SOURCE

CURRENT SCOPE

```

E|
2047 M| STEP_I_FLAG = ON; | ITERATION_DRIVER
2048 M| OLD_FINAL_STEP = FINAL_STEP; | ITERATION_DRIVER
2049 M| SC4 = 0.; | ITERATION_DRIVER
2050 M| DO FOR I_U = 2 TO (STEP_DIM + 1); | ITERATION_DRIVER
2051 M| 1 IF I_U < (FINAL_STEP - 3) THEN | ITERATION_DRIVER
2052 M| 1 DO; | ITERATION_DRIVER
2053 M| 2 I_TIME = I_U; | ITERATION_DRIVER
2054 M| 2 CALL TIME_SET; | ITERATION_DRIVER
2055 M| 2 SC4 = SC4 + PRESENT_TIME_STEP; | ITERATION_DRIVER
2056 M| 1 END; | ITERATION_DRIVER
2057 M| 1 ELSE | ITERATION_DRIVER
2057 M| 1 DO; | ITERATION_DRIVER
2058 M| 2 IF I_U < (FINAL_STEP + 1) THEN | ITERATION_DRIVER
2059 M| 2 SC4 = SC4 + FINAL_TIME_STEP; | ITERATION_DRIVER
2060 M| 2 ELSE | ITERATION_DRIVER
2060 M| 2 SC4 = SC4 + NORM_TIME_STEP; | ITERATION_DRIVER
2061 M| 1 END; | ITERATION_DRIVER
2062 M| 1 U_OLD_TIME = SC4; | ITERATION_DRIVER
S| I_U | ITERATION_DRIVER
2063 M| 1 IF ((ITERATION = 1) AND (MOD(I_U, 2) = 1)) THEN | ITERATION_DRIVER
2064 M| 1 U_TIME_KEEP = U_OLD_TIME ; | ITERATION_DRIVER
S| CEILING(I_U/2) | ITERATION_DRIVER
2065 M| 1 END; | ITERATION_DRIVER
2066 M| [HOLD_U_T] = [U_OLD_TIME]; | ITERATION_DRIVER
E|
2067 M| IF FIRST_ITERATION_FLAG = ON THEN | ITERATION_DRIVER
2068 M| DO; | ITERATION_DRIVER
2069 M| 1 CALL STATE_INTEGRATION; | ITERATION_DRIVER

```


STMT	SOURCE	CURRENT SCOPE
EI		
2070 MI 1	FIRST_ITERATION_FLAG = OFF;	ITERATION_DRIVER
2071 MI	END;	ITERATION_DRIVER
2072 MI	ELSE	ITERATION_DRIVER
2072 MI	DO;	ITERATION_DRIVER
EI		
2073 MI 1	IF OVER_STEP = OFF THEN	ITERATION_DRIVER
EI		
2074 MI 1	DO FOR STEP_I = 1 TO MAX_STEP_I WHILE STEP_I_FLAG = ON;	ITERATION_DRIVER
EI		
2075 MI 2	STEP_SCALE_J = J_SCALE_FACTOR	ITERATION_DRIVER
EI		
2076 MI 2	STEP_SCALE_PSI = PSI_SCALE_FACTOR	ITERATION_DRIVER
2077 MI 2	IF STEP_I = 1 THEN	ITERATION_DRIVER
2078 MI 2	DO;	ITERATION_DRIVER
EI		
2079 MI 3	HOLD_PSI = PSI;	ITERATION_DRIVER
2080 MI 3	J_TIME = CEILING(FINAL_STEP / 2);	ITERATION_DRIVER
2081 MI 3	M1_FLOW_FINAL_STEP = (-X_STORE	ITERATION_DRIVER
SI	FINAL_STEP:5 + X_STORE FINAL_STEP-1:5	
2081 MI 3	FINAL_TIME_STEP;	ITERATION_DRIVER
2082 MI 3	M2_FLOW_FINAL_STEP = (-X_STORE	ITERATION_DRIVER
SI	FINAL_STEP:6 + X_STORE FINAL_STEP-1:6	
2082 MI 3	FINAL_TIME_STEP;	ITERATION_DRIVER
2083 MI 3	M3_FLOW_FINAL_STEP = (-X_STORE	ITERATION_DRIVER
SI	FINAL_STEP:7 + X_STORE FINAL_STEP-1:7	
2083 MI 3	FINAL_TIME_STEP;	ITERATION_DRIVER
2084 MI 3	MASS_FLOW_FINAL_STEP = (-NET_MASS	ITERATION_DRIVER
SI	FINAL_STEP + NET_MASS FINAL_STEP-1	
2084 MI 3	FINAL_TIME_STEP;	ITERATION_DRIVER
2085 MI 3	L_TIME = FINAL_STEP - 1;	ITERATION_DRIVER
2086 MI 3	CALL MODEL_DRIVER;	ITERATION_DRIVER

STMT	SOURCE	CURRENT SCOPE
2097 MI 3	STAGE_SEP = OFF;	ITERATION_DRIVER
2098 MI 3	TURBOJET_POWER = ON;	ITERATION_DRIVER
2099 MI 3	SCRAMJET_POWER = OFF;	ITERATION_DRIVER
2090 MI 3	DO FOR I_INIT = 1 TO NUM_CONSTANT_PARAMETERS;	ITERATION_DRIVER
2091 MI 4	SMALL_G_VEC	ITERATION_DRIVER
SI	I_INIT	
2092 MI 3	END;	ITERATION_DRIVER
2093 MI 3	I_J_J = 0.;	ITERATION_DRIVER
2094 MI 3	I_PSI_J = 0.;	ITERATION_DRIVER
2095 MI 3	* I_PSI_PSI = 0.;	ITERATION_DRIVER
2096 MI 3	CHECK1 = (X_STORE	ITERATION_DRIVER
SI	FINAL_STEP:1	
2096 MI 3) - (2. X_STORE	ITERATION_DRIVER
SI	FINAL_STEP:2	
2097 MI 3	X_STORE	ITERATION_DRIVER
SI	FINAL_STEP:4	
2098 MI 3	LAMSDA	ITERATION_DRIVER
SI	J_TIME:1	
2098 MI 3	LAMSDA	ITERATION_DRIVER
SI	J_TIME:2	
2099 MI 3	LAMSDA	ITERATION_DRIVER
SI	J_TIME:3	
2100 MI 3	LAMSDA	ITERATION_DRIVER
SI	J_TIME:4	
2101 MI 3	LAMSDA	ITERATION_DRIVER
SI	J_TIME:5	
2102 MI 3	LAMSDA	ITERATION_DRIVER
SI	J_TIME:6	
2103 MI 3	LAMSDA	ITERATION_DRIVER
SI	J_TIME:7	
2104 MI 3	* CAP_LAMSDA_1	ITERATION_DRIVER
SI	J_TIME = 0.;	

```

SOURCE
CURRENT SCOPE
2105 M| 3 CAP_LAMBDA_1 J_TIME:1,1 = -1.; ITERATION_DRIVER
S|
2106 M| 3 CAP_LAMBDA_1 J_TIME:2,2 = -1.; ITERATION_DRIVER
S|
2107 M| 3 CAP_LAMBDA_1 J_TIME:5,3 = -1.; ITERATION_DRIVER
S|
2108 M| 3 CAP_LAMBDA_1 J_TIME:6,4 = -1.; ITERATION_DRIVER
S|
2109 M| 3 CAP_LAMBDA_1 J_TIME:7,5 = -1.; ITERATION_DRIVER
S|
2110 M| 3 CAP_LAMBDA_1 J_TIME:4,1 = CHECK1 X_STORE FINAL_STEP:2; ITERATION_DRIVER
S|
2111 M| 3 CAP_LAMBDA_1 J_TIME:4,2 = CHECK1 ((X_STORE FINAL_STEP:1 + EARTH_RADIUS) X_STORE); ITERATION_DRIVER
S|
2111 M| 3 X_STORE FINAL_STEP:4 ) + (NET_R_FORCE / NET_MASS FINAL_STEP); ITERATION_DRIVER
S|
2112 M| 3 CAP_LAMBDA_1 J_TIME:4,3 = CHECK1 M1_FLOW_FINAL_STEP; ITERATION_DRIVER
S|
2113 M| 3 CAP_LAMBDA_1 J_TIME:4,4 = CHECK1 M2_FLOW_FINAL_STEP; ITERATION_DRIVER
S|
2114 M| 3 CAP_LAMBDA_1 J_TIME:4,5 = CHECK1 M3_FLOW_FINAL_STEP; ITERATION_DRIVER
S|
2115 M| 3 E| CAP_LAMBDA_2 = 0.; ITERATION_DRIVER
S|
2116 M| 3 TANK2 = (P P SIN(P) SIN(NOZZLE_ANGLE)) / SIN(P + NOZZLE_ANGLE); ITERATION_DRIVER
S|
2117 M| 3 TANK1 = .5452 P TANK2; ITERATION_DRIVER
S|
2118 M| 3 TANK2 = .0544 (1. - P) TANK2; ITERATION_DRIVER
S|
2119 M| 3 CHECK1 = SIN(NOZZLE_ANGLE) / (SIN(P + NOZZLE_ANGLE) SIN(P)); ITERATION_DRIVER
S|
2120 M| 3 CAP_LAMBDA_2 = CHECK1 TANK1; ITERATION_DRIVER
S|
2121 M| 3 CAP_LAMBDA_2 = CHECK1 TANK2; ITERATION_DRIVER
S|

```

```

STMT          SOURCE          CURRENT SCOPE
2122 M| 3     CAP_LAMBDA_2 = TANK1 / P ;      ITERATION_DRIVER
SI           2,3              2
2123 M| 3     CAP_LAMBDA_2 = TANK2 / P ;      ITERATION_DRIVER
SI           2,4              2
2124 M| 3     CAP_LAMBDA_2 = TANK1 / P ;      ITERATION_DRIVER
SI           7,3              7
2125 M| 3     CAP_LAMBDA_2 = TANK2 / (P - 1.);  ITERATION_DRIVER
SI           7,4              7
2126 M| 3     CAP_LAMBDA_2 = (2. TANK1) / P ;  ITERATION_DRIVER
SI           8,3              8
2127 M| 3     CAP_LAMBDA_2 = (2. TANK2) / P ;  ITERATION_DRIVER
SI           8,4              8
2128 M| 3     CAP_LAMBDA_2 = 1.;             ITERATION_DRIVER
SI           9,5              9
2129 M| 3     SC1 = SIN(P + NOZZLE_ANGLE);     ITERATION_DRIVER
SI           1                  1
2130 M| 3     SC2 = SIN(NOZZLE_ANGLE);        ITERATION_DRIVER
2131 M| 3     SC3 = P * P * SC2 (.0136 - (.008148 P ));  ITERATION_DRIVER
SI           8 8              7
2132 M| 3     SC4 = SIN(P) / SC1;            ITERATION_DRIVER
SI           1                  1
2133 M| 3     DM_DP = (((((P * P) / 4.) (1. - COS(P + NOZZLE_ANGLE))) + (P * SC3)) (SC2 / (
SI           1 2 8 1          2          2          2          2
2133 M| 3     SC1 SC1))) + (.25 (((P * SC2) / SC1) ));  ITERATION_DRIVER
SI           8 6              6
2134 M| 3     IF SCRAMJET_MASS > (MIN_SCRJ_MASS_PER_FT P S9) THEN  ITERATION_DRIVER
SI           2 2              2
2135 M| 3     DFP3 = 15.2 + (4.6 / (P * P ));  ITERATION_DRIVER
SI           3 3              3
2136 M| 3     ELSE                          ITERATION_DRIVER
2136 M| 3     DFP3 = 0.;                      ITERATION_DRIVER
2137 M| 3     DM_DP = (SCRAMJET_MASS / P) + (5. P) + ((P / 4.) (1. + SC4 + (SC2 / SC1)))  ITERATION_DRIVER
SI           2 2 4 8          8          8          8
2137 M| 3     + (SC3 SC4);                  ITERATION_DRIVER
SI           2 2              2

```

STMT	SOURCE	CURRENT SCOPE
2138 MI 3 SI	DM_DP = DFP3 P; 2	ITERATION_DRIVER
2139 MI 3 SI	DM_DP = 5. P; 2	ITERATION_DRIVER
2140 MI 3 SI	DM_DP = P / (8. TAN(P)); 5	ITERATION_DRIVER
2141 MI 3 SI	EI DM_DP = -(P P) / (16. (SIN(P))); 5 5 6	ITERATION_DRIVER
2142 MI 3 SI	DM_DP = P P P SC4 SC2 (-.008148); 7 2 8 8	ITERATION_DRIVER
2143 MI 3 SI	DM_DP = ((P / 4.) (1. + SC4 + (SC2 / SC1))) + ((2. P SC3 SC4) / P) + (P 8 2 8	ITERATION_DRIVER
2143 MI 3	SC2 SC4 .5);	ITERATION_DRIVER
2144 MI 3 SI	DM_DP = .04; 9	ITERATION_DRIVER
2145 MI 3 SI	DM_DP = 1. / 3220.; 10	ITERATION_DRIVER
2146 MI 3	I_TIME_STORE = FINAL_STEP;	ITERATION_DRIVER
2147 MI 3	J_TIME_STORE = CEILING(FINAL_STEP / 2);	ITERATION_DRIVER
2148 MI 3	TIME_STEP = FINAL_TIME_STEP;	ITERATION_DRIVER
2149 MI 3	RK_COLUMNS = 1;	ITERATION_DRIVER
2150 MI 3	DO WHILE I_TIME > 1;	ITERATION_DRIVER
2151 MI 4	I_TIME = I_TIME_STORE;	ITERATION_DRIVER
2152 MI 4	J_TIME = J_TIME_STORE;	ITERATION_DRIVER
2153 MI 4 SI	IF I_TIME = OMEGA_I_TIME THEN 1	ITERATION_DRIVER
2154 MI 4	SCRAMJET_POWER = ON;	ITERATION_DRIVER
2155 MI 4 SI	IF I_TIME = OMEGA_I_TIME THEN 2	ITERATION_DRIVER
2156 MI 4	TURBOJET_POWER = OFF;	ITERATION_DRIVER
2157 MI 4 SI	IF I_TIME = OMEGA_I_TIME THEN 3	ITERATION_DRIVER

STMT	SOURCE	CURRENT SCOPE
2153 MI 4	DO;	ITERATION_DRIVER
EI		
2159 MI 5	SCRANJET_PCKER = OFF;	ITERATION_DRIVER
EI		
2160 MI 5	STAGE_SEP = ON;	ITERATION_DRIVER
2161 MI 4	END;	ITERATION_DRIVER
EI		
2162 MI 4	LAMEDA_FLAG = ON;	ITERATION_DRIVER
2163 MI 4	RK_RCHS = NUM_STATES;	ITERATION_DRIVER
EI		
2164 MI 4	FD_FLAG = ON;	ITERATION_DRIVER
2165 MI 4	DO FOR I_CL = 1 TO 2;	ITERATION_DRIVER
2166 MI 5	CALL RUNSE_KUTTA;	ITERATION_DRIVER
2167 MI 5	DO FOR I_STORE = 1 TO NUM_STATES;	ITERATION_DRIVER
2168 MI 6	LAMEDA J_TIME:I_STORE = RK_VAL_N_PLUS_1 I_STORE,1	ITERATION_DRIVER
EI		
2169 MI 5	END;	ITERATION_DRIVER
2170 MI 4	END;	ITERATION_DRIVER
EI		
2171 MI 4	LAMEDA_FLAG = OFF;	ITERATION_DRIVER
2172 MI 4	I_TIME = I_TIME_STORE;	ITERATION_DRIVER
2173 MI 4	J_TIME = J_TIME_STORE;	ITERATION_DRIVER
EI		
2174 MI 4	CAP_LAMEDA_1_FLAG = ON;	ITERATION_DRIVER
2175 MI 4	RK_COLUMNS = NUM_CONSTRAINTS;	ITERATION_DRIVER
2176 MI 4	DO FOR I_CL = 1 TO 2;	ITERATION_DRIVER
2177 MI 5	CALL RUNSE_KUTTA;	ITERATION_DRIVER
2178 MI 5	DO FOR I_STORE = 1 TO NUM_STATES;	ITERATION_DRIVER
2179 MI 6	DO FOR J_STORE = 1 TO NUM_CONSTRAINTS;	ITERATION_DRIVER
2180 MI 7	CAP_LAMEDA_1 J_TIME:I_STORE, J_STORE = RK_VAL_N_PLUS_1 I_STORE,	ITERATION_DRIVER
EI		


```

SOURCE
CURRENT SCOPE
2205 M I 4      IF I_TIME = 1 THEN      I ITERATION_DRIVER
2206 M I 4      CALL HAM_SUB_U;      I ITERATION_DRIVER
2207 M I 4      I_TIME = I_TIME_STORE; I ITERATION_DRIVER
2208 M I 4      J_TIME = J_TIME_STORE; I ITERATION_DRIVER
                E I
2209 M I 4      SGV_FLAG = ON;      I ITERATION_DRIVER
2210 M I 4      RK_COLUMNS = 1;     I ITERATION_DRIVER
2211 M I 4      CALL RUNGE_KUTTA;    I ITERATION_DRIVER
2212 M I 4      DO FOR I_STORE = 1 TO NJM_CONSTANT_PARAMETERS; I ITERATION_DRIVER
2213 M I 5      S I                SMALL_G_VEC = RK_VAL_N_PLUS_1 I_STORE,1 I_STORE,1
2214 M I 4      END;                I ITERATION_DRIVER
                E I
2215 M I 4      SGV_FLAG = OFF;     I ITERATION_DRIVER
2216 M I 4      I_TIME_STORE = I_TIME; I ITERATION_DRIVER
2217 M I 4      J_TIME_STORE = CEILING(I_TIME_STORE / 2); I ITERATION_DRIVER
2218 M I 4      CALL TIME_SET;      I ITERATION_DRIVER
2219 M I 4      TIME_STEP = PRESENT_TIME_STEP; I ITERATION_DRIVER
                E I
2220 M I 3      END;                I ITERATION_DRIVER
2221 M I 3      I_TIME = FINAL_STEP; I ITERATION_DRIVER
2222 M I 3      I_TIME_STORE = FINAL_STEP; I ITERATION_DRIVER
2223 M I 3      J_TIME_STORE = CEILING(FINAL_STEP / 2); I ITERATION_DRIVER
2224 M I 3      TIME_STEP = FINAL_TIME_STEP; I ITERATION_DRIVER
                E I
2225 M I 3      STAGE_SEP = OFF;    I ITERATION_DRIVER
                E I
2226 M I 3      TURBOJET_FCHER = ON; I ITERATION_DRIVER
                E I
2227 M I 3      SCRAMJET_POWER = OFF; I ITERATION_DRIVER
2228 M I 3      DO WHILE I_TIME > 1; I ITERATION_DRIVER
2229 M I 4      I_TIME = I_TIME_STORE; I ITERATION_DRIVER

```



```

STMT
2230 MI 4          J_TIME = J_TIME_STORE;
2231 MI 4          IF I_TIME = OMEGA_I_TIME THEN
SI
EI
2232 MI 4          SCRAHJET_POWER = ON;
2233 MI 4          IF I_TIME = OMEGA_I_TIME THEN
SI
EI
2234 MI 4          TURBOJET_POWER = OFF;
2235 MI 4          IF I_TIME = OMEGA_I_TIME THEN
SI
EI
2236 MI 4          DO:
EI
2237 MI 5          SCRAHJET_POWER = OFF;
EI
2238 MI 5          STAGE_SEP = ON;
2239 MI 4          END;
EI
2240 MI 4          I_J_J_FLAG = ON;
2241 MI 4          RK_ROWS = 1;
2242 MI 4          RK_COLUMNS = 1;
2243 MI 4          CALL RUNGE_KUTTA;
2244 MI 4          I_J_J = RK_VAL_N_PLUS_1
SI
EI
2245 MI 4          I_J_J_FLAG = OFF;
2246 MI 4          I_TIME = I_TIME_STORE;
2247 MI 4          J_TIME = J_TIME_STORE;
EI
2248 MI 4          I_PSI_J_FLAG = ON;
2249 MI 4          RK_ROWS = NUM_CONSTRAINTS;
2250 MI 4          CALL RUNGE_KUTTA;
2251 MI 4          DO FOR I_STORE = 1 TO NUM_CONSTRAINTS;

```

CURRENT SCOPE

| ITERATION_DRIVER

| ITERATION_DRIVER

| ITERATION_DRIVER

| ITERATION_DRIVER

| ITERATION_DRIVER

| ITERATION_DRIVER

| ITERATION_DRIVER

| ITERATION_DRIVER

| ITERATION_DRIVER

| ITERATION_DRIVER

| ITERATION_DRIVER

| ITERATION_DRIVER

| ITERATION_DRIVER

| ITERATION_DRIVER

| ITERATION_DRIVER

| ITERATION_DRIVER

| ITERATION_DRIVER

| ITERATION_DRIVER

| ITERATION_DRIVER

| ITERATION_DRIVER

| ITERATION_DRIVER

| ITERATION_DRIVER

```

SOURCE
STMT
2252 M| 5      I_PSI_J      = RK_VAL_N_PLUS_1
SI          I_STORE
2253 M| 4      END;
EI
2254 M| 4      I_PSI_J_FLAG = OFF;
2255 M| 4      I_TIME = I_TIME_STORE;
2256 M| 4      J_TIME = J_TIME_STORE;
EI
2257 M| 4      I_PSI_PSI_FLAG = ON;
2259 M| 4      RK_COLUMNS = NUM_CONSTRAINTS;
2259 M| 4      CALL RUNGE_KUTTA;
2260 M| 4      DO FOR I_STORE = 1 TO NUM_CONSTRAINTS;
2261 M| 5          DO FOR J_STORE = I_STORE TO NUM_CONSTRAINTS;
2262 M| 6              I_PSI_PSI      = RK_VAL_N_PLUS_1
SI              I_STORE, J_STORE
2263 M| 5          END;
2264 M| 4      END;
EI
2265 M| 4      I_PSI_PSI_FLAG = OFF;
2266 M| 4      I_TIME_STORE = I_TIME;
2267 M| 4      J_TIME_STORE = CEIL( ( I_TIME_STORE / 2 ) );
2268 M| 4      CALL TIME_SET;
2269 M| 4      TIME_STEP = PRESENT_TIME_STEP;
2270 M| 3      END;
2271 M| 3      DO FOR I_STORE = 2 TO NUM_CONSTRAINTS;
2272 M| 4          DO FOR J_STORE = 1 TO ( I_STORE - 1 );
2273 M| 5              I_PSI_PSI      = I_PSI_PSI
SI              I_STORE, J_STORE
2274 M| 4          END;
2275 M| 3      END;
2276 M| 3      DO FOR CONFIG_INDEX = 1 TO NUM_TRANS_PTS;

```

```

SOURCE
CURRENT SCOPE
STMT
2277 MI 4 J_TIME = CEILING(OMEGA_I_TIME / 2);
SI      CONFIG_INDEX
2278 MI 4 IF ((OMEGA_I_TIME > 1) AND (OMEGA_I_TIME < (
SI      CONFIG_INDEX CONFIG_INDEX
2276 MI 4 FINAL_STEP - 1))) THEN
2279 MI 4 DO;
2280 MI 5 I_TIME = OMEGA_I_TIME;
SI      CONFIG_INDEX
EI
2281 MI 5 T_XDOT = 0.;
EI
2282 MI 5 X_DOT = 0.;
EI
2283 MI 5 STAGE_SEP = OFF;
2284 MI 5 IF I_TIME = OMEGA_I_TIME THEN
SI      I
EI
2285 MI 5 SCRAMJET_POWER = OFF;
2286 MI 5 ELSE
EI
2287 MI 5 SCRAMJET_POWER = ON;
SI      I
EI
2288 MI 5 IF I_TIME < OMEGA_I_TIME THEN
SI      I
EI
2289 MI 5 TURBOJET_POWER = OFF;
2290 MI 5 ELSE
EI
2291 MI 5 TURBOJET_POWER = ON;
EI
2292 MI 5 STATE_INTEGRATION_FLAG = ON;
2293 MI 5 CALL MODEL_DRIVER;
EI
2294 MI 5 STATE_INTEGRATION_FLAG = OFF;
2295 MI 5 T_XDOT = NET_R_FORCE / NET_MASS;
SI      I

```

```

SOURCE
CURRENT SCOPE
STMT
2294 M| 5 T_XDOT = NET_THETA_FORCE / (NET_MASS (X_STORE I_TIME I_TIME:1 +
SI
EARTH_RADIUS));
ITERATION_DRIVER
2294 M| 5 ITERATION_DRIVER
E|
2295 M| 5 IF TURBOJET_POWER = ON THEN
ITERATION_DRIVER
2296 M| 5 T_XDOT = -TJ_FUEL_FLOW;
SI
ITERATION_DRIVER
E|
2297 M| 5 IF SCRAMJET_POWER = ON THEN
ITERATION_DRIVER
2298 M| 5 T_XDOT = -SCRJ_FUEL_FLOW;
SI
ITERATION_DRIVER
E|
2299 M| 5 IF I_TIME = OMEGA_I_TIME THEN
ITERATION_DRIVER
SI
DO;
ITERATION_DRIVER
E|
2300 M| 5 STAGE_SEP = ON;
ITERATION_DRIVER
E|
2301 M| 6 SCRAMJET_POWER = OFF;
ITERATION_DRIVER
E|
2302 M| 6 END;
ITERATION_DRIVER
2303 M| 5 ELSE
ITERATION_DRIVER
2304 M| 5 SCRAMJET_POWER = ON;
ITERATION_DRIVER
E|
2305 M| 5 IF I_TIME > OMEGA_I_TIME THEN
SI
ITERATION_DRIVER
E|
2306 M| 5 TURBOJET_POWER = ON;
ITERATION_DRIVER
2307 M| 5 ELSE
ITERATION_DRIVER
E|
2307 M| 5 TURBOJET_POWER = OFF;
ITERATION_DRIVER
2308 M| 5 L_TIME = I_TIME - 1;
ITERATION_DRIVER
2309 M| 5 T_MASS = NET_MASS I_TIME ;
SI
ITERATION_DRIVER
E|
2310 M| 5 IF I_TIME = OMEGA_I_TIME THEN
SI
ITERATION_DRIVER

```

```

SOURCE
CURRENT SCOPE
2311 MI 5 NET_MASS = T_MASS - HELD_FS_MASS; ITERATION_DRIVER
SI I_TIME
2312 MI 5 CALL MODEL_DRIVER; ITERATION_DRIVER
2313 MI 5 X_DOT = NET_R_FORCE / NET_MASS I_TIME; ITERATION_DRIVER
SI I_TIME
2314 MI 5 X_DOT = NET_THETA_FORCE / (NET_MASS (X_STORE I_TIME + ITERATION_DRIVER
SI I_TIME I_TIME:1
2314 MI 5 EARTH_RADIUS)); ITERATION_DRIVER
EI
2315 MI 5 IF TURBOJET_POMER = ON THEN ITERATION_DRIVER
2316 MI 5 X_DOT = -TJ_FUEL_FLOW; ITERATION_DRIVER
SI 5
EI
2317 MI 5 IF SCRAMJET_POMER = ON THEN ITERATION_DRIVER
2318 MI 5 X_DOT = -SCRJ_FUEL_FLOW; ITERATION_DRIVER
SI 6
EI
2319 MI 5 IF STAGE_SEP = ON THEN ITERATION_DRIVER
2320 MI 5 X_DOT = -SS_FUEL_FLOW; ITERATION_DRIVER
SI 7
EI
2321 MI 5 T_XDOT = T_XDOT - X_DOT; ITERATION_DRIVER
2322 MI 5 NET_MASS = T_MASS; ITERATION_DRIVER
SI I_TIME
2323 MI 4 END; ITERATION_DRIVER
2324 MI 4 ELSE ITERATION_DRIVER
2324 MI 4 T_XDOT = 0.; ITERATION_DRIVER
EI
2325 MI 4 SMALL_G_VEC CONFIG_INDEX+NUM_CONSTANT_PARAMETERS = LAMBDA J_TIME; T_XDOT; ITERATION_DRIVER
SI LAMBDA J_TIME:
EI
2326 MI 4 M_VEC = TRANSPOSE(CAP_LAMBDA_1 J_TIME; T_XDOT; ITERATION_DRIVER
SI J_TIME:
EI
2327 MI 4 DO FOR I_LOOP = 1 TO NUM_CONSTRAINTS; ITERATION_DRIVER

```

```

SOURCE
2329 M I 5          M          I_LOOP,CONFIG_INDEX+NUM_CONSTANT_PARAMETERS = M_VEC          I_LOOP          ;
SI
2329 M I 4          END;
2330 M I 3          END;
2331 M I 3          DO FOR CONFIG_INDEX = 1 TO NUM_CONSTRAINTS;
2332 M I 4          DO FOR I_LOOP = 1 TO NUM_CONSTANT_PARAMETERS;
2333 M I 5          M          CONFIG_INDEX,I_LOOP = -CAP_LAMSDA_2          I_LOOP,CONFIG_INDEX          ;
SI
2334 M I 4          END;
2335 M I 3          END;
2336 M I 2          END;
2337 M I 2          ELSE
E I
2337 M I 2          PSI = HOLD_PSI;
2338 M I 2          CALL DELTA_U_V_CALC;
2339 M I 2          DO FOR I_STORE = 1 TO NUM_CONSTANT_PARAMETERS;
2340 M I 3          P          I_STORE = P          + DELTA_V          I_STORE          ;
SI
2341 M I 2          END;
2342 M I 2          DO FOR I_RCP = 1 TO NUM_TRANS_PTS;
2343 M I 3          SCI = DELTA_V          I_RCP+NUM_CONSTANT_PARAMETERS          / 4.;
SI
2344 M I 3          IF ((SCI < POS_TIME_STEP          I_RCP          ) OR (SCI = POS_TIME_STEP          I_RCP          )) AND ((SCI > -
SI
2344 M I 3          NEG_TIME_STEP          I_RCP          ) OR (SCI = -NEG_TIME_STEP          I_RCP          )) THEN
2345 M I 3          DO;
2346 M I 4          POS_TIME_STEP          I_RCP          = POS_TIME_STEP          I_RCP          - SCI;
SI
2347 M I 4          NEG_TIME_STEP          I_RCP          = NEG_TIME_STEP          I_RCP          + SCI;
SI
2348 M I 4          DELTA_OMEGA_I_TIME          I_RCP          = 0;
SI
2348 M I 4          END;
SI

```

```

SOURCE
CURRENT SCOPE
STMT          2349 MI 3      END;          | ITERATION_DRIVER
              2350 MI 3      ELSE         | ITERATION_DRIVER
              2350 MI 3      DO:          | ITERATION_DRIVER
              2351 MI 4      IF SC1 < 0. THEN | ITERATION_DRIVER
              2352 MI 4      SC2 = DELTA_V    + (4. NEG_TIME_STEP | ITERATION_DRIVER
              SI              I_RCP          );
              2353 MI 4      ELSE         | ITERATION_DRIVER
              2353 MI 4      SC2 = DELTA_V    - (4. POS_TIME_STEP  | ITERATION_DRIVER
              SI              I_RCP          );
              2354 MI 4      SC3 = ABS(SC2 / (4. NORM_TIME_STEP)); | ITERATION_DRIVER
              2355 MI 4      DELTA_OMEGA_I_TIME = 4 CEILING(SC3) SIGN(-SC1); | ITERATION_DRIVER
              SI              I_RCP
              2356 MI 4      SC2 = SC3 - TRUNCATE(SC3);          | ITERATION_DRIVER
              2357 MI 4      IF SC1 < 0. THEN | ITERATION_DRIVER
              2358 MI 4      DO:          | ITERATION_DRIVER
              2359 MI 5      NEG_TIME_STEP = (1. - SC2) NORM_TIME_STEP; | ITERATION_DRIVER
              SI              I_RCP
              2360 MI 5      POS_TIME_STEP = SC2 NORM_TIME_STEP;   | ITERATION_DRIVER
              SI              I_RCP
              2361 MI 4      END;          | ITERATION_DRIVER
              2362 MI 4      ELSE         | ITERATION_DRIVER
              2362 MI 4      DO:          | ITERATION_DRIVER
              2363 MI 5      NEG_TIME_STEP = SC2 NORM_TIME_STEP;   | ITERATION_DRIVER
              SI              I_RCP
              2364 MI 5      POS_TIME_STEP = (1. - SC2) NORM_TIME_STEP; | ITERATION_DRIVER
              SI              I_RCP
              2365 MI 4      END;          | ITERATION_DRIVER
              2366 MI 3      END;          | ITERATION_DRIVER
              2367 MI 2      END;          | ITERATION_DRIVER
              2368 MI 2      DO FOR I_STORE = 1 TO NUM_TRANS_PTS; | ITERATION_DRIVER
              2369 MI 3      OMEGA_I_TIME = OMEGA_I_TIME + DELTA_OMEGA_I_TIME ; | ITERATION_DRIVER
              SI              I_STORE

```

STMT	SOURCE	CURRENT SCOPE
2370 MI 3 SI	IF OMEGA_I_TIME I_STORE > (FINAL_STEP - 12) THEN	ITERATION_DRIVER
2371 MI 3	DO;	ITERATION_DRIVER
2372 MI 4	IF FINAL_STEP > 12 THEN	ITERATION_DRIVER
2373 MI 4 SI	OMEGA_I_TIME I_STORE = FINAL_STEP - 8;	ITERATION_DRIVER
2374 MI 4	ELSE	ITERATION_DRIVER
2374 MI 4 SI	OMEGA_I_TIME I_STORE = 8;	ITERATION_DRIVER
2375 MI 4 SI	NEG_TIME_STEP I_STORE = NORM_TIME_STEP / 2.;	ITERATION_DRIVER
2376 MI 4 SI	POS_TIME_STEP I_STORE = NORM_TIME_STEP / 2.;	ITERATION_DRIVER
2377 MI 3	END;	ITERATION_DRIVER
2378 MI 3 SI	IF OMEGA_I_TIME I_STORE < 8 THEN	ITERATION_DRIVER
2379 MI 3	DO;	ITERATION_DRIVER
2380 MI 4 SI	OMEGA_I_TIME I_STORE = 8;	ITERATION_DRIVER
2381 MI 4 SI	NEG_TIME_STEP I_STORE = NORM_TIME_STEP / 2.;	ITERATION_DRIVER
2382 MI 4 SI	POS_TIME_STEP I_STORE = NORM_TIME_STEP / 2.;	ITERATION_DRIVER
2383 MI 3	END;	ITERATION_DRIVER
2384 MI 2	END;	ITERATION_DRIVER
2385 MI 2 SI	IF OMEGA_I_TIME I_STORE < OMEGA_I_TIME I_STORE THEN	ITERATION_DRIVER
2386 MI 2	DO;	ITERATION_DRIVER
2387 MI 3 SI	OMEGA_I_TIME I_STORE = OMEGA_I_TIME I_STORE; OMEGA_I_TIME I_STORE = OMEGA_I_TIME I_STORE; OMEGA_I_TIME I_STORE = OMEGA_I_TIME I_STORE;	ITERATION_DRIVER
2388 MI 3 SI	NEG_TIME_STEP I_STORE = NEG_TIME_STEP I_STORE; NEG_TIME_STEP I_STORE = NEG_TIME_STEP I_STORE;	ITERATION_DRIVER
2389 MI 3 SI	POS_TIME_STEP I_STORE = POS_TIME_STEP I_STORE; POS_TIME_STEP I_STORE = POS_TIME_STEP I_STORE;	ITERATION_DRIVER

STMT	SOURCE	CURRENT SCOPE
2390 MI 2	END;	ITERATION_DRIVER
2391 MI 2	IF OMEGA_I_TIME < OMEGA_I_TIME THEN	ITERATION_DRIVER
SI	1 2	
2392 MI 2	DO;	ITERATION_DRIVER
2393 MI 3	IF OMEGA_I_TIME < (FINAL_STEP - 12) THEN	ITERATION_DRIVER
SI	2	
2394 MI 3	DO;	ITERATION_DRIVER
2395 MI 4	OMEGA_I_TIME = OMEGA_I_TIME + 6;	ITERATION_DRIVER
SI	1 2	
2396 MI 4	NEG_TIME_STEP = NORM_TIME_STEP / 2.;	ITERATION_DRIVER
SI	1	
2397 MI 4	POS_TIME_STEP = NORM_TIME_STEP / 2.;	ITERATION_DRIVER
SI	1	
2398 MI 3	END;	ITERATION_DRIVER
2399 MI 3	ELSE	ITERATION_DRIVER
2399 MI 3	DO;	ITERATION_DRIVER
2400 MI 4	OMEGA_I_TIME = OMEGA_I_TIME ;	ITERATION_DRIVER
SI	1 2	
2401 MI 4	NEG_TIME_STEP = NEG_TIME_STEP ;	ITERATION_DRIVER
SI	1 2	
2402 MI 4	POS_TIME_STEP = POS_TIME_STEP ;	ITERATION_DRIVER
SI	1 2	
2403 MI 3	END;	ITERATION_DRIVER
2404 MI 2	END;	ITERATION_DRIVER
2405 MI 2	IF (OMEGA_I_TIME - OMEGA_I_TIME) < 8 THEN	ITERATION_DRIVER
SI	2 3	
2406 MI 2	DO;	ITERATION_DRIVER
2407 MI 3	OMEGA_I_TIME = OMEGA_I_TIME ;	ITERATION_DRIVER
SI	2 3	
2408 MI 3	NEG_TIME_STEP = NEG_TIME_STEP ;	ITERATION_DRIVER
SI	2 3	
2409 MI 3	POS_TIME_STEP = POS_TIME_STEP ;	ITERATION_DRIVER
SI	2 3	

START	SOURCE	CURRENT SCOPE
2410 MI 3 SI	IF ((ITERATION < 6) AND (FINAL_STEP > (OMEGA_I_TIME ₂ + 12))) THEN	ITERATION_DRIVER
2411 MI 3	DO:	ITERATION_DRIVER
2412 MI 4 SI	OMEGA_I_TIME ₂ = OMEGA_I_TIME ₂ + 8;	ITERATION_DRIVER
2413 MI 4 SI	NEG_TIME_STEP ₂ = NORM_TIME_STEP / 2.;	ITERATION_DRIVER
2414 MI 4 SI	POS_TIME_STEP ₂ = NORM_TIME_STEP / 2.;	ITERATION_DRIVER
2415 MI 3	END;	ITERATION_DRIVER
2416 MI 2	END;	ITERATION_DRIVER
2417 MI 2 SI	IF (OMEGA_I_TIME ₁ - OMEGA_I_TIME ₂) < 8 THEN	ITERATION_DRIVER
2418 MI 2	DO:	ITERATION_DRIVER
2419 MI 3 SI	OMEGA_I_TIME ₁ = OMEGA_I_TIME ₂ ;	ITERATION_DRIVER
2420 MI 3 SI	NEG_TIME_STEP ₁ = NEG_TIME_STEP ₂ ;	ITERATION_DRIVER
2421 MI 3 SI	POS_TIME_STEP ₁ = POS_TIME_STEP ₂ ;	ITERATION_DRIVER
2422 MI 3 SI	IF ((ITERATION < 9) AND (FINAL_STEP > (OMEGA_I_TIME ₁ + 12))) THEN	ITERATION_DRIVER
2423 MI 3	DO:	ITERATION_DRIVER
2424 MI 4 SI	OMEGA_I_TIME ₁ = OMEGA_I_TIME ₁ + 8;	ITERATION_DRIVER
2425 MI 4 SI	NEG_TIME_STEP ₁ = NORM_TIME_STEP / 2.;	ITERATION_DRIVER
2426 MI 4 SI	POS_TIME_STEP ₁ = NORM_TIME_STEP / 2.;	ITERATION_DRIVER
2427 MI 3	END;	ITERATION_DRIVER
2428 MI 2	END;	ITERATION_DRIVER
2429 MI 2	SC4 = 0.;	ITERATION_DRIVER
2430 MI 2	DO FOR I_U = 2 TO FINAL_STEP;	ITERATION_DRIVER
2431 MI 3	IF I_U < (FINAL_STEP - 3) THEN	ITERATION_DRIVER

STMT	SOURCE	CURRENT SCOPE
2432 MI 3	DO;	ITERATION_DRIVER
2433 MI 4	I_TIME = I_U;	ITERATION_DRIVER
2434 MI 4	CALL TIME_SET;	ITERATION_DRIVER
2435 MI 4	SC4 = SC4 + PRESENT_TIME_STEP;	ITERATION_DRIVER
2436 MI 3	END;	ITERATION_DRIVER
2437 MI 3	ELSE	ITERATION_DRIVER
2437 MI 3	SC4 = SC4 + FINAL_TIME_STEP;	ITERATION_DRIVER
2438 MI 3	U_NEH_TIME = SC4;	ITERATION_DRIVER
2438 MI 3	I_U	
2439 MI 2	END;	ITERATION_DRIVER
2440 MI 2	IF OLD_FINAL_STEP > FINAL_STEP THEN	ITERATION_DRIVER
2441 MI 2	OLD_FINAL_STEP = FINAL_STEP;	ITERATION_DRIVER
2442 MI 2	IF OLD_FINAL_STEP > 9 THEN	ITERATION_DRIVER
2443 MI 2	DO FOR I_U = 5 TO (OLD_FINAL_STEP - 4);	ITERATION_DRIVER
2444 MI 3	IF MOD(I_U, 2) = 1 THEN	ITERATION_DRIVER
2445 MI 3	DO;	ITERATION_DRIVER
2446 MI 4	J_U = CEILING(I_U / 2);	ITERATION_DRIVER
2447 MI 4	LI4 = 4 * NUM_TRANS_PTS;	ITERATION_DRIVER
2448 MI 4	SC4 = (LI4 + .1) * NORM_TIME_STEP;	ITERATION_DRIVER
2449 MI 4	IF (I_U + LI4) < OLD_FINAL_STEP THEN	ITERATION_DRIVER
2450 MI 4	LI5 = LI4;	ITERATION_DRIVER
2451 MI 4	ELSE	ITERATION_DRIVER
2451 MI 4	LI5 = OLD_FINAL_STEP - 1 - I_U;	ITERATION_DRIVER
2452 MI 4	IF (I_U - LI4) < 2 THEN	ITERATION_DRIVER
2453 MI 4	LI4 = I_U - 2;	ITERATION_DRIVER
2454 MI 4	OLD_SC3 = SC4;	ITERATION_DRIVER
2455 MI 4	LI_FLAG = ON;	ITERATION_DRIVER


```

SOURCE
CURRENT SCOPE
2473 MI 8      UV1 = UV1 / (U_OLD_TIME - U_OLD_TIME ) ; ITERATION_DRIVER
SI           I_RCP - U_OLD_TIME I_RCP-1
EI
2474 MI 8      DELTA_U_NEW = DELTA_U - U_OLD_TIME ; ITERATION_DRIVER
SI           J_U: J_RCP: + ((DELTA_U - U_OLD_TIME) / J_RCP)
EI
2474 MI 8      DELTA_U - U_OLD_TIME ; ITERATION_DRIVER
SI           J_RCP-1: UV1);
EI
2475 MI 8      U_NEW = U_ACTIVE (2 J_RCP)-1: + (U_ACTIVE (2 J_RCP)-1: (2 J_RCP)-1: ITERATION_DRIVER
SI
2475 MI 8      J_RCP)-1: - U_ACTIVE (2 J_RCP)-3: UV1); ITERATION_DRIVER
SI
2476 MI 7      END; ITERATION_DRIVER
2477 MI 7      SC4 = SC3; ITERATION_DRIVER
2478 MI 6      END; ITERATION_DRIVER
2479 MI 6      OLD_SC3 = SC3; ITERATION_DRIVER
2480 MI 5      END; ITERATION_DRIVER
2481 MI 4      END; ITERATION_DRIVER
2482 MI 3      END; ITERATION_DRIVER
2483 MI 2      END; ITERATION_DRIVER
2484 MI 2      DO FOR J_U = 4 TO FLOOR((OLD_FINAL_STEP - 5) / 2); ITERATION_DRIVER
2485 MI 3      DELTA_U - U_OLD_TIME ; ITERATION_DRIVER
SI           J_U: J_U:
EI
2486 MI 3      U_ACTIVE (2 J_U)-1: = U_NEW ; ITERATION_DRIVER
SI
2487 MI 2      END; ITERATION_DRIVER
2488 MI 2      DO FOR I_U = 1 TO (FINAL_STEP - 2); ITERATION_DRIVER
2489 MI 3      IF MCD(I_U, 2) = 1 THEN ITERATION_DRIVER
EI           U_ACTIVE I_U: = U_ACTIVE I_U: + DELTA_U CEILING(I_U/2); ITERATION_DRIVER
SI
2490 MI 3      END; ITERATION_DRIVER

```

```

STMT          SOURCE          CURRENT SCOPE
2491 MI 2     END;              ITERATION_DRIVER
2492 MI 2     DO FOR I_U = 1 TO (FINAL_STEP - 3);  ITERATION_DRIVER
2493 MI 3     IF MOD(I_U, 2) /= 1 THEN          ITERATION_DRIVER
2494 MI 3     DO;                            ITERATION_DRIVER
2495 MI 4     IF (((I_U + 1) = OMEGA_I_TIME ) OR ((I_U + 1) = OMEGA_I_TIME ) OR ((I_U + 1)  ITERATION_DRIVER
SI
2495 MI 4     ) = OMEGA_I_TIME ) THEN          ITERATION_DRIVER
SI
2496 MI 4     U_ACTIVE = U_ACTIVE          ITERATION_DRIVER
SI          I_U: I_U-1;
2497 MI 4     ELSE                          ITERATION_DRIVER
SI
2497 MI 4     U_ACTIVE = (U_ACTIVE + U_ACTIVE ) / 2.;  ITERATION_DRIVER
SI          I_U: I_U-1;
2498 MI 3     END;                          ITERATION_DRIVER
2499 MI 2     END;                          ITERATION_DRIVER
SI
2500 MI 2     U_KEEP = U_ACTIVE          ITERATION_DRIVER
SI          FINAL_STEP-2;
2501 MI 2     DO FOR I_U = (FINAL_STEP - 3) TO (STEP_DIM + 1);  ITERATION_DRIVER
2502 MI 3     IF I_U > FINAL_STEP THEN          ITERATION_DRIVER
SI
2503 MI 3     U_ACTIVE = U_ACTIVE          ITERATION_DRIVER
SI          FINAL_STEP - ((U_ACTIVE - U_ACTIVE  ITERATION_DRIVER
SI          FINAL_STEP-4;
2503 MI 3     FINAL_STEP-2; ) (I_U - FINAL_STEP) / 2.);  ITERATION_DRIVER
SI
2504 MI 3     ELSE                          ITERATION_DRIVER
SI
2504 MI 3     U_ACTIVE = U_ACTIVE          ITERATION_DRIVER
SI          FINAL_STEP-4; - ((U_ACTIVE - U_KEEP) (I_U  ITERATION_DRIVER
SI          FINAL_STEP-4;
2504 MI 3     + 4 - FINAL_STEP) (NORM_TIME_STEP / (2. FINAL_TIME_STEP)));  ITERATION_DRIVER
SI
2505 MI 2     END;                          ITERATION_DRIVER
SI
2506 MI 2     CALL STATE_INTEGRATION;        ITERATION_DRIVER
SI

```

```

STMT          SOURCE          CURRENT SCOPE
E1           *
2507 M1 2     IF (((PSI - (PSI_WEIGHT PSI)) < (HOLD_PSI - (PSI_WEIGHT HOLD_PSI))) OR ((PSI_MAG < (
SI           MIN_PSI_THRESHOLD FIRST_PSI_MAG)) AND ((X_STORE FINAL_STEP:5 + X_STORE FINAL_STEP:6
2507 M1 2     X_STORE FINAL_STEP:7 - INTEG_L) < COST))) THEN
SI           FINAL_STEP:7
E1           STEP_I_FLAG = OFF;
2508 M1 2
E1           ELSE IF ((STEP_I_FLAG = OFF) OR (MAX_STEP_I /= STEP_I)) THEN
2509 M1 2
2510 M1 2     DO;
E1           [X_STORE] = [HOLD_X];
2511 M1 3     [NET_MASS] = [HOLD_M];
2512 M1 3     [L_X_STORE] = [HOLD_L_X];
E1           P = HOLD_P;
2513 M1 3     [U_ACTIVE] = [HOLD_U];
E1           [U_OLD_TIME] = [HOLD_U_T];
2514 M1 3     [CHEGA_I_TIME] = [HOLD_T];
E1           [POS_TIME_STEP] = [HOLD_POS_TIME];
2515 M1 3     [NEG_TIME_STEP] = [HOLD_NEG_TIME];
2516 M1 3     END;
2517 M1 3
2518 M1 3     END;
2519 M1 3
2520 M1 2     END;
2521 M1 1     END;
2522 M1     END;
2523 M1 CLOSE ITERATION_DRIVER;

```

**** B L O C K S U M M A R Y ****

OUTER PROCEDURES CALLED

TIME_SET, MODEL_DRIVER, RUNSE_KUTTA, HAM_SUB_U, DELTA_U_V_CALC

COMPOOL VARIABLES USED

NUM_STATES, NUM_CONSTRAINTS, STEP_DIM, NUM_CONTROLS, FINAL_STEP, NORM_TIME_STEP, U_OLD_TIME*, ITERATION, U_TIME_KEEP*

STMT	SOURCE	CURRENT SCOPE
2524 MI	OPTIMIZATION:	OPTIMIZATION
2524 MI	PROCEDURE:	OPTIMIZATION
2525 MI	DECLARE ANGLE_OF_ATTACK_INITIAL ARRAY(STEP_DIM + 1) SCALAR DOUBLE AUTOMATIC;	OPTIMIZATION
2526 MI	DECLARE CAP_PHI_INITIAL ARRAY(STEP_DIM + 1) SCALAR DOUBLE AUTOMATIC;	OPTIMIZATION
2527 MI	DECLARE CP_INDEX ARRAY(23) INTEGER STATIC INITIAL(1, 250, 266, 352, 394, 538, 802, 913, 917, 921	OPTIMIZATION
2527 MI	, 985, 989, 993, 1006, 1026, 1177, 1181, 1185, 1218, 1230, 1254, 1278, 2031);	OPTIMIZATION
2528 MI	DECLARE CP_INIT ARRAY(23) SCALAR DOUBLE STATIC INITIAL(.035, .035, .170, .250, .669, .9, .97,	OPTIMIZATION
2528 MI	.97, .97, .97, .97, .97, .9, .9, .9, .9, .81, .9, .9);	OPTIMIZATION
2529 MI	DECLARE MAX_CP_INDEX INTEGER STATIC INITIAL(23);	OPTIMIZATION
2530 MI	DECLARE W_INDEX ARRAY(5) INTEGER STATIC INITIAL(1, 301, 351, 401, 1001);	OPTIMIZATION
2531 MI	DECLARE W_INIT ARRAY(5, NUM_CONTROLS) SCALAR DOUBLE STATIC INITIAL(5., 1000., 5.,	OPTIMIZATION
2531 MI	1000., 5., 1000., 5., 1000.);	OPTIMIZATION
2532 MI	DECLARE MAX_W_INDEX INTEGER STATIC INITIAL(5);	OPTIMIZATION
2533 MI	DECLARE AA_INDEX ARRAY(31) INTEGER STATIC INITIAL(1, 106, 210, 326, 458, 639, 874, 884, 913	OPTIMIZATION
2533 MI	, 914, 917, 921, 934, 954, 985, 989, 993, 1006, 1036, 1106, 1150, 1170, 1177, 1181, 1185, 1250,	OPTIMIZATION
2533 MI	1259, 1270, 1276, 2001);	OPTIMIZATION
2534 MI	DECLARE AA_INIT ARRAY(31) SCALAR DOUBLE STATIC INITIAL(0., 0., -.120, .020, .090, .210, .215,	OPTIMIZATION
2534 MI	.210, .180, .1496, .148, .14425, .14425, .128, .022, .022, .022, .022, .029, .002,	OPTIMIZATION
2534 MI	.002, .00421, .00453, .00547, .026, .035, .070, .097, .097);	OPTIMIZATION
2535 MI	DECLARE MAX_AA_INDEX INTEGER STATIC INITIAL(31);	OPTIMIZATION
2536 MI	DECLARE P_INITIAL VECTOR(NUM_CONSTANT_PARAMETERS) DOUBLE STATIC INITIAL(.021, 32.157, 9.4, 6.49,	OPTIMIZATION
2536 MI	269.19, 1.222, .416, 161., 33450., 1.8708E06);	OPTIMIZATION
2537 MI	DECLARE OPT_INIT ARRAY(NUM_TRANS_PTS) INTEGER STATIC INITIAL(1181, 989, 917);	OPTIMIZATION
2538 MI	DECLARE FUEL_COST SCALAR DOUBLE AUTOMATIC;	OPTIMIZATION
2539 MI	* [M] = 0.;	OPTIMIZATION
2540 MI	ITERATION = 1;	OPTIMIZATION
2541 MI	DO FOR I_STORE = 1 TO FLOOR((STEP_DIM + 3) / 2);	OPTIMIZATION

STMT	SOURCE	CURRENT SCOPE
2542 M 1	IF ((I_STORE < W_INDEX) AND (ITERATION < MAX_W_INDEX)) THEN	OPTIMIZATION
SI	ITERATION	
2543 M 1	ITERATION = ITERATION + 1;	OPTIMIZATION
2544 M 1	DO FOR IIT = 1 TO NUM_CONTROLS;	OPTIMIZATION
2545 M 2	W_I_STORE:IIT,IIT = W_INIT + ((W_INIT - W_INIT) / (W_INIT - W_INIT))	OPTIMIZATION
SI	ITERATION-1,IIT	
2545 M 2	((I_STORE - W_INDEX) / (W_INDEX - W_INDEX))	OPTIMIZATION
SI	ITERATION-1	
2546 M 1	END;	OPTIMIZATION
2547 M	END;	OPTIMIZATION
2548 M	ITERATION = 1;	OPTIMIZATION
2549 M	DO FOR I_STORE = 1 TO (STEP_DIM + 1);	OPTIMIZATION
2550 M 1	IF ((I_STORE < AA_INDEX) AND (ITERATION < MAX_AA_INDEX)) THEN	OPTIMIZATION
SI	ITERATION	
2551 M 1	ITERATION = ITERATION + 1;	OPTIMIZATION
2552 M 1	ANGLE_OF_ATTACK_INITIAL_I_STORE = AA_INIT + ((AA_INIT - AA_INIT) / (AA_INIT - AA_INIT))	OPTIMIZATION
SI	ITERATION-1	
2552 M 1	((I_STORE - AA_INDEX) / (AA_INDEX - AA_INDEX))	OPTIMIZATION
SI	ITERATION-1	
2553 M	END;	OPTIMIZATION
2554 M	ITERATION = 1;	OPTIMIZATION
2555 M	DO FOR I_STORE = 1 TO (STEP_DIM + 1);	OPTIMIZATION
2556 M 1	IF ((I_STORE < CP_INDEX) AND (ITERATION < MAX_CP_INDEX)) THEN	OPTIMIZATION
SI	ITERATION	
2557 M 1	ITERATION = ITERATION + 1;	OPTIMIZATION
2558 M 1	CAP_PHI_INITIAL_I_STORE = CP_INIT + ((CP_INIT - CP_INIT) / (CP_INIT - CP_INIT))	OPTIMIZATION
SI	ITERATION-1	
2558 M 1	(I_STORE - CP_INDEX) / (CP_INDEX - CP_INDEX))	OPTIMIZATION
SI	ITERATION-1	
2559 M	END;	OPTIMIZATION
2560 M	P = P_INITIAL;	OPTIMIZATION
2561 M	ITERATION = 1;	OPTIMIZATION

STMT

SOURCE

CURRENT SCOPE

```

2562 MI DO FOR I_STORE = 1 TO (STEP_DIM + 1);
2563 MI 1 U_ACTIVE = ANGLE_OF_ATTACK_INITIAL I_STORE;
SI I_STORE:1
2564 MI 1 IF CAP_PHI_INITIAL I_STORE < 1. THEN
SI I_STORE
2565 MI 1 U_ACTIVE = SQR((1. / CAP_PHI_INITIAL I_STORE) - 1.);
SI I_STORE:2
2566 MI 1 ELSE
2566 MI 1 U_ACTIVE I_STORE:2 = 0.;
SI I_STORE:2
2567 MI END;
2568 MI [OMEGA_I_TIME] = [OIT_INIT];
EI
2569 MI [X_STORE] = 0.;
2570 MI [NET_MASS] = 0.;
2571 MI DJS = DJS_INIT;
EI
2572 MI HOLD_P = P;
2573 MI CALL ITERATION_DRIVER;
2574 MI FIRST_PASS_PSI_MAG = PSI_MAG;
EI
2575 MI IF OVER_STEP = OFF THEN
2576 MI DO;
2577 MI 1 FUEL_COST = X_STORE FINAL_STEP:5 + X_STORE FINAL_STEP:6 + X_STORE FINAL_STEP:7;
SI I_STORE:5 I_STORE:6 I_STORE:7
2578 MI 1 COST = FUEL_COST - INTEG_L;
EI
2579 MI 1 ITER_FLAG = ON;
EI
2580 MI 1 OVER_ITER_FLAG = OFF;
2581 MI 1 L_FILE = ITERATION;
EI
2582 MI 1 DO FOR IIT = L_FILE TO MAX_ITERATIONS WHILE (ITER_FLAG AND NOT OVER_ITER_FLAG) = ON;
EI

```

STMT	SOURCE	CURRENT SCOPE
2583 MI 2	IF IIT = MAX_ITERATIONS THEN	OPTIMIZATION
EI		
2584 MI 2	OVER_ITER_FLAG = ON;	OPTIMIZATION
2585 MI 2	ELSE	OPTIMIZATION
2585 MI 2	DO;	OPTIMIZATION
EI		
2586 MI 3	[HOLD_X] = [X_STORE];	OPTIMIZATION
2587 MI 3	[HOLD_M] = [NET_MASS];	OPTIMIZATION
EI		
2588 MI 3	[HOLD_L_X] = [L_X_STORE];	OPTIMIZATION
EI		
2589 MI 3	HOLD_P = P;	OPTIMIZATION
2590 MI 3	ITERATION = ITERATION + 1;	OPTIMIZATION
2591 MI 3	[HOLD_T] = [OMEGA_I_TIME];	OPTIMIZATION
EI		
2592 MI 3	[HOLD_U] = [U_ACTIVE];	OPTIMIZATION
2593 MI 3	[HOLD_PCS_TIME] = [PCS_TIME_STEP];	OPTIMIZATION
2594 MI 3	[HOLD_NEG_TIME] = [NEG_TIME_STEP];	OPTIMIZATION
2595 MI 3	CALL ITERATION_DRIVER;	OPTIMIZATION
2596 MI 3	FIRST_PASS_PSI_MAG = PSI_MAG;	OPTIMIZATION
EI		
2597 MI 3	IF OVER_STEP = OFF THEN	OPTIMIZATION
2598 MI 3	DO;	OPTIMIZATION
2599 MI 4	FUEL_COST = X_STORE + X_STORE + X_STORE + X_STORE	OPTIMIZATION
SI	FINAL_STEP:5 FINAL_STEP:6 FINAL_STEP:7	
2599 MI 4	;	OPTIMIZATION
2600 MI 4	DELTA_COST = COST - FUEL_COST + INTEG_L;	OPTIMIZATION
2601 MI 4	COST = FUEL_COST - INTEG_L;	OPTIMIZATION
2602 MI 4	IF ((ABS(DELTA_COST) < MIN_COST_RQMT) AND (PSI_MAG < MIN_PSI_RQMT)) THEN	OPTIMIZATION
EI		
2603 MI 4	ITER_FLAG = OFF;	OPTIMIZATION
2604 MI 4	ELSE IF ABS(PHI_MAG / FIRST_PSI_MAG) < PHI_CHECK THEN	OPTIMIZATION

```

STMT          SOURCE          CURRENT SCOPE
2605 MI 4      DO:              | OPTIMIZATION
2606 MI 5      IF DELTA_COST > 0. THEN | OPTIMIZATION
2607 MI 5      DO:              | OPTIMIZATION
2608 MI 6      IF DJS < (DELTA_COST_CHECK DELTA_COST) THEN | OPTIMIZATION
2609 MI 6      DJS = DELTA_COST_SHRINK DJS; | OPTIMIZATION
2610 MI 6      IF DJS > -DELTA_COST THEN | OPTIMIZATION
2611 MI 6      DJS = -DELTA_COST; | OPTIMIZATION
2612 MI 6      IF DJS < (2. DJS_INIT) THEN | OPTIMIZATION
2613 MI 6      DJS = 2. DJS_INIT; | OPTIMIZATION
2614 MI 5      END;              | OPTIMIZATION
2615 MI 5      ELSE              | OPTIMIZATION
2615 MI 5      ITER_FLAG = OFF; | OPTIMIZATION
2616 MI 4      END;              | OPTIMIZATION
2617 MI 3      END;              | OPTIMIZATION
2618 MI 2      END;              | OPTIMIZATION
2619 MI 1      END;              | OPTIMIZATION
2620 MI        END;              | OPTIMIZATION
2621 MI CLOSE OPTIMIZATION;

```

**** B L O C K S U M M A R Y ****

OUTER PROCEDURES CALLED
ITERATION_DRIVER

--- COMFOL VARIABLES USED

STEP_DIM, NUM_CONTROLS, NUM_CONSTANT_PARAMETERS, NUM_TRANS_PTS, M*, ITERATION*, ITERATION_P*, U_ACTIVE*, OMEGA_I_TIME*
X_STORE*, DJS_INIT, P, FINAL_STEP, X_STORE, L_FILE*, L_FILE, MAX_ITERATIONS, OMEGA_I_TIME, U_ACTIVE, PDS_TIME_STEP
NEG_TIME_STEP, MIN_COST_RGMT, MIN_PSI_RGMT, FIRST_PSI_MAG, PSI_CHECK, DELTA_COST_CHECK, DELTA_COST_SHRINK

OUTER VARIABLES USED

I_STORE*, I_STORE, IIT*, IIT, NET_MASS*, DJS*, HOLD_P*, FIRST_PASS_PSI_MAG*, PSI_MAG, OVER_STEP, COST*, INTEG_L, ITER_FLAG*
OVER_ITER_FLAG*, ITER_FLAG, OVER_ITER_FLAG, HOLD_X*, HOLD_M*, NET_MASS, HOLD_L_X*, L_X_STORE, HOLD_U*, HOLD_POS_TIME*
HOLD_NEG_TIME*, DELTA_COST*, COST, DELTA_COST, DJS

HAL/S 360-23.05

I N T E R M E T R I C S , I N C .

MARCH 7, 1980

6:29:25.65

PAGE 143

STMT

SOURCE

CURRENT SCOPE

NORM_TIME_STEP, U_TIME_KEEP*

| | |

**** C O M P I L A T I O N L A Y O U T ****

RUN_POOL: EXTERNAL COMPOOL;

AIR_BREATHER_OPTIMIZATION: PROCEDURE;

MODEL_DRIVER: PROCEDURE;

VEHICLE: PROCEDURE;

FIRST_STAGE: PROCEDURE;

SCND_STAGE: PROCEDURE;

ENVIRONMENT: PROCEDURE;

THEISIS_ALGORITHM: PROCEDURE;

U_COMPUTE: PROCEDURE;

STATE_DERIVS: PROCEDURE;

HAM_SUB_U: PROCEDURE;

DELTA_U_V_CALC: PROCEDURE;

RUNSE_KUTTA: PROCEDURE;

RK_DERIV: PROCEDURE;

TIME_SET: PROCEDURE;

ITERATION_DRIVER: PROCEDURE;

STATE_INTEGRATION: PROCEDURE;

OPTIMIZATION: PROCEDURE;

SYMBOL & CROSS REFERENCE TABLE LISTING:

(CROSS REFERENCE FLAG KEY: 4 = ASSIGNMENT, 2 = REFERENCE, 1 = SUBSCRIPT USE, 0 = DEFINITION)

DCL NAME	TYPE	ATTRIBUTES & CROSS REFERENCE
250 A_FIND	BIT(1)	ALIGNED, AUTOMATIC XREF: 0 0250 4 0313 2 0314 4 0318
2533 AA_INDEX	INTEGER ARRAY	ARRAY(31), SINGLE, ALIGNED, STATIC, INITIAL XREF: 0 2533 2 2550 2 2552
2534 AA_INIT	SCALAR ARRAY	ARRAY(31), DOUBLE, ALIGNED, STATIC, INITIAL XREF: 0 2534 2 2552
102 AIR_BREATHING_OPTIMIZATION	PROCEDURE	XREF: 0 0102 NOT REFERENCED
53 ALT_FINAL	SCALAR	DOUBLE, ALIGNED, CONSTANT XREF: 0 0053 2 1920 2 1923
46 ALT_METER_INTERVAL	SCALAR	DOUBLE, ALIGNED, CONSTANT XREF: 0 0046 2 0513 2 0530 2 0534
511 ALTITUDE	SCALAR	DOUBLE, ALIGNED, AUTOMATIC XREF: 0 0511 4 0513 2 0514 2 0529 2 0533
404 ANS_FIND	BIT(1)	ALIGNED, AUTOMATIC XREF: 0 0404 4 0417 2 0410 4 0422
216 ANGLE_OF_ATTACK	SCALAR	DOUBLE, ALIGNED, STATIC XREF: 0 0216 2 0346 2 0347 2 0356 2 0414 2 0419 2 0460 4 0577 4 0581 2 0589 2 0606 2 0694 2 0695
2525 ANGLE_OF_ATTACK_INITIAL	SCALAR ARRAY	ARRAY(2001), DOUBLE, ALIGNED, AUTOMATIC XREF: 0 2525 4 2552 2 2563
236 ASPECT_RATIO	SCALAR	DOUBLE, ALIGNED, STATIC XREF: 0 0236 4 0309 2 0310 2 0315 2 0341 2 0342 2 0348
44 ATM_DENS	SCALAR ARRAY	ARRAY(51), DOUBLE, ALIGNED, CONSTANT XREF: 0 0044 2 0518 2 0525 2 0531 2 0532
43 ATM_TEMP	SCALAR ARRAY	ARRAY(51), DOUBLE, ALIGNED, CONSTANT XREF: 0 0043 2 0519 2 0524 2 0529 2 0530
861 B	5 X 5 MATRIX	DOUBLE, ALIGNED, STATIC XREF: 0 0261 4 0280 2 0294 2 0297 2 0299 2 0308 6 0309 4 0305 6 0306 4 0307 6 0311 6 0317 6 0322 6 0324 2 0331 6 0332 2 0338 6 0339 4 0340 2 0353 2 0355
877 B_HOLD	SCALAR	DOUBLE, ALIGNED, AUTOMATIC XREF: 0 0877 4 0898 2 0900 4 0905 2 0907 4 0931 2 0933 4 0938 2 0940
874 B_INT_1	SCALAR ARRAY	ARRAY(5), DOUBLE, ALIGNED, AUTOMATIC XREF: 0 0874 4 0882 4 0890 2 0895 2 0896 2 0925
875 B_INT_2	SCALAR ARRAY	ARRAY(5), DOUBLE, ALIGNED, AUTOMATIC XREF: 0 0875 4 0893 4 0391 2 0502 2 0903 2 0935
199 BETA_LOWER_BOUND	SCALAR	DOUBLE, ALIGNED, AUTOMATIC XREF: 0 0199 4 0618 2 0622 4 0626 2 0628
201 BETA_NEK_BOUND	SCALAR	DOUBLE, ALIGNED, AUTOMATIC XREF: 0 0201 4 0622 2 0623 2 0625 2 0626
138 BETA_NOSE_SHOCK	SCALAR	DOUBLE, ALIGNED, STATIC XREF: 0 0138 4 0628 2 0629 2 0630 2 1239 2 1250 2 1252 2 1253
213 BETA_THETA_MAX	SCALAR	DOUBLE, ALIGNED, AUTOMATIC XREF: 0 0213 4 0610 2 0611 2 0619
198 BETA_UPPER_BOUND	SCALAR	DOUBLE, ALIGNED, AUTOMATIC XREF: 0 0198 4 0619 2 0622 4 0625 2 0628
239 BODY_WING_MASS	SCALAR	DOUBLE, ALIGNED, AUTOMATIC XREF: 0 0239 4 0268 2 0274
867 C_SUB_J	SCALAR	DOUBLE, ALIGNED, STATIC XREF: 0 0867 4 0961 4 0962 2 0967 2 0969
756 C_SUB_PSI	SCALAR	DOUBLE, ALIGNED, STATIC XREF: 0 0756 4 0958 2 0961 2 0967 2 0969
873 C_SUB_PSI_KEEP	SCALAR	DOUBLE, ALIGNED, STATIC XREF: 0 0873 4 0944 4 0950 4 0951 2 0958

DCL NAME	TYPE	ATTRIBUTES & CROSS REFERENCE
65 CAP_CA	SCALAR	DOUBLE, ALIGNED, INITIAL XREF: 0 0095 2 1163 2 1216 2 2002
733 CAP_LAMBDA_1	7 X 5 MATRIX ARRAY	ARRAY(1001), DOUBLE, ALIGNED, STATIC XREF: 0 0733 2 0554 2 1603 2 1685 2 1687 2 1609 2 1691 2 1799 2 1712 2 1724 4 2104 4 2105 4 2106 4 2107 4 2108 4 2109 4 2110 4 2111 4 2112 4 2113 4 2114 4 2100 2 2326
743 CAP_LAMBDA_1_DOT	7 X 5 MATRIX	DOUBLE, ALIGNED, STATIC XREF: 0 0743 4 1670 4 1672 4 1674 4 1676 4 1678 2 1720
762 CAP_LAMBDA_1_FLAG	BIT(1)	ALIGNED, STATIC XREF: 0 0762 2 1172 2 1165 2 1667 2 1719
1050 CAP_LAMBDA_1_HOLD	7 X 5 MATRIX	DOUBLE ALIGNED, STATIC XREF: 0 1050 4 1177 2 1670 2 1672 2 1674 2 1676 2 1679
734 CAP_LAMBDA_2	10 X 5 MATRIX	DOUBLE, ALIGNED, STATIC XREF: 0 0734 2 1760 4 2115 4 2120 4 2121 4 2122 4 2123 4 2124 4 2125 4 2126 4 2127 4 2129 4 2193 2 2333
744 CAP_LAMBDA_2_DOT	10 X 5 MATRIX	DOUBLE, ALIGNED, STATIC XREF: 0 0744 4 1693 4 1695 4 1697 4 1699 4 1691 2 1722
763 CAP_LAMBDA_2_FLAG	BIT(1)	ALIGNED, STATIC XREF: 0 0763 2 1165 2 1600 2 1721 2 1744
127 CAP_PHI	SCALAR	DOUBLE, ALIGNED, STATIC XREF: 0 0127 2 0305 2 0300 4 0570 4 0582 2 0701 2 1661 2 1476 2 1477 2 1492 2 1495 2 1521 2 1533 2 1598 2 1591 2 1599
2526 CAP_PHI_INITIAL	SCALAR ARRAY	ARRAY(2001), DOUBLE, ALIGNED, AUTOMATIC XREF: 0 2526 4 2558 2 2564 2 2565
83 CAP_Q	SCALAR	DOUBLE, ALIGNED, INITIAL XREF: 0 0093 2 1161 2 1939 2 1600 2 2000
162 CD	SCALAR	DOUBLE, ALIGNED, STATIC XREF: 0 0162 4 0390 6 0393 2 0392 4 0396 4 0562 2 1464
235 CDO	SCALAR	DOUBLE, ALIGNED, STATIC XREF: 0 0235 4 0360 4 0363 4 0376 2 0380
1871 CHECK1	SCALAR	DOUBLE, ALIGNED, AUTOMATIC XREF: 0 1671 4 2096 2 2109 2 2110 2 2111 2 2112 2 2113 2 2114 4 2119 2 2120 2 2121
161 CL	SCALAR	DOUBLE, ALIGNED, STATIC XREF: 0 0161 4 0346 2 0351 2 0350 2 0381 6 0384 2 0391 4 0551 2 1463 2 1479
770 CONFIG_INDEX	INTEGER	SINGLE, ALIGNED, STATIC XREF: 0 0770 4 2276 1 2277 1 2278 1 2290 1 2325 1 2328 4 2331 1 2333
1119 COS_A	SCALAR	DOUBLE, ALIGNED, STATIC XREF: 0 1119 4 1363 2 1364 2 1365 2 1366 2 1367 2 1368 2 1369 2 1455 2 1456 2 1430 2 1431
1070 COS_B_T	SCALAR	DOUBLE, ALIGNED, STATIC XREF: 0 1070 4 1253 2 1259 2 1415 2 1416 2 1417 2 1418 2 1419 2 1420 2 1421 2 1422 2 1423
1067 COS_BETA	SCALAR	DOUBLE, ALIGNED, STATIC XREF: 0 1067 4 1250 2 1255 2 1253 2 1262 2 1263 2 1264 2 1266 2 1267 2 1268 2 1413 2 1415 2 1417
1045 COS_DELTA	SCALAR	DOUBLE, ALIGNED, STATIC XREF: 0 1045 4 1501 2 1507 2 1500 2 1511 2 1512 2 1515 2 1516 2 1578 2 1579
166 COS_VEHICLE_ANGLE	SCALAR	DOUBLE, ALIGNED, STATIC XREF: 0 0166 4 0680 2 0713 2 0714 2 1611 2 1612 2 1614
781 COST	SCALAR	DOUBLE, ALIGNED, STATIC XREF: 0 0781 2 2507 4 2578 2 2600 4 2601
2527 CP_INDEX	INTEGER ARRAY	ARRAY(23), SINGLE, ALIGNED, STATIC, INITIAL XREF: 0 2527 2 2556 2 2558
2528 CP_INIT	SCALAR ARRAY	ARRAY(23), DOUBLE, ALIGNED, STATIC, INITIAL XREF: 0 2528 2 2558
1131 DAE1_DPI	10 - VECTOR	DOUBLE, ALIGNED, STATIC XREF: 0 1131 4 1396 4 1439 4 1445 2 1454 2 1457
1132 DAE2_DPI	10 - VECTOR	DOUBLE, ALIGNED, STATIC XREF: 0 1132 4 1397 4 1440 4 1443 2 1456 2 1458

DCL NAME	TYPE	ATTRIBUTES & CROSS REFERENCE									
1125 DAR_DPI	10 - VECTOR	DOUBLE, ALIGNED, STATIC	XREF: 0 1125	4 1390	4 1450	4 1463	2 1464				
1126 DAMI_DPI	10 - VECTOR	DOUBLE, ALIGNED, STATIC	XREF: 0 1126	4 1391	4 1447	4 1451	2 1463	2 1464			
1127 DAH2_DPI	10 - VECTOR	DOUBLE, ALIGNED, STATIC	XREF: 0 1127	4 1392	4 1402	2 1463	2 1484				
1122 DBETA_DMO	SCALAR	DOUBLE, ALIGNED, STATIC	XREF: 0 1122	4 1240	4 1255	2 1299	2 1300				
1135 DETA_DPI	SCALAR	DOUBLE, ALIGNED, STATIC	XREF: 0 1135	4 1412	2 1413	2 1415	2 1417				
1076 DBETA_DR	SCALAR	DOUBLE, ALIGNED, STATIC	XREF: 0 1076	4 1298	2 1301	2 1304	2 1310				
1078 DBETA_DTDOT	SCALAR	DOUBLE, ALIGNED, STATIC	XREF: 0 1078	4 1300	2 1303	2 1306	2 1312				
1077 DBETA_DUR	SCALAR	DOUBLE, ALIGNED, STATIC	XREF: 0 1077	4 1299	2 1302	2 1305	2 1311				
171 DCD_DCL2	SCALAR	DOUBLE, ALIGNED, STATIC	XREF: 0 0171	4 0243	4 0344	2 0351	2 0380	2 0381	6 0399	4 0560	2 1479
257 DCD0_DMO	SCALAR	DOUBLE, ALIGNED, AUTOMATIC	XREF: 0 0257	4 0359	4 0377	2 0381					
160 DCD1_DAR	SCALAR	DOUBLE, ALIGNED, STATIC	XREF: 0 0160	4 0351	6 0387	4 0398	4 0568	2 1464			
157 DCD1_CMO	SCALAR	DOUBLE, ALIGNED, STATIC	XREF: 0 0157	4 0291	6 0385	4 0397	4 0565	2 1345	2 1349	2 1353	
1101 DCD1_DR	SCALAR	DOUBLE, ALIGNED, STATIC	XREF: 0 1101	4 1345	2 1359						
1109 DCD1_DTDOT	SCALAR	DOUBLE, ALIGNED, STATIC	XREF: 0 1109	4 1353	2 1361						
1105 DCD1_DUR	SCALAR	DOUBLE, ALIGNED, STATIC	XREF: 0 1105	4 1349	2 1360						
158 DCD2_DMO	SCALAR	DOUBLE, ALIGNED, STATIC	XREF: 0 0158	4 0472	4 0476	6 0482	4 0491	4 0566	2 1346	2 1354	
1102 DCD2_DR	SCALAR	DOUBLE, ALIGNED, STATIC	XREF: 0 1102	4 1346	2 1359						
1110 DCD2_DTDOT	SCALAR	DOUBLE, ALIGNED, STATIC	XREF: 0 1110	4 1354	2 1351						
169 DCD2_DUAL	SCALAR	DOUBLE, ALIGNED, STATIC	XREF: 0 0169	4 0464	6 0494	4 0492	2 1479				
1106 DCD2_DUR	SCALAR	DOUBLE, ALIGNED, STATIC	XREF: 0 1106	4 1350	2 1360						
170 DCL_BALPHA	SCALAR	DOUBLE, ALIGNED, STATIC	XREF: 0 0170	4 0345	2 0346	6 0390	4 0559	2 1478	2 1479		
159 DCL1_DAR	SCALAR	DOUBLE, ALIGNED, STATIC	XREF: 0 0159	4 0347	2 0351	6 0398	4 0567	2 1463			
155 DCL1_DMO	SCALAR	DOUBLE, ALIGNED, STATIC	XREF: 0 0155	4 0356	2 0381	6 0386	4 0563	2 1343	2 1347	2 1351	
1099 DCL1_DR	SCALAR	DOUBLE, ALIGNED, STATIC	XREF: 0 1099	4 1343	2 1356						
1107 DCL1_DTDOT	SCALAR	DOUBLE, ALIGNED, STATIC	XREF: 0 1107	4 1351	2 1358						
1103 DCL1_DUR	SCALAR	DOUBLE, ALIGNED, STATIC	XREF: 0 1103	4 1347	2 1357						
156 DCL2_CMO	SCALAR	DOUBLE, ALIGNED, STATIC	XREF: 0 0156	4 0471	4 0475	6 0481	4 0564	2 1344	2 1348	2 1352	
1100 DCL2_DR	SCALAR	DOUBLE, ALIGNED, STATIC	XREF: 0 1100	4 1344	2 1356						
1108 DCL2_DTDOT	SCALAR	DOUBLE, ALIGNED, STATIC	XREF: 0 1108	4 1352	2 1358						
168 DCL2_DUAL	SCALAR	DOUBLE, ALIGNED, STATIC	XREF: 0 0168	4 0463	6 0483	2 1478	1104	DCL2_DUR	XREF: 0 1104	4 1348	2 1357
1143 DD_DPI	SCALAR	DOUBLE, ALIGNED, AUTOMATIC	XREF: 0 1143	4 1464	2 1465		2 1466				
1115 DD_DR	SCALAR	DOUBLE, ALIGNED, STATIC	XREF: 0 1115	4 1359	2 1364	2 1367	1117	DD_DTDOT	XREF: 0 1117	4 1361	2 1369
1152 DD_DUAL	SCALAR	DOUBLE, ALIGNED, STATIC	XREF: 0 1152	4 1479	2 1480	2 1481	1116	DD_DUR	XREF: 0 1116	4 1360	2 1365
1116 DD_DUR	SCALAR	DOUBLE, ALIGNED, STATIC	XREF: 0 1116	4 1360	2 1365	2 1368					

DCL NAME	TYPE	ATTRIBUTES & CROSS REFERENCE
255 DDCD_DCL2_DAR	SCALAR	DOUBLE, ALIGNED, AUTOMATIC XREF: 0 0255 4 0349 4 0350 2 0351
256 DDCD_DCL2_DM0	SCALAR	DOUBLE, ALIGNED, AUTOMATIC XREF: 0 0255 4 0357 2 0381
1039 DDELTA_DR	SCALAR	DOUBLE, ALIGNED, STATIC XREF: 0 1033 4 1497 2 1505 2 1506
1040 DDELTA_DT00T	SCALAR	DOUBLE, ALIGNED, STATIC XREF: 0 1040 4 1499 2 1513 2 1514
1039 DDELTA_DUR	SCALAR	DOUBLE, ALIGNED, STATIC XREF: 0 1039 4 1498 2 1509 2 1510
20 DEGREES_PER_RADIAN	SCALAR	DOUBLE, ALIGNED, CONSTANT XREF: 0 0020 2 0346 2 0347 2 0356 2 1478 2 1479
34 DELIVERED_MASS	SCALAR	DOUBLE, ALIGNED, CONSTANT XREF: 0 0034 2 0412
35 DELIVERED_PLANFORM_AREA	SCALAR	DOUBLE, ALIGNED, CONSTANT XREF: 0 0411
179 DELTA_ANGLE	SCALAR	DOUBLE, ALIGNED, STATIC XREF: 0 0179 2 0245 4 0247
757 DELTA_COST	SCALAR	DOUBLE, ALIGNED, STATIC XREF: 0 0757 4 2600 2 2602 2 2606 2 2608 2 2610 2 2611
80 DELTA_COST_CHECK	SCALAR	DOUBLE, ALIGNED, INITIAL XREF: 0 0080 2 2608
81 DELTA_COST_SURINK	SCALAR	DOUBLE, ALIGNED, INITIAL XREF: 0 0081 2 2609
737 DELTA_HEGA_I_TIME	INTEGER ARRAY	ARRAY(3), SINGLE, ALIGNED, STATIC XREF: 0 0737 4 2340
730 DELTA_U	2 - VECTOR ARRAY	ARRAY(1001), DOUBLE, ALIGNED, STATIC XREF: 0 0730 4 0967
1877 DELTA_U_NEW	2 - VECTOR ARRAY	ARRAY(1001), DOUBLE, ALIGNED, AUTOMATIC XREF: 0 1877 4 2469 4 2474 2 2485
860 DELTA_U_V_CALC	PROCEDURE	XREF: 0 0050 2 2338
731 DELTA_V	13 - VECTOR	DOUBLE, ALIGNED, STATIC XREF: 0 0731 4 0969 2 2340 2 2343 2 2352 2 2353 4 2625
1890 DFP3	SCALAR	DOUBLE, ALIGNED, AUTOMATIC XREF: 0 1890 4 2135 4 2136 2 2138
1024 DFR_DMI	SCALAR	DOUBLE, ALIGNED, STATIC XREF: 0 1024 4 1504 2 1559
1030 DFR_DP	SCALAR ARRAY	ARRAY(10), DOUBLE, ALIGNED, STATIC XREF: 0 1000 4 1578 4 1582 2 1604
1010 DFR_DR	SCALAR	DOUBLE, ALIGNED, STATIC XREF: 0 1010 4 1507 2 1555
1029 DFR_DT00T	SCALAR	DOUBLE, ALIGNED, STATIC XREF: 0 1029 4 1515 2 1557
1147 DFR_DUA	2 - VECTOR	DOUBLE, ALIGNED, STATIC XREF: 0 1147 4 1611 4 1613 2 1618
1025 DFR_DUR	SCALAR	DOUBLE, ALIGNED, STATIC XREF: 0 1025 4 1511 2 1555
1001 DFTHETA_DP	SCALAR ARRAY	ARRAY(10), DOUBLE, ALIGNED, STATIC XREF: 0 1001 4 1579 4 1583 2 1605
1011 DFTHETA_DR	SCALAR	DOUBLE, ALIGNED, STATIC XREF: 0 1011 4 1508 2 1551
1030 DFTHETA_DT00T	SCALAR	DOUBLE, ALIGNED, STATIC XREF: 0 1030 4 1516 2 1563
1148 DFTHETA_DUA	2 - VECTOR	DOUBLE, ALIGNED, STATIC XREF: 0 1143 4 1612 4 1614 2 1619
1026 DFTHETA_DUR	SCALAR	DOUBLE, ALIGNED, STATIC XREF: 0 1026 4 1512 2 1542
1133 D6_DPI	10 - VECTOR	DOUBLE, ALIGNED, STATIC XREF: 0 1133 4 1359 4 1468 2 1470
1091 DISPL_DM2	SCALAR	DOUBLE, ALIGNED, STATIC XREF: 0 1091 4 1313 2 1321 2 1322 2 1323 2 1426 2 1435
1139 DISPL_DP1	SCALAR	DOUBLE, ALIGNED, STATIC XREF: 0 1138 4 1426 2 1431
1092 DISP2_DM2	SCALAR	DOUBLE, ALIGNED, STATIC XREF: 0 1092 4 1315 2 1333 2 1334 2 1335 2 1427 2 1491
1139 DISP2_DP1	SCALAR	DOUBLE, ALIGNED, STATIC XREF: 0 1139 4 1427 2 1433
758 DJS	SCALAR	DOUBLE, ALIGNED, STATIC XREF: 0 0758 2 0959 4 2571 2 2608 6 2609 2 2610 4 2611 2 2612 4 2613
94 DJS_INIT	SCALAR	DOUBLE, ALIGNED, INITIAL XREF: 0 0094 2 2571 2 2612 2 2613
797 DJS_SCALE	SCALAR	DOUBLE, ALIGNED, STATIC XREF: 0 0797 4 0959 2 0961
1142 DL_DPI	SCALAR	DOUBLE, ALIGNED, AUTOMATIC XREF: 0 1142 4 1463 2 1465 2 1466
1112 DL_CR	SCALAR	DOUBLE, ALIGNED, STATIC XREF: 0 1112 4 1356 2 1354 2 1357
1114 DL_DT00T	SCALAR	DOUBLE, ALIGNED, STATIC XREF: 0 1114 4 1358 2 1366 2 1369
1151 DL_DUAL	SCALAR	DOUBLE, ALIGNED, STATIC XREF: 0 1151 4 1478 2 1480 2 1481

TYPE

ATTRIBUTES & CROSS REFERENCE

DCL NAME	TYPE	ATTRIBUTES & CROSS REFERENCE
1113 DL_DUR	SCALAR	DOUBLE, ALIGNED, STATIC XREF: 0 1113 4 1357 2 1365 2 1360
728 DM_DP	SCALAR ARRAY	ARRAY(10), DOUBLE, ALIGNED, STATIC XREF: 0 728 2 1468 2 1578 2 1604 2 1605 4 2133 4 2137 4 2130 4 2139 4 2140 4 2141 4 2142 4 2143 4 2144 4 2145
1008 DMASSFLUX_DP1	SCALAR ARRAY	ARRAY(10), DOUBLE, ALIGNED, STATIC XREF: 0 1008 4 1398 4 1434 6 1457 2 1508
1009 DMASSFLUX_DP2	SCALAR ARRAY	ARRAY(10), DOUBLE, ALIGNED, STATIC XREF: 0 1009 4 1399 4 1435 6 1455 2 1591
1017 DMASSFLUX_DP1	SCALAR	DOUBLE, ALIGNED, STATIC XREF: 0 1017 4 1372 2 1522
1016 DMASSFLUX_DP2	SCALAR	DOUBLE, ALIGNED, STATIC XREF: 0 1016 4 1375 2 1514
1036 DMASSFLUX_DTDOT1	SCALAR	DOUBLE, ALIGNED, STATIC XREF: 0 1036 4 1374 2 1554
1037 DMASSFLUX_DTDOT2	SCALAR	DOUBLE, ALIGNED, STATIC XREF: 0 1037 4 1377 2 1536
1022 DMASSFLUX_DUR1	SCALAR	DOUBLE, ALIGNED, STATIC XREF: 0 1022 4 1373 2 1523
1023 DMASSFLUX_DUR2	SCALAR	DOUBLE, ALIGNED, STATIC XREF: 0 1023 4 1376 2 1535
154 DMCR_DH2	SCALAR	DOUBLE, ALIGNED, STATIC XREF: 0 0154 4 0292 4 0569 2 1332 2 1375 2 1376 2 1377 2 1428
1140 DMCR_DP1	SCALAR	DOUBLE, ALIGNED, STATIC XREF: 0 1140 4 1428 2 1433 2 1435
1058 DM0_DR	SCALAR	DOUBLE, ALIGNED, STATIC XREF: 0 1058 4 1232 2 1298 2 1301 2 1304 2 1310 2 1343 2 1344 2 1345 2 1346
1060 DM0_DTDOT	SCALAR	DOUBLE, ALIGNED, STATIC XREF: 0 1060 4 1034 2 1300 2 1303
1059 DM0_DUR	SCALAR	DOUBLE, ALIGNED, STATIC XREF: 0 1059 4 1033 2 1299 2 1302 2 1305 2 1311 2 1347 2 1348 2 1350
1002 DM1DOT_DP	SCALAR ARRAY	ARRAY(10), DOUBLE, ALIGNED, STATIC XREF: 0 1002 4 1500 4 1509 4 1596 2 1606
1012 DM1DOT_DR	SCALAR	DOUBLE, ALIGNED, STATIC XREF: 0 1012 4 1522 4 1527 4 1545 2 1567
1031 DM1DOT_DTDOT	SCALAR	DOUBLE, ALIGNED, STATIC XREF: 0 1031 4 1524 4 1529 4 1547 2 1569
1144 DM1DOT_DUA	2 - VECTOR	DOUBLE, ALIGNED, STATIC XREF: 0 1144 4 1472 4 1486 4 1487
1027 DM1DOT_DUR	SCALAR	DOUBLE, ALIGNED, STATIC XREF: 0 1027 4 1523 4 1528 4 1546 2 1568
1061 DM2_DBETA	SCALAR	DOUBLE, ALIGNED, STATIC XREF: 0 1061 4 1235 4 1258 2 1301 2 1302 2 1303
1123 DM2_DM0	SCALAR	DOUBLE, ALIGNED, STATIC XREF: 0 1123 4 1241 4 1059 4 1273 4 1282 4 1292 2 1301 2 1302 2 1303
1137 DM2_DP1	SCALAR	DOUBLE, ALIGNED, STATIC XREF: 0 1137 4 1409 4 1415 4 1422 2 1423 2 1424 2 1426 2 1427 2 1428 2 1429 2 1486 2 1491
1079 DM2_DR	SCALAR	DOUBLE, ALIGNED, STATIC XREF: 0 1079 4 1301 2 1304 2 1307 2 1310 2 1321 2 1333 2 1375
1081 DM2_DTDOT	SCALAR	DOUBLE, ALIGNED, STATIC XREF: 0 1081 4 1303 2 1306 2 1309 2 1312 2 1323 2 1335 2 1377
1090 DM2_DUR	SCALAR	DOUBLE, ALIGNED, STATIC XREF: 0 1090 4 1302 2 1305 2 1308 2 1311 2 1322 2 1334 2 1376
1003 DM2DOT_DP	SCALAR ARRAY	ARRAY(10), DOUBLE, ALIGNED, STATIC XREF: 0 1003 4 1591 4 1592 4 1597 2 1607
1013 DM2DOT_DR	SCALAR	DOUBLE, ALIGNED, STATIC XREF: 0 1013 4 1534 4 1539 4 1548 2 1570
1032 DM2DOT_DTDOT	SCALAR	DOUBLE, ALIGNED, STATIC XREF: 0 1032 4 1536 4 1541 4 1550 2 1572
1145 DM2DOT_DUA	2 - VECTOR	DOUBLE, ALIGNED, STATIC XREF: 0 1145 4 1473 4 1491 4 1492 2 1621
1028 DM2DOT_DUR	SCALAR	DOUBLE, ALIGNED, STATIC XREF: 0 1028 4 1535 4 1540 4 1549 2 1571

DCL NAME	TYPE	ATTRIBUTES & CROSS REFERENCE
1004 DM3DOT_DP	SCALAR ARRAY	ARRAY(10), DOUBLE, ALIGNED, STATIC XREF: 0 1004 4 1593
1146 DM3DOT_DUA	2 - VECTOR	4 1599 4 1600 2 1603
1006 DN_DP	SCALAR ARRAY	DOUBLE, ALIGNED, STATIC XREF: 0 1146 4 1474 4 1495 2 1622
1015 DN_DR	SCALAR	ARRAY(10), DOUBLE, ALIGNED, STATIC XREF: 0 1003 4 1456
1014 DN_DTDOT	SCALAR	2 1468 2 1578 2 1579
723 DN_DUA	2 - VECTOR	DOUBLE, ALIGNED, STATIC XREF: 0 1015 4 1367 2 1385 2 1506
1020 DN_DUR	SCALAR	DOUBLE, ALIGNED, STATIC XREF: 0 1034 4 1369 2 1514
1005 DP_DP	SCALAR ARRAY	DOUBLE, ALIGNED, STATIC XREF: 0 0723 4 1401 2 1612
1014 DP_DR	SCALAR	2 1624 4 2340
1033 DP_DTDOT	SCALAR	DOUBLE, ALIGNED, STATIC XREF: 0 1020 4 1368 2 1365 2 1510
722 DP_DUA	2 - VECTOR	ARRAY(10), DOUBLE, ALIGNED, STATIC XREF: 0 1005 4 1455
1019 DP_DUR	SCALAR	2 1490 2 1577
1153 DFHI_DUA2	SCALAR	DOUBLE, ALIGNED, STATIC XREF: 0 1014 4 1364 2 1385 2 1505
145 DRAG	SCALAR	DOUBLE, ALIGNED, STATIC XREF: 0 1033 4 1366 2 1367 2 1513
126 DRO_DR	SCALAR	DOUBLE, ALIGNED, STATIC XREF: 0 0722 4 1460 2 1611 2 1612
1063 DRO2_DBETA	SCALAR	2 1624 4 2639
1074 DRO2_DHO	SCALAR	DOUBLE, ALIGNED, STATIC XREF: 0 1019 4 1365 2 1366 2 1509
1121 DRO2_DR2	SCALAR	DOUBLE, ALIGNED, STATIC XREF: 0 1153 4 1476 2 1477 2 1487
1134 DRO2_DPI	SCALAR	2 1492 2 1495
1088 DRO2_DR	SCALAR	DOUBLE, ALIGNED, STATIC XREF: 0 0145 4 0693 2 0696 2 0697
1075 DRO2_DRO_0	SCALAR	2 1359 2 1360 2 1361
1090 DRO2_DTDOT	SCALAR	DOUBLE, ALIGNED, STATIC XREF: 0 0126 4 0534 4 0571 2 1310
1089 DRO2_DUR	SCALAR	2 1358 2 1359 2 1359 2 1360
253 DRY_TANK_VOLUME	SCALAR	DOUBLE, ALIGNED, STATIC XREF: 0 1063 4 1237 4 1266 2 1268
1007 DT_DP	SCALAR ARRAY	DOUBLE, ALIGNED, STATIC XREF: 0 1074 4 1268 4 1276 4 1295
1016 DT_DR	SCALAR	4 1295 2 1310 2 1311 2 1312
1035 DT_DTDOT	SCALAR	DOUBLE, ALIGNED, STATIC XREF: 0 1121 4 1239 4 1269 2 1310
1149 DT_DUA	2 - VECTOR	2 1311 2 1312
1021 DT_DUR	SCALAR	DOUBLE, ALIGNED, STATIC XREF: 0 1134 4 1407 4 1413 4 1424
1128 DTH1_DPI	10 - VECTOR	2 1431 2 1433 2 1434 2 1435
1129 DTH2_DPI	10 - VECTOR	DOUBLE, ALIGNED, STATIC XREF: 0 1068 4 1310 2 1321 2 1333
1096 DTH2_DR	SCALAR	2 1372 2 1375
1093 DTH2_DTDOT	SCALAR	DOUBLE, ALIGNED, STATIC XREF: 0 1075 4 1269 4 1277 4 1286
1097 DTH2_DUR	SCALAR	4 1286 2 1310
		DOUBLE, ALIGNED, STATIC XREF: 0 1090 4 1312 2 1323 2 1335
		2 1374 2 1377
		DOUBLE, ALIGNED, STATIC XREF: 0 1089 4 1311 2 1322 2 1334
		2 1373 2 1376
		DOUBLE, ALIGNED, AUTOMATIC XREF: 0 0253 4 0259 2 0270
		2 0272
		ARRAY(10), DOUBLE, ALIGNED, STATIC XREF: 0 1007 4 1462
		2 1469 2 1475 2 1577
		DOUBLE, ALIGNED, STATIC XREF: 0 1016 4 1380 2 1395 2 1505
		DOUBLE, ALIGNED, STATIC XREF: 0 1035 4 1392 2 1397 2 1513
		DOUBLE, ALIGNED, STATIC XREF: 0 1149 4 1475 4 1477 2 1611
		2 1612 2 1613 2 1614 2 1624
		DOUBLE, ALIGNED, STATIC XREF: 0 1021 4 1381 2 1386 2 1509
		DOUBLE, ALIGNED, STATIC XREF: 0 1128 4 1393 4 1431 6 1454
		2 1462 2 1466
		DOUBLE, ALIGNED, STATIC XREF: 0 1129 4 1394 4 1433 6 1456
		2 1462 2 1491
		DOUBLE, ALIGNED, STATIC XREF: 0 1096 4 1333 4 1358 2 1390
		DOUBLE, ALIGNED, STATIC XREF: 0 1098 4 1335 4 1340 2 1382
		DOUBLE, ALIGNED, STATIC XREF: 0 1097 4 1334 4 1339 2 1381

ATTRIBUTES & CROSS REFERENCE

DCL NAME	TYPE	ATTRIBUTES & CROSS REFERENCE
1130 DTH3_DPI	10 - VECTOR	DOUBLE, ALIGNED, STATIC XREF: 0 1130 4 1395 4 1461 2 1462
153 DT0_DR	SCALAR	DOUBLE, ALIGNED, STATIC XREF: 0 0153 4 0550 4 0570 2 1232
1093 DT1_DR	SCALAR	DOUBLE, ALIGNED, STATIC XREF: 0 1093 4 1321 4 1326 2 1380
1095 DT1_DTDOT	SCALAR	DOUBLE, ALIGNED, STATIC XREF: 0 1095 4 1328 4 1362
1094 DT1_DUR	SCALAR	DOUBLE, ALIGNED, STATIC XREF: 0 1094 4 1322 4 1327 2 1301
1062 DT2_DSETA	SCALAR	DOUBLE, ALIGNED, STATIC XREF: 0 1062 4 1236 4 1262 2 1264
1072 DT2_DTH	SCALAR	DOUBLE, ALIGNED, STATIC XREF: 0 1072 4 1264 4 1274 4 1283
1120 DT2_DH2	SCALAR	DOUBLE, ALIGNED, STATIC XREF: 0 1120 4 1238 4 1287 2 1304
1136 DT2_DPI	SCALAR	DOUBLE, ALIGNED, STATIC XREF: 0 1136 4 1408 4 1417 4 1423
1082 DT2_DR	SCALAR	DOUBLE, ALIGNED, STATIC XREF: 0 1082 4 1304 2 1307
1084 DT2_DTDOT	SCALAR	DOUBLE, ALIGNED, STATIC XREF: 0 1084 4 1305 2 1309
1073 DT2_DTH	SCALAR	DOUBLE, ALIGNED, STATIC XREF: 0 1073 4 1265 4 1275 4 1284
1083 DT2_DUR	SCALAR	DOUBLE, ALIGNED, STATIC XREF: 0 1083 4 1305 2 1308
1064 DU2_DH2	SCALAR	DOUBLE, ALIGNED, STATIC XREF: 0 1064 4 1244 2 1246 2 1307
1141 DU2_DPI	SCALAR	DOUBLE, ALIGNED, STATIC XREF: 0 1141 4 1429 2 1431 2 1433
1085 DU2_DR	SCALAR	DOUBLE, ALIGNED, STATIC XREF: 0 1085 4 1307 2 1321 2 1333
1087 DU2_DTDOT	SCALAR	DOUBLE, ALIGNED, STATIC XREF: 0 1087 4 1309 2 1323 2 1335
1065 DU2_DTH	SCALAR	DOUBLE, ALIGNED, STATIC XREF: 0 1065 4 1246 2 1307 2 1308
1086 DU2_DUR	SCALAR	DOUBLE, ALIGNED, STATIC XREF: 0 1086 4 1303 2 1322 2 1334
103 DYNAMIC_PO	SCALAR	DOUBLE, ALIGNED, STATIC XREF: 0 0103 2 0391 2 0392 2 0465
5 EARTH_MASS	SCALAR	DOUBLE, ALIGNED, CONSTANT XREF: 0 0586 2 1357 2 1359
11 EARTH_OMEGA	SCALAR	DOUBLE, ALIGNED, CONSTANT XREF: 0 1161 2 1478 2 1936 2 1938
3 EARTH_RADIUS	SCALAR	DOUBLE, ALIGNED, CONSTANT XREF: 0 1999 2 2000
508 ENVIRONMENT	PROCEDURE	DOUBLE, ALIGNED, CONSTANT XREF: 0 0005 2 0540 2 1503
151 EXPANSION_FLAG	BIT(1)	DOUBLE, ALIGNED, CONSTANT XREF: 0 0011 2 0538 2 1230
211 EXTREMAL_ARRAY	SCALAR ARRAY	DOUBLE, ALIGNED, CONSTANT XREF: 0 1941 2 1971
740 F	7 X 7 MATRIX	DOUBLE, ALIGNED, CONSTANT XREF: 0 0003 2 0572 2 0842
786 FD_COUNT	INTEGER	DOUBLE, ALIGNED, CONSTANT XREF: 0 1941 2 1959 2 1971 2 2096 2 2111
790 FD_FLAG	BIT(1)	DOUBLE, ALIGNED, CONSTANT XREF: 0 0508 2 0591
45 FEET_PER_METER	SCALAR	DOUBLE, ALIGNED, CONSTANT XREF: 0 0151 4 0557 4 0642 2 1279 2 1419

DCL NAME	TYPE	ATTRIBUTES & CROSS REFERENCE
100 FINAL_STEP	INTEGER	SINGLE, ALIGNED XREF: 0 0100 2 0923 2 0824 2 0963 4 2004 2 2048 2 2051 2 2050 2 2030 1 2081 1 2002 1 2083 1 2004 2 2085 1 2086 1 2110 1 2111 2 2106 2 2147 2 2221 2 2222 2 2223 2 2278 2 2370 2 2372 2 2373 2 2393 2 2413 2 2422 2 2430 2 2431 2 2440 2 2441 2 2403 2 2492 1 2500 2 2501 2 2502 3 2503 3 2504 1 2507 1 2577 1 2599 4 2622 DOUBLE, ALIGNED, STATIC XREF: 0 0754 4 1990 2 1982 2 2059 2 2081 2 2082 2 2093 2 2054 2 2148 2 2224 2 2437 2 2504 4 2630 ARRAY(4), DOUBLE, ALIGNED, STATIC XREF: 0 1899 4 1952 2 1985 2 1986 ALIGNED, AUTOMATIC XREF: 0 0242 4 0365 2 0366 4 0373 ALIGNED, STATIC XREF: 0 0720 2 1169 4 1171 4 1784 4 1804 4 1815 4 1828 4 2637 ALIGNED XREF: 0 0074 2 2057 4 2070 4 2643 DOUBLE, ALIGNED, STATIC XREF: 0 0608 2 0960 4 2574 4 2596 DOUBLE, ALIGNED XREF: 0 0072 2 0946 2 0960 2 2507 2 2604 4 2644 DOUBLE, ALIGNED, STATIC XREF: 0 0976 4 1793 2 1836 XREF: 0 0234 2 0499 2 0503 DOUBLE, ALIGNED, STATIC XREF: 0 0117 4 0274 2 0700 2 0941 2 1648 2 1932 DOUBLE, ALIGNED, STATIC XREF: 0 0161 2 0266 2 0257 4 0549 ARRAY(5), DOUBLE, ALIGNED, CONSTANT XREF: 0 0033 2 0310 2 0315 2 0341 2 0342 2 0347 2 0348 2 0350 DOUBLE, ALIGNED, CONSTANT XREF: 0 0030 2 0338 2 0340 2 0353 2 0355 DOUBLE, ALIGNED, CONSTANT XREF: 0 0031 2 0337 2 0339 2 0352 2 0354 DOUBLE, ALIGNED, STATIC XREF: 0 0222 4 0392 2 0393 4 0395 4 0689 2 0693 SINGLE, ALIGNED, CONSTANT XREF: 0 0052 2 1467 2 1575 2 1602 DOUBLE, ALIGNED, STATIC XREF: 0 0221 4 0391 4 0688 2 0692 ARRAY(10), DOUBLE, ALIGNED, CONSTANT XREF: 0 0032 2 0323 2 0328 2 0336 2 0356 2 0357 DOUBLE, ALIGNED, AUTOMATIC XREF: 0 2538 4 2577 2 2578 4 2599 2 2600 2 2601 DOUBLE, ALIGNED, AUTOMATIC XREF: 0 0238 4 0267 2 0268 DOUBLE, ALIGNED, AUTOMATIC XREF: 0 0254 4 0266 2 0267 2 0269 DOUBLE, ALIGNED, AUTOMATIC XREF: 0 0191 4 0336 2 0337 2 0338 2 0339 2 0340 4 0341 2 0344 2 0345 2 0352 2 0353 2 0354 2 0355 4 0382 2 0383 2 0394 2 0385 2 0397 2 0388 2 0389 2 0390 4 0453 2 0454 2 0455 2 0456 2 0457 4 0460 2 0461 2 0462 2 0467 2 0468 2 0469 2 0470 4 0478 2 0479 2 0490 2 0481 2 0482 2 0483 2 0484 4 0531 2 0532 2 0533 2 0534 4 0594 2 0696 2 0697 DOUBLE, ALIGNED, STATIC XREF: 0 0977 4 1630 2 1670 DOUBLE, ALIGNED, STATIC XREF: 0 0978 4 1637 2 1672 DOUBLE, ALIGNED, AUTOMATIC XREF: 0 0192 4 0532 2 0533 4 0695 2 0696 2 0697 DOUBLE, ALIGNED, STATIC XREF: 0 0979 4 1642 2 1674 DOUBLE, ALIGNED, AUTOMATIC XREF: 0 0193 4 0651 2 0652 4 0659 2 0660
1899 FINAL_U_STORE	2 - VECTOR ARRAY	
242 FIND_FLAG	BIT(1)	
720 FIRST_DERIV_FLAG	BIT(1)	
74 FIRST_ITERATION_FLAG	BIT(1)	
808 FIRST_PASS_PSI_MAG	SCALAR	
72 FIRST_PSI_MAG	SCALAR	
976 FIRST_RK_VAL_N	10 X 5 MATRIX	
234 FIRST_STAGE	PROCEDURE	
117 FIRST_STAGE_DRY_MASS	SCALAR	
181 FIRST_STAGE_LENGTH	SCALAR	
33 FS_A_VAL	SCALAR ARRAY	
30 FS_CD_MAT	5 X 10 MATRIX	
31 FS_CL_MAT	5 X 10 MATRIX	
222 FS_DRAG	SCALAR	
52 FS_FIXED_PARAMETERS	INTEGER	
221 FS_LIFT	SCALAR	
32 FS_M_VAL	SCALAR ARRAY	
2538 FUEL_COST	SCALAR	
238 FUSELAGE_SURFACE_AREA	SCALAR	
254 FUSELAGE_VOLUME	SCALAR	
191 F1	SCALAR	
977 F1	7 X 7 MATRIX	
978 F2	7 X 7 MATRIX	
192 F2	SCALAR	
979 F3	7 X 7 MATRIX	
193 F3	SCALAR	

ATTRIBUTES & CROSS REFERENCE

DCL NAME	TYPE	ATTRIBUTES & CROSS REFERENCE
980 F4	7 X 7 MATRIX	DOUBLE, ALIGNED, STATIC XREF: 0 0930 4 1649 2 1676
194 F4	SCALAR	DOUBLE, ALIGNED, AUTOMATIC XREF: 0 0194 4 0529 2 0630
981 F5	7 X 7 MATRIX	DOUBLE, ALIGNED, STATIC XREF: 0 0645 2 0650
195 F5	SCALAR	DOUBLE, ALIGNED, AUTOMATIC XREF: 0 0681 4 1054 2 1678
167 G	SCALAR	DOUBLE, ALIGNED, STATIC XREF: 0 0167 4 0540 2 0713 2 1612
86 G_D	SCALAR	DOUBLE, ALIGNED, INITIAL XREF: 0 0005 2 1162 2 1153 2 1216
132 G_LOAD	SCALAR	DOUBLE, ALIGNED, STATIC XREF: 0 0132 4 0715 2 1162 2 1163
732 G_MAT	7 X 2 MATRIX ARRAY	DOUBLE, ALIGNED, STATIC XREF: 0 1624 2 1469 2 1623
15 GAM10	SCALAR	ARRAY(1001), DOUBLE, ALIGNED, STATIC XREF: 0 0732 2 0955
17 GAM1	SCALAR	DOUBLE, ALIGNED, CONSTANT XREF: 0 0015 2 0016 2 0018
18 GAM2	SCALAR	DOUBLE, ALIGNED, CONSTANT XREF: 0 0530 2 0632 2 0575
16 GAM3	SCALAR	DOUBLE, ALIGNED, CONSTANT XREF: 0 0018 2 0609 2 0631
47 GROUND_RO	SCALAR	DOUBLE, ALIGNED, CONSTANT XREF: 0 0018 2 0609 2 0631
12 G0	SCALAR	DOUBLE, ALIGNED, CONSTANT XREF: 0 0018 2 0609 2 0631
176 H_C	SCALAR	DOUBLE, ALIGNED, STATIC XREF: 0 0176 2 0260 2 0303 4 0544
177 H_C_TJ	SCALAR	DOUBLE, ALIGNED, STATIC XREF: 0 0177 2 0264 2 0303 4 0545
729 H_SUB_U	2 - VECTOR ARRAY	ARRAY(1001), DOUBLE, ALIGNED, STATIC XREF: 0 0729 4 0855
851 HAM_SUB_U	PROCEDURE	XREF: 0 0551 2 0967 2 1707 2 1709
240 HC_TANK_MASS	SCALAR	DOUBLE, ALIGNED, AUTOMATIC XREF: 0 0240 4 0271 2 0274
106 HC_TANK_VOL	SCALAR	DOUBLE, ALIGNED, STATIC XREF: 0 0106 4 0270 2 0271 2 2041
180 HC_TANK_VOL_FRACTION	SCALAR	DOUBLE, ALIGNED, STATIC XREF: 0 0100 2 0270 2 0272 4 0548
794 HELD_FS_MASS	SCALAR	DOUBLE, ALIGNED, STATIC XREF: 0 0794 2 1223 4 1932 2 2311
252 HIGH_A	INTEGER	SINGLE, ALIGNED, AUTOMATIC XREF: 0 0252 4 0311 4 0317
510 HIGH_ALT	INTEGER	2 0322 1 0339 1 0340 1 0341 1 0347 1 0350 1 0352 1 0353
406 HIGH_ANGLE	INTEGER	1 0354 1 0355
229 HIGH_CD	SCALAR	SINGLE, ALIGNED, AUTOMATIC XREF: 0 0510 4 0528 1 0529
246 HIGH_C00	SCALAR	1 0530 1 0531
231 HIGH_CL	SCALAR	SINGLE, ALIGNED, AUTOMATIC XREF: 0 0406 4 0415 4 0421
		2 0426 1 0431 1 0432 1 0438 1 0439 1 0456 1 0457 1 0460
		1 0463 1 0464 1 0467 1 0468 1 0469 1 0470
		DOUBLE, ALIGNED, AUTOMATIC XREF: 0 0229 4 0340 2 0345
		2 0344 2 0350 4 0355 2 0357 4 0432 4 0439 4 0457 2 0462
		2 0464 4 0470 2 0472
		DOUBLE, ALIGNED, AUTOMATIC XREF: 0 0246 4 0371 2 0376
		2 0377
		DOUBLE, ALIGNED, AUTOMATIC XREF: 0 0231 4 0339 2 0345

DCL NAME	TYPE	ATTRIBUTES & CROSS REFERENCE									
226 HIGH_M	INTEGER	2 0347	4 0354	2 0356	4 0431	4 0438	4 0456	2 0461	2 0463		
		4 0469	2 0471								
		SINGLE, ALIGNED, AUTOMATIC XREF: 0 0206 4 0207 2 0270									
		1 0291	1 0292	4 0324	4 0330	2 0335	1 0336	1 0337	1 0338		
		1 0339	1 0340	1 0330	1 0355	1 0355	1 0357	4 0449	2 0452		
		1 0453	1 0454	1 0453	1 0456	1 0457	1 0469	1 0470	1 0471		
		1 0472									
247 HIGH_M_S	SCALAR	DOUBLE, ALIGNED, AUTOMATIC XREF: 0 0247 4 0372 2 0376									
		2 0377									
206 HIGH_M_2	SCALAR	DOUBLE, ALIGNED, AUTOMATIC XREF: 0 0206 4 0648 2 0651									
		6 0655	2 0658	4 0662							
208 HIGH_NU	SCALAR	DOUBLE, ALIGNED, AUTOMATIC XREF: 0 0208 4 0652 2 0653									
800 HOLD_L_X	7 - VECTOR ARRAY	ARRAY(2001), DOUBLE, ALIGNED, STATIC XREF: 0 0800 2 2513									
		4 2568									
799 HOLD_M	SCALAR ARRAY	ARRAY(2001), DOUBLE, ALIGNED, STATIC XREF: 0 0799 2 2512									
		4 2597									
806 HOLD_NEG_TIME	SCALAR ARRAY	ARRAY(3), DOUBLE, ALIGNED, STATIC XREF: 0 0806 2 2519									
		4 2594									
801 HOLD_P	10 - VECTOR	DOUBLE, ALIGNED, STATIC XREF: 0 0801 2 2514 4 2572 4 2589									
805 HOLD_POS_TIME	SCALAR ARRAY	ARRAY(3), DOUBLE, ALIGNED, STATIC XREF: 0 0805 2 2510									
		4 2593									
1902 HOLD_FSI	5 - VECTOR	DOUBLE, ALIGNED, STATIC XREF: 0 1902 4 2079 2 2337 2 2507									
803 HOLD_T	INTEGER ARRAY	ARRAY(3), SINGLE, ALIGNED, STATIC XREF: 0 0803 2 2517									
		4 2591									
804 HOLD_U	2 - VECTOR ARRAY	ARRAY(2001), DOUBLE, ALIGNED, STATIC XREF: 0 0804 2 2515									
		4 2592									
802 HOLD_U_T	SCALAR ARRAY	ARRAY(2001), DOUBLE, ALIGNED, STATIC XREF: 0 0802 4 2066									
		2 2516									
798 HOLD_X	7 - VECTOR ARRAY	ARRAY(2001), DOUBLE, ALIGNED, STATIC XREF: 0 0798 2 2511									
		4 2566									
8 HYDROCARBON_DENSITY	SCALAR	DOUBLE, ALIGNED, CONSTANT XREF: 0 0003 2 0271 2 2041									
7 H2_DENSITY	SCALAR	DOUBLE, ALIGNED, CONSTANT XREF: 0 0207 2 0273 2 2042									
241 H2_TANK_MASS	SCALAR	DOUBLE, ALIGNED, AUTOMATIC XREF: 0 0241 4 0273 2 0274									
105 H2_TANK_VOL	SCALAR	DOUBLE, ALIGNED, STATIC XREF: 0 0105 4 0272 2 0273 2 2042									
196 I_BETA	INTEGER	SINGLE, ALIGNED, AUTOMATIC XREF: 0 0196 4 0621 4 0657									
		NOT REFERENCED									
789 I_CL	INTEGER	SINGLE, ALIGNED, STATIC XREF: 0 0789 2 0854 2 1192 4 2165									
		4 2176	4 2189	4 2200							
719 I_FD	INTEGER	SINGLE, ALIGNED, STATIC XREF: 0 0719 2 1669 2 1671 2 1673									
		2 1675	2 1677	2 1682	2 1684	2 1686	2 1688	2 1690	2 1695		
		2 1697	2 1699	2 1781	4 1783	4 1783	2 1797	4 1800	4 1801		
		4 1803	2 1825	4 1826	4 1827	4 2636					
1055 I_FK	INTEGER	SINGLE, ALIGNED, STATIC XREF: 0 1055 4 1202 1 1203 1 1206									
		4 1226	1 1227	4 1400	2 1401	2 1405	2 1437	2 1442	2 1444		
		2 1445	2 1448	1 1454	1 1456	1 1457	1 1458	2 1460	1 1462		
		1 1463	1 1464	1 1465	1 1466	2 1467	1 1468	1 1470	4 1574		
		2 1575	1 1577	1 1578	1 1579	1 1582	1 1583	1 1589	1 1589		
		1 1591	1 1592	1 1593	1 1596	1 1597	2 1598	1 1599	1 1600		
		2 1602	1 1604	1 1605	1 1606	1 1607	1 1608	4 1617	1 1608		
		1 1619	1 1620	1 1621	1 1622	1 1624	1 1625				
1874 I_INIT	INTEGER	SINGLE, ALIGNED, AUTOMATIC XREF: 0 1874 4 2090 1 2091									
759 I_J_J	SCALAR	DOUBLE, ALIGNED, STATIC XREF: 0 0759 2 0761 4 2090 1 2091									
		4 2234									
760 I_J_J_DOT	SCALAR	DOUBLE, ALIGNED, STATIC XREF: 0 0760 4 1707 2 1726									
765 I_J_J_FLAG	BIT(1)	ALIGNED, STATIC XREF: 0 0765 2 1702 2 1706 2 1725 2 1767									

ATTRIBUTES & CROSS REFERENCE

DCL NAME	TYPE	ATTRIBUTE	CROSS REFERENCE
783 I_TIME_STORE	INTEGER	SINGLE, ALIGNED, STATIC	XREF: 0 0783 2 1205 4 2146 2 2151 2 2172 2 2195 2 2193 2 2207 4 2216 2 2217 4 2222 2 2229 2 2245 2 2255 4 2266 2 2267
1881 I_U	INTEGER	SINGLE, ALIGNED, STATIC	XREF: 0 1831 4 2050 2 2051 2 2053 2 2059 1 2062 2 2063 1 2064 4 2430 2 2431 2 2433 1 2438 4 2443 2 2444 2 2446 2 2449 2 2451 2 2452 2 2453 2 2456 1 2460 1 2455 1 2468 4 2489 2 2490 1 2493 4 2492 2 2493 2 2495 1 2496 1 2497 4 2501 2 2502 3 2503 3 2504 DOUBLE, ALIGNED, STATIC
862 I_VEC_1	5 - VECTOR	XREF: 0 0652 4 0653 2 0667	
863 I_VEC_2	5 - VECTOR	XREF: 0 0653 4 0655 2 0661 2 0667	
864 I_VEC_3	5 - VECTOR	XREF: 0 0664 4 0954 2 0955 2 0951	
243 I_ZLD	INTEGER	DOUBLE, ALIGNED, STATIC	XREF: 0 0243 4 0316 1 0367
780 IIT	INTEGER	SINGLE, ALIGNED, STATIC	XREF: 0 0780 4 2544 1 2545 4 2582 2 2583
870 IN_I	INTEGER	SINGLE, ALIGNED, AUTOMATIC	XREF: 0 0370 4 0885 1 0937 1 0989 2 0990 4 0897 1 0898 1 0899 1 0900 4 0902 1 0916 1 0907 4 0909 2 0910 1 0911 4 0913 2 0914 1 0917 4 0928 2 0929 1 0932 1 0933 4 0937 1 0938 1 0939 1 0940
871 IN_J	INTEGER	SINGLE, ALIGNED, AUTOMATIC	XREF: 0 0871 4 0886 1 0887 1 0889 2 0991 4 0995 1 0899 1 0920 4 0904 1 0905 1 0956 1 0907 4 0915 2 0916 1 0917 4 0920 2 0921 1 0922 4 0930 1 0931 1 0932 1 0933 4 0935 2 0936 1 0939 1 0940
872 IN_K	INTEGER	SINGLE, ALIGNED, AUTOMATIC	XREF: 0 0872 4 0881 3 0982 3 0883 1 0884 2 0885 2 0886 1 0890 1 0891 1 0895 3 0956 1 0898 1 0899 1 0902 3 0903 1 0905 1 0906 2 0910 1 0911 2 0914 2 0916 1 0917 2 0921 1 0922 1 0924 2 0926 6 0927 1 0928 2 0929 1 0931 1 0932 1 0935 2 0936 1 0938 1 0939 DOUBLE, ALIGNED, STATIC
787 INTEG_L	SCALAR	XREF: 0 0787 2 1741 4 1845 4 1927	
779 ITER_FLAG	BIT(1)	XREF: 0 0779 2 2573 2 2601	
71 ITERATION	INTEGER	ALIGNED, STATIC	XREF: 0 0779 4 2579 2 2582 4 2603 4 2615 SINGLE, ALIGNED
1870 ITERATION_DRIVER	PROCEDURE	XREF: 0 0071 2 0943 2 2053 2 2410 2 2422	
869 J_DU	INTEGER	4 2540 3 2542 6 2543 1 2543 4 2548 3 2550 6 2551 1 2552 4 2554 3 2556 6 2557 1 2559 2 2561 2 2591 6 2590 XREF: 0 1070 2 2573 2 2595	
866 J_MAT	2 X 5 MATRIX	SINGLE, ALIGNED, STATIC	XREF: 0 0659 4 0963 1 0964 2 0965 1 0967
1893 J_OMEGA	INTEGER	DOUBLE, ALIGNED, STATIC	XREF: 0 0866 4 0964 2 0967 SINGLE, ALIGNED, STATIC
1879 J_RCP	INTEGER	1 1835 1 1866	
989 J_RK	INTEGER	SINGLE, ALIGNED, AUTOMATIC	XREF: 0 1879 4 2459 1 2469 1 2470 1 2474 1 2475
78 J_SCALE_FACTOR	SCALAR	XREF: 0 0989 1 1720 1 1722 1 1730	
777 J_STORE	INTEGER	SINGLE, ALIGNED, STATIC	XREF: 0 0989 1 1760 4 1775 1 1776 4 1790 1 1792 4 1753 1 1754 4 1759 1 1760 4 1775 1 1776 4 1790 1 1792 1 1793 1 1794 4 1809 1 1811 1 1812 4 1819 1 1821 1 1822 4 1833 1 1835 1 1836
785 J_TIME	INTEGER	DOUBLE, ALIGNED, INITIAL	XREF: 0 0079 2 2075

DCL NAME	TYPE	ATTRIBUTES & CROSS REFERENCE
1680 J_TIME_STORE	INTEGER	1 2102 1 2103 1 2104 1 2105 1 2106 1 2107 1 2108 1 2109 1 2110 1 2111 1 2112 1 2113 1 2114 4 2152 1 2168 4 2173 1 2180 4 2186 4 2199 4 2203 4 2208 4 2230 4 2247 4 2255 4 2277 1 2325 1 2326 SINGLE, ALIGNED, STATIC XREF: 0 1890 4 2147 2 2152 2 2173 2 2186 2 2199 4 2217 4 2223 2 2230 2 2247 2 2256 4 2267
1882 J_U	INTEGER	SINGLE, ALIGNED, AUTOMATIC XREF: 0 1082 4 2446 1 2469
741 K	7 X 10 MATRIX	1 2470 1 2474 1 2475 4 2464 1 2485 1 2486 DOUBLE, ALIGNED, STATIC XREF: 0 0741 4 1573 4 1604 4 1605 4 1606 4 1607 4 1608 2 1631 2 1633 2 1643 2 1655 2 1655 4 1675 1 1177
1053 K_RK	INTEGER	SINGLE, ALIGNED, STATIC XREF: 0 1053 4 1173 1 1175 1 1177
982 KA	7 X 10 MATRIX	DOUBLE, ALIGNED, STATIC XREF: 0 0932 4 1631 2 1603 2 1696
983 KB	7 X 10 MATRIX	DOUBLE, ALIGNED, STATIC XREF: 0 0985 4 1639 2 1685
984 KC	7 X 10 MATRIX	DOUBLE, ALIGNED, STATIC XREF: 0 0924 4 1643 2 1607 2 1698
985 KD	7 X 10 MATRIX	DOUBLE, ALIGNED, STATIC XREF: 0 0935 4 1650 2 1609
986 KE	7 X 10 MATRIX	DOUBLE, ALIGNED, STATIC XREF: 0 0935 4 1655 2 1691 2 1700
1051 KEEP_MASS	SCALAR	DOUBLE, ALIGNED, STATIC XREF: 0 1051 4 1222 2 1661
972 KO	10 X 5 MATRIX	DOUBLE, ALIGNED, STATIC XREF: 0 0972 4 1792 2 1812
973 K1	10 X 5 MATRIX	DOUBLE, ALIGNED, STATIC XREF: 0 0973 4 1811 2 1812 2 1822
974 K2	10 X 5 MATRIX	DOUBLE, ALIGNED, STATIC XREF: 0 0974 4 1821 2 1822 2 1836
975 K3	10 X 5 MATRIX	DOUBLE, ALIGNED, STATIC XREF: 0 0975 4 1835 2 1836
200 L_BETA	SCALAR	DOUBLE, ALIGNED, AUTOMATIC XREF: 0 0200 4 0620 2 0624
1048 L_CONST	SCALAR	DOUBLE, ALIGNED, STATIC XREF: 0 1048 4 1216 2 1227 2 1379 2 1470 2 1624
21 L_D_SCALE_FACTOR	SCALAR	DOUBLE, ALIGNED, CONSTANT XREF: 0 0021 2 0382 2 0470
73 L_FILE	INTEGER	SINGLE, ALIGNED XREF: 0 0073 4 2501 2 2582
788 L_FINAL	SCALAR	DOUBLE, ALIGNED, STATIC XREF: 0 0708 4 1998 4 2000 6 2002 2 2100
1054 L_FK	INTEGER	SINGLE, ALIGNED, AUTOMATIC XREF: 0 1054 4 1176 1 1177
996 L_SUB_P	10 - VECTOR	DOUBLE, ALIGNED, STATIC XREF: 0 0996 4 1213 4 1470 2 1632 2 1644 2 1656
997 L_SUB_P_1	10 - VECTOR	DOUBLE, ALIGNED, STATIC XREF: 0 0997 4 1632 2 1696
999 L_SUB_P_3	10 - VECTOR	DOUBLE, ALIGNED, STATIC XREF: 0 0998 4 1644 2 1698
999 L_SUB_P_5	10 - VECTOR	DOUBLE, ALIGNED, STATIC XREF: 0 0999 4 1656 2 1700
1150 L_SUB_U	2 - VECTOR	DOUBLE, ALIGNED, STATIC XREF: 0 1150 4 1624 4 1625 2 1633 2 1645 2 1658
811 L_SUB_U_L	2 - VECTOR	DOUBLE, ALIGNED, STATIC XREF: 0 0911 2 0359 4 1658
809 L_SUB_U_1	2 - VECTOR	DOUBLE, ALIGNED, STATIC XREF: 0 0809 2 0855 4 1633
810 L_SUB_U_3	2 - VECTOR	DOUBLE, ALIGNED, STATIC XREF: 0 0610 2 0856 4 1645
995 L_SUB_X	7 - VECTOR	DOUBLE, ALIGNED, STATIC XREF: 0 0995 4 1212 4 1227 4 1385 4 1386 4 1387 2 1666
134 L_TIME	INTEGER	SINGLE, ALIGNED, STATIC XREF: 0 0134 1 0581 1 0582 4 1196 2 1197 4 1198 4 1211 1 1362 1 1363 1 1412 1 1476 1 1500 4 2085 4 2308
727 L_X_STORE	7 - VECTOR ARRAY	ARRAY(2001), DOUBLE, ALIGNED, STATIC XREF: 0 0727 2 1666 4 1933 4 1939 4 1940 4 1941 4 1966 4 1969 4 1970 4 1971 4 2513 2 2588
748 LAMBDA	7 - VECTOR ARRAY	ARRAY(1003), DOUBLE, ALIGNED, STATIC XREF: 0 0748 2 0855 2 0856 2 0855 2 1696 2 1698 2 1700 2 1749 4 2097 4 2098 4 2099 4 2100 4 2101 4 2102 4 2103 4 2168 2 2325
742 LAMBDA_DOT	7 - VECTOR	DOUBLE, ALIGNED, STATIC XREF: 0 0742 4 1666 2 1718
761 LAMBDA_FLAG	BIT(1)	ALIGNED, STATIC XREF: 0 0761 2 1172 2 1174 2 1185 2 1190

DCL NAME	TYPE	ATTRIBUTES & CROSS REFERENCE
1049 LAMBDA_HOLD	7 - VECTOR	2 1665 2 1717 2 1744 2 1767 2 1825 4 1906 4 2162 4 2171
1895 LI_FLAG	BIT(1)	DOUBLE, ALIGNED, STATIC XREF: 0 1049 4 1175 2 1666
144 LIFT	SCALAR	ALIGNED, AUTOMATIC XREF: 0 1895 4 2455 2 2456 4 2462
1893 LI4	INTEGER	DOUBLE, ALIGNED, STATIC XREF: 0 0144 4 0592 2 0696 2 0697
1894 LI5	INTEGER	2 1356 2 1357 2 1358 SINGLE, ALIGNED, AUTOMATIC XREF: 0 1093 4 2447 2 2448
251 LOW_A	INTEGER	2 2449 2 2450 2 2452 4 2453 2 2455 SINGLE, ALIGNED, AUTOMATIC XREF: 0 1894 4 2450 4 2451
509 LOW_ALT	INTEGER	2 2456 SINGLE, ALIGNED, AUTOMATIC XREF: 0 0251 4 0322 1 0337
405 LOW_ANGLE	INTEGER	1 0330 1 0341 1 0347 1 0350 1 0352 1 0353 1 0354 1 0355 SINGLE, ALIGNED, AUTOMATIC XREF: 0 0509 4 0514 2 0515
230 LOW_CD	SCALAR	2 0522 2 0528 3 0529 1 0530 1 0531 3 0532 SINGLE, ALIGNED, AUTOMATIC XREF: 0 0405 4 0426 1 0429
244 LOW_C00	SCALAR	1 0430 1 0436 1 0437 1 0454 1 0455 1 0460 1 0463 1 0464 1 0467 1 0468 1 0469 1 0470 DOUBLE, ALIGNED, AUTOMATIC XREF: 0 0230 4 0338 2 0344
232 LOW_CL	SCALAR	2 0350 4 0353 2 0357 4 0439 4 0437 4 0455 2 0462 2 0464 4 0468 2 0472 DOUBLE, ALIGNED, AUTOMATIC XREF: 0 0244 4 0369 2 0376
227 LOW_M	INTEGER	2 0377 DOUBLE, ALIGNED, AUTOMATIC XREF: 0 0232 4 0337 2 0345
245 LOW_M_S	SCALAR	2 0347 4 0352 2 0356 4 0429 4 0436 4 0454 2 0461 2 0463 4 0467 2 0471 SINGLE, ALIGNED, AUTOMATIC XREF: 0 0227 4 0290 1 0291
205 LOW_M_2	SCALAR	1 0292 4 0335 1 0336 1 0337 1 0339 1 0340 1 0352 1 0353 1 0356 1 0357 4 0452 1 0453 1 0454 1 0455 1 0456 1 0457 1 0467 1 0468 1 0471 1 0472 DOUBLE, ALIGNED, AUTOMATIC XREF: 0 0245 4 0370 2 0376
749 M	5 X 13 MATRIX	2 0377 DOUBLE, ALIGNED, AUTOMATIC XREF: 0 0205 4 0647 2 0648
233 M_FIND	BIT(1)	2 0658 4 0663 DOUBLE, ALIGNED, STATIC XREF: 0 0749 2 0880 2 0954 2 0956
1876 M_VEC	5 - VECTOR	4 2328 4 2333 ALIGNED, AUTOMATIC XREF: 0 0233 4 0326 2 0327 4 0331
23 M_ZLD	SCALAR ARRAY	4 0444 2 0445 4 0449 DOUBLE, ALIGNED, STATIC XREF: 0 1876 4 2326 2 2328
587 M_1	5 X 2 MATRIX	ARRAY(16), DOUBLE, ALIGNED, CONSTANT XREF: 0 0023 2 0359
207 M_2_FLAG	BIT(1)	2 0362 2 0367 2 0370 2 0372 DOUBLE, ALIGNED, AUTOMATIC XREF: 0 0997 4 1712 2 1713
771 MASS_FLOW_FINAL_STEP	SCALAR	ALIGNED, AUTOMATIC XREF: 0 0207 4 0649 2 0650 4 0654
2535 MAX_AA_INDEX	INTEGER	DOUBLE, ALIGNED, STATIC XREF: 0 0771 4 2034 2 2100
42 MAX_ALT	INTEGER	SINGLE, ALIGNED, STATIC, INITIAL XREF: 0 2535 2 2550
876 MAX_B	SCALAR	SINGLE, ALIGNED, CONSTANT XREF: 0 0042 2 0043 2 0044 2 0515 1 0518 1 0519 DOUBLE, ALIGNED, AUTOMATIC XREF: 0 0376 4 0384 2 0687
64 MAX_BETA_CYCLES	INTEGER	4 0639 SINGLE, ALIGNED, CONSTANT XREF: 0 0064 2 0621 2 0657
2529 MAX_CP_INDEX	INTEGER	SINGLE, ALIGNED, STATIC, INITIAL XREF: 0 2529 2 2556
66 MAX_CUTOFF_ITERATIONS	INTEGER	SINGLE, ALIGNED, CONSTANT XREF: 0 0066 2 1956 2 1963
28 MAX_FS_AR_INDEX	INTEGER	2 1978 SINGLE, ALIGNED, CONSTANT XREF: 0 0028 2 0030 2 0031
29 MAX_FS_M_INDEX	INTEGER	2 0033 1 0310 2 0311 2 0314 1 0342 1 0348 SINGLE, ALIGNED, CONSTANT XREF: 0 0029 2 0030 2 0031
		2 0032 1 0323 2 0324 2 0327

DCL NAME	TYPE	ATTRIBUTES & CROSS REFERENCE
95 MAX_ITERATIONS	INTEGER	SINGLE, ALIGNED, INITIAL XREF: 0 0095 2 2582 2 2583
183 MAX_ROCKET_THRUST	SCALAR	DOUBLE, ALIGNED, STATIC XREF: 0 0183 2 0410 4 0551 2 0685
36 MAX_SS_ANGLE_INDEX	INTEGER	SINGLE, ALIGNED, CONSTANT XREF: 0 0036 2 0038 2 0039
37 MAX_SS_M_INDEX	INTEGER	2 0041 1 0414 2 0415 3418 XREF: 0 0037 2 0038 2 0039
91 MAX_STEP_I	INTEGER	SINGLE, ALIGNED, CONSTANT XREF: 1 0436 1 0437 1 0439 1 0442 2 0445
2532 MAX_M_INDEX	INTEGER	SINGLE, ALIGNED, INITIAL XREF: 0 0091 2 2074 2 2509
22 MAX_ZLD_INDEX	INTEGER	SINGLE, ALIGNED, STATIC, INITIAL XREF: 0 2532 2 2542
27 PCR_C	SCALAR ARRAY	SINGLE, ALIGNED, CONSTANT XREF: 0 0022 2 0023 2 0024
249 HCR_FLAG	BIT(1)	ARRAY(15), DOUBLE, ALIGNED, CONSTANT XREF: 0 0027 2 0280
26 PCR_M	SCALAR ARRAY	ALIGNED, AUTOMATIC XREF: 0 0249 4 0532 2 0283 4 0286
25 HCR_MAX_INDEX	INTEGER	ARRAY(15), DOUBLE, ALIGNED, CONSTANT XREF: 0 0026 2 0279
146 PD_MASS	SCALAR	2 0284 2 0291 2 0592 XREF: 0 0025 2 0026 2 0027
209 MID_M_2	SCALAR	SINGLE, ALIGNED, CONSTANT XREF: 1 0279 1 0280 2 0293
210 MID_MU	SCALAR	DOUBLE, ALIGNED, STATIC XREF: 0 0146 4 0693 6 0700 2 0713
92 MIN_COST_RIGHT	SCALAR	2 0715 2 1227 2 1379 2 1468 XREF: 0 0209 4 0659 2 0659
93 MIN_PSI_RIGHT	SCALAR	DOUBLE, ALIGNED, AUTOMATIC XREF: 0 0662 2 0565
90 MIN_PSI_THRESHOLD	SCALAR	DOUBLE, ALIGNED, AUTOMATIC XREF: 0 0110 4 0660 2 0661
14 MIN_SCRJ_MASS_PER_FT	SCALAR	DOUBLE, ALIGNED, INITIAL XREF: 0 0092 2 2602
172 MODEL_DRIVER	PROCEDURE	DOUBLE, ALIGNED, INITIAL XREF: 0 0093 2 2602
130 M0	SCALAR	DOUBLE, ALIGNED, INITIAL XREF: 0 0090 2 2507
407 M0_FLAG	BIT(1)	DOUBLE, ALIGNED, CONSTANT XREF: 0 0014 2 0261 2 0262
135 M0_2	SCALAR	2 2134 XREF: 0 0172 2 1214 2 1930 2 1935 2 1961 2 2086 2 2291
186 M1	SCALAR	2 2312 XREF: 0 0130 2 0323 2 0326 2 0335
57 M1_FINAL	SCALAR	DOUBLE, ALIGNED, STATIC XREF: 0 0376 2 0427 2 0434 2 0442 2 0446
772 M1_FLOW_FINAL_STEP	SCALAR	2 0359 2 0362 2 0367 2 0376 2 0427 2 0434 2 0442 2 0446
202 M1_2	SCALAR	2 0453 4 0539 2 0595 2 0601 2 0605 2 0517 2 1229 2 1232
137 M2	SCALAR	2 1233 2 1234 2 1255 2 1259 2 1264 2 1268 2 1273 2 1274
50 M2_FINAL	SCALAR	2 1276 2 1282 2 1283 2 1285 XREF: 0 0407 4 0441 4 0458 2 0465
773 M2_FLOW_FINAL_STEP	SCALAR	ALIGNED, AUTOMATIC XREF: 0 0135 4 0605 2 0609 2 0611
202 M2_2	SCALAR	DOUBLE, ALIGNED, STATIC XREF: 0 0632 2 0633 2 0637 2 0644
137 M2	SCALAR	2 0625 2 0630 2 0631 2 0632 2 0633 2 0637 2 0644
59 M3_FINAL	SCALAR	2 0647 2 0656 4 1229 2 1254 2 1255 2 1259 2 1262
773 M3_FLOW_FINAL_STEP	SCALAR	2 1266 2 1273 2 1274 2 1276 2 1282 2 1285 2 1312 2 1413
202 M3_2	SCALAR	2 1415 2 1417 XREF: 0 0186 4 0601 4 0670 2 0672
59 M3_FINAL	SCALAR	DOUBLE, ALIGNED, STATIC XREF: 0 0186 4 0601 4 0670 2 0672
773 M3_FLOW_FINAL_STEP	SCALAR	2 0674 XREF: 0 0057 2 1924
202 M3_2	SCALAR	DOUBLE, ALIGNED, STATIC XREF: 0 0772 4 2081 2 2112
137 M3	SCALAR	DOUBLE, ALIGNED, AUTOMATIC XREF: 0 0202 4 0630 4 0636
59 M3_FINAL	SCALAR	4 0665 2 0666 2 0670 XREF: 0 0137 2 0277 2 0279 2 0284
773 M3_FLOW_FINAL_STEP	SCALAR	DOUBLE, ALIGNED, STATIC XREF: 0 0302 4 0594 4 0674 2 1246 2 1291 2 1282
202 M3_2	SCALAR	2 1267 2 1288 2 1313 2 1314 2 1315 2 1414 2 1415 2 1422
59 M3_FINAL	SCALAR	2 1423 2 1424 XREF: 0 0058 2 1925
773 M3_FLOW_FINAL_STEP	SCALAR	DOUBLE, ALIGNED, CONSTANT XREF: 0 0773 4 2082 2 2113
202 M3_2	SCALAR	DOUBLE, ALIGNED, STATIC XREF: 0 1124 2 1279 4 1281 2 1282
59 M3_FINAL	SCALAR	2 1263 2 1267 2 1268 2 1421 2 1422 2 1423 2 1424
773 M3_FLOW_FINAL_STEP	SCALAR	DOUBLE, ALIGNED, CONSTANT XREF: 0 0059 2 1926

DCL NAME	TYPE	ATTRIBUTES & CROSS REFERENCE	
774 MS_FLCL_FINAL_STEP	SCALAR	DOUBLE, ALIGNED, STATIC XREF: 0 0774 4 0003 2 2114	
112 N_AERO	SCALAR	DOUBLE, ALIGNED, STATIC XREF: 0 0112 4 0897 2 0713 2 0714	
67 NEG_TIME_STEP	SCALAR ARRAY	2 0715 2 1385 2 1386 2 1397 2 1468 2 1480 2 1505 2 1509	
		2 1515 2 1524	
		ARRAY(3), DOUBLE, ALIGNED, INITIAL XREF: 0 0067 2 1059	
726 NET_MASS	SCALAR ARRAY	2 1864 2 2344 6 2347 2 2352 4 2359 4 2363 4 2375 4 2381	
		6 2398 4 2398 6 2401 6 2408 4 2413 6 2420 4 2425 4 2519	
		2 2594	
		ARRAY(2001), DOUBLE, ALIGNED, STATIC XREF: 0 0726 2 1022	
110 NET_R_FORCE	SCALAR	6 1223 2 1507 2 1555 2 1556 2 1557 2 1558 2 1561 2 1582	
111 NET_THETA_FORCE	SCALAR	2 1563 2 1564 2 1664 2 1685 2 1612 2 1610 2 1619 2 1624	
1154 NET_THRUST	SCALAR	4 1661 4 1346 6 1848 4 1971 2 2004 2 2090 2 2111 2 2293	
147 NET_X_FORCE	SCALAR	2 2294 2 2309 4 2311 2 2313 2 2314 4 2322 4 2512 4 2570	
60 NORM_TIME_STEP	SCALAR	2 2587 4 2624	
		DOUBLE, ALIGNED, STATIC XREF: 0 0110 4 0713 2 0844 2 1558	
		2 1604 2 1612 2 2111 2 2295 2 2315	
		DOUBLE, ALIGNED, STATIC XREF: 0 0111 4 0714 2 0846 2 1561	
		2 1564 2 1605 2 1611 2 2008 2 2094 2 2314	
		DOUBLE, ALIGNED, STATIC XREF: 0 1154 4 1215 2 1468 2 1477	
		2 1506 2 1510 2 1514 2 1624	
		DOUBLE, ALIGNED, STATIC XREF: 0 0147 4 0712 2 0713 2 0714	
		2 0715 2 1385 2 1386 2 1397	
		DOUBLE, ALIGNED, CONSTANT XREF: 0 0060 2 1853 2 1934	
		2 2060 2 2334 2 2339 2 2350 2 2353 2 2354 2 2375 2 2376	
		2 2361 2 2382 2 2398 2 2397 2 2413 2 2414 2 2425 2 2426	
		2 2448 2 2504 2 2630 2 2633	
150 NORMAL_SHOCK_FLAG	BIT(1)		
174 NOSE_ANGLE	SCALAR	ALIGNED, STATIC XREF: 0 0150 4 0556 4 0635 2 1271 4 2143	
6 NOZZLE_ANGLE	SCALAR	DOUBLE, ALIGNED, STATIC XREF: 0 0174 2 0666 2 0267 4 0542	
		2 0606	
48 NUM_CONSTANT_PARAMETERS	INTEGER	DOUBLE, ALIGNED, CONSTANT XREF: 0 0006 2 0266 2 0267	
		2 2116 2 2119 2 2129 2 2130 2 2133	
		SINGLE, ALIGNED, CONSTANT XREF: 0 0049 2 0051 2 0075	
		2 0728 2 0731 2 0734 2 0741 2 0744 2 0747 2 0749 2 0750	
		2 0901 2 0965 2 0982 2 0983 2 0984 2 0985 2 0986 2 0987	
		2 0997 2 0999 2 0999 2 1000 2 1001 2 1002 2 1003 2 1004	
		2 1005 2 1006 2 1007 2 1008 2 1009 2 1125 2 1126 2 1127	
		2 1128 2 1129 2 1130 2 1131 2 1132 2 1133 2 1134 2 1574	
		2 1758 2 1764 2 2060 2 2128 2 2191 2 2212 1 2325 1 2329	
		2 2332 2 2339 1 2343 1 2352 1 2353 2 2359	
51 NUM_CONSTRAINTS	INTEGER	SINGLE, ALIGNED, CONSTANT XREF: 0 0051 2 0052 2 0724	
		2 0725 2 0733 2 0734 2 0735 2 0736 2 0739 2 0743 2 0744	
		2 0745 2 0745 2 0749 2 0851 2 0852 2 0853 2 0854 2 0865	
		2 0866 2 0874 2 0875 2 0881 2 0885 2 0886 2 0897 2 0904	
		2 0909 2 0913 2 0915 2 0920 2 0930 2 0937 2 0972 2 0973	
		2 0974 2 0975 2 0976 2 0987 2 1050 2 1176 2 1753 2 1759	
		2 1770 2 1774 2 1775 2 1876 2 1882 2 2175 2 2179 2 2182	
		2 2249 2 2251 2 2259 2 2260 2 2261 2 2271 2 2287 2 2331	
49 NUM_CONTROLS	INTEGER	SINGLE, ALIGNED, CONSTANT XREF: 0 0049 2 0069 2 0076	
		2 0722 2 0733 2 0729 2 0730 2 0732 2 0736 2 0804 2 0809	
		2 0810 2 0811 2 0856 2 0937 2 1144 2 1145 2 1146 2 1147	
		2 1149 2 1149 2 1150 2 1617 2 1877 2 1899 2 1901 2 1903	
		2 2531 2 2544	
2 NUM_STATES	INTEGER	SINGLE, ALIGNED, CONSTANT XREF: 0 0002 2 0098 2 0727	
		2 0732 2 0733 2 0739 2 0740 2 0741 2 0742 2 0743 2 0748	
		2 0798 2 0800 2 0977 2 0978 2 0979 2 0980 2 0981 2 0982	

DCL NAME	TYPE	ATTRIBUTES & CROSS REFERENCE
50 NUM_TRANS_PTS	INTEGER	2 0993 2 0994 2 0995 2 0995 2 1049 2 1050 2 1050 2 1157 2 1173 1 1750 1 1741 2 1748 2 1752 2 1842 1 1845 2 1875 2 1913 2 2165 2 2167 2 2178 XREF: 0 0050 2 0061 2 0067 SINGLE, ALIGNED, CONSTANT XREF: 0 0050 2 0061 2 0067 2 0068 2 0070 2 0731 2 0737 2 0749 2 0750 2 0803 2 0905 2 0806 2 0818 2 0865 2 1202 2 1854 2 2276 2 2342 2 2369 2 2447 2 2537 XREF: 0 0203 4 0645 2 0646 DOUBLE, ALIGNED, AUTOMATIC XREF: 0 0203 4 0645 2 0646 2 0661 XREF: 0 0204 4 0645 2 0653 ALIGNED, STATIC XREF: 0 0149 4 0555 4 0615 2 1247 2 1410 4 2647 ALIGNED, STATIC XREF: 0 0792 4 1199 4 1207 2 1210 2 1220 2 1660 ARRAY(3), SINGLE, ALIGNED, STATIC, INITIAL XREF: 0 2537 2 2568 SINGLE, ALIGNED, STATIC XREF: 0 1898 4 2048 2 2440 4 2441 2 2442 2 2443 2 2449 2 2451 2 2484 DOUBLE, ALIGNED, AUTOMATIC XREF: 0 1898 4 2454 2 2461 4 2479 ARRAY(3), SINGLE, ALIGNED XREF: 0 0070 2 1203 2 1206 2 1220 2 1660 2 1847 2 1857 2 1859 2 1863 2 1865 2 2013 2 2018 2 2021 2 2026 2 2028 2 2153 2 2155 2 2157 2 2231 2 2233 2 2235 2 2277 2 2273 2 2280 2 2294 2 2298 2 2299 8 2 2305 2 2310 6 2369 2 2373 4 2374 2 2378 4 2390 2 2385 6 2387 2 2391 2 2393 6 2400 2 2405 6 2407 2 2410 6 2412 2 2417 6 2419 2 2422 6 2424 2 2495 4 2517 4 2550 2 2591 XREF: 0 2524 2 2641 PROCEDURE XREF: 0 2524 2 2641 SCALAR XREF: 0 1071 4 1254 2 1258 2 1259 4 1379 2 1385 2 1386 2 1387 XREF: 0 0782 4 2580 2 2592 4 2584 ALIGNED, STATIC XREF: 0 0784 2 1934 4 2034 2 2037 2 2073 2 2575 2 2597 4 2631 DOUBLE, ALIGNED XREF: 0 0075 2 0542 2 0543 2 0544 2 0545 2 0546 2 0547 2 0548 2 0549 2 0550 2 0551 2 1402 2 1412 2 1434 2 1435 2 1439 2 1440 2 1443 2 1445 2 1447 2 1450 2 1451 2 1454 2 1456 2 1521 2 1533 2 2043 2 2116 2 2117 2 2118 2 2119 2 2122 2 2123 2 2124 2 2125 2 2126 2 2127 2 2129 2 2131 2 2132 2 2133 2 2134 2 2135 2 2137 2 2138 2 2139 2 2140 2 2141 2 2142 2 2143 6 2340 4 2514 4 2550 2 2572 2 2589 XREF: 0 0113 4 0696 2 0712 2 1460 DOUBLE, ALIGNED, STATIC XREF: 0 0113 4 0696 2 0712 2 1460 2 1481 2 1506 2 1510 2 1514 2 1624 DOUBLE, ALIGNED, STATIC, INITIAL XREF: 0 2536 2 2560 ALIGNED, STATIC XREF: 0 0721 2 1180 4 1182 4 1785 4 1805 4 1829 4 2639 DOUBLE, ALIGNED, STATIC XREF: 0 1892 4 1928 2 1957 4 2031 ARRAY(3), DOUBLE, ALIGNED, INITIAL XREF: 0 0058 2 1850 2 1866 2 2344 6 2346 2 2353 4 2360 4 2364 4 2370 4 2392 6 2389 4 2397 6 2402 6 2409 4 2414 6 2421 4 2426 4 2518 2 2593 DOUBLE, ALIGNED, STATIC XREF: 0 0791 4 1853 4 1858 4 1860 4 1864 4 1866 2 1944 2 1959 2 1980 2 2055 2 2219 2 2269 2 2435 4 2633
203 NU0	SCALAR	
204 NU1	SCALAR	
149 OBLIQUE_SHOCK_FLAG	BIT(1)	
792 OIT_FLAG	BIT(1)	
2537 OIT_INIT	INTEGER ARRAY	
1898 OLD_FINAL_STEP	INTEGER	
1896 OLD_SC3	SCALAR	
70 OMEGA_I_TIME	INTEGER ARRAY	
2524 OPTIMIZATION	PROCEDURE	
1071 OSC1	SCALAR	
782 OVER_ITER_FLAG	BIT(1)	
784 OVER_STEP	BIT(1)	
75 P	10 - VECTOR	
113 P_AERO	SCALAR	
2536 P_INITIAL	10 - VECTOR	
721 PARTIAL_DERIV_FLAG	BIT(1)	
1892 PAST_INTEG_L	SCALAR	
68 POS_TIME_STEP	SCALAR ARRAY	
791 PRESENT_TIME_STEP	SCALAR	

ATTRIBUTES & CROSS REFERENCE

DCL NAME	TYPE	ATTRIBUTES & CROSS REFERENCE
735 PSI	5 - VECTOR	DOUBLE, ALIGNED, STATIC XREF: 0 0735 2 0953 4 2039 4 2040 4 2041 4 2042 4 2043 2 2044 2 2079 4 2337 2 2507
96 PSI_CHECK	SCALAR	DOUBLE, ALIGNED, INITIAL XREF: 0 0096 2 2604
89 PSI_COST_MIX	SCALAR	DOUBLE, ALIGNED, INITIAL XREF: 0 0039 2 0530
778 PSI_MAG	SCALAR	DOUBLE, ALIGNED, STATIC XREF: 0 0778 2 0946 4 2044 2 2507 2 2374 2 2596 2 2602 2 2604
79 PSI_SCALE_FACTOR	SCALAR	DOUBLE, ALIGNED, INITIAL XREF: 0 0679 2 2076
65 PSI_START	SCALAR	DOUBLE, ALIGNED, CONSTANT XREF: 0 0065 2 0944 2 0946 2 0949 2 0950
868 PSI_VAL	SCALAR	DOUBLE, ALIGNED, AUTOMATIC XREF: 0 0068 4 0946 2 0947 4 0948 2 0949 2 0951
62 PSI_WEIGHT	5 X 5 MATRIX	DOUBLE, ALIGNED, CONSTANT XREF: 0 0062 2 2044 2 2507
184 P0	SCALAR	DOUBLE, ALIGNED, STATIC XREF: 0 0134 4 0539 2 0598 2 0631 2 0637 2 0667
187 P1	SCALAR	DOUBLE, ALIGNED, STATIC XREF: 0 0197 4 0598 4 0631 4 0637 4 0667 2 0671
84 Q_D	SCALAR	DOUBLE, ALIGNED, INITIAL XREF: 0 0084 2 1160 2 1161 2 1936 2 1938 2 1955 2 1968 2 1999 2 2000
217 R	SCALAR	DOUBLE, ALIGNED, STATIC XREF: 0 0217 2 0540 4 0572 2 0574 2 0598
97 R_CUTOFF_CHECK	SCALAR	DOUBLE, ALIGNED, INITIAL XREF: 0 0097 2 1949
197 R_NEW_BOUND	SCALAR	DOUBLE, ALIGNED, AUTOMATIC XREF: 0 0197 4 0623 2 0624
19 R_0	SCALAR	DOUBLE, ALIGNED, CONSTANT XREF: 0 0019 2 0538 2 0539 2 0671 2 0672 2 1231 2 1244
512 REL_RO	SCALAR	DOUBLE, ALIGNED, AUTOMATIC XREF: 0 0512 4 0518 4 0525 4 0533 2 0534 2 0537
122 RESHAPE_FLAG	BIT(1)	ALIGNED, STATIC XREF: 0 0122 2 0258 2 0408 2 0496 4 0505 2 0552 4 1929
769 RK_COLUMNS	INTEGER	SINGLE, ALIGNED, STATIC XREF: 0 0769 2 1780 2 1790 2 1809 2 1819 2 1833 4 1914 4 2149 4 2175 4 2242 4 2259
990 RK_D_VAL	SCALAR	DOUBLE, ALIGNED, STATIC XREF: 0 0990 4 1159 4 1161 6 1163 4 1165 4 1718 4 1720 4 1722 4 1724 4 1726 4 1728 4 1730 2 1792 2 1811 2 1821 2 1835
994 RK_DERIV	PROCEDURE	XREF: 0 0994 2 1791 2 1810 2 1820 2 1834
768 RK_ROWS	INTEGER	SINGLE, ALIGNED, STATIC XREF: 0 0768 2 1780 2 1787 2 1806 2 1816 2 1830 4 1913 4 2163 4 2183 4 2241 4 2249
991 RK_STEP	INTEGER	SINGLE, ALIGNED, STATIC XREF: 0 0991 6 1160 4 1179 2 1177 4 1739
724 RK_VAL_N	10 X 5 MATRIX	DOUBLE, ALIGNED, STATIC XREF: 0 0724 2 1175 2 1177 4 1739 4 1741 4 1749 4 1754 4 1760 4 1765 4 1768 4 1771 4 1776 2 1793 6 1794 6 1812 6 1822
725 RK_VAL_N_PLUS_1	10 X 5 MATRIX	DOUBLE, ALIGNED, STATIC XREF: 0 0725 4 1836 2 1843 2 1845 2 2168 2 2180 2 2193 2 2213 2 2244 2 2252 2 2262
123 RO_0	SCALAR	DOUBLE, ALIGNED, STATIC XREF: 0 0123 4 0537 2 0539 2 0592 2 0599 2 1266 2 1269 2 1276 2 1277 2 1286 2 1356 2 1359 2 1413 2 1839 2 1940 2 1941 2 1969 2 1970 2 1971 2 1972
188 RO_1	SCALAR	DOUBLE, ALIGNED, STATIC XREF: 0 0188 4 0599 4 0671 2 0676
124 RO_2	SCALAR	DOUBLE, ALIGNED, STATIC XREF: 0 0124 2 0505 2 0508 4 0555 4 0676 2 1269 2 1277 2 1285 2 1286 2 1289 2 1317 2 1321 2 1322 2 1323 2 1333 2 1334 2 1335 2 1372 2 1373 2 1374 2 1375 2 1376 2 1377 2 1424 2 1430 2 1431 2 1432 2 1433 2 1434 2 1435 2 1457 2 1458
13 ROCKET_ISP	SCALAR	DOUBLE, ALIGNED, CONSTANT XREF: 0 0013 2 0711 2 1495 2 1599
173 ROCKET_MAX_T	SCALAR	DOUBLE, ALIGNED, STATIC XREF: 0 0173 4 0683 4 0685 2 0701
116 ROCKET_THRUST	SCALAR	DOUBLE, ALIGNED, STATIC XREF: 0 0116 4 0701 2 0711 2 0712

ATTRIBUTES & CROSS REFERENCE

TYPE

1	RUN_FOOL	COMPOOL	2 1215 2 1495						
971	RUNGE_KUTTA	PROCEDURE	EXTERNAL, VERSION=1	XREF: 0 0001					
			XREF: 0 0971 2 1945	2 1962 2 2166	2 2177 2 2190	2 2190	2 2211		
403	SCND_STAGE	PROCEDURE	2 2243 2 2250 2 2259						
141	SCRAMJET_ISP	SCALAR	XREF: 0 0403 2 0500	2 0504					
			DOUBLE, ALIGNED, STATIC	XREF: 0 0141 4 0302	2 0308 2 0705				
			2 1330 2 1333 2 1334	2 1335 2 1432	2 1433 2 1409	2 1409	2 1491		
			2 1492						
129	SCRAMJET_MASS	SCALAR	DOUBLE, ALIGNED, STATIC	XREF: 0 0129 4 0260	2 0261 4 0262				
			6 0263 2 0274 2 2134	2 2137					
119	SCRAMJET_POWER	BIT(1)	ALIGNED, STATIC	XREF: 0 0119	2 0277 2 0306	2 1330	2 1432		
			2 1455 2 1489 2 1531	2 1590 4 1918	4 2016 4 2022	4 2029			
			4 2089 4 2154 4 2159	4 2227 4 2232	4 2237 4 2255	4 2286			
			2 2297 4 2302 4 2304	2 2317					
114	SCRAMJET_THRUST	SCALAR	DOUBLE, ALIGNED, STATIC	XREF: 0 0114 4 0307	4 0308 4 0666				
			2 0705 2 0712 2 1215	2 1332 2 1333	2 1334 2 1335	2 1433			
			2 1455 2 1491 2 1492						
109	SCRJ_FUEL_FLOW	SCALAR	DOUBLE, ALIGNED, STATIC	XREF: 0 0109 4 0705	4 0709 2 0940				
			2 2298 2 2318						
128	SCRJ_MASS_CAPTURE_RATIO	SCALAR	DOUBLE, ALIGNED, STATIC	XREF: 0 0128 4 0280	4 0291 2 0294				
			4 0396 4 0300 2 0309	4 0690 2 1330	2 1332 2 1375	2 1376			
			2 1377 2 1432 2 1433	2 1435 2 1458					
10	SCRJ_MAX_FUEL_AIR_RATIO	SCALAR	DOUBLE, ALIGNED, CONSTANT	XREF: 0 0010	2 0308 2 1533				
			2 1591						
1886	SC1	SCALAR	DOUBLE, ALIGNED, STATIC	XREF: 0 1886	4 1938 2 1939	2 1640			
			2 1941 4 1968 2 1969	2 1970 2 1971	4 1983 2 1984	2 1985			
			2 1986 4 2129 2 2132	2 2133 2 2137	2 2143 4 2343	2 2344			
			2 2346 2 2347 2 2351	2 2355 2 2357					
1887	SC2	SCALAR	DOUBLE, ALIGNED, STATIC	XREF: 0 1887	4 1954 2 1984	2 1985			
			2 1929 4 2130 2 2131	2 2133 2 2137	2 2142 2 2143	4 2352			
			4 2353 2 2354 4 2356	2 2359 2 2360	2 2363 2 2364				
1888	SC3	SCALAR	DOUBLE, ALIGNED, STATIC	XREF: 0 1888	4 2131 2 2133	2 2137			
			2 2143 4 2354 2 2355	2 2356 4 2460	2 2461 2 2453	2 2477			
			2 2479						
1889	SC4	SCALAR	DOUBLE, ALIGNED, STATIC	XREF: 0 1889	4 2049 6 2055	6 2059			
			6 2060 2 2062 4 2132	2 2137 2 2142	2 2143 4 2429	6 2435			
			6 2437 2 2438 4 2448	2 2454 2 2463	4 2477				
1047	SG	SCALAR	DOUBLE, ALIGNED, STATIC	XREF: 0 1047	4 1503 2 1504	2 1507			
			2 1578						
747	SGV_DOT	10 - VECTOR	DOUBLE, ALIGNED, STATIC	XREF: 0 0747	4 1696 4 1698	4 1700			
			2 1724						
764	SGV_FLAG	BIT(1)	ALIGNED, STATIC	XREF: 0 0764	2 1693 2 1723	2 1763	2 1799		
			4 1909 4 2209	4 2215					
1118	SIN_A	SCALAR	DOUBLE, ALIGNED, STATIC	XREF: 0 1118	4 1362 2 1364	2 1365			
			2 1366 2 1367 2 1368	2 1369 2 1455	2 1466 2 1480	2 1481			
1069	SIN_B_T	SCALAR	DOUBLE, ALIGNED, STATIC	XREF: 0 1069	4 1252 2 1255	2 1258			
			2 1259 2 1414	2 1415					
1066	SIN_BETA	SCALAR	DOUBLE, ALIGNED, STATIC	XREF: 0 1066	4 1249 2 1251	2 1255			
			2 1258 2 1261 2 1262	2 1264 2 1266	2 1268 2 1413	2 1415			
			2 1416 2 1417						
212	SIN_BETA_THETA_MAX	SCALAR	DOUBLE, ALIGNED, AUTOMATIC	XREF: 0 0212	4 0609 2 0610				
			2 0611						
1046	SIN_DELTA	SCALAR	DOUBLE, ALIGNED, STATIC	XREF: 0 1046	4 1502 2 1507	2 1508			
			2 1511 2 1512 2 1515	2 1516 2 1578	2 1579				
165	SIN_VEHICLE_ANGLE	SCALAR	DOUBLE, ALIGNED, STATIC	XREF: 0 0165	4 0679 2 0713	2 0714			

ATTRIBUTES & CROSS REFERENCE

DCL NAME	TYPE	ATTRIBUTES & CROSS REFERENCE
1068 SIN_2_BETA	SCALAR	2 1611 2 1612 2 1613 DOUBLE, ALIGNED, STATIC XREF: 0 1068 4 1251 2 1254 2 1255 2 1258 2 1259 2 1261 2 1262 2 1266 2 1412 2 1413 2 1415 2 1416 2 1417
750 SMALL_G_VEC	13 - VECTOR	DOUBLE, ALIGNED, STATIC XREF: 0 0750 2 0954 2 0961 2 0969 2 1765 4 2091 4 2213 4 2325
1057 SPEED_OF_SOUND_2	SCALAR	DOUBLE, ALIGNED, STATIC XREF: 0 1057 4 1231 2 1232 2 1233 2 1234
1052 SR	SCALAR	DOUBLE, ALIGNED, STATIC XREF: 0 1052 4 1195 2 1232 2 1234 2 1355 2 1356 2 1358 2 1359 2 1351 2 1486 2 1489 2 1499 2 1500 2 1503 2 1507 2 1557 2 1551 2 1552 2 1563 2 1554 2 1605 2 1619
41 SS_ANGLE_OF_ATTACK_VAL	SCALAR ARRAY	ARRAY(5), DOUBLE, ALIGNED, CONSTANT XREF: 0 0041 2 0414 2 0419 2 0460 2 0463 2 0464
164 SS_CD	SCALAR	DOUBLE, ALIGNED, STATIC XREF: 0 0164 4 0462 6 0480 2 0486 4 0490 2 1454
39 SS_CD_MAT	5 X 16 MATRIX	DOUBLE, ALIGNED, CONSTANT XREF: 0 0039 2 0430 2 0432 2 0437 2 0439 2 0455 2 0457 2 0468 2 0470
163 SS_CL	SCALAR	DOUBLE, ALIGNED, STATIC XREF: 0 0153 4 0461 6 0479 2 0485 2 1463
38 SS_CL_MAT	5 X 16 MATRIX	DOUBLE, ALIGNED, CONSTANT XREF: 0 0038 2 0429 2 0431 2 0436 2 0438 2 0454 2 0456 2 0467 2 0469
224 SS_DRAG	SCALAR	DOUBLE, ALIGNED, STATIC XREF: 0 0224 4 0465 2 0487 4 0409 2 0693
120 SS_DRY_MASS	SCALAR	DOUBLE, ALIGNED, STATIC XREF: 0 0120 4 0410 2 0693 2 0839 2 1846 2 1931
108 SS_FUEL_FLOW	SCALAR	DOUBLE, ALIGNED, STATIC XREF: 0 0108 4 0711 2 0849 2 2320 2 2321
223 SS_LIFT	SCALAR	DOUBLE, ALIGNED, STATIC XREF: 0 0223 4 0405 2 0692 ARRAY(16), DOUBLE, ALIGNED, CONSTANT XREF: 0 0040 2 0427 2 0434 2 0442 2 0446 2 0453 2 0471 2 0472
182 SS_MAX_FUEL_LOAD	SCALAR	DOUBLE, ALIGNED, STATIC XREF: 0 0182 2 0410 2 0411 4 0550 2 0485 2 0486 4 0411 2 0485 2 0486 4 0411 2 1478 2 1479 2 1356 2 1357 2 1358 2 1359 2 1350 2 1351 2 1478 2 1479
143 SS_PLANFORM_AREA	SCALAR	ALIGNED, STATIC XREF: 0 0134 2 0498 2 0593 2 0682 2 0689 2 0702 2 0840 2 1242 2 1370 2 1403 2 1467 2 2011 4 2015 4 2037
104 STAGE_SEP	BIT(1)	4 2160 4 2225 4 2238 4 2233 4 2301 2 2319 4 2160 4 2225 4 2238 4 2233 4 2301 2 2319
993 START_RK_COLUMNS	INTEGER	SINGLE, ALIGNED, STATIC XREF: 0 0993 4 1733 4 1808 2 1809 4 1818 2 1819 4 1832 2 1835 XREF: 0 0536 2 1755
856 STATE_DEPVS	PROCEDURE	XREF: 0 1905 2 2069 2 2506
1905 STATE_INTEGRATION	PROCEDURE	ALIGNED, STATIC XREF: 0 0133 2 0575 2 1155 2 1734 2 1039 2 1855 4 1919 2 1934 4 2035 2 2007 4 2292 4 2646
133 STATE_INTEGRATION_FLAG	BIT(1)	SINGLE, ALIGNED, CONSTANT XREF: 0 0063 2 0076 2 0077 2 0098 2 0099 2 0726 2 0727 2 0729 2 0730 2 0732 2 0733 2 0751 2 0752 2 0798 2 0799 2 0800 2 0802 2 0804 2 1877 2 2033 2 2050 2 2501 2 2525 2 2525 2 2541 2 2549 2 2555 2 2562 2 2622
63 STEP_DIM	INTEGER	SINGLE, ALIGNED, STATIC XREF: 0 0807 2 0878 4 2074 2 2075 2 2076 2 2077 2 2509 4 2623
807 STEP_I	INTEGER	ALIGNED, STATIC XREF: 0 1900 4 2047 4 2508 2 2509 4 2075 2 0959 4 2075
1900 STEP_I_FLAG	BIT(1)	DOUBLE, ALIGNED, INITIAL XREF: 0 0088 2 0958 4 2076 2 0959 4 2075
88 STEP_SCALE_J	SCALAR	DOUBLE, ALIGNED, INITIAL XREF: 0 0087 2 0958 4 2076 4 2075
87 STEP_SCALE_PSI	SCALAR	ALIGNED, STATIC XREF: 0 0152 4 0558 4 0597 2 1293 4 2650 4 2650
152 SUBSONIC_FLAG	BIT(1)	DOUBLE, ALIGNED, STATIC XREF: 0 1041 4 1332 2 1333 4 1332 2 1333
1041 S2	SCALAR	

DCL NAME	TYPE	ATTRIBUTES & CROSS REFERENCE
1042 S3	SCALAR	2 1335 4 1500 2 1501 2 1502 DOUBLE, ALIGNED, STATIC XREF: 0 1042 4 1496 2 1497 2 1498 2 1499
1043 S5	SCALAR	DOUBLE, ALIGNED, STATIC XREF: 0 1043 4 1505 2 1507 2 1508 4 1509 2 1511 2 1512 4 1513 2 1515 2 1516 4 1521 2 1522 2 1523 2 1524 4 1533 2 1534 2 1535 2 1536 4 1577 2 1578 2 1579
1044 S6	SCALAR	DOUBLE, ALIGNED, STATIC XREF: 0 1044 4 1506 2 1507 2 1508 4 1510 2 1511 2 1512 4 1514 2 1515 2 1516
1091 S9	SCALAR	DOUBLE, ALIGNED, STATIC, INITIAL XREF: 0 1091 2 2134 BIT(1)
793 T_FLAG	SCALAR	ALIGNED, AUTOMATIC XREF: 0 0793 4 1200 4 1205 2 1210
1097 T_MASS	SCALAR	DOUBLE, ALIGNED, STATIC XREF: 0 1097 4 2309 2 2311 2 2322
1056 T_VAL	SCALAR	DOUBLE, ALIGNED, STATIC XREF: 0 1056 4 1230 2 1232 2 1234 2 1355 2 1356 2 1358 2 1359 2 1361 2 1496 2 1497 2 1498 2 1500
1875 T_XDOT	7 - VECTOR	DOUBLE, ALIGNED, STATIC XREF: 0 1875 4 2281 4 2293 4 2294 4 2296 4 2298 6 2321 4 2324 2 2325 2 2326
214 TAN_THETA_MAX	SCALAR	DOUBLE, ALIGNED, AUTOMATIC XREF: 0 0214 4 0611 2 0612
1072 TANK1	SCALAR	DOUBLE, ALIGNED, AUTOMATIC XREF: 0 1072 4 2117 2 2120 2 2122 2 2124 2 2126
1073 TANK2	SCALAR	DOUBLE, ALIGNED, AUTOMATIC XREF: 0 1073 4 2116 2 2117 6 2118 2 2121 2 2123 2 2125 2 2127 XREF: 0 0718 2 2451
718 THESIS_ALGORITHM	PROCEDURE	
82 THETA_DOT_INITIAL	SCALAR	DOUBLE, ALIGNED, INITIAL XREF: 0 0082 2 1948 2 1975
54 THETA_FINAL	SCALAR	DOUBLE, ALIGNED, CONSTANT XREF: 0 0054 2 1922
215 THETA_MAX	SCALAR	DOUBLE, ALIGNED, AUTOMATIC XREF: 0 0215 4 0612 2 0613
139 THETA_NOISE	SCALAR	DOUBLE, ALIGNED, STATIC XREF: 0 0139 4 0606 2 0607 2 0613 2 0616 2 0620 2 0630 2 0646 2 1252 2 1253
755 TIME_INTERVAL	SCALAR	DOUBLE, ALIGNED, STATIC XREF: 0 0755 4 1737 4 1745 4 1746 2 1792 2 1811 2 1821 2 1835 XREF: 0 1851 2 1943 2 1955 2 2054 2 2218 2 2268 2 2434
1051 TIME_SET	PROCEDURE	
1085 TIME_SIGN	SCALAR	DOUBLE, ALIGNED, STATIC XREF: 0 1085 4 1976 4 1977 2 1980
753 TIME_STEP	SCALAR	DOUBLE, ALIGNED, STATIC XREF: 0 0753 2 1737 2 1745 2 1746 4 1944 4 1959 6 1980 2 1983 2 1990 4 2148 4 2219 4 2224 4 2269
107 TJ_FUEL_FLOW	SCALAR	DOUBLE, ALIGNED, STATIC XREF: 0 0107 4 0704 4 0708 2 0847 2 2295 2 2316
9 TJ_MAX_FUEL_AIR_RATIO	SCALAR	DOUBLE, ALIGNED, CONSTANT XREF: 0 0009 2 0305 2 1521 2 1558
1052 TSI	INTEGER	SINGLE, ALIGNED, AUTOMATIC XREF: 0 1952 4 1854 1 1657
140 TURBOJET_ISP	SCALAR	1 1058 1 1059 1 1060 1 1063 1 1064 1 1065 1 1066 DOUBLE, ALIGNED, STATIC XREF: 0 0140 4 0301 2 0305 2 0704 2 1319 2 1321 2 1322 2 1323 2 1430 2 1431 2 1464 2 1466 2 1487
237 TURBOJET_MASS	SCALAR	DOUBLE, ALIGNED, AUTOMATIC XREF: 0 0237 4 0264 2 0274
118 TURBOJET_POWER	BIT(1)	ALIGNED, STATIC XREF: 0 0118 2 0303 2 1319 2 1430 2 1453 2 1484 2 1519 2 1587 4 1917 4 2020 4 2027 4 2088 4 2156 4 2226 4 2234 4 2288 4 2289 2 2295 4 2306 4 2307 2 2315
115 TURBOJET_THRUST	SCALAR	DOUBLE, ALIGNED, STATIC XREF: 0 0115 4 0304 4 0687 2 0704 2 0712 2 1215 2 1321 2 1322 2 1323 2 1454 2 1486 2 1487
136 T0	SCALAR	DOUBLE, ALIGNED, STATIC XREF: 0 0136 4 0519 4 0524 4 0529 2 0538 2 0539 2 0600 2 0632 2 0639 2 0668 2 1231 2 1232 2 1262 2 1265 2 1274 2 1275 2 1283 2 1284 2 1417
109 T1	SCALAR	DOUBLE, ALIGNED, STATIC XREF: 0 0109 4 0600 4 0632 4 0638

DCL NAME	TYPE	ATTRIBUTES & CROSS REFERENCE
148 T2	SCALAR	4 0666 2 0567 6 0668 2 0671 2 0672 2 0677 4 0677 2 1244 DOUBLE, ALIGNED, STATIC XREF: 0 0149 4 0537 2 1245 2 1246 2 1265 2 1275 2 1284 2 1287 2 1423
796 U	2 X 2 MATRIX	DOUBLE, ALIGNED, STATIC XREF: 0 0795 4 0831 4 0832 2 0967
813 U_A	INTEGER	2 1707 2 1709 2 1713 4 2634 XREF: 0 0913 4 0819 2 0820
76 U_ACTIVE	2 - VECTOR ARRAY	SINGLE, ALIGNED, AUTOMATIC 4 0821 2 0826 XREF: 0 0076 2 0577 2 0578
814 U_B	INTEGER	ARRAY(2001), DOUBLE, ALIGNED 2 0581 2 0582 2 1362 2 1363 2 1412 2 1476 2 1500 2 1952 6 1955 4 1983 2 2470 2 2475 4 2495 6 2496 6 2497 2 2500 6 2503 6 2504 4 2515 4 2563 4 2565 4 2566 2 2592
812 U_COMPUTE	PROCEDURE	SINGLE, ALIGNED, AUTOMATIC 4 0824 2 0826 XREF: 0 0314 4 0822 2 0223
815 U_I	INTEGER	XREF: 0 0812 2 0966 2 1705
751 U_J_OLD_TIME	SCALAR ARRAY	SINGLE, ALIGNED, AUTOMATIC XREF: 0 0815 4 0818 2 0819 2 0822 4 0926 1 0827 1 0930 1 0931 1 0932
1901 U_KEEP	2 - VECTOR	ARRAY(1001), DOUBLE, ALIGNED, STATIC XREF: 0 0751 2 0927
1903 U_NEW	2 - VECTOR ARRAY	2 0030 4 1996 4 2027 DOUBLE, ALIGNED, AUTOMATIC XREF: 0 1901 4 2500 2 2504
752 U_NEW_TIME	SCALAR ARRAY	ARRAY(1001), DOUBLE, ALIGNED, AUTOMATIC XREF: 0 1903 4 2470 4 2475 2 2486
99 U_OLD_TIME	SCALAR ARRAY	ARRAY(2001), DOUBLE, ALIGNED, STATIC XREF: 0 0752 4 2438 2 2460 2 2465 2 2466 4 2629
218 U_R	SCALAR	ARRAY(2001), DOUBLE, ALIGNED XREF: 0 0099 6 1992 2 1996 4 2062 2 2064 2 2066 2 2460 2 2465 2 2466 2 2468 2 2473 4 2516 4 2628
55 U_R_FINAL	SCALAR	DOUBLE, ALIGNED, STATIC XREF: 0 0218 4 0573 2 0589 2 0590
816 U_SET	BIT(1)	DOUBLE, ALIGNED, CONSTANT XREF: 0 0055 2 1921
220 U_T_AIR	SCALAR	ALIGNED, AUTOMATIC XREF: 0 0816 4 0825 2 0826 4 0829
219 U_THETA	SCALAR	DOUBLE, ALIGNED, STATIC XREF: 0 0220 4 0588 2 0589 2 0590
56 U_THETA_FINAL	SCALAR	DOUBLE, ALIGNED, STATIC XREF: 0 0219 4 0574 2 0583
795 U_TIME	INTEGER	DOUBLE, ALIGNED, CONSTANT XREF: 0 0056 2 1923
77 U_TIME_KEEP	SCALAR ARRAY	SINGLE, ALIGNED, STATIC XREF: 0 0795 2 0819 2 0822 1 0827 1 0350 4 0965 4 1704
817 U_VAL	SCALAR	ARRAY(1001), DOUBLE, ALIGNED XREF: 0 0077 2 0827 2 0830 4 2064 4 2635
4 UNIVERSAL_G_CONSTANT	SCALAR	DOUBLE, ALIGNED, AUTOMATIC XREF: 0 0617 4 0830 2 0831
1904 UV1	SCALAR	2 0832
185 U0	SCALAR	DOUBLE, ALIGNED, CONSTANT XREF: 0 0004 2 0540 2 1593 DOUBLE, ALIGNED, AUTOMATIC XREF: 0 1934 4 2465 6 2469 2 2469 2 2470 6 2473 2 2474 2 2475
190 U1	SCALAR	DOUBLE, ALIGNED, STATIC XREF: 0 0185 2 0539 4 0590 2 0592
125 U2	SCALAR	2 0602
61 V	13 X 13 MATRIX	DOUBLE, ALIGNED, STATIC XREF: 0 0190 4 0602 4 0672 2 0675 DOUBLE, ALIGNED, STATIC XREF: 0 0125 2 0305 2 0308 4 0525 4 0675 2 1317 2 1321 2 1322 2 1323 2 1334 2 1335 2 1372 2 1373 2 1374 2 1375 2 1376 2 1377 2 1430 2 1431 2 1432 2 1433 2 1434 2 1435 2 1457 2 1458
992 VAL_1	INTEGER	DOUBLE, ALIGNED, INITIAL XREF: 0 0061 2 0880 2 0954 2 0956
225 VEHICLE	PROCEDURE	2 0951 2 0969
131 VEHICLE_ANGLE	SCALAR	SINGLE, ALIGNED, STATIC XREF: 0 0992 2 1183 4 1780 XREF: 0 0225 2 0553 2 0681
837 VEHICLE_MASS	SCALAR	DOUBLE, ALIGNED, STATIC XREF: 0 0131 4 0589 2 0679 2 0680 DOUBLE, ALIGNED, AUTOMATIC XREF: 0 0837 4 0839 6 0841 2 0844 2 0846

DCL NAME	TYPE	ATTRIBUTES & CROSS REFERENCE
1111 V0_2	SCALAR	DOUBLE, ALIGNED, STATIC XREF: 0 1111 4 1355 2 1356 2 1357 2 1358 2 1359 2 1360 2 1361
69 M	2 X 2 MATRIX ARRAY	ARRAY(1001), DOUBLE, ALIGNED XREF: 0 0069 2 0331 2 0832 4 2539 4 2545
2530 H_INDEX	INTEGER ARRAY	ARRAY(5), SINGLE, ALIGNED, STATIC, INITIAL
2531 H_INIT	SCALAR ARRAY	2 2542 2 2545 ARRAY(5*2), DOUBLE, ALIGNED, STATIC, INITIAL 2 2545
175 H_SCRJ	SCALAR	DOUBLE, ALIGNED, STATIC XREF: 0 0175 2 0263 2 0264 2 0266 2 0267 2 0305 2 0308 4 0543
142 KING_AREA	SCALAR	DOUBLE, ALIGNED, STATIC XREF: 0 0142 4 0265 2 0268 2 0309 2 0391 2 0392 2 1356 2 1357 2 1358 2 1359 2 1360 2 1361 2 1447 2 1463 2 1484 2 1478 2 1479
178 KING_SPAN	SCALAR	DOUBLE, ALIGNED, STATIC XREF: 0 0178 2 0265 2 0309 4 0546
739 X_DOT	7 - VECTOR	DOUBLE, ALIGNED, STATIC XREF: 0 0739 4 0843 4 0844 4 0845 4 0846 4 0847 4 0848 4 0849 2 1185 4 2302 4 2313 4 2314 4 2316 4 2318 4 2320 2 2321
838 X_R	SCALAR	DOUBLE, ALIGNED, AUTOMATIC XREF: 0 0838 4 0842 2 0844 2 0846
98 X_STORE	7 - VECTOR ARRAY	ARRAY(2001), DOUBLE, ALIGNED XREF: 0 0098 2 0513 2 0572 2 0573 2 0574 2 0699 2 0319 2 0942 2 0673 2 0844 2 0845 2 0846 2 1195 2 1230 2 1233 2 1355 2 1357 2 1360 2 1496 2 1497 2 1499 2 1500 2 1555 2 1557 2 1561 2 1562 2 1563 2 1739 4 1843 2 1846 4 1920 4 1921 4 1922 4 1923 4 1924 4 1925 4 1926 2 1939 2 1940 2 1941 2 1948 2 1969 2 1970 2 1971 2 1975 2 2039 2 2040 2 2041 2 2042 2 2043 2 2081 2 2082 2 2083 2 2086 2 2110 2 2111 2 2094 2 2314 2 2507 4 2511 4 2569 2 2577 2 2586 2 2599 4 2645 ARRAY(16), DCUBLE, ALIGNED, CONSTANT XREF: 0 0024 2 0360 2 0363 2 0369 2 0371
24 ZLD	SCALAR ARRAY	

BUILT-IN FUNCTION CROSS REFERENCE

(CROSS REFERENCE FLAG KEY: 2 = REFERENCE, 1 = SUBSCRIPT USE)

NAME	CROSS REFERENCE
ABS	XREF: 2 0897 2 2354 2 2460 2 2602 2 2604
COS	XREF: 2 0611 2 0623 2 0620 2 0695 2 1250 2 1363 2 1412 2 1450 2 1501 2 2133
EXP	XREF: 2 0302 2 0532 2 0533 2 1315
LOG	XREF: 2 0531
MAX	XREF: 2 0619
MOD	XREF: 2 1201 2 1946 2 1995 2 2009 2 2063 2 2444 2 2457 2 2469 2 2493
SIN	XREF: 2 0266 2 0267 2 0623 2 0629 2 0630 2 0679 2 0694 2 1249 2 1252 2 1362 2 1451 2 1502 2 2116 2 2119
TAN	2 2129 2 2130 2 2132 2 2141
SIGN	XREF: 2 0265 2 0611 2 0620 2 0623 2 2140
SQRT	XREF: 2 2355
FLOOR	XREF: 2 0582 2 0478 2 0539 2 0590 2 0609 2 0643 2 0644 2 0651 2 0659 2 0670 2 0672 2 0715 2 0946 2 1244
ARCSIN	2 1254 2 1273 2 1282 2 1422 2 2565
ARCTAN	XREF: 2 0514 2 0523 2 0524 2 0963 2 1188 2 2484 2 2541
CEILING	XREF: 2 0599 2 0512 2 0645 2 0652 2 0660 2 1500
TRUNCATE	XREF: 1 1995 1 2064 2 2080 2 2147 2 2203 2 2217 2 2223 2 2267 2 2277 2 2355 2 2446 2 2459 1 2490
TRANSPOSE	XREF: 2 2356
	2 1696 2 1698 2 1700 2 1709 2 1712 2 1713 2 2326
	2 1676 2 1678 2 1679 2 1683 2 1687 2 1689 2 1691

LIST OF REFERENCES

1. "Space Manufacturing Facilities (Space Colonies)," Jerry Grey, editor, American Institute of Aeronautics and Astronautics, Inc., New York, 1977, pp. 51-76.
2. Avery, W.H., "Twenty-five Years of Ramjet Development," Jet Propulsion, Vol. 25, No. 11, Nov. 1955, pp. 604-614.
3. Dugger, G.L., "Comparison of Hypersonic Ramjet Engines with Subsonic and Supersonic Combustion," Combustion and Propulsion, Fourth AGARD Colloquium, High Mach Number Air-Breathing Engines, A.L. Jaumotte, A.H. Lefebvre, A.M. Rothrock, editors, Pergamon Press, New York, 1961, pp. 84-110.
4. Hunter, Maxwell W. II, "Commercial Space Transportation Possibilities," American Astronautical Society paper no. 67-134, 1967.
5. Henry, John R. and Charles H. McLellan, "The Air-Breathing Launch Vehicle for Earth-Orbit Shuttle—New Technology and Development Approach," American Institute of Aeronautics and Astronautics paper no. 70-269, 1970.
6. Gregory, Thomas J., Louis J. Williams, and Darrell E. Wilcox, "The Air-Breathing Launch Vehicle for Earth-Orbit Shuttle—Performance and Operation," American Institute of Aeronautics and Astronautics paper no. 70-270, 1970.
7. Hunter, Maxwell W. II and Dietrich W. Fellenz, "The Hypersonic Transport—The Technology and the Potential," American Institute of Aeronautics and Astronautics paper no. 70-1218, 1970.
8. Johnston, P.J., J.M. Cabbage, and J.P. Weidner, "Studies of Engine-Airframe Integration on Hypersonic Aircraft," American Institute of Aeronautics and Astronautics paper no. 70-542, 1970.

LIST OF REFERENCES (CONT.)

9. Edwards, C.L.W., W.J. Small, J.P. Weidner, and P.J. Johnston, "Studies of Scramjet/Airframe Integration Techniques for Hypersonic Aircraft," American Institute of Aeronautics and Astronautics paper no. 75-58, 1975.
10. Weidner, J.P., W.J. Small, and J.A. Penland, "Scramjet Integration on Hypersonic Research Airplane Concepts," American Institute of Aeronautics and Astronautics paper no. 76-755, 1976.
11. Wieting, Allan R. and Robert W. Guy, "Preliminary Thermal-Structural Design and Analysis of an Airframe-Integral Hydrogen-Cooled Scramjet," American Institute of Aeronautics and Astronautics paper no. 75-137, 1975.
12. Rogers, R.C., "Effects of Fuel Temperature on Supersonic Mixing and Combustion of Hydrogen," American Institute of Aeronautics and Astronautics paper no. 77-17, 1977.
13. Hearth, Donald P. and Albert E. Preyss, "Hypersonic Technology—Approach to an Expanded Program," Astronautics and Aeronautics, Vol. 14, No. 12, Dec. 1976, pp. 20-37.
14. Hankey, Wilbur L., "Some Design Aspects of Hypersonic Vehicles," Aerospace Research Laboratories Report no. 70-0049, March 1970.
15. Bryson, A.E., Stanley E. Ross, "Optimum Rocket Trajectories with Aerodynamic Drag," Jet Propulsion, July, 1958, pp. 465-469.
16. Bryson, A.E., W.F. Denham, "A Steepest-Ascent Method for Solving Optimum Programming Problems," Journal of Applied Mechanics, June, 1962, pp. 247-257.
17. Wilhite, Alan W., "Optimization of Rocket Propulsion Systems for Advanced Earth-to-Orbit Shuttles," Journal of Spacecraft and Rockets, Vol. 17, No. 2, March-April, 1980, pp. 99-104.
18. Nicolai, Leland M., Fundamentals of Aircraft Design, E.P. Domicone Printing Services, Fairborn, Ohio, pp. E4-E5.
19. C.S. Draper Laboratory Statement Level Simulator, Lift and Drag Data Set.
20. Martin, James Arthur, Aerospaceplane Optimization and Performance Estimation, Master's Thesis, Massachusetts Institute of Technology, August, 1967, p. 9.

LIST OF REFERENCES (CONT.)

21. Liepmann, H.W. and A. Roshko, Elements of Gas Dynamics, John Wiley and Sons, Inc., New York, 1957, p. 59.
22. Ibid., p. 86-87.
23. Ibid., p. 53, p. 99.
24. JP-121 course notes, California Institute of Technology, 1974.
25. "Scramjet Performance Characteristics" paper draft, Langley Research Center, 1978, Figure 16.
26. Ibid.
27. Jones, Robert A. and Paul W. Huber, "Airframe Integrated Propulsion System for Hypersonic Cruise Vehicles", paper presented at the 11th Congress of the International Council of the Aeronautical Sciences, September, 1978, p. 5.
28. Ibid., p. 2.
29. Shuttle Operational Data Book, Volume II, "Mission Mass Properties", September, 1975.
30. C.S. Draper Laboratory Statement Level Simulator, Lift and Drag Data Set.
31. U.S. Standard Atmosphere, 1962, U.S. Government Printing Office, Washington, D.C., December, 1962.
32. Beer, F.P. and E.R. Johnston, Vector Mechanics for Engineers: Statics and Dynamics, McGraw-Hill Book Company, New York, 1962, p. 467.
33. Henry, Beverly Z. and John P. Decker, "Future Earth Orbit Transportation Systems/Technology Implications," Astronautics and Aeronautics, Vol. 14, No. 9, Sept. 1976, p. 25.
34. Voss, Janice, Optimization of Variable Mixture Ratio Rocket Boosters, Masters Thesis, Massachusetts Institute of Technology, May, 1977.
35. Satellite Power Systems (SPS) Concept Definition Study, Final Report (Exhibit C), Volume IV, "Transportation Analysis", Appendix A.

BIOGRAPHY

Philip David Hattis was born in Chicago, Illinois on 18 July 1952. He received his early education at public schools in Winnetka, Illinois and graduated from New Trier East High School in 1970. He entered Northwestern University as an undergraduate in 1970 and received his Bachelor of Science degree in Mechanical Engineering in 1973. Having enrolled in the graduate school of the California Institute of Technology in 1973, he was granted the Master of Science degree in Aeronautics in 1974. Since 1974, Mr. Hattis has been pursuing his doctoral degree in the Department of Aeronautics and Astronautics at the Massachusetts Institute of Technology (MIT).

While attending graduate school at MIT, Mr. Hattis has been a Draper Fellow at The Charles Stark Draper Laboratory (CSDL). On two occasions, he has also been a Summer Staff member at CSDL.

Mr. Hattis is a member of the Pi Tau Sigma, Tau Beta Pi, and Sigma Xi honorary societies and is also a member of the American Society of Mechanical Engineers and the American Institute of Aeronautics and Astronautics.